

**The Role of Mitochondria in Regulating
Smooth Muscle Cell Proliferation and
Migration in Pulmonary Hypertension**

A thesis presented by

AbdulHadi Salem H. Burzangi

Pharm.D, M.Sc.

In fulfilment of the requirements for the degree of Doctor of Philosophy

2018

Strathclyde Institute of Pharmacy and Biomedical Sciences

University of Strathclyde, Glasgow, UK.

This thesis is the result of the author's original research. It has been composed by the author and has not been previously submitted for examination which has led to the award of a degree.

The Copyright of this thesis belongs to the author under the terms of the United Kingdom Copyright Acts as qualified by University of Strathclyde Regulation 3.50. Due acknowledgement must always be made of the use of any material contained in, or derived from, this thesis.

Acknowledgements

This thesis would not have been possible without the blessings of Almighty Allah (God).

First and foremost, I wish to express my deepest gratitude to my supervisor Dr Paul Coats for his unlimited guidance, encouragement and supervision during the production of this work. During my years of study I encountered many obstacles, which would not have been possible to overcome without his support. I appreciate all his contribution of time, help and ideas.

I am also extremely thankful to my second supervisor Prof. Robin Plevin who provided me with a lot of advice during my PhD journey. He also assisted me in running some experiments and analysing some of the data in his lab. Therefore, I would like also to thank Robin lab group for their cooperation. I want to express my great appreciation to Ahlam Al-Obaidi for her time and help especially in the FACs work. Big thanks go to Yousif Khalaf and Gary who have given me a lot of advice and shared ideas with me.

I would also like to thank Mr Graeme MacKenzie for his friendship and for his help during my lab work, especially appreciated for his time in the epi-fluorescence microscopic work. Big thanks to Dr Rothwelle Tate for his advice related to the PCR work. A special thank goes to my colleagues in the CV lab: Molly Huq and Rachel Donaghy.

Furthermore, I would like to express the deepest gratitude to my parents for their endless support and encouragement. I would also like to thank my siblings for giving me the strength to finish my study.

I would like to thank all my friends both at university and those I have met in Glasgow and especially those in Saudi Arabia who may have been far from me physically but have never been far from me in spirit and for whose help and friendship I will be forever thankful.

Finally, I would like to express my highest gratitude to King AbdulAziz University, for their support by covering my tuition fees and living expenses, all pharmacology department staff and the Cultural Bureau, Embassy of Saudi Arabia. Special thanks to Ms Asma Omar for her supervision and help throughout the scholarship years.

Abstract:

Remodeling of the pulmonary arteries with proliferation and migration of pulmonary arterial smooth muscle cell (PASMC) is the hallmark of pulmonary hypertension, a proliferative disease with poor prognosis, which is exacerbated by hypoxic conditions. Hyperproliferation of PASMC underlies the failure of current therapy directed at vasodilation. Therefore, more direct anti-proliferative treatment, which targets the pulmonary vasculature is urgently sought. Signalling mechanisms that cause these cells to proliferate during hypoxia remain unclear. Recent studies highlight the role of mitochondrial alteration in PASMC of pulmonary hypertension, which is characterized by the glycolysis shift in metabolism and the increase in mitochondrial fragmentation that is also observed in cancer.

The work presented in this thesis describes the influence of the mitochondria (particularly mitochondrial fission) on cell proliferation and migration of PASMCs during a short period of hypoxia and identifying the mitochondrial-dependent signalling in response to platelet-derived growth factor (PDGF) and hypoxia. Aims were first to determine the appropriate model of hypoxia-induced cell proliferation among different degrees of hypoxia. The second aim was to investigate the role of the mitochondria in regulating cell proliferation and migration using the established hypoxic cell model (3% O₂).

PASMCs were isolated from Sprague-Dawley rats. Cells were maintained under hypoxia for 24 h and compared with normoxic cultures. Cell proliferation was measured by [³H]-thymidine incorporation assay. The effect of mitochondrial inhibition was studied using mitochondrial dynamin-related protein-1 (DRP1) inhibitor Mdivi-1 (10 μM). The signalling proteins and genes were measured by Western blot and real-time qPCR techniques, respectively. Mitochondrial functions were assessed by measuring ATP level, reactive oxygen species (ROS; superoxide and H₂O₂) production, and cellular apoptosis. Mitochondrial morphology was examined using an epi-fluorescence microscope.

During hypoxia, data show PDGF significantly enhances cell proliferation, HIF1α expression, and promotes mitochondrial dysfunction by decreasing mitochondrial

fission, ATP, ROS (H₂O₂ release) and cellular apoptosis, which all exhibit the proliferative/apoptotic-resistant phenotype of PASMCs compared to PDGF stimulated cells in normoxia. In comparison to hypoxic background cells (cells quiesced with 0.1% FCS and maintained in 3% O₂), PDGF caused a reduction in DRP1 expression and mitochondrial fragmentation, an increase in mTORC1 expression and a decrease in hypoxic genes (HIF1 α and FIH-1).

Interestingly, despite the reduced DRP1 expression and the presence of elongated mitochondria that were observed in the PDGF stimulated cells during hypoxia, inhibiting mitochondrial fission in these cells with Mdivi-1 slows cell proliferation and migration. It causes further reduction in HIF1 α and DRP1 expression, promotes hyper-fused mitochondria, upregulates FIH-1 gene expression, inhibits mTORC1 expression and recovers the mitochondrial function possibly via increasing mitochondrial COX-II and ATPase 6 gene expression. Taken together, these data suggest PDGF under hypoxic conditions increases mTORC1 which could control mitochondrial fission and hypoxic genes (HIF1 α and FIH-1) and significantly stimulates cell proliferation. However, DRP1 still seems essential in regulating cell proliferation.

Therefore, the effect of mTORC1 knockdown in PDGF stimulated cells during hypoxia was studied to confirm the role of mTORC1 in mediating cell proliferation. Knockdown of the mTORC1 gene caused a significant decrease in cell proliferation associated with an increase in DRP1, HIF1 α and FIH-1 gene expression. Finally, the inhibitory mechanism of Mdivi-1 following mTORC1 knockdown was studied. Mdivi-1 caused further reduction in cell proliferation, an increase in HIF1 α gene and a decrease in FIH-1 expression in cells treated with siRNA against mTORC1. The results also showed Mdivi-1 enhanced HIF1 α and FIH-1 expression and decreased mTORC1 expression in hypoxic background cells. Taken together, Mdivi-1 inhibits PDGF induced cell proliferation during hypoxia by increasing FIH-1, which is responsible for HIF1 α degradation, via its direct inhibitory effect on mTORC1.

Conferences and Publication

- 1. Poster communication.** Hypoxia has a role in regulating proliferation in pulmonary vascular cells and vascular remodeling. Presented at the Scottish cardiovascular forum, Glasgow, February 2017

- 2. Published abstract.** Burzangi A, Plevin R, Coats P. Mitochondria has a role in regulating Hypoxic dependent cell proliferation in pulmonary cells and vascular remodelling. Heart 2017 10.1136/heartjnl-2017-311433.14

- 3. Article.** Alamri A, Burzangi A, Coats P, Watson D. 2018. Untargeted metabolic profiling cell-based approach of pulmonary artery smooth muscle cells in response to high glucose and roles of antioxidants vitamin D and E (In press).

CONTENTS

Page

Acknowledgements	I
Abstract	II
Conferences and Publication	IV
Contents	V
List of Figures	XI
List of Tables	XVI
List of Abbreviations	XVII
Chapter 1. General Introduction	
Pulmonary Hypertension	2
1.1 Definition and Classification	2
1.2 Pulmonary arterial hypertension (PAH)	2
1.3 Structure of pulmonary vascular wall	5
1.3.1 Tunica Adventitia	5
1.3.2 Tunica Media	5
1.3.2.1 Phenotypic changes of resident PASMCs in response to hypoxia	7
1.3.3 Tunica Intima	8
1.4 Pathophysiology of Pulmonary Hypertension	8
1.4.1 Hypoxic Pulmonary Vasoconstriction	10
1.4.2 Pulmonary Vascular Remodeling	11
1.5 Current PAH therapeutics	16
1.5.1 Calcium channel blockers	18
1.5.2 Endothelin receptor antagonist	18
1.5.3 Phosphodiesterase-type 5 (PDE-5) inhibitor	19
1.5.4 Synthetic prostacyclin and its analogues	20
1.5.5 Developing future therapeutic target: Tyrosine kinase inhibitors	21
1.6 Hypoxia as an experimental model of pulmonary hypertension	21
1.7 Hypoxia-inducible factor 1 (HIF-1) signalling	22
1.8 Mitogen Activated Protein Kinases (MAPK) signalling	24
1.9 The mammalian target of rapamycin (mTOR) signalling pathway	28
1.10 The Role of Mitochondria in Cardiovascular disease	31
1.11 Mitochondrial dysfunction and PAH	33
1.12 Mitochondrial Pharmacology	35
1.13 Aims and Hypothesis	37

Chapter 2. General Methods

2.1	Materials	39
2.2	Cell harvest and culture	41
2.2.1	Cell count and subculture	42
2.3	Immunohistochemical (IHC) confirmation of the isolated PSMCs	42
2.4	Experimental set-up: cells exposure to hypoxia	43
2.5	Western Blot	44
2.5.1	Preparation of whole cell extracts and stimulation	44
2.5.2	SDS-Polyacrylamide Gel Electrophoresis (SDS-PAGE)	45
2.5.3	Electrophoretic transfer of proteins onto a nitrocellulose membrane	45
2.5.4	Immunological detection of protein	46
2.5.5	Re-probing and stripping of nitrocellulose membranes	47
2.5.6	Scanning densitometry	47
2.6	Amido black protein assay	47
2.7	Cell proliferation [³H]-thymidine incorporation assay	48
2.8	Cell migration assay	49
2.9	Polymerase chain reaction (PCR) amplification	49
2.9.1	RNA isolation for PCR	49
2.9.2	cDNA preparation	50
2.9.3	Quantitative qRT-PCR amplification	51
2.9.4	Relative quantification [$\Delta\Delta C_t$] method for real time PCR	51
2.9.5	PCR primers for SYBR green based real time assays	51
2.10	Fluorescence-activating cell sorting (FACS) analysis	54
2.11	Reactive oxygen species (ROS)	54
2.12	Cellular ATP assay	55
2.13	Cell apoptosis assay	55
2.14	Generation of mito-depleted PSMCs	56
2.15	siRNA transfection of mTORC1 in PSMCs	56
2.16	Immuno-fluorescence staining of PCNA	57
2.17	Identification of Mitochondrial morphology	57
2.18	Data and Statistical Analysis	58

Chapter 3. The Role of Hypoxia in Regulating Pulmonary Artery Smooth Muscle Cell Proliferation

3.1	Introduction	60
3.2	The effect of Hypoxia on PSMCs in PAH	61

3.3	Chapter Aims	65
3.4	Results	66
3.5	Isolation of Smooth Muscle Cell, Culture and Characterisation	66
3.6	Effect of Foetal Calf Serum (FCS) on PASMC Proliferation	69
3.7	Effect of Acute Hypoxia (10% O₂) on PASMC Proliferation	71
3.8	Effect of Acute Hypoxia (10% O₂) on ERK1/2 phosphorylation	73
3.9	Effect of Acute Hypoxia (5% O₂) on PASMC Proliferation	77
3.10	Effect of Acute Hypoxia (5% O₂) on ERK1/2 phosphorylation	79
3.11	Effect of Acute Hypoxia (3% O₂) on PASMC Proliferation	81
3.12	The effect of Hypoxia (3% O₂) on Proliferative Marker Genes	83
3.13	Hypoxic Marker Genes	87
3.14	Effect of Hypoxia (3% O₂) on MAPK phosphorylation	90
3.15	Effect of Hypoxia (3% O₂) on PI3K/mTOR signalling pathway	94
3.16	Discussion	96
3.17	The primary detaches of the pulmonary artery	96
3.18	Effects of Serum concentration on cell Proliferation	97
3.19	The effect of Acute Hypoxia on PASMC Proliferation	97
3.20	The Effect of Hypoxia (10% and 5% O₂) on ERK1/2 phosphorylation	98
3.21	The Effect of Hypoxia (3% O₂) on PASMC Proliferation	99
3.22	The Effect of Hypoxia (3% O₂) on p38 MAPK phosphorylation	102
3.23	The effect of Hypoxia (3% O₂) on mTOR signalling pathway	102
3.24	Main Findings	103

Chapter 4. The Role of Mitochondria in Regulating PASMC Proliferation and Migration

4.1	Introduction	105
4.2	Mitochondria and PASMC proliferation	106
4.3	Mitochondrial fission protein DRP1 as a potential therapeutic target in pulmonary hypertension	109
4.4	Chapter Aims	110
4.5	Results	111
4.6	The combined effects of Hypoxia and PDGF on cell Proliferation	111
4.7	Effect of Mdivi-1 on Hypoxic-PDGF induced cell Proliferation	114
4.8	Effect of Mdivi-1 on Hypoxic-FCS induced cell Proliferation	116
4.9	Effect of Hypoxia on PDGF induced PASMC Migration	118
4.10	The effect of Mdivi-1 on PDGF induced PASMC Migration	120

4.11	Effect of Mdivi-1 on cell cycle progression	125
4.12	The effect of Mdivi-1 on cyclin D1 protein expression	127
4.13	The effect of Mdivi-1 on cell regulatory gene expression	129
4.14	Mitochondrial functions	134
4.14.1	Effect of Mdivi-1 on Reactive Oxygen Species (ROS)	134
4.14.2	Effect of Mdivi-1 on ATP production	140
4.14.3	The effect of Mdivi-1 on mitochondrial ATPase 6 gene expression	142
4.14.4	Effect of Mdivi-1 on cytochrome c protein expression	144
4.14.5	Effect of Mdivi-1 on Cellular Apoptosis (Caspase 3/7 release)	146
4.15	The effect of Mdivi-1 on mitochondrial marker gene expression	148
4.15.1	The effect of Mdivi-1 on DRP1 gene expression	148
4.15.2	The effect of Mdivi-1 on TFAM gene expression	150
4.15.3	The effect of Mdivi-1 on COX-II gene expression	153
4.16	The effect of Mdivi-1 on Mitochondrial Morphology	156
4.17	The effect of Mdivi-1 on mitochondrial morphology and localization in FCS stimulated cells during hypoxia	159
4.18	Generation of Mitochondrial-depleted cells (Rho cells)	162
4.19	The effect of PDGF on Mito-depleted Rho cell Proliferation	164
4.20	Discussion	166
4.21	The study of PDGF signalling in pulmonary hypertension	166
4.22	Effect of mitochondrial inhibition on PASMC proliferation	168
4.23	Mitochondrial DRP1 role in cell proliferation during normoxia	169
4.24	Mitochondrial DRP1 role in cell proliferation during hypoxia	172
4.25	The effect of Mdivi-1 on cell cycle progression	175
4.26	The effect of Mdivi-1 on PASMC Migration	179
4.27	Effect of Mdivi-1 on Cell apoptosis	180
4.28	Summary of Results	180

Chapter 5. The Mechanism of Mdivi-1-Dependent Inhibition of PASMC Proliferation and Migration under Hypoxia

5.1	Introduction	183
5.2	Chapter Aims	184
5.3	Results	185
5.4	The effect of PDGF on HIF-1α gene expression	185
5.5	The effect of PDGF receptor antagonist on HIF-1α protein expression in hypoxic-PDGF stimulated cells	187

5.6	The effect of Mdivi-1 on HIF-1α gene expression in PDGF stimulated cells during hypoxia	189
5.7	The effect of Mdivi-1 on FIH-1 gene expression in PDGF stimulated cells during hypoxia	192
5.8	Effect of Mdivi-1 on MAPK signalling pathway in PDGF stimulated cells during hypoxia	195
5.8.1	Effect of Mdivi-1 on ERK1/2 phosphorylation	195
5.8.2	Effect of Mdivi-1 on p38 MAPK phosphorylation	197
5.8.3	Effect of Mdivi-1 on JNK phosphorylation	199
5.9	Effect of Mdivi-1 on PI3K/mTOR signalling pathway in PDGF stimulated cells during hypoxia	201
5.9.1	The effect of Mdivi-1 on PI3K gene expression	201
5.9.2	The effect of Mdivi-1 on PTEN gene expression	204
5.9.3	The effect of Mdivi-1 on PDK-1 phosphorylation	206
5.9.4	The effect of Mdivi-1 on AKT gene expression	208
5.9.5	The effect of Mdivi-1 on mTORC1 gene expression	211
5.9.6	The effect of Mdivi-1 on 4EBP1 gene expression	214
5.9.7	The effect of Mdivi-1 on P70s6k gene expression	216
5.10	The effect of mTORC1 knockdown alone and with Mdivi-1 on PDGF-induced cell proliferation during hypoxia	218
5.10.1	The transfection efficacy of mTORC1 siRNA	218
5.10.2	Effect of mTORC1 knockdown alone and with Mdivi-1 on cell Proliferation	220
5.10.3	The effect of mTORC1 knockdown alone and with Mdivi-1 on mitochondrial DRP1 gene expression	222
5.10.4	The effect of mTORC1 knockdown alone and with Mdivi-1 on HIF-1α gene expression	224
5.10.5	The effect of mTORC1 knockdown alone and with Mdivi-1 on FIH-1 gene expression	226
5.11	Discussion	228
5.12	The involvement of HIF-1α gene expression in mitochondrial-dependent proliferation of PSMCs	228
5.13	MAPK phosphorylation following mitochondrial inhibition	229
5.14	The participation of the mitochondrial fission protein DRP1 in the mTOR signalling pathway	229
5.15	The effect of Mdivi-1 on PSMC Migration	232
5.16	The mechanism of Mdivi-1 on hypoxic genes	234

5.17	Summary of Results	236
Chapter 6. General Discussion		
6.1	General Discussion	238
6.2	Cell signalling in a Hypoxic cell Model	238
6.3	DRP1 Role in cell Proliferation and Migration during Hypoxia	242
6.4	Study Limitations and Future Work	245
6.5	Conclusion	246
	References	247-276

List of Figures

	Page
<u>Chapter 1. Introduction</u>	
Figure 1.1	Phenotypic changes in VSMC 7
Figure 1.2	Pathogenesis of PAH 9
Figure 1.3	Histological changes of pulmonary arteries observed in patients with PAH 12
Figure 1.4	Pulmonary Vascular Arteriogram 13
Figure 1.5	Schematic representation of the pathological remodeling processes of pulmonary artery 15
Figure 1.6	Major signalling pathways approved for PAH therapy 17
Figure 1.7	Oxygen dependent regulation of HIF-1 α 23
Figure 1.8	Mitogen Activated Protein Kinases (MAPK) signalling pathways 25
Figure 1.9	The modulation of MEK1/2/ERK1/2 phosphorylation 27
Figure 1.10	PI3K/AKT/mTORC1 signalling pathway 30
<u>Chapter 2. Materials and Methods</u>	
Figure 2.1	Dissected Proximal Pulmonary Artery from a Sprague-Dawley rat 41
Figure 2.2	Demonstration of mitochondrial length quantification within a cell using Image J 58
<u>Chapter 3. The Role of Hypoxia in Regulating Pulmonary Artery Smooth Muscle Cell Proliferation</u>	
Figure 3.1	Signalling mechanisms involved in hypoxia-dependent activation of different transcription factors in PASMCs to mediate pulmonary hypertension 63
Figure 3.2	Rat Pulmonary Artery Smooth Muscle cells (PASMCs) observed under phase contrast microscope (x10) 67
Figure 3.3	Immunofluorescence for α -actin and myosin heavy chain (MHC) in PASMCs 68
Figure 3.4	Effects of incremental serum concentrations on [³ H]-thymidine incorporation in PASMCs 70
Figure 3.5	The effect of hypoxia (10% O ₂) on serum-stimulated [³ H]-thymidine incorporation in PASMCs 72
Figure 3.6	Time course of serum-induced ERK activation in PASMCs 74

Figure 3.7	The combined effect of incremental serum concentrations and hypoxia (10% O ₂) on ERK1/2 phosphorylation in PSMCs	76
Figure 3.8	The effect of hypoxia (5% O ₂) on serum-stimulated [³ H]-thymidine incorporation in PSMCs	78
Figure 3.9	The effect of hypoxia (5% O ₂) on ERK1/2 phosphorylation	80
Figure 3.10	The combined effect of incremental serum concentrations and hypoxia (3% O ₂) on [³ H]-thymidine incorporation in PSMCs	82
Figure 3.11	The effect of hypoxia (3% O ₂) on the proliferative marker genes; PCNA, ERK1 and cyclin D1 expression in serum-stimulated PSMCs	84
Figure 3.12	The effect of hypoxia (3% O ₂) on PCNA expression in serum-stimulated PSMCs	85
Figure 3.13	The effect of hypoxia (3% O ₂) on Cdkn2a gene expression in serum-stimulated PSMCs	86
Figure 3.14	Expression of HIF-1 α and HIF-2 α genes in serum-stimulated PSMCs during hypoxia (3% O ₂)	88
Figure 3.15	The effect of hypoxia (3% O ₂) on arginase-1 expression in serum-stimulated PSMCs	89
Figure 3.16	The effect of hypoxia (3% O ₂) on serum-induced ERK1/2 phosphorylation in PSMCs	91
Figure 3.17	The effect of hypoxia (3% O ₂) on serum stimulation of p38 MAPK phosphorylation in PSMCs	92
Figure 3.18	The effect of hypoxia (3% O ₂) on JNK phosphorylation in PSMCs	93
Figure 3.19	The effect of hypoxia (3% O ₂) on PI3K/AKT/mTORC1 cascade in serum-stimulated PSMCs	95

Chapter 4. The Role of Mitochondria in Regulating Pulmonary Artery Smooth

Muscle Cell Proliferation and Migration

Figure 4.1	The mitochondrial effect on PSMC proliferation/apoptosis balance in PAH	108
Figure 4.2	Mitochondrial fusion and fission processes and their major mediators	110
Figure 4.3	The effect of PDGF on pulmonary artery smooth muscle cell proliferation	112
Figure 4.4	The effect of hypoxia on PDGF induced cell proliferation	113
Figure 4.5	The effect of Mdivi-1 on PDGF induced PSMC proliferation	115
Figure 4.6	The effect of Mdivi-1 on 10% FCS induced PSMC proliferation	117

Figure 4.7	The effect of hypoxia on PDGF stimulated PASMC migration	119
Figure 4.8	The effect of Mdivi-1 on PDGF induced PASMC migration	122
Figure 4.9	The effect of Mdivi-1 on PDGF induced PASMC migration during hypoxia	124
Figure 4.10	The effect of Mdivi-1 on cell cycle progression in stimulated cells	126
Figure 4.11	The effect of Mdivi-1 on cyclin D1 protein expression in PDGF stimulation during hypoxia	128
Figure 4.12	The effect of Mdivi-1 on cyclin D1 gene expression in background hypoxic cells	130
Figure 4.13	The effect of Mdivi-1 on cyclin D1 gene expression in PDGF stimulated cells during hypoxia	131
Figure 4.14	The effect of Mdivi-1 on P53 gene expression in PDGF stimulated cells during hypoxia	133
Figure 4.15	Reactive oxygen species (ROS) production (superoxide) in pulmonary artery smooth muscle cells	135
Figure 4.16	The effect of Mdivi-1 on ROS production (superoxide) in PDGF stimulated cells during hypoxia	136
Figure 4.17	H ₂ O ₂ levels in pulmonary artery smooth muscle cells	138
Figure 4.18	The effect of Mdivi-1 on H ₂ O ₂ levels in PDGF stimulated cells during hypoxia	139
Figure 4.19	The effect of Mdivi-1 on mitochondrial ATP production in PDGF stimulated cells during hypoxia	141
Figure 4.20	The effect of Mdivi-1 on mitochondrial ATPase 6 gene expression in PDGF stimulated cells during hypoxia	143
Figure 4.21	The effect Mdivi-1 on cytochrome c protein expression in PDGF stimulation during hypoxia	145
Figure 4.22	The effect of Mdivi-1 on apoptotic activity in PDGF stimulated cells during hypoxia	147
Figure 4.23	The effect of Mdivi-1 on DRP1 gene expression in PDGF stimulated cells during hypoxia	149
Figure 4.24	The effect of Mdivi-1 on TFAM expression in PDGF stimulated cells	151
Figure 4.25	Data extracted from Figure 4.24 A and B to highlight the effect of hypoxia on mitochondrial TFAM gene expression in (A) quiescent cells and in (B) PDGF stimulated cells	152
Figure 4.26	The effect of Mdivi-1 on mitochondrial COX-II gene expression in quiescent hypoxic cells	154

Figure 4.27	The effect of Mdivi-1 on mitochondrial COX-II gene expression in PDGF stimulated cells during hypoxia 155	
Figure 4.28	Representative images show mitochondrial morphology in the quiescent cells and after stimulating the cells with PDGF following Mdivi-1 treatment during normoxia and hypoxia	157
Figure 4.29	The mitochondrial length in the quiescent cells, PDGF stimulated cells and stimulated cells following Mdivi-1 treatment during normoxia and hypoxia 158	
Figure 4.30	Representative images show mitochondrial morphology in 10% serum stimulated cells and stimulated cells with Mdivi-1 during normoxia and hypoxia	160
Figure 4.31	The mitochondrial length in the quiescent cells, 10% serum stimulated cells and stimulated cells with Mdivi-1 during normoxia and hypoxia 161	
Figure 4.32	The loss of mitochondrial marker genes in the mitochondrial-depleted Rho cells	163
Figure 4.33	The effect of PDGF stimulation on the proliferative response of mitochondrial-depleted Rho cells under normoxic and hypoxic conditions	165

Chapter 5. The Mechanism of Mdivi-1-Dependent Inhibition of PASMC

Proliferation and Migration under Hypoxia

Figure 5.1	The effect of PDGF on HIF-1 α gene expression during hypoxia	186
Figure 5.2	The effect of PDGF receptor antagonist on HIF-1 α protein expression in PDGF stimulated cells during hypoxia	188
Figure 5.3	The effect of Mdivi-1 on HIF-1 α expression in cells stimulated with PDGF	190
Figure 5.4	The effect of Mdivi-1 on HIF-1 α gene expression in quiescent cells and PDGF stimulated cells during hypoxia	191
Figure 5.5	The effect of Mdivi-1 on FIH-1 gene expression in hypoxic cells	193
Figure 5.6	The effect of Mdivi-1 on FIH-1 gene expression in PDGF stimulated cells during hypoxia	194
Figure 5.7	The effect Mdivi-1 on ERK1/2 phosphorylation in PDGF stimulation during hypoxia	196
Figure 5.8	The effect Mdivi-1 on p38 MAPK phosphorylation in PDGF stimulation during hypoxia	198

Figure 5.9	The effect Mdivi-1 on JNK phosphorylation in PDGF stimulation during hypoxia	200
Figure 5.10	The effect of Mdivi-1 on PI3K expression in quiescent hypoxic cells	202
Figure 5.11	The effect of Mdivi-1 on PI3K gene expression in PDGF stimulated cells during hypoxia	203
Figure 5.12	The effect of Mdivi-1 on PTEN gene expression in PDGF stimulated cells during hypoxia	205
Figure 5.13	The effect Mdivi-1 on PDK1 phosphorylation in PDGF stimulation during hypoxia	207
Figure 5.14	The effect of Mdivi-1 on AKT expression in quiescent hypoxic cells	209
Figure 5.15	The effect of Mdivi-1 on AKT gene expression in PDGF stimulated cells during hypoxia	210
Figure 5.16	The effect of Mdivi-1 on mTORC1 gene expression in quiescent hypoxic cells	212
Figure 5.17	The effect of Mdivi-1 on mTORC1 gene expression in PDGF stimulated cells during hypoxia	213
Figure 5.18	The effect of Mdivi-1 on 4EPB1 gene expression in PDGF stimulated cells during hypoxia	215
Figure 5.19	The effect of Mdivi-1 on P70s6K gene expression in PDGF stimulated cells during hypoxia	217
Figure 5.20	The transfection efficacy of siRNA for mTORC1 in PSMCs	219
Figure 5.21	The effect of siRNA mTORC1 alone and with Mdivi-1 on PDGF-induced cell proliferation during hypoxia	221
Figure 5.22	The effect of siRNA mTORC1 alone and with Mdivi-1 on DRP1 gene expression upon PDGF stimulated cells during hypoxia	223
Figure 5.23	The effect of siRNA mTORC1 alone and with Mdivi-1 on HIF-1 α gene expression upon PDGF stimulated cells during hypoxia	225
Figure 5.24	The effect of siRNA mTORC1 alone and with Mdivi-1 on FIH-1 gene expression upon PDGF stimulated cells during hypoxia	227

Chapter 6. General Discussion

Figure 6.1	Schematic diagram summarises the main findings in the established hypoxia cell model	241
Figure 6.2	The mitochondrial role in Hypoxic-PDGF induced cell proliferation (Schematic summary)	244

List of Tables

	Page
<u>Chapter 1. Introduction.</u>	
Table 1.1 WHO classification of pulmonary hypertension	4
Table 1.2 NYHA/WHO classification of functional status of patients with pulmonary hypertension	5
<u>Chapter 2. Material and Methods.</u>	
Table 2.1 Primary antibodies for Western blot analysis	46
Table 2.2 Primers for real-time PCR analysis	53

List of Abbreviations (alphabetical order)

Adenosine triphosphate (ATP)
Analysis of Variance (ANOVA)
Apoptosis-inducing factor (AIF)
Basic fibroblast growth factor (bFGF)
Bone morphogenetic protein (BMP)
Break point cluster/Abelson (Bcr/ABL)
C-jun amino-terminal kinases/stress-activated protein kinase (JNK/SAPK)
CREB-binding protein (CBP)
Cyclic adenosine monophosphate (cAMP)
Cyclic AMP response element binding protein (CREB)
Cyclic guanosine monophosphate (cGMP)
Cyclin-Dependent Kinase (CDK)
Cyclin-dependent kinase Inhibitor 2A (Cdkn2A)
Cytochrome c oxidase subunit 2 (COX-II)
Deoxyribonucleic Acid (DNA)
Diamidino-2-Phenylindole (DAPI)
Dichloroacetate (DCA)
Dichlorofluorescein (DCF)
Dichlorofluorescein diacetate (DCFH-DA)
Dihydroethidium (DHE)
Dual leucine zipper kinase (DLK)
Dynamin-related protein-1 (DRP1)
Endoplasmic reticulum (ER)
Endothelial cells (ECs)
Endothelial nitric oxide synthase (eNOS)
Endothelin converting enzyme-1 (ECE-1)
Endothelin-1 (ET-1)
Epidermal growth factor (EGF)
Eukaryotic initiation factor 4E (eIF4E)
Extracellular signal- regulated kinases 1/2 (ERK1/2)
Factor-inhibiting HIF-1 (FIH-1)
Fatty acid oxidation (FAO)

Fibroblast growth factor-2 (FGF2)
Fluorescence-activating cell sorting (FACS)
Foetal calf serum (FCS)
Glucose transporter (GLUT)
Glyceraldehyde 3-Phosphate Dehydrogenase (GAPDH)
GTPase activating protein (GAP)
Guanine nucleotide exchange factor (GEF)
Hexokinase 2 (HK2)
Human umbilical vein endothelial cells (HUVECs)
Hypoxia inducible factor 1 (HIF-1)
Hypoxia response element (HRE)
Hypoxic pulmonary vasoconstriction (HPV)
Initiation factor 4E binding protein 1 (4EBP1)
Insulin-like growth factor-1 (IGF-1)
I κ B kinase- β (IKK β)
Lactate dehydrogenase A (LDHA)
Manganese superoxide dismutase (MnSOD)
Matrix metalloproteinase-2 (MMP-2)
Mean pulmonary arterial pressure (mPAP)
Messenger ribonucleic acid (mRNA)
Mitochondria transition pore (MTP)
Mitochondrial Division-Inhibitor 1 (Mdivi-1)
Mitochondrial fission 1 (Fis1)
Mitochondrial fission factor (Mff)
Mitochondrial membrane potential ($\Delta\Psi$ m)
Mitochondrial outer membrane permeabilization (MOMP)
Mitochondrial transcription factor A (TFAM)
Mitofusin 1 (MFN1)
Mitofusin 2 (MFN2)
Mitogen-activated protein kinase (MAPK)
Myosin heavy chain (MHC)
National Institute of Health (NIH)
New York Heart Association (NYHA)
Nitric oxide (NO)

Nuclear factor of activated T cell (NFAT)
Optic atrophy-1 (OPA1)
Oxidative phosphorylation (OXPHOS)
P70 ribosomal protein S6 kinase1 (S6K1)
Phosphatase and Tensin Homolog Deleted on Chromosome 10 (PTEN)
Phosphate Buffered Saline (PBS)
Phosphofructokinase 2 (PFKFB2)
Phosphoinositide 3-kinase (PI3K)
Phosphoinositide-dependent protein kinase 1 (PDK1)
Phospholipase C (PLC)
Platelet-derived growth factor (PDGF)
Polymerase chain reaction (PCR)
Proliferating Cell Nuclear Antigen (PCNA)
Prolyl hydroxylase domain (PHD)
Prostacyclin (PGI₂)
Protein kinase C (PKC)
Protein tyrosine phosphatase (PTP)
Pulmonary arterial hypertension (PAH)
Pulmonary arterial pressure (PAP)
Pulmonary artery endothelial cells (PAECs)
Pulmonary artery smooth muscle cells (PASMCs)
Pulmonary vascular resistance (PVR)
Pulmonary wedge pressure (PWP)
Pyruvate dehydrogenase (PDH)
Ras homolog enriched in brain (Rheb)
Reactive oxygen species (ROS)
Receptor tyrosine kinase (RTK)
Relative fluorescent units (RFU)
Relative light units (RLU)
Right ventricular hypertrophy (RVH)
Small interfering RNA (siRNA)
Smooth muscle cell (SMC)
Sodium dodecyl sulphate (SDS)
Superoxide dismutase-2 (SOD2)

The mammalian target of rapamycin complex1 (mTORC1)

Transforming growth factor- β (TGF- β)

Tuberous sclerosis complex (TSC1/2)

Tumour necrosis factor- α (TNF- α)

Ubiquitin C (UBC)

Ultraviolet (UV)

Uncoupling protein 2 (Ucp2)

Vascular endothelial growth factor (VEGF)

Vascular smooth muscle cell (VSMC)

Von Hippel Lindau (VHL)

Wild type (WT)

Chapter 1

General Introduction

Pulmonary Hypertension

1.1 Definition and Classification

Pulmonary hypertension is clinically defined as occurring when the mean pulmonary arterial pressure (mPAP) is greater than 25 mmHg at rest or higher than 30 mmHg during exercise (Badesch et al., 2009). This is almost twice as high as the normal range (14-20 mmHg) of the mean PAP that is found in a normal person. In all randomised controlled trials the measurement of this value is the most common way to identify patients with pulmonary arterial hypertension (PAH) (Humbert et al., 2013). An increase in vascular resistance and cardiac pressure, which result from pulmonary arterioles narrowing, are considered primary features of pulmonary hypertension. The narrowing of the pulmonary artery is due to excessive proliferation of pulmonary artery smooth muscle cells (Rabinovitch, 2008). An increase in the pulmonary arterial pressure leads to right ventricular hypertrophy, which eventually causes right heart failure and death.

The Fifth World Symposium (2013) on pulmonary hypertension categorized pulmonary hypertension into five clinical classifications (Table 1.1). Each category shares common pathophysiological features. However, the reason for classifying the diseases into categories was to identify the aetiological factors associated with pulmonary hypertension in each situation and to improve the therapeutic options.

1.2 Pulmonary Arterial Hypertension (PAH)

Group 1, pulmonary arterial hypertension (PAH), comprises a life-threatening form of the disease, which is characterized by pulmonary vascular remodeling and a subsequent increase in pulmonary vascular resistance (Archer et al., 2010). The measurement of pulmonary wedge pressure (PWP), using an inserted pulmonary catheter with an inflated balloon into a small pulmonary arterial branch, is considered an important tool for differentiating between groups. Pulmonary arterial hypertension (PAH) is recognized with a pulmonary wedge pressure of < 15 mmHg which is classified as pre-capillary pulmonary hypertension (Simonneau et al., 2009, Galie et al., 2009a). Right cardiac catheterisation is used to confirm the diagnosis of pulmonary hypertension. The most common symptoms of PAH are

chest pain, shortness of breath, fatigue and syncope. However, these symptoms do not frequently appear at an early stage and they could occur at a later stage of the disease. Studies have claimed that it can take up to two years to detect and diagnose the disease (Humbert et al., 2006, Badesch et al., 2009). This means that PAH diagnosis often occurs when the disease has developed and become extremely severe. Moreover, patients with pulmonary hypertension are also classified into four groups depending on the severity of their manifestations of the disease and their ability to carry out physical tasks using the New York Heart Association (NYHA) scale on heart failure (Table 1.2). Class I represents the earliest stage of PAH, whereas Class IV includes patients with right heart failure. The purpose of this classification is to identify the severity of pulmonary hypertension and the impact on the heart. This classification can help in predicting the patient's life expectancy. For example, the survival time of patients with Class III is 2.5 years, whereas it decreases significantly to 6 months in patients with Class IV (D'Alonzo et al., 1991). The incidence of the disease in the United Kingdom and Northern Ireland is approximately 1.1 cases per million annually and prevalence of 6.6 cases per million in 2009 (Ling et al., 2012). In Scotland it accounts for about 7.1 cases per million annually whereas the prevalence is predicted to be 26 cases per million in 2005 (Peacock et al., 2007). However, the worldwide prevalence of the disease is difficult to estimate because of the lack of accurate diagnosis and the accessibility to hospitalization data is restricted in many regions (Archer et al., 2010). Moreover, it has been reported that females are more likely to develop PAH compared to males with a ratio of 4.3: 1 (Walker et al., 2006).

<p>1 Pulmonary arterial hypertension</p> <p>1.1 Idiopathic</p> <p>1.2 Heritable</p> <p> 1.2.1 Bone morphogenetic protein receptor type 2 (BMP2)</p> <p> 1.2.2 Activin receptor-like kinase 1 (ALK1), endoglin (ENG), SMAD family member 9 (SMAD9), caveolin 1 (CAV1), potassium two pore domain channel subfamily K member 3 (KCNK3)</p> <p> 1.2.3 Unknown</p> <p>1.3 Drug and toxin-induced</p> <p>1.4 Associated with</p> <p> 1.4.1 Connective tissue disease</p> <p> 1.4.2 Portal hypertension</p> <p> 1.4.3 HIV infection</p> <p> 1.4.4 Congenital heart diseases</p> <p> 1.4.5 Schistosomiasis</p> <p>1' Pulmonary veno-occlusive disease and/or pulmonary capillary hemangiomatosis</p> <p>1'' Persistent pulmonary hypertension of the newborn (PPHN)</p>
<p>1 Pulmonary hypertension due to left heart disease</p> <p>2.1 Left ventricular systolic dysfunction</p> <p>2.2 left ventricular diastolic dysfunction</p> <p>2.3 Valvular disease</p> <p>2.4 Congenital/acquired left heart inflow/outflow tract obstruction and congenital cardiomyopathies</p>
<p>2 Pulmonary hypertension due to lung diseases and /or hypoxia</p> <p>3.1 chronic obstructive pulmonary disease (COPD)</p> <p>3.2 Interstitial lung disease</p> <p>3.3 Other pulmonary disease with mixed restrictive and obstructive patterns</p> <p>3.4 Sleep-related breathing behaviour</p> <p>3.5 Alveolar hypoventilation disorders</p> <p>3.6 Chronic exposure to high altitudes</p> <p>3.7 Developmental lung disease</p>
<p>4 Chronic thromboembolic pulmonary hypertension (CTEPH)</p>
<p>5 Pulmonary hypertension with unclear multifactorial mechanisms</p> <p>5.1 Hematologic disorders: chronic haemolytic anaemia, splenectomy</p> <p>5.2 Systemic disorders: sarcoidosis, pulmonary histiocytosis</p> <p>5.3 Metabolic disorders: glycogen storage disease, Gaucher disease, thyroid disorders</p> <p>5.4 Others: tumoral obstruction, fibrosing mediastinitis, chronic renal failure</p>

Table 1.1 WHO classification of pulmonary hypertension. Adapted from (Simonneau et al., 2013).

Class	Description
I	Ordinary physical activity does not cause any symptoms/ patients without limitation of physical activity
II	Symptoms are associated with ordinary physical activity/ patients have mild limitation of physical activity
III	Symptoms with less than ordinary activity/ patients have marked limitation of physical activity
IV	Symptoms exist at rest and with any activity/ patients are unable to perform any physical activity without symptoms

Table 1.2 NYHA/WHO classification of the functional status of patients with pulmonary hypertension. Adapted from (McLaughlin and McGoon, 2006).

1.3 Structure of pulmonary vascular wall

The pulmonary vascular wall consists of three main layers: the tunica adventitia, the tunica media and the tunica intima.

1.3.1 Tunica Adventitia

The outermost layer is known as the tunica adventitia, which contains adventitial fibroblasts, elastin and collagen (Stenmark et al., 2006a). The importance of the cellular components within the adventitia is to support the structural integrity of the vascular wall.

1.3.2 Tunica Media

The thickest layer of the pulmonary vascular wall is termed as the tunica media. It includes pulmonary artery smooth muscle cells (PASMCs) organized in a matrix of elastin fibers and collagen, which provide their strength. The main function of the smooth muscle cells is vessel contraction and they have a major role in maintaining the vascular tone and the blood pressure (Frid et al., 1997). These cells can present

different phenotypes including their shape, their proliferative and migratory rates and the expression of various marker proteins, which all depend on their functions (Bochaton-Piallat and Gabbiani, 2005). For example, spindle shaped smooth muscle cells with a low rate of proliferation and migration refer to the contractile (quiescent) phenotype, whereas the other smooth muscle cells with a rhomboid cellular shape and higher proliferative and migratory rates characterise the synthetic phenotype, which is present during response to injury (Figure 1.1) (Milewicz et al., 2010). The mechanisms contributing to the phenotypic conversion of smooth muscle cell (SMC) include signalling pathways/mediators such as platelet-derived growth factor (PDGF), transforming growth factor- β (TGF- β), tumour necrosis factor- α (TNF- α) and angiotensin II (Rensen et al., 2007). The isolated PASMCs from patients with pulmonary arterial hypertension show a remarkable resistance to the proteins which induce apoptosis such as bone morphogenetic proteins such as bone morphogenetic protein 2 (BMP2) and bone morphogenetic protein 7 (BMP7), and exhibits more proliferative and migratory phenotypes. This suggests the impaired apoptosis and the increased proliferation/ migration of PASMC can concomitantly mediate thickening of the pulmonary artery. Consequently, this results in vascular lumen occlusion and increased pulmonary vascular resistance (Voelkel and Tuder, 1997, Savai et al., 2014).

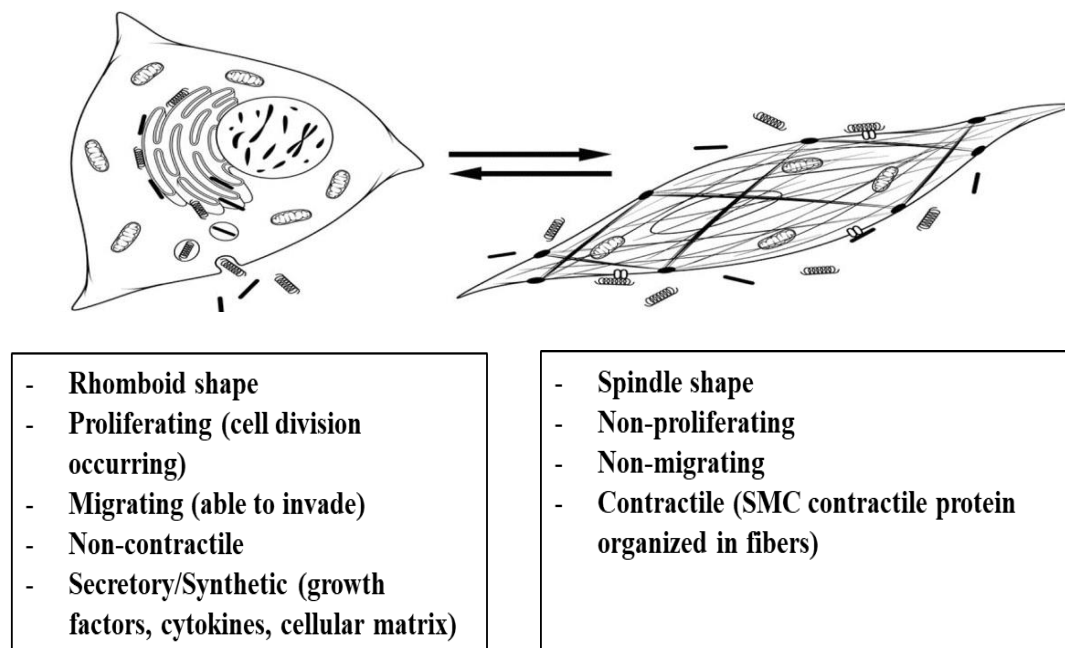


Figure 1.1 Phenotypic changes in VSMC. The right side represents a differentiated/contractile smooth muscle cell phenotype, which has numerous contractile fibres. The left side shows a dedifferentiated/synthetic cell phenotype, which is able to proliferate, migrate and modify the extracellular matrix to repair the vessel wall in response to vascular injury. Adapted from (Milewicz et al., 2010).

1.3.2.1 Phenotypic changes of resident PASMCs in response to hypoxia

Damage to the endothelial cell basement membrane is considered as one of the histological changes in the development of pulmonary hypertension (Stenmark et al., 1999). This damage facilitates the access of mitogens and growth factors, either from the serum or from adjacent endothelial cells, to the underlying smooth muscle cells and matrix, thus permitting a change in PASMC behaviour and function (Cowan et al., 2000). Pulmonary artery endothelial cells (PAECs) can directly affect the phenotype of PASMCs during PAH pathogenesis. They are capable of secreting growth factors that stimulate PASMC proliferation, such as PDGF and fibroblast growth factor-2 (FGF2), or they fail to produce factors that inhibit PASMC proliferation, such as apelin (Crosswhite and Sun, 2014). Moreover, inflammatory cells contribute to SMC hypertrophy and neointimal formation in PAH and can also produce proteins such as MMP-2, which degrade the extracellular matrix and release matrix-bound growth factors, such as basic

fibroblast growth factor (bFGF), which promote smooth muscle cell proliferation (Thompson and Rabinovitch, 1996).

1.3.3 Tunica Intima

The thin inner layer of the vascular wall is the tunica intima, which includes the endothelial cells (ECs) arranged as a monolayer on a connective tissue matrix. Endothelial cells are in direct contact with the blood in the vessel and regulate the lumen environment. They have the ability to modulate overall vascular tone by the release of several vasodilators and vasoactive substances (Aaronson et al., 2002). All cellular components within the pulmonary vascular wall act differently in modulating the vascular response to injury or stress.

1.4 Pathophysiology of Pulmonary Hypertension

Abnormal changes in the pulmonary arterioles phenotype leads to pulmonary vascular dysfunction, an increase in cardiac pressure and eventually right heart failure, which are all considered pathophysiological risk factors for the development of pulmonary hypertension. The presence of predisposing genetic factors, vascular stress, and environmental or biological mediators of vascular injury have a strong impact on cell-signalling pathway dysregulation, which ultimately affects the function and the structure of the pulmonary arterioles (Figure 1.2). For example, hypoxia promotes higher vasoconstriction and causes apparent defects in Ca^{2+} and K^+ balance within the PASMC, which lead to a reduction in the lumen size (Wang et al., 2005, Yuan et al., 1998). Another study on cultured PASMCs isolated from bovine showed vasoconstriction when the cells were exposed to hypoxia (Murray et al., 1990). The alteration of oxygen levels is assumed to be controlled by PASMCs, not PAECs. This was supported by a study by (Marshall and Marshall, 1992), which showed hypoxia can accelerate pulmonary vasoconstriction in arteries denuded of their endothelium. The action of both Ca^{2+} and K^+ ions within the cells plays a vital role in controlling vessel haemostasis. High levels of the cytosolic Ca^{2+} can trigger smooth muscle cell contraction (Somlyo and Somlyo, 1994). PASMCs exposed to hypoxia shows a decrease in K^+ channel activity, which can modulate intracellular Ca^{2+} levels resulting in hypoxic

pulmonary vasoconstriction (Wang et al., 2007, Platoshyn et al., 2001, Sommer et al., 2008).

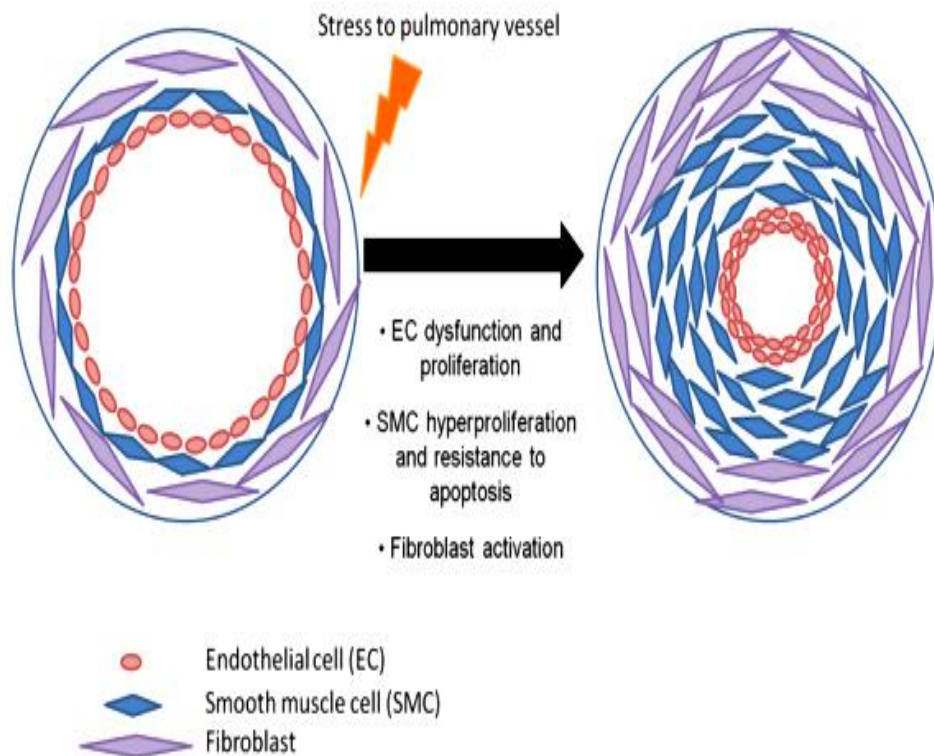


Figure 1.2 Pathogenesis of PAH. Vascular stress (e.g. injury, hypoxic exposure or inflammation) to the small pulmonary arteries enhances the activity of adventitial fibroblasts and promotes SM and EC proliferation leading to hypertrophy of the medial and intimal layers of the pulmonary arterial wall. Vasoconstriction, vascular remodeling and endothelial dysfunction participate to form plexiform lesions in PAH. Adapted from (Grant et al., 2013).

1.4.1 Hypoxic Pulmonary Vasoconstriction:

Vasoconstriction is considered as the main initiating factor in PAH pathogenesis. Hypoxic pulmonary vasoconstriction (HPV) is caused by alveolar hypoxia, which distributes pulmonary capillary blood flow to areas with high oxygen levels. This process highlights the inhibitory effect of hypoxia on K^+ channel activation, which potentially results in Ca^{2+} influx, which enhances Ca^{2+} release leading to PASMC contraction (Di Mise et al., 2017). In addition, it has been reported that reactive oxygen species (ROS) were involved in HPV. For example, increased ROS levels were observed when PASMCs were exposed to hypoxia (Marshall et al., 1996). Moreover, it has been reported that excessive ROS, generated from the mitochondria within the PASMCs, were able to enhance cytosolic Ca^{2+} levels leading to HPV (Rathore et al., 2006). In addition, vasodilator pathways are reduced, while the mitogenic activity and vasoconstrictor pathways are increased in PAH patients. Continuous vasoconstriction caused endothelial cell dysfunction together with the reduced release of vasodilator agents. Nitric oxide (NO) and prostacyclin which are released by endothelial cells, were decreased during the early stage of the disease (Maron and Loscalzo, 2013). Endothelin-1 is an important cellular mediator associated with hypoxic pulmonary vasoconstriction. It is well-known as a potent vasoconstrictor (Maguire et al., 2001, Giaid, 1998). It has been demonstrated that stimulation with ET-1 caused higher levels of hypoxia-induced vasoconstriction (Sham et al., 2000). Moreover, blocking of ET-1 receptors was found to inhibit the hypoxic pulmonary vasoconstriction process suggesting that the release of ET-1 by endothelial cells is required for PASMC to respond to hypoxia and the subsequent vasoconstriction (Liu et al., 2001, Oparil et al., 1995). Another cellular mediator involved in PAH is serotonin, which plays a major role in vascular cells mitogenesis (Ren et al., 2011). It has been reported that mitogen-activated protein kinase (MAPK) signalling pathway, the main proliferative pathway in smooth muscle cells, is activated by the expression of the serotonin transporter found in hypertensive arteries (Eddahibi et al., 2001). Several pathways have also been identified to be linked with pulmonary vascular remodeling including changes in potassium channel expression, changes in vascular elastases stimulation, and upregulation of inflammatory cytokines (Humbert et al., 2004a). Therefore, it is necessary to improve the understanding of signalling pathways

involved in PASMC proliferation and vasoconstriction, which result from the initial causative cellular injury such as hypoxic exposure, in order to develop a valid therapeutic option for PAH.

1.4.2 Pulmonary Vascular Remodeling

As mentioned above, the initiation of endothelial cell dysfunction has a vital role in promoting PASMC contraction and vasoconstriction. Endothelial cell apoptosis is initiated during the early stages of pulmonary arterial remodeling. As PAH progresses, endothelial cells become apoptotic-resistant and proliferation increases alongside their damage (Sakao et al., 2009). Moreover, endothelial cells associated with PAH lose vasculo-protective factors such as nitric oxide and this increases the underlying vascular SMC contraction/ proliferation (Lin et al., 2016).

The sustained vasoconstriction and the vascular remodeling of the pulmonary arteries are considered the main histopathological characteristics of pulmonary hypertension (Maron and Loscalzo, 2013, Stacher et al., 2012). These processes involve intimal thickening, apoptosis-resistant PAECs, proliferation, migration and increased glycolytic metabolism in PASMCs and an increase in fibroblasts within the vessel wall (Farber and Loscalzo, 2004, Abe et al., 2010, Archer et al., 2010). Histopathological abnormalities of vascular remodeling in PAH patients are shown in Figure 1.3 compared to the normal pulmonary artery.

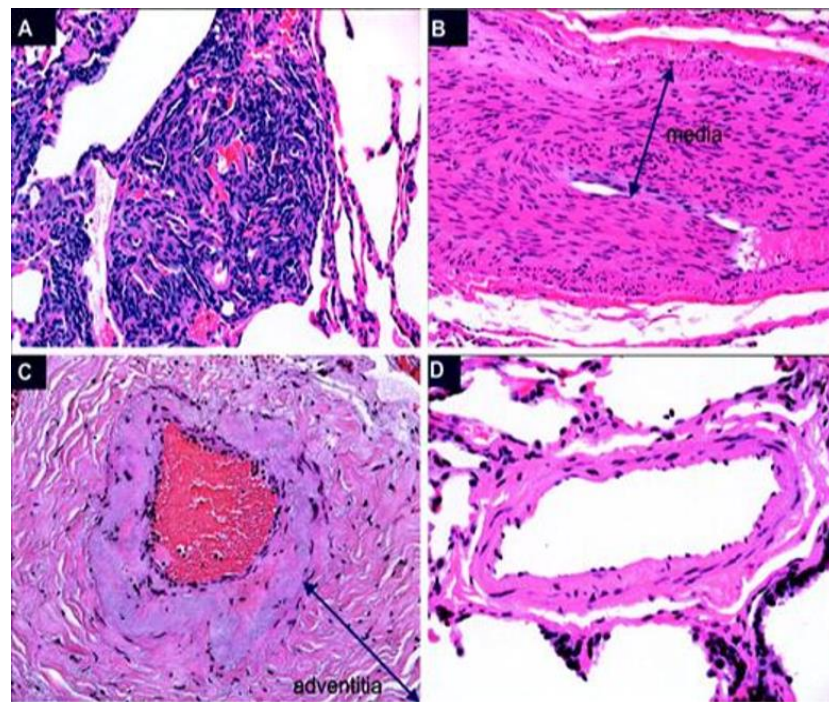


Figure 1.3 Histological changes of pulmonary arteries observed in patients with PAH. A) Plexiform lesion characterized by obliteration of the lumen and hyper-proliferation of cells in diseased artery. B) Hypertrophy/hyperplasia of the medial layer in a moderate PAH patient. C) Fibrosis of the adventitia in a moderate PAH patient. D) A characteristic pulmonary artery in a human without PAH (normal). Adapted from (Cool et al., 2005).

Remodeling commonly occurs in small distal pulmonary arteries. In normal physiology, small distal pulmonary arteries are thin-walled vessels, not muscularised, and their medial smooth muscle is completely diminished. These arteries consist of endothelial cells and pericytes (undifferentiated smooth muscle cells) to aid the blood-gas exchange. However, during the early stages of PAH, tunica intima thickening can effect pericytes to differentiate into smooth muscle cells (Ricard et al., 2014). A vessel with hyper-proliferation of the PSMCs is defined as a vessel with a double elastic laminae, while a non-muscular vessel is

associated with a single elastic lamina. In the pulmonary artery, PASMCs can migrate to the terminal arterioles (Sheikh et al., 2014). In addition to proliferation and migration of PASMCs, upregulation of collagen and elastin synthesis also contributes to PASMC phenotypic changes and the development of pulmonary vascular remodeling (Hongfang et al., 2006, Todorovich-Hunter et al., 1988). The hypertrophic remodeling of large proximal pulmonary arteries combined with PASMC hyperplasia and adventitial fibrosis have resulted in a severe narrowing of the lumen and subsequent atrophic loss of many peripheral pulmonary arteries within the lung (Moledina et al., 2011). The effect of the loss of blood flow regions within the distal pulmonary arteries is termed “vascular pruning” and was confirmed in PAH patients (Figure 1.4) by arteriograms (Reid, 1986).

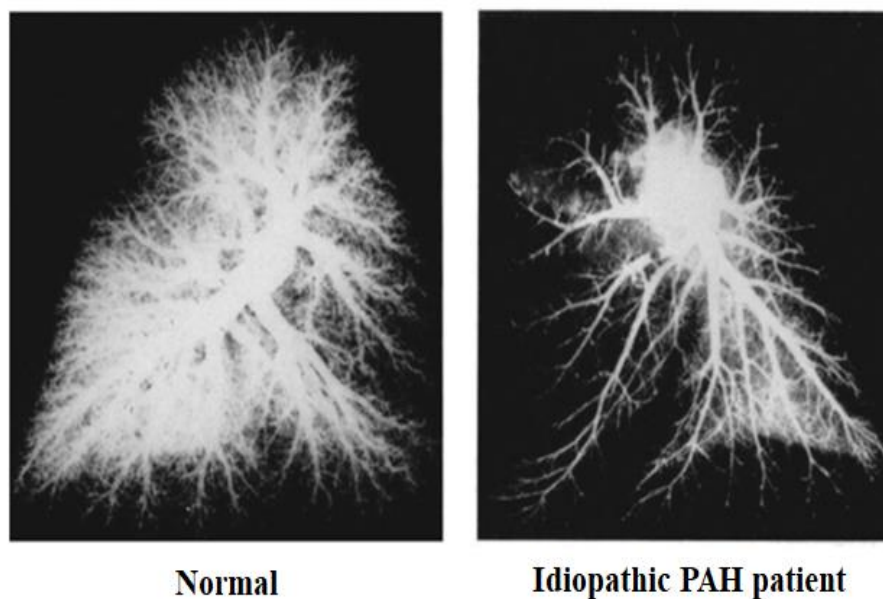


Figure 1.4 Pulmonary Vascular Arteriogram. Pulmonary arteriogram obtained from a healthy adult lung (left) and from an idiopathic PAH patient lung (right). The extensive loss of the peripheral pulmonary vasculature “vascular pruning” was observed in PAH lung. Adapted from (Reid, 1986).

Severe PAH can be recognized by the existence of neointima formations, which originates from the extracellular matrix and numerous cells located between the tunica intima and the internal elastic laminae (Yi et al., 2000). Neointima formation

is associated with the absence of endothelial cell markers and higher expression of the contractile marker α -smooth muscle actin (Yi et al., 2000). This suggests that these cells are more likely to be considered as SMCs. They may have formed from stem cells, fibrocytes or endothelial cells (Frid et al., 2002, Davie et al., 2004). Pulmonary vascular remodeling also affects the proximal pulmonary arteries. In the final stage of PAH, plexiform lesions are frequently detected, which are caused by hyper-proliferation and migration of endothelial cells surrounded by myofibroblasts, smooth muscle cells and connective tissue matrix (Pietra et al., 2004). Angiogenesis markers, such as vascular endothelial growth factor (VEGF) and VEGF receptors are increased in proliferating endothelial cells. In addition, platelet and fibrin thrombi frequently exist in plexiform lesions and both macrophages and inflammatory cells: T cells and B cells are also believed to be included in the progression of these lesions (Rabinovitch, 2008). Targeting proliferation, migration, inflammation and angiogenesis is thought to inhibit the pathological remodeling process and is considered an attractive therapeutic target for PAH. A schematic representation of the main pathological remodeling processes of the pulmonary artery is presented in Figure 1.5.

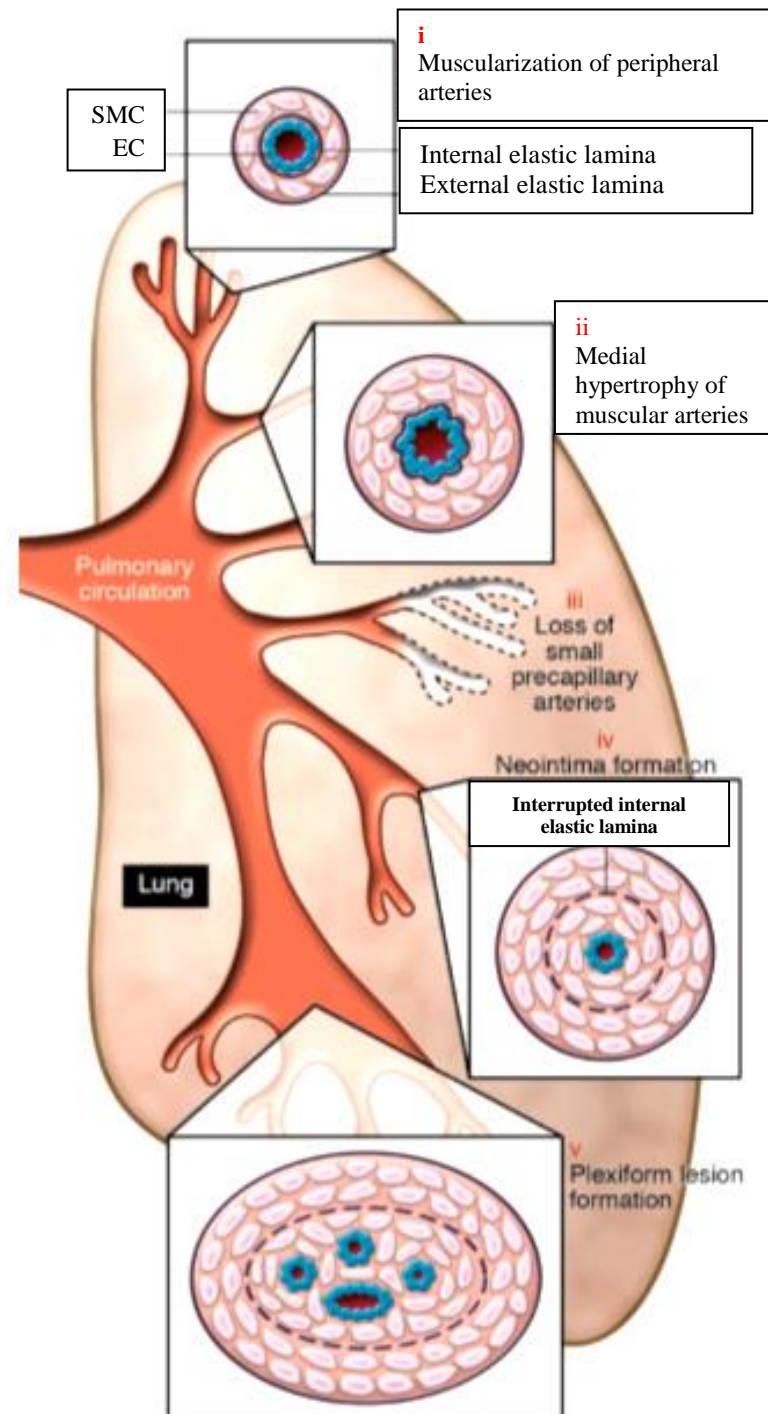


Figure 1.5 Schematic representation of the pathological remodeling processes of pulmonary artery. The figure shows the different pathological changes of pulmonary arterial remodeling. These include: (i) Muscularization of the distal pulmonary arteries, (ii) Medial thickening of the proximal pulmonary arteries, (iii) Extensive loss of distal arteries, (iv) Neointimal formation and pulmonary lumen occlusion, and (v) Formation of plexiform lesions. Adapted from (Rabinovitch, 2008).

1.5 Current PAH therapeutics

The complex multifactorial nature of the disease has impeded the development of PAH therapies. In addition, the incomplete understanding of various molecular signalling pathways involved in PAH, and the delayed detection of the disease due to the lack of symptomatic manifestations are the main reasons provided to explain why a specific treatment strategy cannot easily be identified. Despite the fact that current PAH therapies can apparently relieve patient symptoms and reduce the clinical deterioration rate, PAH remains an incurable disease (Galie et al., 2009b).

The main pathways approved for PAH therapy include the endothelin, nitric oxide and prostacyclin pathways (Figure 1.6). The life expectancy of the patient is now improved in comparison to the 1980's. According to the UK and Ireland National Institute of Health (NIH) registry, the mortality rate has decreased from 66% in the 1980's to 40% in 2012 (Rich et al., 1987, Ling et al., 2012). However, these mortality rates remain unacceptably high and the current therapies have many systemic side effects. Thus, there is great rational to consider new therapeutics directions.

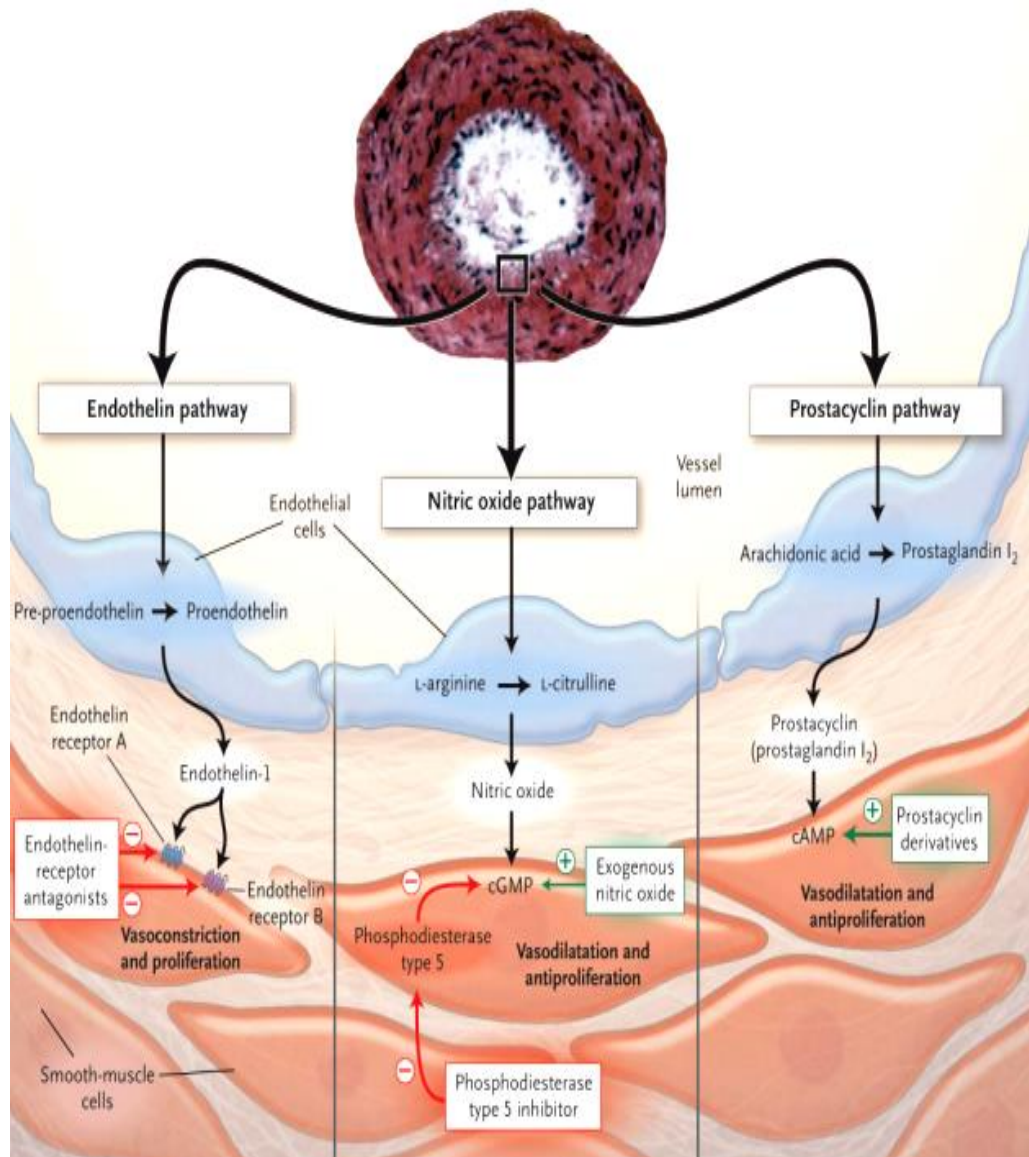


Figure 1.6 Major signalling pathways approved for PAH therapy

At the top of the figure, the transverse section of the pulmonary artery is shown. The figure displays the mechanisms of how the drugs target three major pathways contributing to hyper-proliferation and contraction of PSMCs of the pulmonary artery in PAH patients. Pathways include endothelin-1, nitric oxide and prostacyclin pathways. Therapies include endothelin-receptor antagonists, nitric oxide and phosphodiesterase type 5 inhibitors and prostacyclin derivatives. Adapted from (Humbert et al., 2004b).

1.5.1 Calcium channel blockers

Sustained vasoconstriction of pulmonary arteries is a major hallmark of PAH pathogenesis. An increase in intracellular Ca^{2+} within the PASMCs causes vasoconstriction resulting in an increase in pulmonary vascular resistance. The influx of Ca^{2+} into PASMCs through channels can be targeted to suppress vasoconstriction, promote vasodilation and eventually reduce pulmonary vascular resistance. However, the use of Ca^{2+} channel blocker drugs in PAH is quite limited. It has been reported that these drugs are only recommended for patients who have a positive response following a vasodilatory test. Responders represent roughly 5-10% of PAH patients (Sitbon et al., 2005).

1.5.2 Endothelin receptor antagonist

Endothelin-1 (ET-1) is a highly potent vasoconstrictor molecule which has an important role in regulating vascular tone (Yanagisawa et al., 1988). The ET_A receptor is located on VSMCs while the ET_B receptor is found on both ECs and VSMCs (Seo et al., 1994). According to Firth and Ratcliffe (1992), the distribution of endothelin-1 is five times higher in the lung in comparison to other organs. This suggests the majority of endothelin-1 is synthesised within the pulmonary circulation (Firth and Ratcliffe, 1992).

Endothelial cells within the pulmonary artery play an important role in PAH pathogenesis and their dysfunction is highly regulated by ET-1 (Galie et al., 2004). Endothelin-receptor activation stimulates the phospholipase C (PLC) signalling pathway in VSMCs. PLC converts phosphatidylinositol bisphosphate to inositol triphosphate and diacylglycerol. Inositol triphosphate increases intracellular Ca^{2+} concentrations and participates in vasoconstriction (Bouallegue et al., 2007). The vasoconstrictive and proliferative characteristics driven by endothelin-1 are enhanced following receptor binding leading to alterations in the structure and function of the pulmonary arterial wall (MacLean et al., 1994, Davie et al., 2002). In addition, it has been reported that the severity of pulmonary hypertension is correlated with increasing ET-1 concentrations within the pulmonary circulation (Stewart et al., 1991). Targeting endothelin-1 production and action through either inhibiting endothelin converting enzyme-1 (ECE-1) or blocking endothelin

receptors may diminish ET-1 dependent processes. However, there are other pathways which can interact with ET-1 levels. Therefore, targeting the enzyme would not be a suitable therapeutic strategy. Blocking of both ET_A and ET_B receptors may be the most effective approach as targeting one receptor can be compensated by the activity of the other. Several studies highlight the use of dual receptor antagonists in PAH treatment. It has been reported that blocking both ET_A and ET_B receptors can diminish the proliferative capacity of human PASMCs and reduce right ventricular hypertrophy (RVH) (Davie et al., 2002). In addition, the use of bosentan, a dual endothelin-1 receptor antagonist, in PAH therapy has been shown to improve pulmonary arterial pressure (PAP), pulmonary vascular resistance (PVR) and the severity of the disease on the heart (Sitbon et al., 2003). Bosentan and macitentan are example of drugs which have a similar mode of action in blocking both ET_A and ET_B receptors and are approved by the Food and Drug Administration (FDA) for PAH treatment. They show improvement in the PAH associated clinical outcomes (Pulido et al., 2013, Rubin et al., 2002).

1.5.3 Phosphodiesterase-type 5 (PDE-5) inhibitor

Nitric oxide (NO) is a major regulator of vascular tone in the pulmonary vasculature (Steudel et al., 1997, Fagan et al., 1999, Jin and Loscalzo, 2010). It is released from endothelial cells from the conversion of L-arginine to citrulline by endothelial nitric oxide synthase (eNOS) (Palmer et al., 1988). Nitric oxide stimulates soluble guanylate cyclase to enhance the intracellular cyclic guanosine monophosphate (cGMP) concentration resulting in the relaxation and inhibition of PASMC proliferation (Lucas et al., 2000). Nitric oxide deficiency has been identified in patients with pulmonary hypertension and the reduction in endothelial nitric oxide synthase (eNOS) levels has been associated with vasoconstriction of the pulmonary artery in PAH patients (Giaid and Saleh, 1995). Upregulation of cGMP levels results in activation of cGMP-dependent protein kinase within the PASMCs, which induces vasodilation (Michelakis, 2003). The key enzyme phosphodiesterase-type 5 is primarily expressed in PASMCs and its hyper-activity was observed in an animal model of pulmonary hypertension, which accelerates cGMP degradation in PASMCs to terminate the effect of cGMP (Corbin et al., 2005). Phosphodiesterase-type 5 inhibitors such as sildenafil, tadalafil and

verdenafil are approved for the treatment of patients with PAH. Oral sildenafil therapy has been reported to inhibit hypoxia and monocrotaline-induced pulmonary hypertension in humans, mice (Zhao et al., 2001) and rats (Schermyly et al., 2004).

1.5.4 Synthetic prostacyclin and its analogues

Prostacyclin (PGI₂) is released from PAECs (Gryglewski, 1980, Gryglewski et al., 2005). Cyclooxygenase (COX) enzyme metabolises arachidonic acid to prostacyclin H₂, which is converted into prostacyclin by prostacyclin synthase. Prostacyclin induces vasodilation and causes a reduction in platelet aggregation. It also has an inhibitory effect on PASMC proliferation through its ability to increase cyclic AMP levels within the cells (Moncada and Vane, 1981). Another metabolite produced by the arachidonic acid breakdown is thromboxane A₂, which is metabolised by thromboxane synthase. Thromboxane A₂ has the opposite action in comparison to prostacyclin. It is a potent pulmonary vasoconstrictor and stimulates platelet aggregation. An imbalance between these two vasoactive metabolites has been detected in PAH patients (Christman et al., 1992). Prostacyclin synthase and prostacyclin production are downregulated in PAH patients whereas thromboxane A₂ is upregulated (Christman et al., 1992, Tuder et al., 1999). In animal studies, a knockdown of prostacyclin receptors in mice under hypoxic conditions promotes pulmonary arterial remodeling and causes severe pulmonary hypertension compared to the wild type (WT) mice (Hoshikawa et al., 2001). Another study showed that over-expressing prostacyclin synthase selectivity in mice has a protective effect against hypoxia-induced pulmonary hypertension (Geraci et al., 1999). Since studies have shown that low levels of prostacyclin contributed to PAH, targeting the prostacyclin signalling provides an ideal therapeutic strategy. The use of a synthetic analogue of prostacyclin is selected for PAH treatment due to the vasodilator effect of prostacyclin and its ability to inhibit platelet aggregation. Epoprostenol was the first prostacyclin analogue to be used in PAH therapy (Mubarak, 2010).

1.5.5 Developing future therapeutic target: Tyrosine kinase inhibitors

As the understanding of pulmonary hypertension pathophysiology increases, the use of cancer drugs is also being identified as a potential therapeutic strategy in PAH. This possibly highlights the abnormal proliferative feature of the cells and the increase in growth factor receptors or tyrosine kinase receptors in both cancer and pulmonary hypertension diseases. Imatinib is a tyrosine kinase inhibitor originally developed to target the break point cluster/Abelson (Bcr/ABL) tyrosine kinase in chronic myeloid leukaemia. Imatinib can also antagonize platelet-derived growth factor (PDGF) receptors and c-KIT signalling, both of which are involved in PAH development and PASMC proliferation (Hoeper et al., 2013). In two animal models of pulmonary hypertension, imatinib showed a reduction in right ventricle pressure and hypertrophy in rats injected with monocrotaline and in mice exposed to chronic hypoxia, which reached near normal values (Schermlay et al., 2005). In addition, imatinib was found to inhibit PASMC proliferation and induce an apoptotic action on PASMC obtained from idiopathic PAH patients (Nakamura et al., 2012). In order to evaluate the long-term safety and efficacy of imatinib, a 204 week randomized efficacy study was conducted. Results show a high discontinuation rate and a severe adverse effect (subdural hematoma) was observed in patients, resulting in the limiting of imatinib in PAH therapy (Frost et al., 2015).

1.6 Hypoxia as an experimental model of pulmonary hypertension

A number of stimuli have been used to study the changes in pulmonary hypertension; but the most widely used are hypoxia and monocrotaline models. For the purpose of this thesis, cell proliferation models and the investigation of cell signalling pathways are considered. Therefore, work with acute hypoxic cell models is the most relevant. An acute hypoxic cell model has the benefit of studying a battery of specific cell signalling pathways, treatment options and drug concentrations on readily available cells isolated from normal animals. An *in vitro* model has been used to study the contractile characteristics of the pulmonary arteries (Martinez-Lemus et al., 1999) or the behaviour of the isolated cultured cells. Another study (Du et al., 2003) also showed that cultured endothelial cells isolated from the pulmonary artery were associated with specific signalling, such as angiotensin signalling cascade. PASMC proliferation and apoptosis were also

studied in response to cGMP-dependent protein kinase transfection in the cultured cells (Chiche et al., 1998). Regarding hypoxia, the hypoxic cell model has been studied in mesenchymal stem cells isolated from the human umbilical cord to investigate hypoxia-dependent cell proliferation signalling in comparison to the normoxic cultured cells (Lavrentieva et al., 2010). Moreover, the effect of hypoxia on PASMC proliferation and apoptosis has been studied through obtaining the cells from the peripheral human pulmonary artery and exposing them to hypoxia (Howard et al., 2012).

1.7 Hypoxia-inducible factor 1 (HIF-1) signalling

Hypoxia-inducible factor 1 (HIF-1) is the main transcription factor in hypoxic signalling which has been identified in relation to the hypoxia-responsive element in the erythropoietin gene (Wang et al., 1995). The HIF-1 pathway is found in all cell types and recognised as a ubiquitous mediator of cellular responses to hypoxic stimuli. Regulation of cell function in response to hypoxia is generally mediated by HIF-1, which is a heterodimer protein containing two constitutively transcribed proteins: HIF-1 α and HIF-1 β (Schofield and Ratcliffe, 2004).

During normal oxygen condition, HIF-1 α has a very short half-life due to rapid degradation (Salceda and Caro, 1997). Proline residues in HIF-1 α are hydroxylated by prolyl hydroxylase domain (PHD) and the hydroxylated HIF-1 α binds to the Von Hippel Lindau (VHL) protein, which causes recognition through the ubiquitination leading to proteasomal degradation of HIF-1 α (Figure 1.7). In addition, HIF-1 α is also hydroxylated by factor-inhibiting HIF-1 (FIH-1) at the asparagine residue during normoxia, which inhibits its interaction with the transcription coactivator, P300 (Mahon et al., 2001, Coleman and Ratcliffe, 2009). Therefore, HIF-1 α is constitutively degraded under normoxia.

However, during hypoxia, the activity of PHD and FIH-1 proteins are decreased due to the requirement of oxygen molecules to exert their functions as the hydroxylation reactions cannot occur during hypoxic condition resulting in a reduction in HIF-1 α degradation with a subsequent increase in HIF-1 protein

complex stability. Following stabilization, HIF reacts with hypoxia-responsive elements to stimulate various genes including the proliferative genes (Figure 1.7).

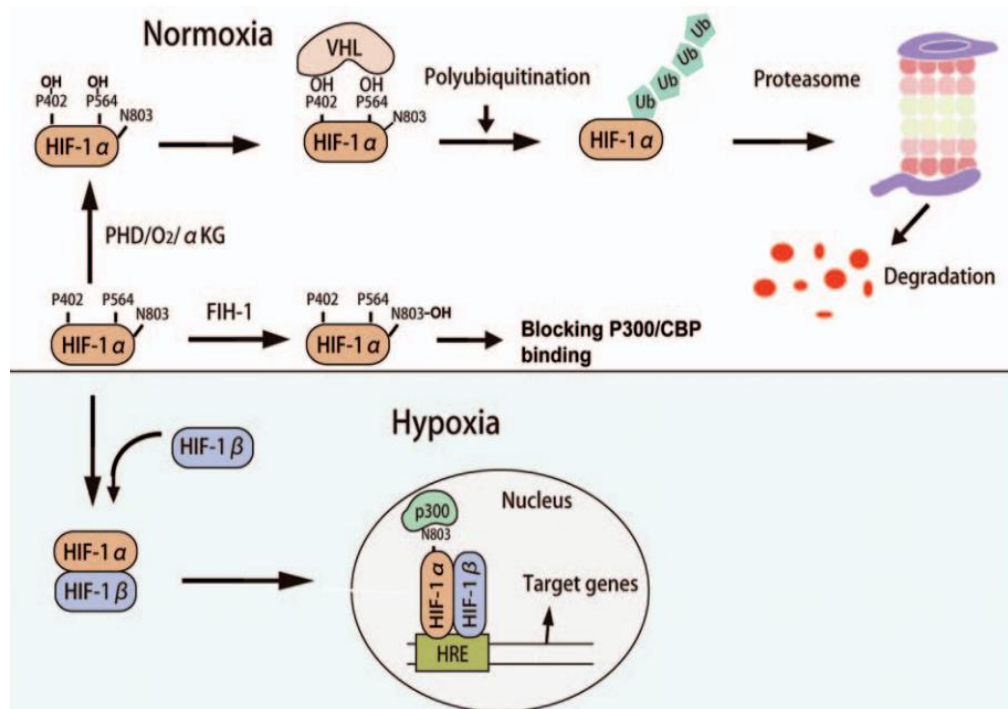


Figure 1.7 Oxygen-dependent regulation of HIF-1 α

In normoxia, HIF-1 α is hydroxylated by prolyl hydroxylase domain (PHD) protein and factor-inhibiting HIF-1 (FIH-1). Hydroxylation of proline residues (P402 and P564) results in binding of von Hippel-Lindau E3 ubiquitin ligase (VHL), which promotes the polyubiquitination and proteasomal degradation of HIF-1 α . Hydroxylation of an asparagine residue N803 prevents the interaction with transcriptional activators such as P300 or cyclic AMP response element binding protein CREB-binding protein (CBP). In hypoxia, the hydroxylation reactions are repressed. HIF-1 α becomes stable and dimerizes with HIF-1 β . The dimerized $\alpha\beta$ heterodimer then translocates to the nucleus and the recruitment of co-activators (e.g. P300/CBP) occurs. The HIF heterodimer then binds to the hypoxia response element (HRE) of target genes to regulate transcription. Adapted from (Lin et al., 2014).

1.8 Mitogen-Activated Protein Kinases (MAPK) signalling

Extracellular signals have a strong influence on cellular activities such as differentiation, growth, apoptosis, mediator synthesis, and gene transcription. A number of extracellular stimuli (such as Ultraviolet (UV) radiation, hypoxia and mitogens) have been studied in MAPK signalling activation (Muthusamy and Piva, 2013, Scott et al., 1998, Milanini et al., 1998). Extracellular stimuli activate various cell receptor complexes associated with subsequent activation (e.g. by phosphorylation) of upstream kinase proteins in the MAPK cascade. The signalling events result in activation of three-kinase architecture including a MAPK and two upstream kinases: MEK kinase and MAPKK kinase (Figure 1.8). Initially, the signal is amplified by the two previous kinase steps resulting in MAPK protein phosphorylation at tyrosine/threonine residues (Ray and Sturgill, 1987). Following phosphorylation, MAPK has the ability to act directly and activate substrate proteins in the cytoplasm (Northwood et al., 1991) or to translocate from the cytoplasm into the nucleus and phosphorylate certain transcription factors (Chen et al., 1992). Therefore, the MAPK signalling cascade acts as a critical link between the extracellular signals acting on cell membrane receptors and the cell nuclear events (Figure 1.8).

The most common subgroups which belong to MAPKs are extracellular signal-regulated kinases 1/2 (ERK1/2), c-jun amino-terminal kinases/stress-activated protein kinase (JNK/SAPK) and p-38 MAPK (Johnson and Lapadat, 2002). These distinct MAPK subfamilies have a major role in proliferation and differentiation in mammals (Zhang and Liu, 2002). In particular, ERK1/2, the typical MAPK, mainly contributes to activation of constitutive signalling dependent cell proliferation, which is mediated by certain growth factors whereas JNK/SAPK and p38 MAPK are known as important regulators of cellular responses to stress signals (e.g. UV radiation and hypoxia) and are involved in cell inflammation and apoptosis (Robinson and Cobb, 1997, Ip and Davis, 1998).

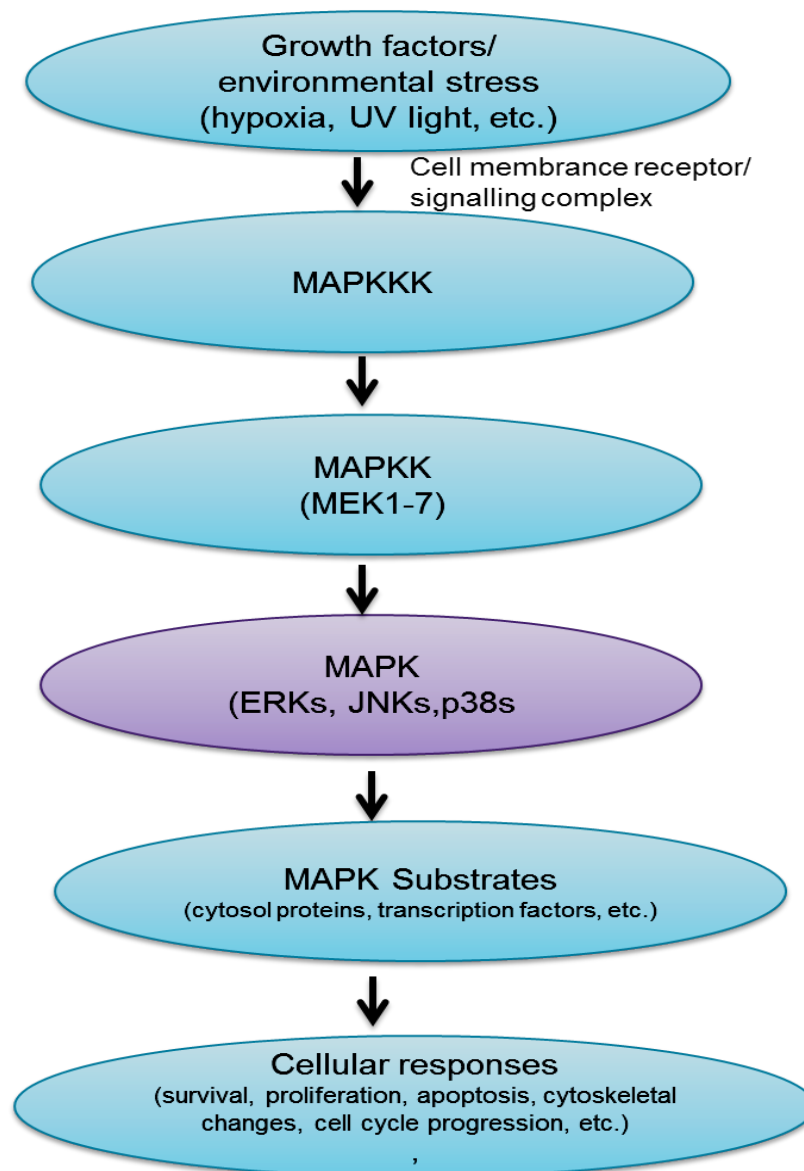


Figure 1.8 Mitogen-Activated Protein Kinases (MAPKs) signalling pathways. MAPKs participate and process several extra-cellular signals. The MAPK cascade contains three protein kinases: a MAPK and two upstream kinases a MAPK Kinase (MAPKK or MEK) and MAPKK Kinase (MAPKKK such as rho kinase). ERK: extracellular signal-related kinase. JNK: c-Jun-N-terminal kinase.

Several growth factors or ligands cause phosphorylation of receptor tyrosine kinases (RTK) through dimerization of two subunits of the receptor (Ihle et al., 1994, Ahn et al., 1992). Phosphorylated tyrosine kinase receptors enhance the cytosolic recruitment of the adapter protein: growth factor receptor-bound protein-2 (GRB-2), which is bound to the Ras-activator protein: Sos (son of sevenless) or Ras-activating guanine nucleotide exchange factor (GEF). This protein stimulates the membrane-bound protein (Ras) to transfer GDP for GTP to maintain the activity of Ras (Egan et al., 1993, Chardin et al., 1993). Thereafter, activated Ras protein binds to several effector proteins. For example, extracellular mitogens signalling through Ras-Raf-ERK1/2 is well characterized (Reuter et al., 2000). GTP-Ras during ERK1/2 cascade binds to A-Raf, B-Raf (the main effector of Ras) and C-Raf kinases (Andreadi et al., 2012, Brown and Sacks, 2008). Once Raf kinases are activated, they stimulate MEK and eventually lead to ERK1/2 phosphorylation (Shaul and Seger, 2007) (Figure 1.9). As a result, MAPK protein (ERK1/2) phosphorylation leads to target both cytosolic and nuclear substrates (Brown and Sacks, 2008).

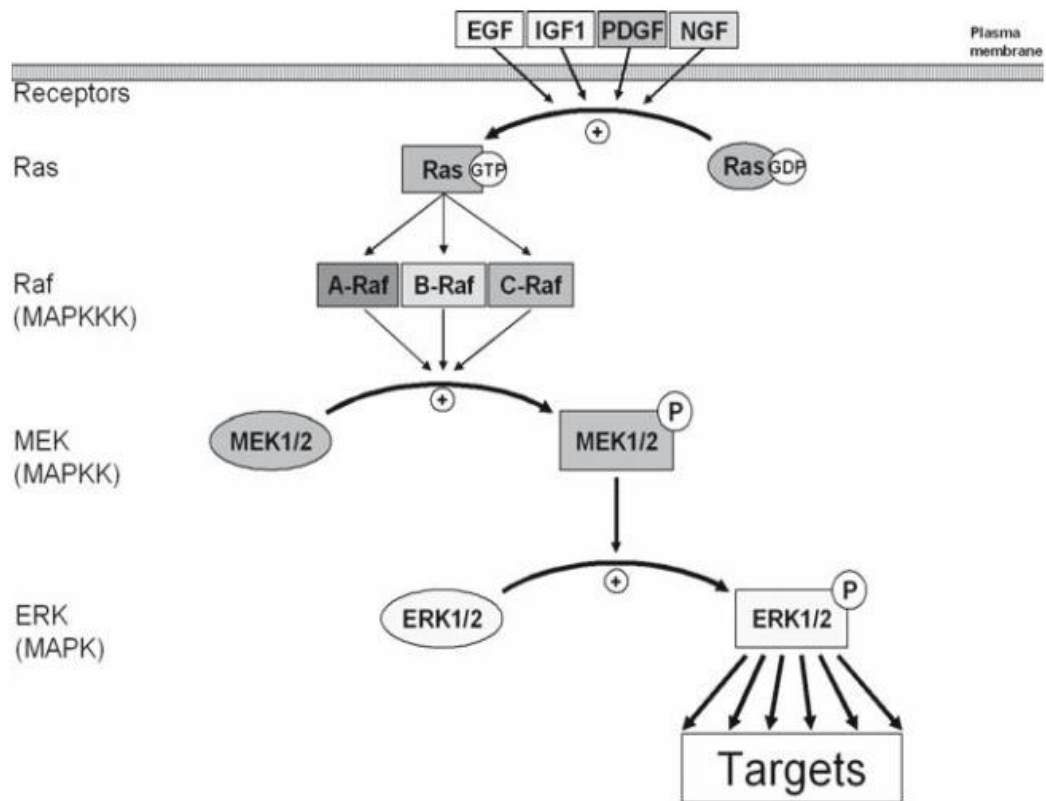


Figure 1.9 The modulation of MEK1/2/ERK1/2 phosphorylation

Growth factors such as epidermal growth factor (EGF) and PDGF induce Ras activation via the stimulation of the transfer of Ras-GDP to Ras-GTP, which eventually activates Raf kinases (MAPKKK) and the downstream kinase (MEK1/2). Phosphorylated MEK1/2 cause the phosphorylation of ERK1/2, which stimulates cytosolic and nuclear substrates. Adapted from (Brown and Sacks, 2008).

The p38 MAPK family consists of different isoforms (α , β , γ and δ) (Cuenda and Rousseau, 2007). They are regularly stimulated by environmental stress, heat and G-protein coupled receptors (Lagneux et al., 2001, Yamauchi et al., 1997). All p38 MAPK isoforms are phosphorylated by MEK3 and MEK6 (Han and Sun, 2007). Signal transduction of the p38 MAPK pathway has an important role in the regulation of many cellular activities such as proliferation, migration, inflammation, angiogenesis, and cytokine production (Brown and Sacks, 2008, Pearson et al., 2001).

The last main member of the MAPK family is JNK which consists of JNK1, JNK2 and JNK3 isoforms (Derijard et al., 1994, Kallunki et al., 1994, Gupta et al., 1996). Extracellular or intracellular signals which cause DNA synthesis inhibition will activate JNK protein (Hsu et al., 2009). JNK kinases are targets of upstream kinases such as MEK4 and dual leucine zipper kinase (DLK) (Fukuyama et al., 2000, Peti and Page, 2013). Finally, JNK phosphorylation leads to translocation of JNK to the nucleus leading to the activation of transcription factors such as c-jun, STAT3 and ATF-2 (Dunn et al., 2002, Lim and Cao, 1999, Gupta et al., 1995). The JNK signalling cascade has an important role in the regulation of apoptosis and the initiation of immune cell development (Roux and Blenis, 2004, Brown and Sacks, 2008).

1.9 The mammalian target of rapamycin (mTOR) signalling pathway

The mammalian target of rapamycin (mTOR) is an essential pathway preserved serine/threonine protein kinase that serves as a key regulator for cell metabolism, growth, proliferation and survival (Cargnello et al., 2015, Yu and Cui, 2016). The mTOR signalling has been found to be an important cell signalling pathway in the initiation, progression, and proliferation involved in cancer and cardiovascular diseases (Guertin and Sabatini, 2007, Humar et al., 2002). The mTOR inhibitors are currently being used in clinical trial studies of pulmonary hypertension. However, due to their various adverse effects, there is still a need for using these inhibitors with careful monitoring and generating more selective inhibitors that would be specific for the hyperproliferative phenotype of the PASMC. Therefore, this highlights the need to explore a novel signalling mechanism that includes mTOR proteins.

The intracellular and extracellular signals are processed by two distinct complexes: mTOR complex1 (mTORC1) and mTOR complex2 (mTORC2). Each complex differs in its composition, its downstream target and its sensitivity to rapamycin (Hara et al., 2002, Sarbassov et al., 2004). mTORC1 activates biosynthesis of proteins, lipids and other anabolic processes to regulate cell proliferation and growth (Laplane and Sabatini, 2012).

The mammalian target of rapamycin complex 1 (mTORC1) is activated by different signals including growth factors, energy status, oxygen level and amino acids (Dibble and Cantley, 2015). Growth factors bind to the cell receptors such as tyrosine kinase or G-protein coupled receptors at the cell surface resulting in the activation of the PI3K/AKT/mTOR pathway (Figure 1.10). Phosphorylation of AKT inhibits the tuberous sclerosis complex (TSC1/2), which serves as a GTPase activating protein (GAP) complex towards Ras homolog enriched in brain (Rheb) (Tee et al., 2003). Therefore, inactivation of TSC1/2 complex enhances the level of Rheb and results in stimulation of mTORC1 (Figure 1.10). mTORC1 directly phosphorylates a number of substrates including eukaryotic initiation factor 4E (eIF4E), binding protein 1 (4EBP1) and p70 ribosomal protein S6 kinase1 (S6K1), which mediates the regulation of anabolic metabolism and cell proliferation (Richter and Sonenberg, 2005). For example, pro-inflammatory cytokines such as tumor necrosis factor (TNF α) can inactivate TSC1/2 by I κ B kinase- β (IKK β) stimulation, which subsequently leads to mTORC1 activation (Lee et al., 2008). In addition, the energy status and the exposure to hypoxia also can contribute to mTORC1 regulation. For example, hypoxia stimulates AMP kinase (AMPK), when the ATP levels are decreased, leading to activation of TSC1/2 and inhibition of mTORC1 signalling (Arsham et al., 2003). mTORC1 can also be inhibited through TSC1/2 activation by transcriptional regulation of DNA damage response (REDD1) during hypoxic conditions (DeYoung et al., 2008).

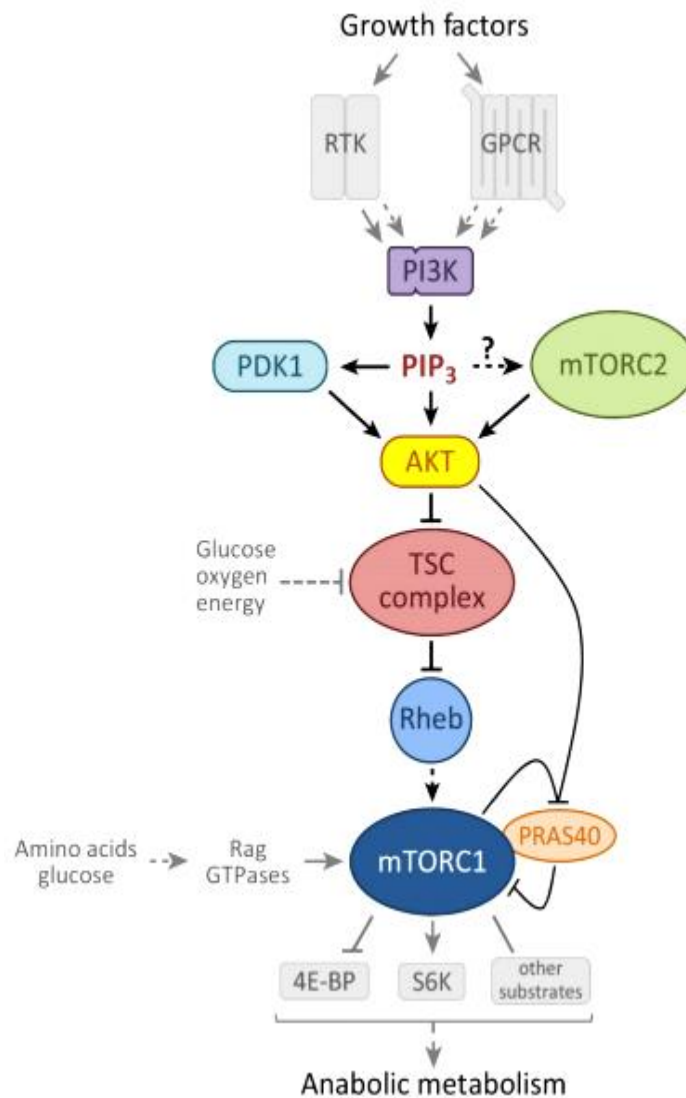


Figure 1.10 PI3K/AKT/mTORC1 signalling pathway

Growth factor activates receptor tyrosine kinase (RTK) or G-protein coupled receptor results in phosphoinositide 3-kinase (PI3K) activation. PI3K forms phosphatidylinositol-3,4,5-trisphosphate (PIP₃) which binds to phosphoinositide-dependent kinase1 (PDK1) and AKT resulting in PDK1 and AKT activation. The activated form of AKT represses the tuberous sclerosis complex (TSC1/2) function, which allows the small GTPase Ras homolog enriched in brain (Rheb) to become activated and stimulate mTORC1 activity. Adapted from (Dibble and Cantley, 2015).

1.10 The Role of Mitochondria in Cardiovascular disease

Mitochondria are small organelles that are best recognized for regulating energy metabolism within cells. They consist of two distinct cellular membranes, which are the outer membrane and the inner membrane. The inner membrane is the site for the electron transport chain enzymes and it encloses mitochondrial DNA and mitochondrial matrix proteins, whereas the outer membrane encircles the intermembrane space and the inner membrane and has pores and channels for the passage of various molecules and ions (Reichert and Neupert, 2002). Mitochondria are responsible for producing the energy-containing molecule adenosine triphosphate (ATP) and play a major role in cell signalling, cell proliferation and apoptosis (Frohman, 2010). In the pulmonary vasculature, mitochondria act also as oxygen sensors via reactive oxygen species (ROS) generation resulting in alteration of the redox state and regulation of various effectors (ion channel and kinases) leading to hypoxic pulmonary vasoconstriction (Weir et al., 2005).

Previously, mitochondria were believed to be static organelles but recent research has highlighted the dynamic state of the mitochondria in which they quickly divide (fission) and elongate together (fusion) to keep steady-state mitochondrial morphology (Suen et al., 2008). The balance between fission/fusion processes is firmly regulated and can be affected by cell cycle kinases, oxidative stress, intracellular Ca^{2+} and metabolism. These processes are mediated by specific proteins. Mitochondrial division (fission) is found to be mediated by dynamin-related protein-1 (DRP1) (Cribbs and Strack, 2009), whereas mitochondrial fusion is mediated by the outer mitochondrial membrane GTPases: mitofusin 1 (MFN1) and mitofusin 2 (MFN2) and the inner mitochondrial membrane GTPase, optic atrophy-1 (OPA1) (Ishihara et al., 2009).

The increased mitochondrial length and the presence of a sequence of invaginations termed cristae within the inner mitochondrial membrane can undertake changes in the mitochondrial structure to regulate mitochondrial function. For example, mitochondrial cristae remodeling and fusion have been shown to promote cell apoptosis through their participation in cytochrome c release from the intermembrane space (Zamzami and Kroemer, 2001).

During the apoptotic signalling pathway driven by the mitochondria, caspase proteases, which are required in the apoptotic pathway, are activated by the release of the mitochondrial cytochrome c protein (Tait and Green, 2010). The release of cytochrome c into the cytosol is accomplished by Bax, a pro-apoptotic member of the Bcl-2 family that forms pores and results in mitochondrial outer membrane permeabilization (MOMP) (Fulda et al., 2010). The role of Bax and Bad in regulating apoptosis and mitochondrial morphology has been shown to be regulated through their interaction with a MFN2 protein that mediates the fusion process (Karbowski et al., 2006).

Recently, various studies have highlighted the role of mitochondria in which they can contribute not only to apoptotic signalling but also to other biological processes such as mitogenic signalling and hypoxia signalling, by being initiators and transducers of the cellular signalling pathway (Antico Arciuch et al., 2012, Chandel, 2010). They can regulate signalling through either serving as a platform in which the interaction of the proteins occurs or through their role in the regulation of intracellular signalling molecules such as Ca^{2+} and ROS (Finkel, 2011). For example, it has demonstrated that the generation of ROS is triggered when cells lack MFN2 (Munoz et al., 2013). This was also supported by another study which showed the lack of mitochondrial fusion protein MFN2 within cardiomyocyte cells, causes an increase in ROS production and the fission of the mitochondria resulting finally in cell apoptosis (Tang et al., 2017).

On the other hand, an inhibition of DRP1 protein and mitochondrial fission process shows an important intervention in preventing smooth muscle cell proliferation, migration and cardiovascular diseases (Ikeda et al., 2015). For example, it has been demonstrated that impaired function of mitochondrial fission protein, particularly DRP1, can protect the heart from myocardial ischemia (Ong et al., 2010). In addition, Marsboom and colleagues (2012) have reported that increases in mitochondrial DRP1 protein, mitochondrial fission and cell proliferation were observed in the PAH-PASMCs, in comparison to the control PASMCs, when HIF-1 α was activated (Marsboom et al., 2012).

This study suggested that the activation of mitochondrial fission by DRP1 could be mediated through the presence of HIF-1 α . The same study also demonstrated that inhibiting the fission process through reducing DRP1 activity caused a reduction in PASMC proliferation. The relationship between HIF-1 α , ROS generation and mitochondrial dynamic activity (through DRP1 up-regulation) has been suggested as an explanation for the increase in PASMC proliferation observed in PAH. A study by Dromparis et al (2010) has demonstrated the signalling mechanisms involved in PASMC proliferation. They have reported that the low level of mitochondrial ROS caused the apoptotic resistant feature of PASMCs due to the closure of the redox-sensitive K⁺ channels which led to an increase in intracellular K⁺ and Ca²⁺ ions resulting in activation of transcription factors such as HIF-1 α and NFAT, enhancing proliferation and vascular contraction (Dromparis et al., 2010). This study highlighted the involvement of HIF-1 α in regulating cell proliferation. However, the exact link between mitochondrial fission, particularly mitochondrial DRP1, hypoxia signalling and PASMC proliferation and migration requires further clarification and investigation.

1.11 Mitochondrial dysfunction and PAH

Mitochondrial dysfunction is classified into two types: primary and secondary. The primary class is caused by pathological events originally initiated by the mitochondria such as a mutation in a gene encoded by mtDNA, or mutation of the nuclear genes that encode mitochondrial proteins. By contrast, secondary mitochondrial disruption results from pathological actions originating outside the mitochondria (Smith et al., 2012). For example, several disorders lead to extensive secondary dysfunction such as ischemia/reperfusion injury, diabetes, metabolic syndrome and cancer (Murphy and Steenbergen, 2011, Wallace et al., 2010). Thus, treating and correcting both primary and secondary mitochondrial pathologies is a challenging area for future therapy.

There are three common pathological causes of mitochondrial damage that have contributed to both primary and secondary mitochondrial dysfunction; excessive ROS generation, elevation of cytosolic Ca²⁺, and defective mitochondrial ATP supply (Smith et al., 2012). There is some evidence of mitochondrial dysfunctional

mechanisms being linked with lung remodeling in pulmonary arterial hypertension. Archer et al. (2010) have reported the link between the impairment of the mitochondrial redox state and the proliferative phenotype of PASMCs, which is related to the deficiency of the mitochondrial superoxide dismutase-2 (SOD2) enzyme (Archer et al., 2010). Further evidence is the disruption of the mitochondria/endoplasmic reticulum (ER) coupling which has also been identified as the lack of uncoupling protein 2 (Ucp2) within the mitochondria enhances ER stress to reduce mitochondrial Ca^{2+} levels and to weaken the activity of Ca^{2+} dependent respiratory complexes (Dromparis et al., 2013).

Moreover, excessive PASMC proliferation and remodeling of the pulmonary vasculature in PAH share several mitochondrial abnormalities that are also found in cancer. In particular, the metabolic theory originated in several cellular processes found in both PAH and cancer that depend on the mitochondria as the hallmark of metabolic control and regulation. An alternative form of metabolism was first explained by Warburg (1956) and is defined as the Warburg effect or aerobic glycolysis in which pyruvate is removed from the tricarboxylic acid cycle (TCA cycle) and is metabolized to lactate instead of its oxidation to produce ATP. Importantly, the end product of the conversion of pyruvate to lactate is NAD^+ , which further enhances the glycolytic activity. This glycolytic shift is utilized by cancer cells, regardless of whether oxygen is present or not, to sustain uncontrolled tumor growth (Warburg, 1956). Similarly, the hyperproliferative and glycolytic phenotype is also observed in the pulmonary vasculature in PAH, which contributes to cell proliferation, high expression of cellular growth factors, and a strong resistance to apoptosis (Tuder et al., 2012, Archer et al., 2010).

In the setting of hypoxia and hypoxia-induced PAH, this metabolic shift is also named as the Pasteur effect in which cells are more dependent on the glycolytic and lactic acid fermentation pathways to generate ATP rather than the pyruvate-dependent oxidative phosphorylation route (Cottrill and Chan, 2013). There are some known mechanisms by which mitochondrial metabolism is dysregulated in hypoxia-induced PAH. Recently, the HIF-1 pathway has been identified as connecting HIF-1 to the glycolytic shift (Semenza, 2007, Kelly et al., 2008). It has

been reported that the mitochondrial enzymes pyruvate dehydrogenase (PDH) and pyruvate dehydrogenase kinase-1, are vital enzymes that mediate the causal link between hypoxia and the metabolic glycolytic effect (Kim et al., 2006). PDH is the gate keeping enzyme that is responsible for pyruvate conversion into acetyl-CoA and facilitates the entry of pyruvate into the mitochondria (Kim and Dang, 2005). High expression of pyruvate dehydrogenase kinase-1 by HIF-1 plays an important role in the suppression of glucose oxidation during hypoxic conditions. This is identified when the deficiency of HIF-1 α within fibroblast cells shows an increase in mitochondrial ROS generation during hypoxia, suggesting persistent glucose oxidation. Accordingly, transfecting these cells with an expression vector encoding pyruvate dehydrogenase kinase caused a reduction in ROS activity (Kolb et al., 2011).

Moreover, hypoxia-inducible factor (HIF) also enhances the glycolytic pathway in numerous ways such as its ability to activate lactate dehydrogenase A (LDHA), which mediates pyruvate metabolism into lactate (Semenza et al., 1996). It has a role in activating glucose transporters (Koppenol et al., 2011), and also in cytochrome c oxidase COX4-1 subunit degradation and COX4-2 subunit upregulation which collectively enhance the activity of cytochrome c oxidase (COX) under aerobic situations within the hypoxic cells (Fukuda et al., 2007).

1.12 Mitochondrial pharmacology

The focus of this thesis is to inhibit the mitochondria pharmacologically through the use of a promising compound called Mitochondrial Division-Inhibitor 1 (Mdivi-1), which acts on a mitochondrial specific target, the mitochondrial outer membrane protein dynamin-related protein-1 (DRP1), which is required for mitochondrial fission and fragmentation process (Westermann, 2010). Phosphorylation of DRP1 is initiated by cyclin B1/cyclin-dependent kinase 1 (cyclin B1/CDK1) resulting in DRP1 activation and its translocation from the cytoplasm to the mitochondrial outer membrane for the fission process (Marsboom et al., 2012).

Mitochondrial fragmentation may play an essential role in sustaining daughter cell generation in the hyperproliferative state, which finds this process as a possible

intervention via the activation of dynamin-related protein-1 (DRP1) protein (Chang and Blackstone, 2007). Cassidy-Stone and co-workers first characterized the DRP1 inhibitor (Mdivi-1) through the screening of molecules that affect the morphology of the mitochondria (Cassidy-Stone et al., 2008). They have reported that Mdivi-1 selectively targets DRP1 by binding to an allosteric binding site and stabilizing a conformational un-assembled DRP1 form that binds to GTP. This conformational change inhibits DRP1 from accumulating into spiral filaments and blocks their polymerisation resulting in an inhibition of mitochondrial fission (Cassidy-Stone et al., 2008). When DRP1 is inhibited, the process of mitochondrial fission that has recently been linked with cell proliferation and cell cycle progression is inhibited. The morphological changes to mitochondria are important in determining cellular functions. Correct balance of mitochondrial fission and fusion in healthy cells keeps mitochondria within size ranges appropriate for the maintenance of cellular physiology (Flippo and Strack, 2017). In contrast, disruptions in the balance of fission-fusion events can induce a disease phenotype (Smith and Gallo, 2017). In PASMCs from PAH patients, the expression of mitochondrial fission protein DRP1 is increased and the mitochondria are fragmented (Marsboom et al., 2012). DRP1-dependent fission of the mitochondrial networks influences important cellular functions including Ca^{2+} signalling, which contributes to cell proliferation (Szabadkai et al., 2004).

Therefore, the study of the mitochondrial dynamics and the differences in mitochondrial morphology and its relation to cell proliferation is more likely to be necessary which may affect many cellular functions.

1.13 Aims and Hypothesis

In this thesis, the hypothesis is that mitochondrial fission is linked to PASMCM proliferation and migration during hypoxia.

The aims of this thesis are to establish a cell-based model of where cell hypoxic-dependent proliferation is reliable and reproducible. With this established, the aim is to determine the signalling mechanisms driving the increased proliferative response of PASMCMs to hypoxia. Moreover, to investigate the potential role of mitochondria in cell proliferation and migration under the established hypoxic-proliferative model using a dynamin-related protein-1 (DRP1) inhibitor, Mdivi-1. And finally, to identify signalling pathways involved in DRP1-dependent cell proliferation and migration under hypoxic conditions.

Chapter 2

General Methods

2.1 Materials

- Foetal calf serum (Sigma, UK)
- Ham's F12 medium (Gibco, UK)
- Paraformaldehyde (Sigma, UK)
- Penicillin streptomycin (Gibco, UK)
- Sodium hydroxide (Sigma, UK)
- Sodium lauryl sulphate (Sigma, UK)
- Trichloroacetic acid (Sigma, UK)
- Triton X 100 (Sigma, UK)
- Emulsifier-safe scintillation fluid (PerkinElmer, USA)
- Mitochondrial inhibitor Mdivi-1 (Sigma, UK)
- Anti phospho/Total ERK1/2 antibody (Cell Signalling, UK)
- Anti phospho p38 MAPK antibody (Cell signalling Tech., USA)
- Anti phospho JNK antibody (Cell Signalling, UK)
- Anti GAPDH antibody (abcam, UK)
- Anti-cytochrome c antibody (abcam, UK)
- Anti- phospho PDK1 (Ser241) antibody (Cell Signalling, UK)
- Anti-cyclin D1 antibody (Santa Cruz, UK)
- Anti α -actin (Sigma, UK)
- ^3H thymidine solution (Amersham, UK)
- Waymouth's medium (Gibco, UK)
- Anti-mouse IgG HRP-linked secondary antibody (Cell Signalling, UK)
- Anti-rabbit IgG HRP-linked secondary antibody (Cell Signalling, UK)
- Platelet Derived Growth Factor (PDGF) (Sigma,UK)
- ApoTox-Glo reagent (Promega, Madison, USA)
- ROS-Glo H_2O_2 reagent (Promega, Madison, USA)
- ToxGlo reagent (Promega, Madison, USA)
- Ethidium bromide (Life Technologies, Paisley, UK)
- Sodium Pyruvate (Sigma, UK)
- Uridine (Sigma, UK)
- Isolate II RNA mini kit (Bioline, London, UK)
- Tetro cDNA synthesis kit (Bioline, London, UK)
- RT2 SYBR Green Mastermix (QIAGEN, USA)

- MicroAmp tubes (Applied Biosystems, Paisley, UK)
- mTORC1 siRNA silencer (Life Technologies, Paisley, UK)
- Cell culture plates (Applied Biosystems, Paisley, UK)
- Taqman master mix (Applied Biosystem, Paisley, UK)
- Vector-shield containing DAPI (Vector laboratories, USA)
- Tris (2-carboxyethyl) phosphine (TCEP, Sigma, UK)
- TrypLE™ Express (Life Technologies)
- Penicillin and streptomycin (PEN-STREP® BioWhittaker™)
- Hoechst 33342 (Thermo Scientific, UK)
- Anti-mouse Fluorescein (Vector Labs)
- Anti-rabbit Fluorescein (Vector Labs)
- Dihydroethidium (abcam, UK)
- Dichlorofluorescein (Sigma, UK)
- Enhanced Chemiluminescence reagent (Thermo Fisher Scientific, UK)
- MitoTracker® (Life Technologies, Paisley, UK)

Methods

2.2 Cell harvest and cell culture

Twelve-week-old male Sprague-Dawley rats of body weight ~300g were used. They were euthanized by schedule 1 CO₂ asphyxiation and exsanguination. All cell culture procedures were conducted in class II biological safety cabinet and following strict aseptic condition. This project includes the study of pulmonary arterial smooth muscle cells (PASMCs). Therefore, the proximal pulmonary arteries (Figure 2.1) were harvested from adult Sprague-Dawley rats and cut into approximately 3 mm long rings and cleaned independently. Small rings of the vessels were transferred into T25 tissue culture flasks containing 5 ml of a mixture (50:50) of F-12 medium (Invitrogen) and Waymouth's medium (Invitrogen) with 10% (v/v) foetal calf serum (FCS) and 5% (v/v) penicillin streptomycin (PEN-STREP® BioWhittaker™). The PASMCs were cultured under standard normoxic conditions at 37° C in a 21% O₂/5% CO₂ incubator for approximately three weeks until confluent. The medium was changed every 48-72 hours and the cellular growth was monitored using a light microscope until they reached 70-80% confluency.

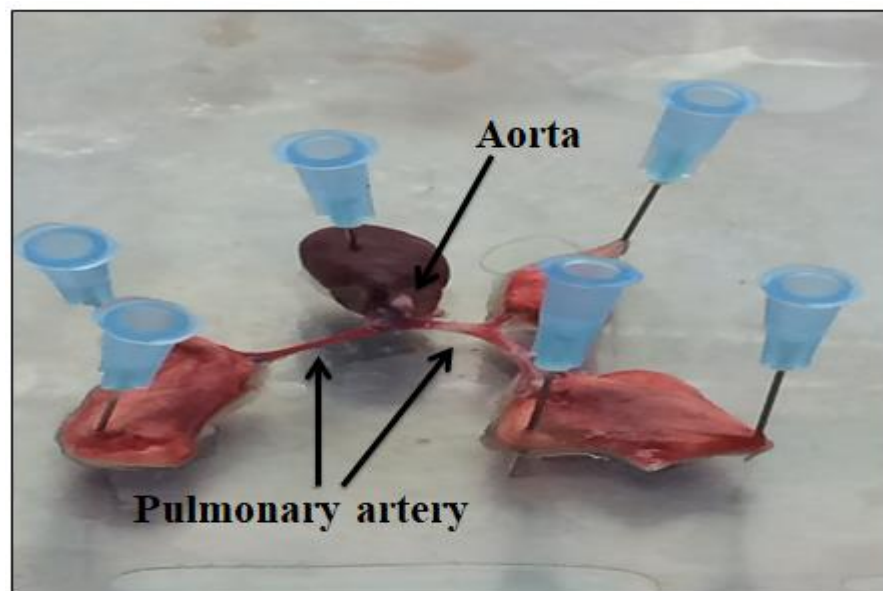


Figure 2.1 Dissected Proximal Pulmonary Artery from a Sprague-Dawley rat

2.2.1 Cell count and subculture

Rat vascular smooth muscle cell passaging was required when the cells reached the desired confluency (Passage 0). After 21 days of incubation, the media was aspirated from 25 cm² cell culture flasks and the small arterial rings were discarded and the seeded PASMCs were transferred into new cell-culture flasks. In order to split the cells (Passage 0) into 75 cm³ cell culture flasks (Passage 1), cells were detached by the addition of 4 ml of TrypLE™ Express (Life Technologies). Afterwards, the flask was kept in a CO₂ incubator for five minutes to accelerate the TrypLE™ Express role. Then, the solution was transferred to a conical 15 ml tube and the tube was centrifuged (1000 x RPM) for 10 minutes. Following the supernatant aspiration, 1 ml of media (containing 10% FCS) was added as a feeder source and mixed gently to achieve a good cell suspension for passaging. Cells were then allowed to grow in 75 cm³ cell culture flasks containing 10 ml media with 10% FCS to 70% confluency (Passage 1) and they were again split into six well plates (2 ml media with 10% FCS each well), 24 well plates (1 ml media with 10% FCS each well) or 96 well plates (0.2 ml media with 10% FCS each well) for further analysis. A haemocytometer was used for cell counting with the injection of 10 µL of the cell aliquot into the haemocytometer from both sides. The cells were counted in three squares at each side (a total of six squares) under the microscope at x40 magnification. The splitting of VSMCs was conducted when the cells were ~70-80% confluent. It is known that cells obtained from primary sources can undergo loss of phenotypic characteristics after repeated passage (Anderson et al., 1970). Therefore, in an attempt to maintain a near wild type phenotype a low-passage number (2 – 4) was studied.

2.3 Immunohistochemical (IHC) confirmation of the isolated PASMCs

To confirm smooth muscle cells were being isolated from the rat pulmonary artery, immunohistochemical staining was performed. Glass cover slips were added into each well of a six-well plate prior to use under sterilized conditions. PASMCs were then seeded and grown on coverslips until they reached 70% confluence. The cells were then fixed in 4% paraformaldehyde for 10 minutes. To permeabilise the cells, 0.1% (v/v) Triton X-100 was added for 10 minutes to permit the interaction of the antibody with the targeted protein marker within the cells. Cells were blocked with

1% (w/v) bovine serum albumin (BSA) in PBST (PBS with 0.1% (v/v) tween and 22.5 mg/ml glycine) for 1 hour at room temperature. Thereafter, smooth muscle cell markers primary antibodies such as anti- α -actin (1:400 dilution, Sigma, UK) and myosin heavy chain (1:100 dilution, R&D Systems) were diluted in 0.1% (w/v) BSA for overnight incubation at 4 °C. Coverslips were washed three times with PBS before adding the secondary antibodies. Suitable fluorescent secondary antibodies, such as anti-mouse Fluorescein (1:150 dilution, Vector Labs) and anti-rabbit Fluorescein (1:150 dilution, Vector Labs), were prepared in 0.1% (w/v) BSA and added for 1 hour in darkness. While maintaining the coverslips in darkness, coverslips were washed three times with PBS. In order to visualize the cellular nuclei, Hoechst stain (Molecular Probes) was utilized for 1 minute followed by rinsing with PBS. Coverslips were mounted on to slides by a drop of DPX Mountant Media (Sigma, UK). The slides were stored in darkness before visualisation. The cells were visualized using an epifluorescence upright microscope (Nikon Eclipse E600 microscope with a Hamamatsu C11440-36U camera and Nikon Plan Apo 60x / 1.40 Oil microscope lens). A DAPI filter set (with excitation and emission wavelengths of 365 nm and 435-485 nm respectively) was used to detect the Hoechst-stained nuclei, whilst a FITC filter set (excitation and emission wavelengths of 470 nm and 515-555 nm respectively) was selected for protein visualization.

2.4 Experimental set-up: cells exposure to acute hypoxia

The hypoxic exposure was carried out by maintaining the PSMCs in a nitrogen-supplemented, humidified, temperature-controlled incubator (Panasonic MCO-19M), which allows control of the internal oxygen levels (0%-21%) while the CO₂ level was kept at 5%. In order to sustain a proper degree of hypoxia, a large amount of nitrogen was required. Thus, nitrogen cylinders were connected by an automatic gas cylinder change over units to provide a fresh supply of nitrogen as needed. The effect of acute hypoxia on cell proliferation and vascular remodeling is generally studied by the culture of vascular cells. Cells are usually exposed to hypoxia (0–10% O₂), for 24 hours, with measurement of cell proliferation or the signalling pathways that regulate cell proliferation (Welsh et al., 2001, Hou et al., 2007, Zhang et al., 2014). Therefore, in keeping with previous published studies PSMCs were exposed to hypoxia for 24 hours.

PASMCs were seeded at 5×10^3 density into two 6 well culture plates. Each plate was labelled: one plate as a normoxic group and the second plate as a hypoxic group. Plates were subsequently incubated in a CO₂ incubator at 37°C/5% CO₂ until cells reached ~60% confluency. Then, the cell culture plate which was labelled as hypoxic was transferred to the hypoxic incubator whereas the normoxic plate was kept in the normoxic incubator. Three wells were used. The first well had the quiescent 0.1% FCS (background) while the other two wells had the stimulant (10% FCS or PDGF) with/ without Mdivi-1. Mdivi-1 was added 30 minutes prior to stimulation. Following the same cell culture conditions (outlined above) cells were processed for Western blot (section 2.5) and qRT-PCR experiments (section 2.9). In this project I have used 10 µM Mdivi-1 as previously published studies have demonstrated that 10 µM Mdivi-1 in vascular smooth muscle cells inhibits mitochondrial fission-fusion with a good effect (Salabei and Hill, 2013, Zhuang et al., 2017). As Mdivi-1 was dissolved in dimethyl sulfoxide (w/v), vehicle control experiments were performed (0.2% (v/v) dimethyl sulfoxide) when the effect of Mdivi-1 was studied.

2.5 Western blot

2.5.1 Preparation of whole cell extracts and stimulation

PASMCs were split into two 6-well plates: a hypoxic plate and a normoxic plate. Cells were grown to 70% confluence in a standard CO₂ incubator using 10% FCS media and then quiesced with 0.1% FCS for 24 h. When the cells were stimulated with FCS or a specific mitogen such as PDGF, the normoxic 6-well plate was maintained in a standard CO₂ incubator with normal oxygen level (21% O₂) while the hypoxic 6-well plate was transferred into the hypoxic incubator (Panasonic MCO-19M) and kept for 24 h. Following stimulation, 200 µL of pre-heated sample buffer (63 mM Tris-HCl (pH6.8), 2 mM Na₄P₂O₇, 5 mM EDTA, 10% (v/v) glycerol, 2% (w/v) SDS, 50 mM DTT, 0.007 (w/v) bromophenol blue) was added into each well, and the cells were then scraped from the wells onto ice. Samples (the lysate) were then transferred to labelled Eppendorf tubes and stored at -20°C. The samples were boiled for 5 minutes for protein denaturation prior to use.

2.5.2 SDS-Polyacrylamide Gel Electrophoresis (SDS-PAGE)

Running component was prepared at 10% (w/v) acrylamide as follows: (N, N'-methylenebis-acrylamide (30: 0.8), 0.375 M Tris (pH 8.8), 0.1% (w/v) SDS and 10% (w/v) ammonium persulfate (APS). In addition, 0.05% (v/v) TEMED (N, N, N, N', N'-tetramethylethylenediamine) was added to initiate the polymerisation step. The running gel solution was then dispensed via a plastic bulb pipette between two assembled glass plates. Isopropanol (20 μ L) was layered to top/ flatten the running component of the gel. The gel plates were then kept at 35-40°C for 30 minutes in a drying oven. Once polymerised, the excess isopropanol/ polyacrylamide was rinsed off with distilled water, and the loading gel was prepared. This contained (10% (v/v) N, N'-methylenebis-acrylamide (30:0.8), 125 mM Tris pH 6.6, 0.1% (w/v) SDS, 0.05% (v/v) APS and 0.05% (v/v) TEMED). The loading gel was added over the running gel. The proper well comb was carefully inserted into the loading gel and left to set for 30 minutes at room temperature. After polymerisation, the comb was removed and the polyacrylamide gels were placed into an electrophoresis tank (Bio-Rad Mini-PROTEAN®-3). An electrophoresis buffer (25 mM Tris, 192 mM glycine, 0.1% (w/v) SDS) was added to the tank. The SDS-PAGE molecular weight ladder and the protein samples were loaded into the wells of the loading gel using a Hamilton syringe and then separated by electrophoresis (for 45 minutes at a voltage of 200 V).

2.5.3 Electrophoretic transfer of proteins onto a nitrocellulose membrane

The separated proteins were transferred onto a nitrocellulose membrane (GE Healthcare, Life Sciences) through electrophoretic blotting. The gel was carefully removed from the glass plates and placed to form the transfer sandwich. The transfer sandwich included a nitrocellulose membrane in the middle against the gel, two blot papers and two Nylon pads. The transfer buffer (25 mM Tris, 195 mM glycine, 20% (v/v) methanol) was added into a Bio-Rad Mini-Trans-Blot™ tank, which included the immersed cassette, and a constant voltage (100 V) was applied for 1 hour. The tank required the ice reservoir to be cold.

2.5.4 Immunological detection of protein

Following transfer, the nitrocellulose membranes were then carefully removed from the cassettes and the blocking of non-specific binding proteins was achieved with the use of 3% (w/v) BSA in Tris-Tween buffered saline solution (TTBS – 150 mM sodium chloride, 20 mM Tris base pH 7.4, 0.02% (w/v) Tween-20) for 1 h at room temperature on a slow rocking plate. The nitrocellulose membranes were then removed from the blocking buffer and incubated with specific antibodies overnight in a cold room. Table 2.1 shows the primary antibodies utilized in this study.

Primary antibody	Dilution	Company
Anti-phospho/Total ERK1/2	(1:7500)	Cell Signalling, UK
Anti-phospho p38 MAPK	(1:1000)	Cell signalling Tech., USA
Anti-phospho JNK	(1:1000)	New England Biolabs, UK
Anti-cyclin D1	(1:1000)	Santa Cruz Biotechnology Inc., USA
Anti-cytochrome C	(1:5000)	Abcam, UK
Anti-HIF-1 α	(1:3000)	Santa Cruz Biotechnology Inc., USA
Anti-phospho PDK1	(1:1000)	Cell Signalling, UK
Anti-GAPDH	(1:40000)	Cell Signalling Tech., USA
Actin	(1:1000)	Cell Signalling, UK

Table 2.1 Primary antibodies for Western blot analysis

Following the incubation with the primary antibodies, membranes were incubated with the secondary antibodies (1% (w/v) BSA + TTBS dilution) for 1 hour at room temperature when the washing step was completed (4 x 10 minutes with TTBS on a rocking plate). The nitrocellulose membranes were then washed with TTBS (3 x 10 minutes) at room temperature on the rocking plate. Enhanced chemiluminescence reagent (ECL) was added in the dark room and applied to each nitrocellulose membrane for 1 minute with agitation, lifted from the tray onto a paper towel to remove any excess ECL. The membranes were then placed in exposure cassettes with an X-ray film on top (Kodak Ls X-OMAT) for the required exposure time

under dark room conditions and developed using X-OMAT (KODAK M35-M X-OMAT processor).

2.5.5 Re-probing and stripping of nitrocellulose membrane

To re-probe the nitrocellulose membrane for measuring the total loading protein, the membranes were stripped by incubating the nitrocellulose membrane in 15 ml of stripping buffer (0.05M Tris-HCl, 2% (v/v) SDS, and 0.1M β -mercaptoethanol). This stage included incubation of the membrane at 60°C for 1 hour with shaking to eliminate the original antibodies from the membrane. The stripping buffer was then discarded and the membrane washed 3 times every 15 minutes in TTBS to remove the residual stripping buffer. After the last wash, the membrane was incubated with the appropriate primary antibody overnight with 1% (w/v) BSA in TTBS. The blots at this stage were then ready for the immunological detection protocol as explained previously.

2.5.6 Scanning Densitometry:

All film obtained from Western blotting were scanned using a GS-800 Calibrated Densitometer (Bio-Rad) and the exposed blots were analysed by densitometry through the use of Image J software.

2.6 Amido black protein assay

Following whole cell extraction and sample preparation, an Amido black protein assay was used in order to measure and normalize protein concentration of each sample and to ensure the loading protein of each test sample was equal. A series of 1:1 dilutions in sampling buffer was prepared and the standard curve was performed by the use of 1 g/ml BSA stock (in H₂O). The samples and each BSA dilution was spotted (5 μ L) on a strip of cellulose acetate and then left to dry. The strip of cellulose was stained with Amido black stain (0.25% (v/v) Amido black, 45% (v/v) methanol, 45% (v/v) dH₂O, 10% (v/v) glacial acid) at room temperature for 10 minutes with shaking. The excess stain was washed by the use of Amido black destain buffer (45% (v/v) methanol, 45% (v/v) dH₂O, 10% (v/v) glacial acid) until the background became closely white. The strip was then left to dry at room

temperature and each sample spot was placed in a 1.5 ml Eppendorf tube and dissolved in 500 μ L dissolving solution (80 ml formic acid, 10 ml glacial acid and 1 ml 100% (v/v) TCA). All Eppendorf sample tubes were kept in a water bath (60° C) for 30 minutes and 250 μ L from each sample was added to a 96-well plate and was measured at 620 nm. Finally, the BSA standard curve was plotted and the concentration of the test samples was interpolated.

2.7 Cell proliferation [³H]-thymidine incorporation assay

DNA synthesis was used as a measure of PASMC proliferation. DNA synthesis was measured by the [³H]-thymidine incorporation assay. Cells were grown to around 70-80 % confluence into a T75 flask and then were seeded into pairs of 24-well plates and incubated in a CO₂ incubator (21% oxygen) until they were 60 % confluent. Cells were then quiesced with 0.1% foetal calf serum (FCS) overnight. Cells were then exposed to a suitable agonist or treatment (as described in section 2.4) and immediately transferred from the CO₂ incubator to the hypoxic incubator (Panasonic MCO-19M) for 24 h in comparison to the corresponding cell condition that was maintained in a CO₂ incubator (normoxia) as a control. The hypoxic level in the hypoxic incubator was adjusted based on study intervention (10%, 5% and 3% oxygen). ³H-thymidine aqueous solution (GE Healthcare®) was added (2 μ L /9.25 kBq) to each well after 18 h stimulation. The assay was terminated at 24 h and ³H incorporated DNA synthesis was measured by scintillation counting.

Finally, media in each group was disposed of and each well was washed one time with 1 ml cold PBS for 10 minutes and 4 times with 1 ml 10% (v/v) trichloroacetic acid (TCA, Sigma) for 10 minutes. Following the washing step, 250 μ L 0.1% (v/v) sodium hydroxide/sodium lauryl sulphate (SDS) solution was added into each well. 2 ml of Emulsifier-safe™ scintillation fluid (PerkinElmer, Boston, USA) was added to the scintillation vials and mixed gently with the well contents. Each vial was loaded into the scintillation machine in order to measure the radioactive counts. Counts were expressed as disintegrations per minute (DPM) and each stimulant was replicated in quadruplicate.

2.8 Cell migration assay

Pulmonary artery smooth muscle cells (PASMCs) were seeded in 6 well plates and incubated with 10% FCS in the CO₂ incubator. When the cells reached 90% confluency, they were quiesced with 0.1% FCS for 24 h. A vertical scratch was then created in the middle of the well using a sterile cell scraper which crosses a horizontal black mark that was drawn on the bottom of each well. Once the scratch was performed, the bottom side of the plate was cleaned to remove the black mark in order to start taking the scratch image at 0 h (the background control image) using a Motic inverted light microscope. Then, cells were stimulated with PDGF (5 ng/ml) and the normoxic and the hypoxic plates were incubated in a normoxic (21% oxygen) and hypoxic (3% oxygen) incubator, respectively for 48 h. Mitochondrial treatment (Mdivi-1) was added 30 minutes before stimulation. During stimulation, images were taken at 12 h, 24 h and 48 h. Captured images of the cells at different stimulation times show how cells migrate from both border sides to the scratch area of each well and the distance was measured and analysed using ImageJ software. For example, in order to investigate the ability of the cells to migrate from both scratch sides, as a result from PDGF stimulation, a photomicrograph of the scratch distance was immediately taken once the scratch was created and the cells were stimulated (a photomicrograph at 0 h). This time represents the total scratch distance (100%) as a control that was compared to the scratch distance at each stimulation time (Figure 4.7). PASMCs were stimulated with PDGF for 12, 24 and 48 h. Therefore, the gap closure, the migratory effect, was checked after 12, 24 and 48 h under normoxic and hypoxic conditions. A similar process was used when the effect of Mdivi-1 on cell migration was studied.

2.9 Polymerase chain reaction (PCR) amplification

2.9.1 RNA isolation for PCR

After the incubation period, total RNA was isolated using isolate II RNA Mini Kit (Bioline, London, UK). The cells were trypsinized, transferred into 15 ml tubes and centrifuged at 1500 rpm for 10 minutes. Following centrifuging, the supernatant was aspirated and the cell pellet was kept in the tube. The Cell lysis step was initiated by adding 350 μ L of lysis buffer and 3.5 μ L of β -Mercaptoethanol into the cell pellet. The lysate was transferred into isolate II filter (violet) in a 2 ml

collection tube and centrifuged at 11000 g for 1 minute at room temperature. The isolate II filter was then discarded and 350 μL of 70% ethanol was added to the homogenized lysate and mixed by pipetting up and down 5 times. Each sample was then loaded into isolate II RNA Mini Column (blue) in a new 2 ml collection tube and centrifuged at 11000 g for 30 seconds. The silica membrane was then desalted by adding 350 μL membrane desalting buffer and centrifuged at 11000 g for a minute in order to dry the membrane. The DNase I reaction mixture was prepared to use in the DNA digestion step by adding 10 μL of reconstituted DNase I to 90 μL of reaction buffer for DNase I. The DNA digestion step was then performed by applying 95 μL of DNase I reaction mixture directly onto the centre of the silica membrane of each column and the column was then incubated for 15 minutes at room temperature. The silica membrane was then washed once with 200 μL wash buffer RW1 and centrifuged at 11000 g for 30 seconds. The membrane was then washed with 600 μL wash buffer RW2 and centrifuged at 11000 g for 30 seconds and finally with 250 μL wash buffer RW2 and centrifuged at 11000 g for two minutes to dry the membrane completely. The final step was eluting the RNA, which is accomplished by adding 60 μL RNase-free water directly onto the centre of the silica membrane and the column was centrifuged at 11000 g for 1 minute. Total RNA sample concentrations were measured using the Nano Drop spectrophotometer.

2.9.2 cDNA preparation:

Total RNA was reversed transcribed to complementary DNA (cDNA) using a Tetro cDNA synthesis kit (Bioline, London, UK) in order to quantify the mRNA transcripts of target genes. All RNA concentrations were normalised to be equal in all reactions and diluted to 12 μL with DEPC-treated water. Then, the mixture was prepared by adding 1 μL of oligo-dT primer mixture as the first strand synthesis primer, 1 μL of dNTP mixture (10 mM), 4 μL of 5x RT buffer, 1 μL of RiboSafe RNase inhibitor and 1 μL of Tetro Reverse Transcriptase to be completed to 20 μL . The samples were then mixed gently by pipetting, reactions incubated at 45°C for 30 minutes and terminated by incubating at 85°C for 5 minutes followed by chilling on ice. Samples were stored at -20°C until real-time PCR experiments.

2.9.3 Quantitative Real-Time Polymerase Chain Reaction (qRT-PCR)

amplification

The real-time Q-PCR was carried out by placing the samples in sterile PCR Cycle plate (Applied thermoFisher). Each 10 μl PCR reaction contained; 5 μL SYBR select Master (Applied Biosystems), 0.3 μl of 1 pmol/ μL of both reverse and forward primes, 1 μL of the cDNA template and 3.4 ml of DEPC- treated water, triplicate were generated for each sample. The thermal cycling and detection were carried out on a stepOne Plus real-time PCR system. The thermal cycle consisted of an initial uracil-DNA glycosylase activation of 2 minutes at 50°C (UNG incubation), the AmpliTaq Gold activation for 10 minutes at 95°C, followed by 1 cycle 15 seconds at 95 °C (denature) then 1 minute at 60°C 40 cycles (Anneal/Extend).

2.9.4 Relative quantification [$\Delta\Delta\text{Ct}$] method for real-time PCR:

The quantification method used with the PCR results was the relative quantification ($\Delta\Delta\text{Ct}$) method. This method normalises Ct values of the target gene to the Ct value of the reference gene in order to get the fold change in gene expression between the control and treated samples according to the following equations:

- 1- $(\Delta\text{Ct}) = \text{Ct}_{\text{target}} - \text{Ct}_{\text{reference gene}}$ (This is to calculate the difference between the treated and control samples).
- 2- $(\Delta\Delta\text{Ct}) = (\text{Ct}_{\text{target}} - \text{Ct}_{\text{reference}})_{\text{treated}} - (\text{Ct}_{\text{target}} - \text{Ct}_{\text{reference}})_{\text{control}}$ (This is to calculate the difference between the ΔCt s of the treated and control samples). $\Delta\Delta\text{Ct} = \Delta\text{Ct}_{\text{treated}} - \Delta\text{Ct}_{\text{control}}$
- 3- The fold change in the samples = $2^{-\Delta\Delta\text{Ct}}$

2.9.5 PCR primers for SYBR green based real-time assays:

Primers were designed to ensure that they only bind to their target genes and avoid non-specific products in SYBR green assays. All primers were designed as described in the following process; Sequences of the genes were obtained from GeneBank. To identify potential primer pairs, the sequences were imported into the PrimerQuest web tool (<http://eu.idtdna.com/Primerquest/Home/Index>) in the

Integrated DNA Technologies (IDT) website (<http://eu.idtdna.com/site>). “qPCR – 2 Primers and Intercalating dye” was chosen in the setting. Amplicon size between 90 – 140 was chosen to maximise PCR efficiency. Primer sequences were generated and only the one with good specificity was selected and validated using Primer-BLAST (Basic Local Alignment Search Tool) in the National Centre for Biotechnology Information (NCBI) website (<http://ncbi.nlm.nih.gov/tools/primer-blast/index.cgi>). Melting temperature (T_m) of all primers was selected between 47 - 62°C and the ΔT_m between the forward and the reverse was less or equal to 1°C. Primer lengths were selected between 18-30 bases and the primers GC content was between 35- 70%.

Genes	Forward Primer	Reverse Primer
UBC	GGTCAAACAGGAAGACAGACGTA	CACACCCAAGAACAAGCACA
PCNA	ACCTCACCAGCATGTCCAA	CATAGTCTGAAACTTTCTCTTGAT TTG
ERK1	GGATCCGCTAGCGAGCCCAGGGG AACTGC	GCGGATCCTTAGGGGGCCTCTGG TGC
Cyclin D1	GAGAAGTTGTGCATCTACTG	AAATGAACTTCACATCTGTGGC
Cdkn2a	GGCACCAGAGGCAGTAACCAT	GACCTTCCGCGGCATCTATG
HIF-1α	GTTTACTAAAGGACAAGTCACC	TTCTGTTTGTGAAGGGAG
HIF-2α	TGCTCCCACGGCCTGTAC	TTGTCACACCTATGGCATATCAC A
FIH-1	GCCCCTACTATGTGCGTTTC	GGCCCAAATAAATACTATCTGA
PI3K	CGCCCCCTTAATCTCTTACA	TGGATGTTCTCCTAACCATCTG
mTORC1	TTGAGGTTGCTATGACCAGAGAGA A	TTACCAGAAAGGACACCAGCCAA TG
Akt	CTTCGTGAACATTAACGACAGGGC C	AATGGCCACCCTGACTAAGGAGT GG
P70s6k	GGAGCCTGGGAGCCCTGATGTA	GAAGCCCTCTTTGATGCTGTCC
PTEN	AGACCATAACCCACCACAGC	TTACACCAGTCCGTCCTTTCC
4EBP1	TAGCCCTACCAGCGATGAGCCT	GTATCAACAGAGGCACAAGGAG GTAT
P53	ATTTGTATCCCGAGTATCTG	GGTATACTCAGAGCCGGCCT
ATPase 6	CCTCTTTCATTACCCCAACA	GAATTACGGCTCCTGCTCA
DRP1	AGACCTCTCATTCTGCAACTG	TTACCCATTCTTCTGCTTCC
Arg1	TTCTCAAAAGGACAGCCTCG	AGCTCTTCATTGGCTTTCCC
TFAM	AGTTCATACCTTCGATTTTC	TGACTTGGAGTTAGCTGC
COX-II	GGCTTACCCATTTCAACTTGCC	CACCTGGTTTTAGGTCATTGGTTG

Table 2.2 Primers for real-time PCR analysis

2.10 Fluorescence-activating cell sorting (FACS) analysis

Cells were cultured with 10% FCS and maintained in a normal CO₂ incubator until they reached 70% confluency. Cells were quiesced for 24 h and then washed with PBS. Cells were then treated with PDGF and exposed to hypoxia for 72 h prior to analysis. Mdivi-1 (10 μM) was added 30 minutes before PDGF stimulation. At the end of the stimulation period, the media was aspirated and the cells were trypsinized, transferred into 15 ml tubes and centrifuged at 1500 rpm for 10 minutes. Following centrifuging, the supernatant was aspirated (avoiding pellet contact) and 1 ml of cold ethanol 70% (v/v) was added. Cells were then stored at -20°C until the day of analysis. Cells were washed with 1 ml of cold PBS, centrifuged at 3000 rpm for 10 minutes and then re-suspended in 250 μL cold PBS. Cells then were transferred into FACS tubes and 5 μL RNase A (50 μg/ml) was added into the tubes and incubated at 37°C and 5% CO₂ for 60 minutes. Finally, 13.5 μL propidium iodide (50 μg/ml) was added to each sample and samples were vortexed before analysis. Samples were read in FACSCANTO II (BD Bioscience Boston, USA) flow cytometer and data were analyzed using FACS Diva software (FACS scan, Becton Dickinson, Oxford, UK). A total of 10000 events were measured per sample and gating was determined using propidium iodide stained populations. Cell cycle events were gated on G1, S, G2/M and sub G1 and the % of total events in each phase was measured.

2.11 Reactive oxygen species (ROS)

To measure ROS generation by PSMCs, dihydroethidium (DHE) and dichlorofluorescein (DCF) fluorescent dyes were used to detect the superoxide (O₂⁻) level and intracellular hydrogen peroxide release, respectively. PSMCs were seeded at 2 × 10³ cells/well in black clear bottom 96-well plates (one labelled as a normoxic plate and the other was labelled as a hypoxic plate). Initially, both plates were cultured with 10% FCS and maintained in a normal CO₂ incubator until they reached 70% confluency. Then, the cells were quiesced for 24 h with 0.1% FCS. Cells in the 96-well plate (labelled as a hypoxic plate) were then exposed to hypoxia (3% oxygen) for 24 h with/without PDGF (5 ng/ml) in comparison to each parallel condition under normoxic condition (21% oxygen). Mdivi-1 (10 μM) was added 30 minutes before PDGF stimulation. At the end of the 24 h stimulation,

dihydroethidium (DHE) or dichlorofluorescein (DCF) were added to each well and incubated at room temperature for 30 minutes. The fluorescence of each sample was then measured in a POLARstar plate reader (Omega; SciQuip, Cambridge, UK) which corresponds to the level of ROS released by the cells in each treatment. Data were obtained at excitation and emission wavelengths of 518/605 nm and 485/520 nm for superoxide ($O_2^{\cdot-}$) and hydrogen peroxide detection, respectively.

2.12 Cellular ATP assay

PASMCs were cultured in 96 well plates until they reached ~70% confluency. Cells were quiesced for 24 h (0.1% FCS) and were then stimulated with 0.1% FCS or 10% FCS or PDGF (5 ng/ml) and exposed to different oxygen levels: normoxia (21% oxygen) and hypoxia (3% oxygen) for 24 h. Drugs such as Mdivi-1 and imatinib were added to the cells 30 minutes before stimulation. At the end of the 24 h stimulation, 100 μ l of mitochondrial ToxGlo reagent (Promega, Madison, USA) was added to each well and incubated at room temperature for 30 minutes. The luminescence of each sample was then measured in a polar star plate reader which corresponds to the level of ATP released by the cells in each treatment.

2.13 Cell apoptosis assay

PASMCs were cultured in 96 well plates until they reached ~70% confluency. Cells were quiesced for 24 h using 0.1% FCS and subsequently exposed to hypoxia and stimulated with/without 5 ng/ml PDGF for 24 h. The mitochondrial treatment (Mdivi-1) was added to the cells 30 minutes before stimulation. As a positive apoptotic control, one well of stimulated cells was treated with 1 μ M paclitaxel. At the end of the 24 h stimulation, 100 μ L of ApoTox-Glo reagent (Promega, Madison, USA) was added to each well and incubated at room temperature for 1 hour. The luminescence of each sample was then measured in a polar star plate reader which corresponds to the caspase 3/7 release within the cells.

2.14 Generation of Mito-depleted PSMCs

Chronic exposure of cells to ethidium bromide leads to the selective inhibition of mitochondrial DNA replication and the generation of cell lines that lack mitochondrial DNA (termed Rho cells) (Chandel and Schumacker, 1999). Cells depleted of mitochondrial DNA (Rho cells) were generated by incubation in 10% FCS media (10 ml per T75 flask) containing ethidium bromide (50 ng/ml) for 21 days. The media was also supplemented with 50 ng uridine and 1 mM sodium pyruvate. Control cells were incubated in the same media lacking ethidium bromide for 21 days. The efficiency of the mitochondrial loss of bioactivity was measured by the level of expression of mitochondrial marker genes at the end of the 21 day incubation.

2.15 siRNA transfection of mTORC1 in PSMCs

Small interfering RNA (siRNA) is a molecular biology method, which is utilized to study the role of various genes in cellular processes; it causes the switching off of the expression of the gene of interest. In order to examine the knockdown of mTORC1 in PSMCs, cells were transfected with siRNA against mTORC1 (Life Technologies, Paisley, UK) in comparison to non-target siRNA (NT). PSMCs were seeded in 6 well plates and cultured until they reached 50-60% confluence prior to transfection. Two Eppendorf tubes were prepared: Tube A and Tube B. Tube A contained the siRNA mixture, a known amount of siRNA was required to prepare the specific concentration of siRNA then completed the volume to 100 μ L of Optimum media (Life Technologies, Paisley, UK). Tube B contained 5 μ L of Lipofectamine RNAiMAX[®] (Invitrogen[®], Paisley, UK) and 95 μ L of Optimum media. Tube A was then added to Tube B and mixed gently. The tubes were left for 20 minutes at room temperature to allow complex formation. Full media was removed from the cells and final mixture (200 μ L) was added into the well to make it up to the total volume of 1 ml of Optimum. Cells were incubated at 37°C in a 5% CO₂ incubator for 8 h. The transfection mixture was then replaced with normal media and cells then were incubated for 72 h at 37°C in a 5% CO₂ incubator. Cells were then lysed and RNA was isolated for further PCR analysis to measure the expression of genes listed in Table 2.2.

2.16 Immuno-fluorescence staining of PCNA

Using the protocol detailed in section 2.3, anti-PCNA primary antibody (1:1000 dilution, abcam, UK) and the appropriate fluorescent secondary antibody anti-rabbit Fluorescein (1:150 dilution, Vector Labs) were used. PCNA inside the cell nuclei of PSMCs was visualized by epifluorescence upright microscope (Nikon Eclipse E600 microscope with Hamamatsu C11440-36U camera and Nikon Plan Apo 60x / 1.40 Oil microscope lens). The FITC filter (at excitation and emission wavelengths of 470 nm and 515-555 nm) was selected. The intensity of PCNA positive area was quantified using Image J software (version 1.50d). A rectangular shape was placed around the nuclei (the region of interest, ROI), followed by clicking 'M' which generates the density for PCNA. For each nuclei, measurements were normalized using the same ROI (Equal ROI was saved by clicking 'T'). In each condition (either normoxia or hypoxia), three ROI were measured and the mean was calculated using excel.

2.17 Identification of Mitochondrial morphology

PASMCs were grown on coverslips until they reached 70% confluence. Cells were stimulated with suitable agonists and immediately incubated in a normoxic/hypoxic incubator for 24 hours. To mark mitochondria, cells were stained with the MitoTracker[®] dye (Life Technologies, Paisley, UK) for 30 minutes in a normoxic/hypoxic incubator. Following incubation, media was aspirated and the cells were washed 2 times with PBS. Cells were fixed with 4% paraformaldehyde for 15 minutes at room temperature and were then washed 2 times with PBS. Coverslips were mounted on to slides by a drop of DPX Mountant Media (Sigma, UK). The mitochondria were visualized using an epifluorescence upright microscope. The microscopic images were then opened using Image J software (version 1.50d) and the mitochondrial length was quantified. A free hand line was traced on the individual mitochondria. Each line was measured by clicking 'M' which generates a value that directly related to the estimated mitochondrial length in Pixels (Figure 2.2). At least 10 mitochondrial lengths were analysed per cell and the mean mitochondrial length per cell was calculated using excel.

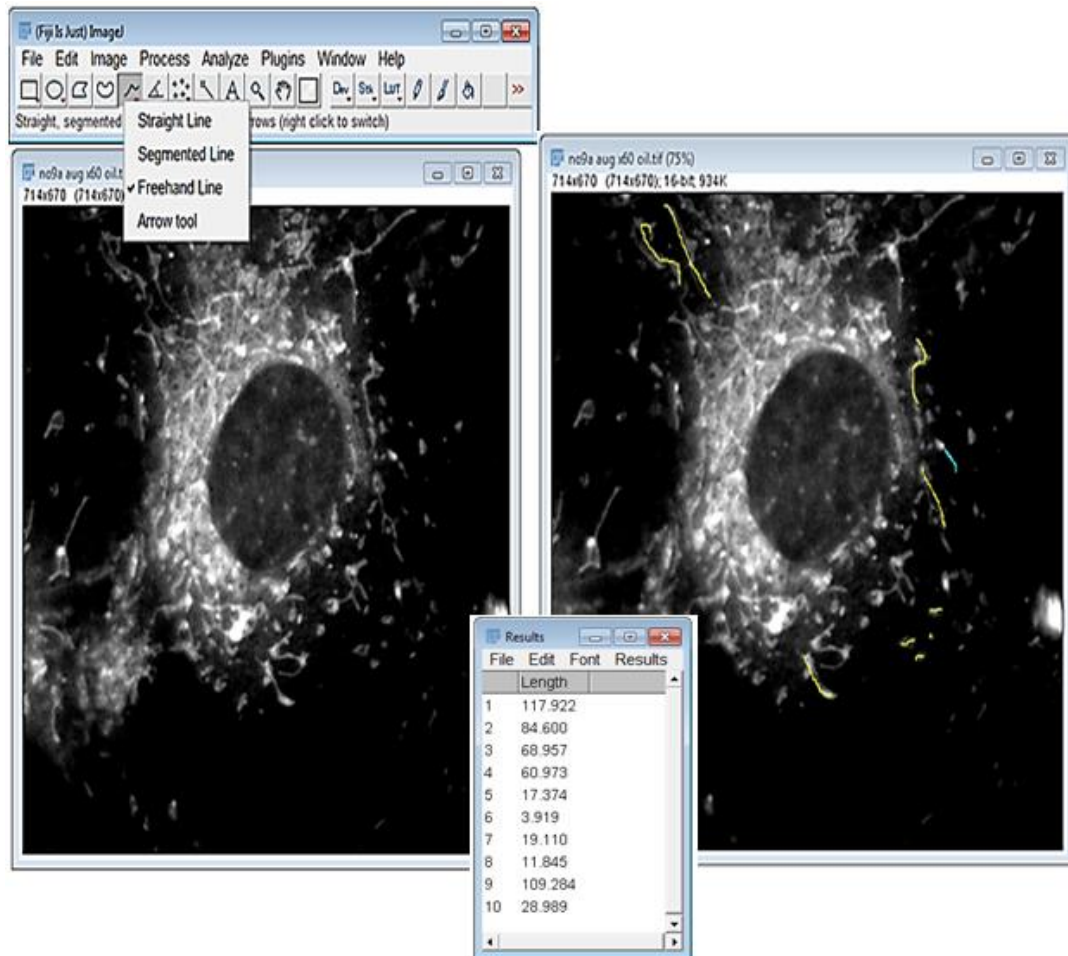


Figure 2.2 Demonstration of mitochondrial length quantification within a cell using Image J. a Tiff image of PASMCS stained with MitoTracker was opened on image J (the left image). A free hand line was selected to trace individual mitochondria manually (shown by the yellow line, the right image). At least 10 mitochondria were measured within a cell. Corresponding lengths of mitochondria were generated automatically as shown in the table.

2.18 Data and statistical analysis:

Values reported are presented as mean \pm SEM (standard error of the mean). Microsoft Excel 2010 was used to generate the figures. Comparisons between groups were assessed with one and two way analysis of variance (ANOVA) followed by Tukey's multiple comparison tests, as appropriate. Significance was considered if $p < 0.05$.

Chapter 3

The Role of Hypoxia in Regulating Pulmonary Artery Smooth Muscle Cell Proliferation

3.1 Introduction

Vascular smooth muscle cells are the main cellular elements of the vascular medial layer, which regulate vasoconstriction and dilation in response to stimuli (Rudijanto, 2007). Hypoxia is considered one of the main reasons for vascular constriction, enhanced pulmonary artery smooth muscle cell (PASMC) proliferation, and pulmonary artery pressure increasing (Eddahibi et al., 1999). The involvement of hypoxia in the pulmonary vascular remodeling of many lung diseases is considered one of the major categories in the updated clinical classification of pulmonary hypertension (See Chapter1 Table 1.1). Bronchial inflammation is thought to be central to the cellular changes and the pathogenesis of many lung disorders such as asthma, COPD and idiopathic pulmonary hypertension (Dorfmuller et al., 2002, Savai et al., 2012). These disorders may lead to acute or chronic hypoxia that mediates the vasoconstriction of the pulmonary artery and eventually leads to hypertrophic remodeling through the induction of proliferation of all cells of the pulmonary artery (Kato and Staub, 1966, Stenmark et al., 2006b). Howell and co-workers found that the sizes of the intimal and the adventitial layer from rat lungs exposed to hypoxia were increased 1.5 fold and the size of the medial layer was enlarged six-fold in comparison to the corresponding controls in normoxia (Howell et al., 2003).

Hypoxia has been well recognized to promote pulmonary cell proliferation and vascular remodeling but the exact mechanisms are not fully understood. Hypoxia is able to stimulate cell proliferation by inhibiting the production or the release of vasodilators substances such as nitric oxide and by promoting the release of various growth factors/mitogens such as endothelin-1, PDGF, VEGF and inflammatory mediators (e.g. interleukin IL-6), from the pulmonary vasculature including fibroblasts, SMCs, ECs and platelets (Zhang et al., 2003, Ying-fang et al., 2007, Kourembanas et al., 1991, Fike and Kaplowitz, 1996, Kwasiborski et al., 2012). In addition, over-expression of extracellular matrix proteins has been observed in response to hypoxia (Mandegar et al., 2004). Furthermore, hypoxia and HIF-1 α have been shown to play an important role in promoting the proliferative responses of PASMCs to specific mediators. For example, it has been reported that hypoxia increases PASMC proliferation via its ability to enhance the mitogenic

responses of PASMC to growth factors such as PDGF, FGF-2 and EGF, which mediate PASMC proliferation by mechanisms which involve the activation of cell cycle regulator proteins such as cyclin A (Schultz et al., 2006). Various signal transduction systems have been suggested to translate the cellular stimuli that regulate cell growth and proliferation, such as the MAPKs (Aguado et al., 2013, Gan et al., 2013) or the PI3K (Gan et al., 2013, Goncharova et al., 2002) or the NF κ B pathway (Ying-fang et al., 2007). Activation of the MAPK pathway occurs continually and starts with a stimulant such as an inflammatory cytokine or growth factor, leading to a cascade of protein phosphorylation, which results in stimulation of transcription factors, which regulate cellular events such as proliferation or apoptosis (Todd et al., 2014). The mechanism of chronic hypoxia on SMC phenotypic changes was demonstrated by Stenmark and his colleagues (2006) through a variety of intracellular signalling mechanisms including MAPK, protein kinase C (PKC), PI3K, Rho kinases and increased intracellular Ca²⁺ entry, which all cooperatively act to regulate cell contraction, proliferation, differentiation and matrix protein synthesis (Stenmark et al., 2006b). However, the participation of hypoxia in these signalling cascades, which regulate PASMC proliferation, is not fully understood.

3.2 The effect of Hypoxia on PASMCs in PAH

As described in (Chapter 1, section 1.4), increased Ca²⁺ signalling caused by vascular stress (hypoxia) is critical to the hypoxia-induced alteration of the pulmonary vascular wall and cell proliferation. It is well known that hypoxia also promotes intracellular reactive oxygen species (ROS) generation in PASMCs and it causes oxidative damage leading to impairment of cell functions (Brennan et al., 2003, Waypa et al., 2006). For example, reactive oxygen species (ROS) play an important role in enhanced intracellular Ca²⁺ levels leading to PASMC contraction and hypoxic vasoconstriction (Rathore et al., 2006). The combined effects of hypoxia, oxidative stress, intracellular Ca²⁺ elevation and the loss of K⁺ channel are implicated in a variety of cellular events. These involve mitochondria, the sarcoplasmic reticulum and the nuclei of PASMC. The combined effects result in constriction, proliferation, migration and over-expression of vasoactive and inflammatory substances that promote pulmonary hypertension (Figure 3.1).

Numerous studies have reported that many transcription factors such as hypoxia-inducible factor 1 alpha (HIF-1 α) (Yu et al., 1999, Shimoda et al., 2000, Hu et al., 1998), nuclear factor κ -B (NF- κ B) (Kimura et al., 2009, Cummins et al., 2006) and extracellular signal-regulated kinase (ERK1/2) (Kyaw et al., 2002, Kawanabe et al., 2002) have critical roles in hypoxic-dependent oxidative stress, intracellular Ca²⁺ disruption and the loss of K⁺ channel in PASMCs leading to cell proliferation and the development of pulmonary hypertension (Figure 3.1). Moreover, increased expression of PDGF receptor, the stimulation of Rho protein and its downstream effector such as Rho-kinase and activation of protein kinase C have contributed to hypoxia-induced proliferation of PASMCs (Wang et al., 2016, Dempsey et al., 1991).

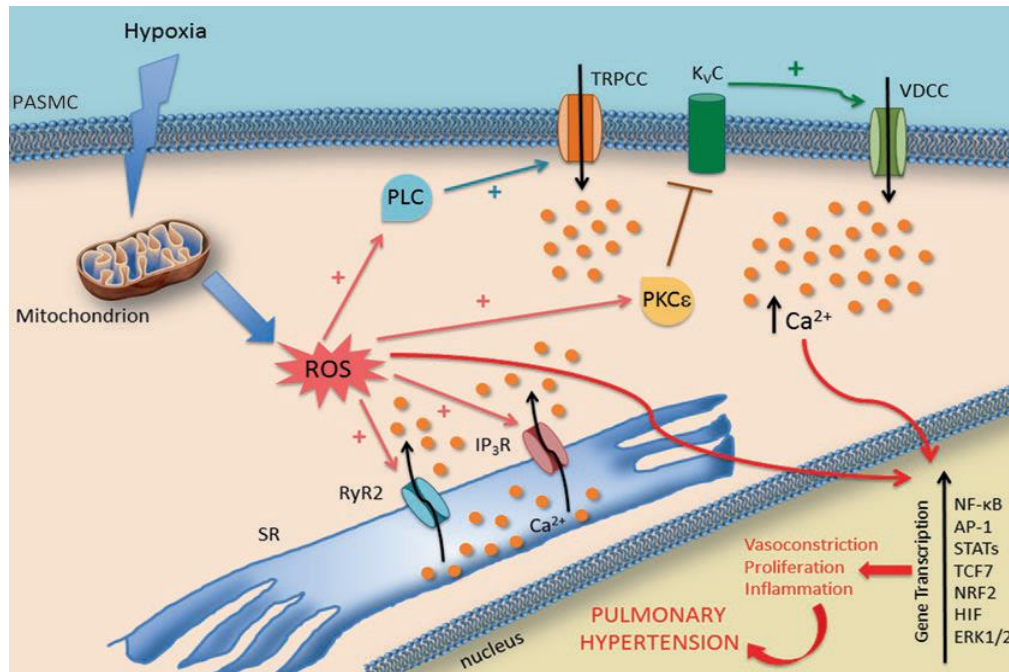


Figure 3.1 Signalling mechanisms involved in hypoxia-dependent activation of different transcription factors in PASMCs to mediate pulmonary hypertension. Hypoxia elevates intracellular ROS, opens RyR2 (ryanodine receptor-2/ Ca^{2+} release channel) and activates IP₃R (inositol triphosphate receptor/ Ca^{2+} release channel) on the sarcoplasmic reticulum (SR), stimulates transient receptor potential canonical channel (TRPCC) and voltage-dependent Ca^{2+} channel (VDCC) on the plasmalemmal membrane, inhibits voltage-dependent K^{+} channel (K_vC) and elevates Ca^{2+} signalling. The elevated ROS and increased Ca^{2+} synergistically lead to activation of different transcription factors such as hypoxia-inducible factor-1 α (HIF-1 α), nuclear factor- κ B (NF- κ B), extra-cellular signal-regulated kinase (ERK1/2) and other transcription factors. The activated transcription factors enhance the transcription of the proliferative and pro-inflammatory genes to mediate the cellular events in pulmonary hypertension. Adapted from (Di Mise et al., 2017).

Several *in vitro* studies of hypoxia on PASMC proliferation have shown the controversy surrounding the identified effect of acute hypoxia on smooth muscle cell proliferation. For example, Michiels et al. and Vender showed that acute exposure of hypoxia has a major role in the initiation of events culminating in smooth muscle cell proliferation (Michiels et al., 1994, Vender, 1992). Conversely, Stiebellehner et al. and Eddahibi et al. demonstrated that acute hypoxia causes a reduction in the proliferative responses whereas another study conducted by Lanner and colleagues reported that there was no link between hypoxia and PASMC proliferation (Eddahibi et al., 1999, Stiebellehner et al., 2003, Lanner et al., 2005).

The main reason for the discrepancies reported above is most likely due to the changes in the experimental conditions during cell preparation. For example, the use of specific mitogens to stimulate the cells during hypoxia could result in an increase in cell proliferation. Humar and colleagues demonstrated different VSMC proliferative responses when cells were exposed to hypoxia and stimulated with different pro-mitogens such as platelet-derived growth factor (PDGF), basic fibroblast growth factor (bFGF) and serum (Humar et al., 2002). As a result, their study concluded that hypoxia promotes VSM proliferation mediated by PDGF and bFGF but not in response to serum stimulation. Moreover, different concentrations of serum used in stimulating cell growth during hypoxia may also be considered. Studies by Lanner et al. (2005) and Stiebellehner et al. (2003) demonstrated that hypoxia did not induce further PASMC proliferation above basal stimulation mediated by 5% and 10% serum. Furthermore, changes in the oxygen level used in diverse experiments also can provide different responses in terms of cellular growth and proliferation. For example, studies have shown hypoxia increases PASMC proliferation at 3% oxygen level when cells were cultured in 0.1% FCS media (Dempsey et al., 1991) or at 5% oxygen level when cells were stimulated with 2% FCS (Cooper and Beasley, 1999). Therefore, using a variety of basal stimulation situations and different oxygen environments, the work presented in this chapter is to determine the baseline data to investigate the role of acute hypoxia on PASMC proliferation.

3.3 Chapter Aims

This chapter aims to:

- Isolate primary PASMC cultures from rat pulmonary artery.
- Establish a reliable and reproducible experimental hypoxic cell culture model.
- Investigate the impact of a range of hypoxic culture conditions on PASMCs.
- Study the effect of hypoxia on cell proliferation and key signalling pathways.

3.4 Results

3.5 Isolation of Smooth Muscle Cell, Culture and Characterisation

Pulmonary artery smooth muscle cells (PASMCs) were derived and cultured from the rat pulmonary artery as described in Method Section (2.2). Identification of “Hill and Valley” pattern consistent with vascular smooth muscle cell morphology was examined by microscopy. PASMCs were grown out from the rat pulmonary arterial ring which was immersed and cultured in 10% serum growing media over 21 days. Cells were photographed at approximately 20, 75 and 100% confluency and recognized by their morphological characteristic organization, which designated in “Hill and Valley” formation (Figure 3.2).

In order to confirm the identity of PASMCs, cells were visualized using smooth muscle cell specific markers such as α -actin and myosin heavy chain by epifluorescence microscope (Figure 3.3). Smooth muscle α -actin is considered as the main component for the cytoskeletal structure of the cell and contractile filaments, which are restricted to differentiated vascular smooth muscle cells. On the other hand, the expression of myosin heavy chain is believed to be linked only with the contractile function of smooth muscle cells (Rensen et al., 2007). Under epifluorescence microscopic analysis, Figure 3.3A shows the expression of actin filaments of the cells in green colour whereas Figure 3.3B displays the intensity of the green stain of the cells depicting myosin heavy chain expression. The nuclei of the cells in both Figure 3.3A and Figure 3.3B were detected by DAPI stain.

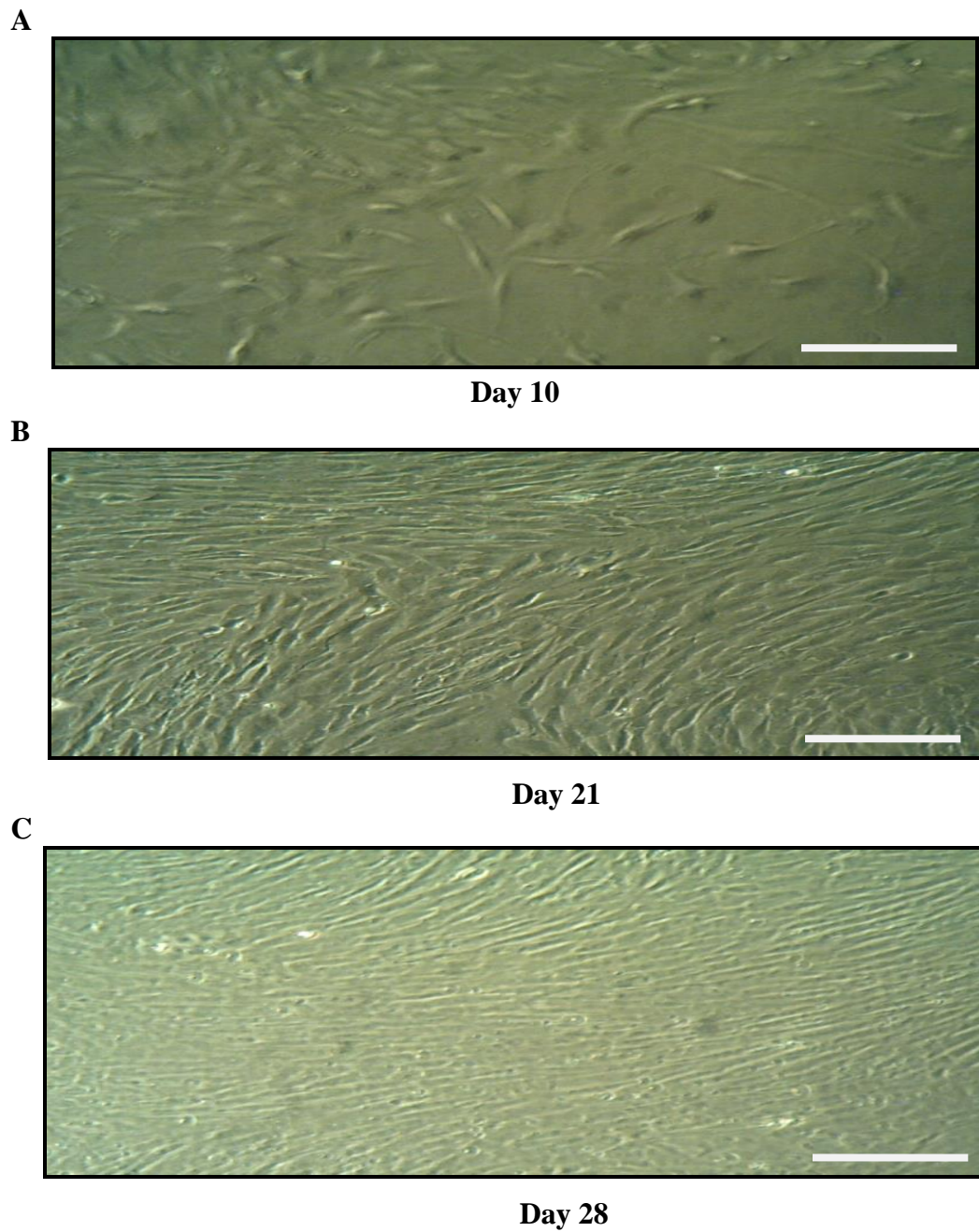


Figure 3.2 Rat Pulmonary Artery Smooth Muscle cells (PASMCs) observed under phase contrast microscope (x10). Cells at estimated 20, 75 and 100% confluency on day 10, 21 and 28 are represented in picture A, B and C respectively. Scale bar is 10 μm in all images.

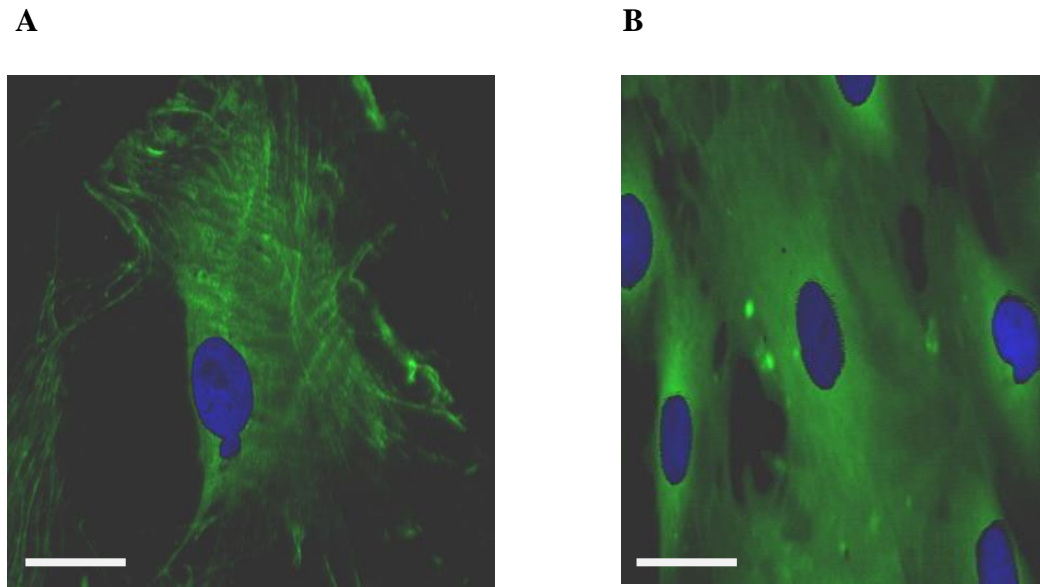


Figure 3.3 Immunofluorescence for α -actin and myosin heavy chain (MHC) in PASMCs. Fluorescent image **A** shows actin filaments (green) in PASMC after adding 1:400 dilutions of α -actin antibody. Fluorescent image **B** indicates the localization of myosin heavy chain (green) in PASMC. The antibody was applied at 1:100 dilutions. Both images were taken at x60 magnification. Scale bar is 10 μ m in both images. PASMC nucleus stained with DAPI (blue) as shown in the above images (n=3).

3.6 Effect of Foetal Calf Serum (FCS) on PASMC Proliferation

PASMC proliferation was investigated using [³H]-thymidine incorporation assay (see Chapter 2, section 2.7) as a measurement of DNA synthesis in the cells. Figure 3.4 shows a stepwise increase in DNA synthesis with increasing foetal calf serum (FCS) concentration. FCS stimulated a concentration-dependent increase in DNA synthesis. The highest concentration of 10% FCS gave a 14.9 ± 1.17 fold increase in DNA synthesis, whereas 2.5% and 5% FCS also gave stepwise increases which were also statistically significant (10.1 ± 1.5 fold, 12.1 ± 1.3 fold) relative to control (0.1% FCS). Statistical analysis also showed no significant difference in DNA synthesis detected in response to 0.5% FCS and 1% FCS, relative to control (0.1% FCS).

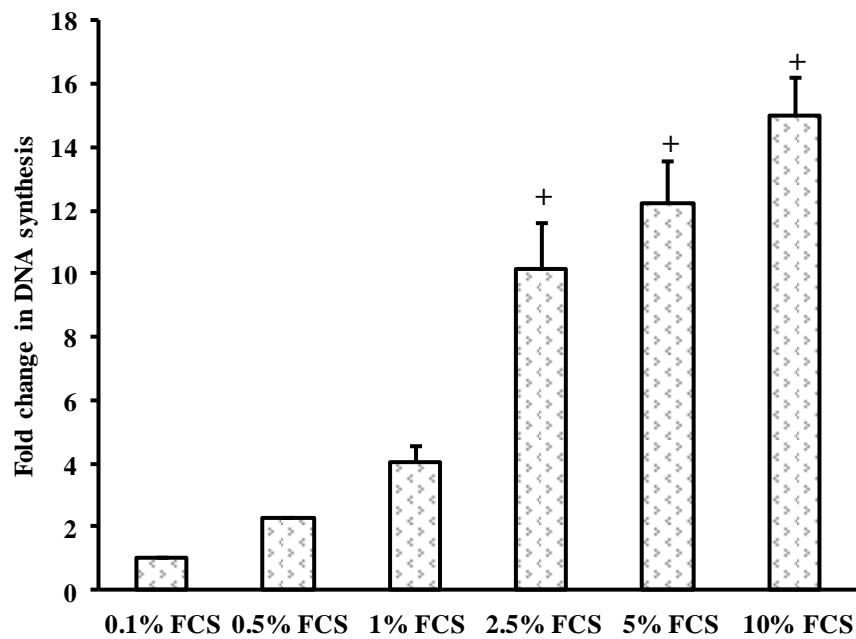


Figure 3.4 Effects of incremental serum concentrations on [³H]-thymidine incorporation in PASMCs. Cells were quiesced with 0.1% FCS for 24 h and were stimulated with different foetal calf serum (FCS) concentrations for 24 h. [³H]-thymidine incorporation assay was performed for the evaluation of DNA synthesis (as an index of cell proliferation). Radioactive counts were measured in disintegrations per minute (DPM) and normalized to the control group (0.1% FCS). +p <0.05 vs. (0.1% FCS). Experiments were conducted in quadruple (24 observations from six independent cell cultures). Each value represents the mean \pm SEM (n=6).

3.7 Effect of acute hypoxia (10% O₂) on PASMC proliferation

Data show PASMCs exposed to hypoxia (10% O₂) did not increase cell proliferation in quiescent cells (cells with 0.1% FCS) (Figure 3.5). In addition, in the presence of serum, proliferative effects were seen in the hypoxic group in a concentration-dependent manner. However, hypoxia (10% O₂) did not show any significant difference in DNA synthesis values, as an index of cell proliferation, compared to normoxia (21% O₂) among all serum concentrations (Figure 3.5).

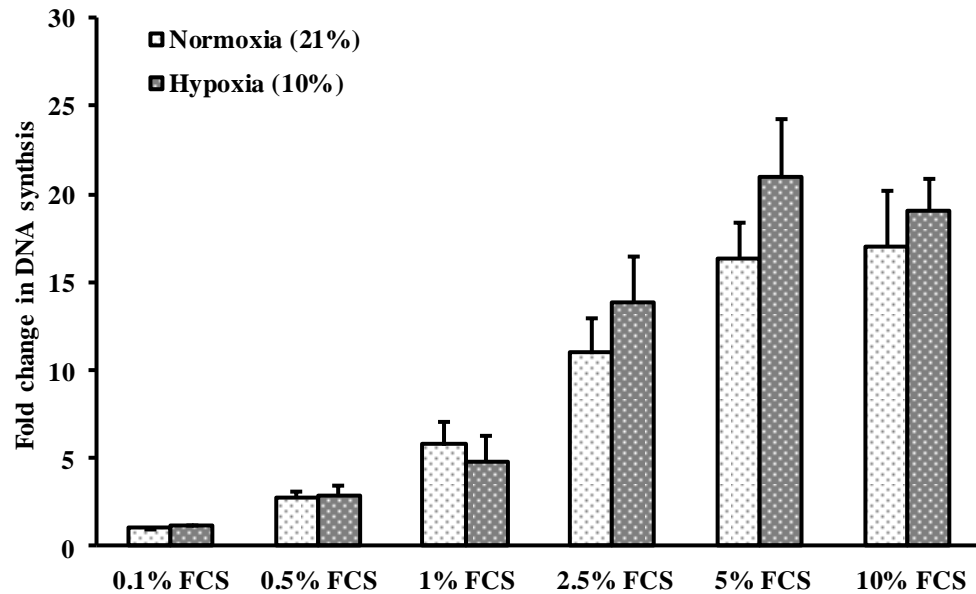


Figure 3.5 The effect of hypoxia (10% O₂) on serum-stimulated [³H]-thymidine incorporation in PASMCs. Cells were quiesced for 24 h. Then, cells were exposed to hypoxia (10% O₂) and stimulated with different serum concentrations for 24 h. [³H]-thymidine incorporation assay was performed for DNA synthesis evaluation (as an index of cell proliferation). Radioactive counts were measured in disintegrations per minute (DPM) and normalized to the control group (quiescent cells). Experiments were conducted in quadruplicate (number of wells). Each value represents the mean ± SEM (n=4).

3.8 Effect of Acute Hypoxia (10% O₂) on ERK1/2 phosphorylation

In order to study the role of MAPK signalling in PASMCM proliferation, it was initially important to perform and optimize the time course stimulation experiment for the activity of MAPK signalling. Using Western blot, phosphorylation of ERK1/2 by 10% serum was examined at different time points: 5, 15, 30 and 60 minutes and 24 hours in PASMCMs (Figure 3.6). The optimal measurement point for ERK phosphorylation was 15 minutes and the gradual reduction of the phosphorylated 42 (ERK1) and 44 kDa (ERK2) proteins was clearly observed after this time (Figure 3.6).

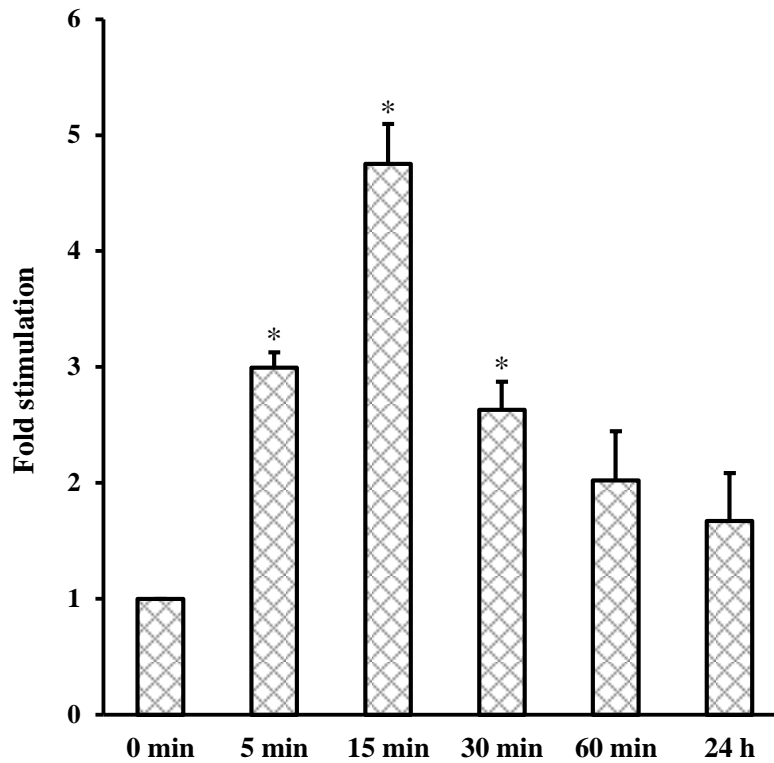
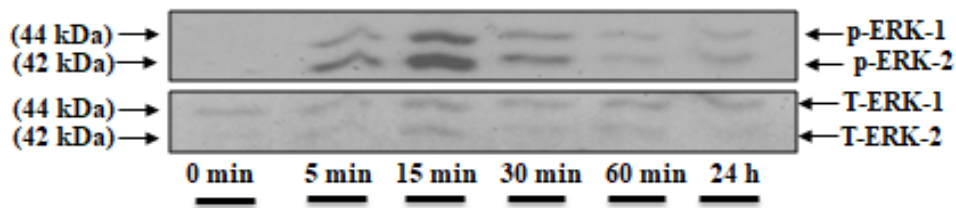


Figure 3.6 Time course of serum-induced ERK activation in PSMCs. Cells were seeded in pairs of 6 well plates. At 70-80% confluence, cells were quiesced with 0.1 % FCS for 24 hours. Cells were then stimulated with 10 % FCS for the times indicated. Blots were assessed by semi-quantitative densitometry and results expressed as fold stimulation relative to control (cells without 10% FCS, 0 min). Whole cell extracts were prepared and analysed using Western blot for p-ERK1/2 (42-44 kDa) expression and its total (42-44 kDa). ERK1/2 phosphorylation was measured relative to total ERK. Each value represents the mean \pm SEM. * $p < 0.05$ vs. cells without 10% FCS ($n=3$).

The study of hypoxic stimuli (10% O₂) on ERK-1/2 MAPK phosphorylation was performed by exposing PASMCs to a 10% O₂ environment for 24 hours and stimulating them with different serum concentrations for 15 minutes. A concentration-dependent increase in ERK1/2 phosphorylation was observed with increasing serum stimulation (Figure 3.7). However, hypoxia (10% O₂) did not trigger an increase in p-ERK protein after 24 hours of exposure. Furthermore, despite the fact that an increase in ERK1/2 phosphorylation was clearly observed in parallel to increase serum concentrations, there was no difference detected in ERK1/2 phosphorylation in response to hypoxia (10% O₂) relative to normoxic conditions (Figure 3.7).

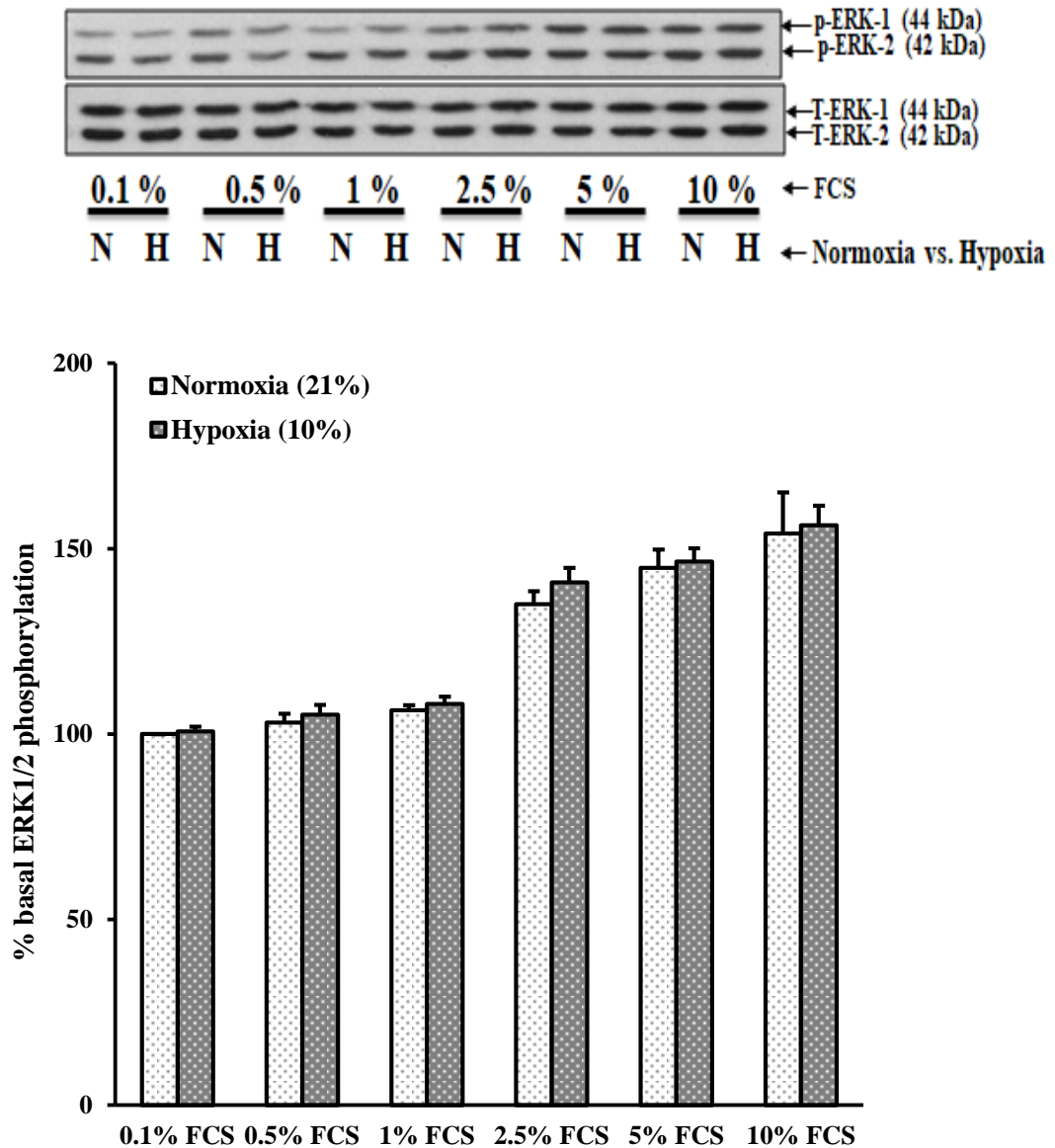


Figure 3.7 The combined effect of incremental serum concentrations and hypoxia (10% O₂) on ERK1/2 phosphorylation in PSMCs. Cells were seeded in pairs of 6 well plates. At 70-80% confluence, cells were quiesced for 24 hours. Then, cells were incubated at different oxygen levels; 21% oxygen (normoxia) and 10% oxygen (hypoxia) for 24 hours and were stimulated with increasing FCS concentrations (0.1%, 0.5%, 1%, 2.5%, 5% and 10%) for 15 minutes. Blots were assessed by semi-quantitative densitometry and results expressed as % basal ERK1/2 phosphorylation relative to control (quiescent cells, cells with 0.1% FCS during normoxia). Whole cell extracts were prepared and analysed using Western blot for p-ERK1/2 (42-44 kDa) expression and its total (42-44 kDa), which was used as a loading control. Each value represents the mean \pm SEM (n=3).

3.9 Effect of Acute Hypoxia (5% O₂) on PASMC Proliferation

The effect of hypoxia (5% O₂) on PASMC proliferation was performed by measuring [³H]-thymidine incorporation in hypoxic cells with incremental serum concentrations in cells that had been kept at 5% oxygen level for 24 hours (Figure 3.8). In control cells, serum at 1% and 10% caused a marked increase in [³H]-thymidine incorporation (5.7 ± 1.3 fold and 17 ± 1.8 fold respectively). However, there was no significant effect of hypoxia (5% O₂) at either serum concentration.

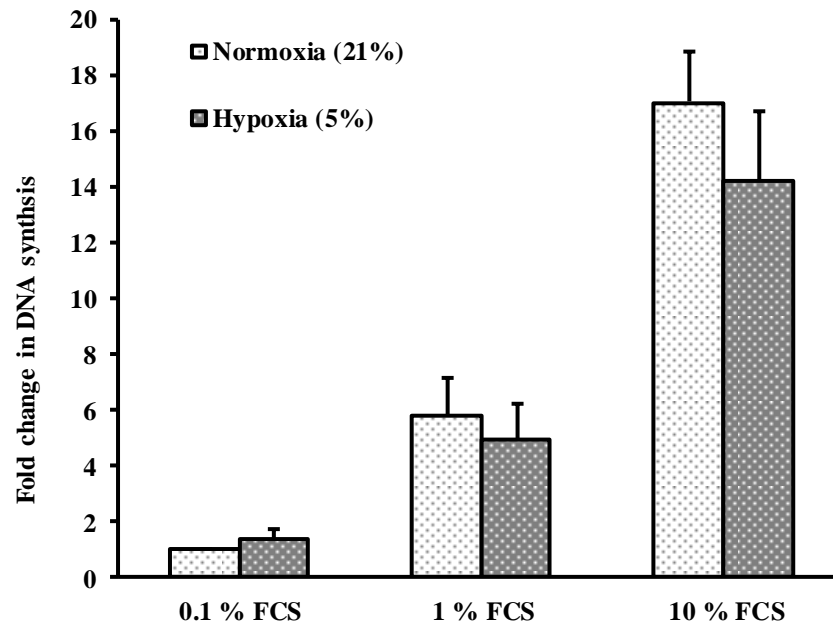


Figure 3.8 The effect of hypoxia (5% O₂) on serum-stimulated [³H]-thymidine incorporation in PASMCs. Cells were quiesced for 24 h. Then, cells were exposed to hypoxia (5% O₂) and stimulated with 1% and 10% foetal calf serum (FCS) for 24 h. [³H]-thymidine incorporation assay was performed for DNA synthesis evaluation (as an index of cell proliferation). Radioactive counts were measured in disintegrations per minute (DPM) and normalized to the control group (quiescent cells). Experiments were conducted in quadruplicate (number of wells). Each value represents the mean \pm SEM (n=5).

3.10 Effect of Acute Hypoxia (5% O₂) on ERK1/2 phosphorylation

Cells were stimulated with 1% and 10% foetal calf serum (FCS) for 15 minutes after 5% O₂ incubation (24 hours). Figure 3.9 shows an increase in ERK1/2 phosphorylation when stimulating the cells with 1% FCS and 10% FCS compared to control (0.1% FCS). However, hypoxia (5% O₂) (Figure 3.9) had similar effects as 10% O₂ (Figure 3.7), which both failed to enhance ERK1/2 protein phosphorylation in the absence or presence of serum in comparison to normoxia (no significant difference, $p > 0.05$).

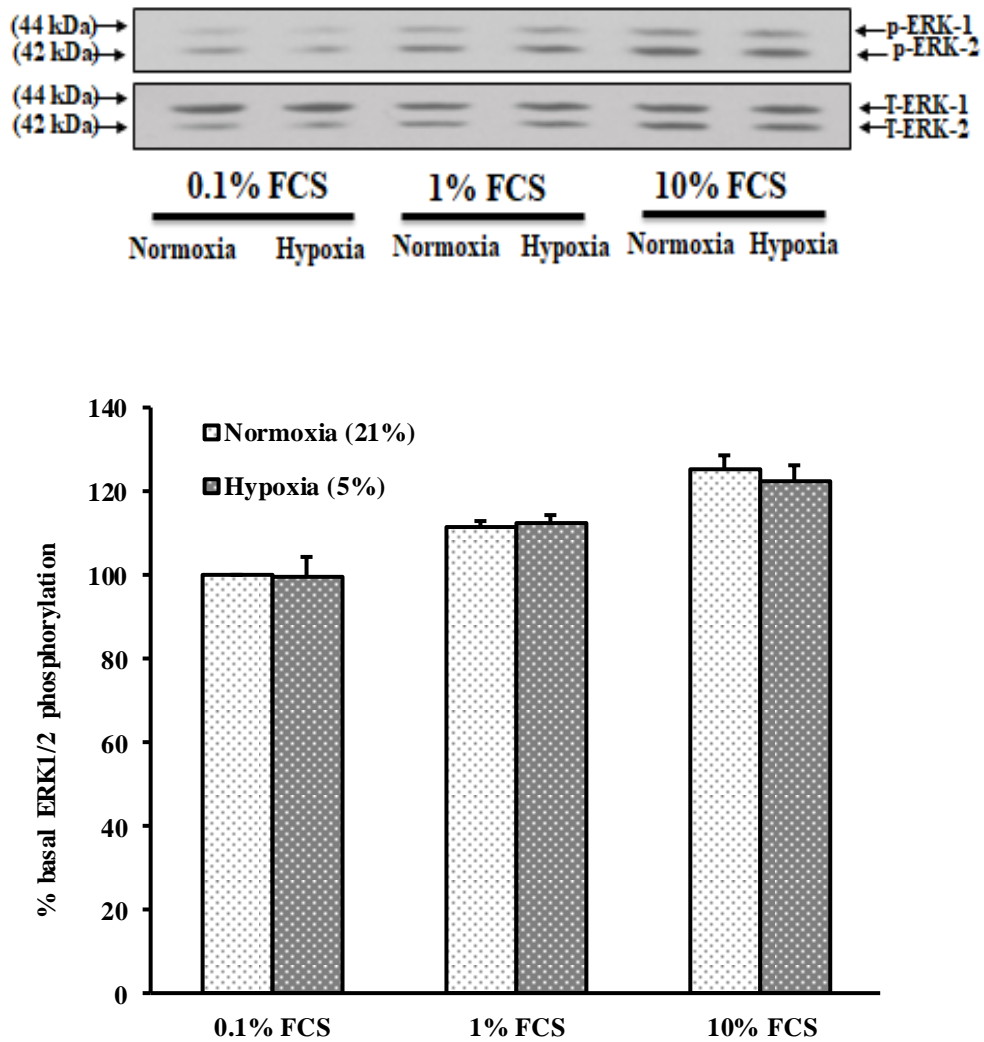


Figure 3.9 The effect of hypoxia (5% O₂) on ERK1/2 phosphorylation in PASMCs. Cells were seeded in pairs of 6 well plates. At 70-80% confluence, cells were quiesced for 24 hours. Cells were then incubated at different oxygen levels; 21% oxygen (normoxia) and 5% oxygen (hypoxia) for 24 hours and were stimulated with 1% FCS or 10% FCS for 15 minutes. Blots were assessed by semi-quantitative densitometry and results expressed as % basal ERK1/2 phosphorylation relative to control (quiescent cells, cells with 0.1% FCS during normoxia). Whole cell extracts were prepared and analysed using Western blot for p-ERK1/2 (42-44 kDa) expression and its total (42-44 kDa), which was used as a loading control. Each value represents the mean \pm SEM (n=3).

3.11 Effect of Acute Hypoxia (3% O₂) on PASMC Proliferation

As shown previously, exposing to 10% O₂ or 5% O₂ had no effect in terms of cellular proliferation in [³H]-thymidine incorporation measurements. Thus, a further reduction in the oxygen level to 3% was examined (Figure 3.10). In resting cells, 3% oxygen caused a small but insignificant increase in [³H]-thymidine incorporation (1.5 ± 0.3 fold). This outcome was also observed for 1% FCS (1.4 ± 0.19 fold) and the trend become significant following 10% FCS stimulation (1.5 ± 0.13 fold).

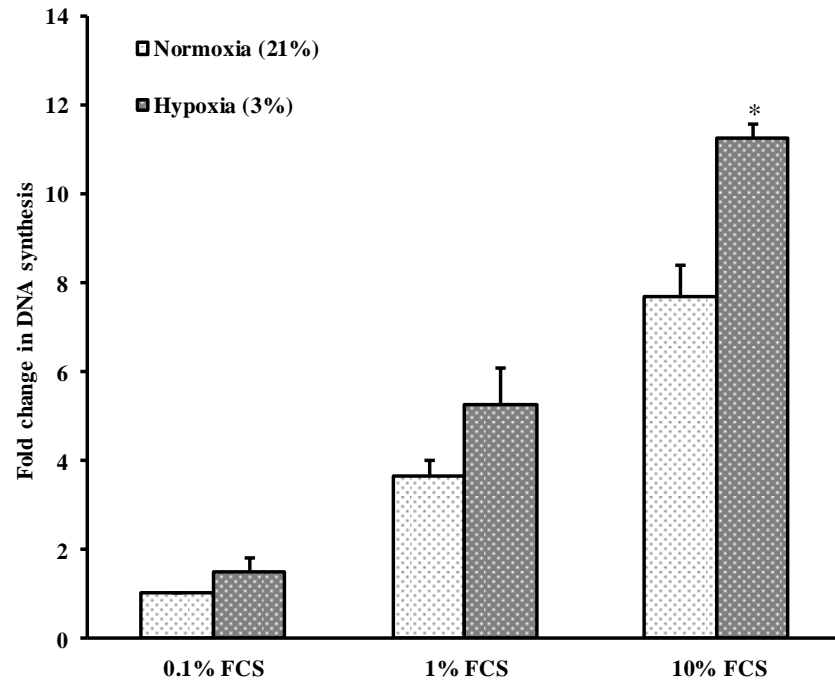


Figure 3.10 The combined effect of incremental serum concentrations and hypoxia (3% O₂) on [³H]-thymidine incorporation in PSMCs. Cells were quiesced for 24 h in 0.1% FCS. Cells were then exposed to hypoxia (3% O₂) and stimulated with 1% and 10% foetal calf serum (FCS) for 24 h. A [³H]-thymidine incorporation assay was performed for DNA synthesis (as an index of cell proliferation). Radioactive counts were measured in disintegrations per minute (DPM) and normalized to the control group (quiescent cells). Experiments were conducted in quadruplicate (number of wells). Each value represents the mean ± SEM. *p < 0.05 vs. cells cultured in normoxia (n=4).

3.12 The effect of Hypoxia (3% O₂) on Proliferative Marker Genes

The previous result (Figure 3.10) showed hypoxia (3% O₂) caused a significant increase in serum-stimulated DNA synthesis. Therefore, additional experiments to identify whether hypoxia leads to increased cell proliferation were performed. A number of key genes implicated in cell proliferation such as proliferating cell nuclear antigen (PCNA) gene, extracellular regulated kinase 1 (ERK1) gene and cyclin D1 gene were examined. Data show PCNA, ERK1 and cyclin D1 genes were increased to 2.8 ± 0.1 , 17.2 ± 2.8 and 15.9 ± 1.1 fold compared to their level in the normoxic control group (Figure 3.11). Also, PCNA inside the cell nuclei of PASMCs was microscopically investigated using an immunofluorescence staining technique for both the normoxic and hypoxic groups (Figure 3.12). The results display a notable existence of PCNA in both stimulated cells. However, the PCNA expression inside the nuclei of hypoxic cells was higher (1.7 ± 0.03 fold, Figure 3.12).

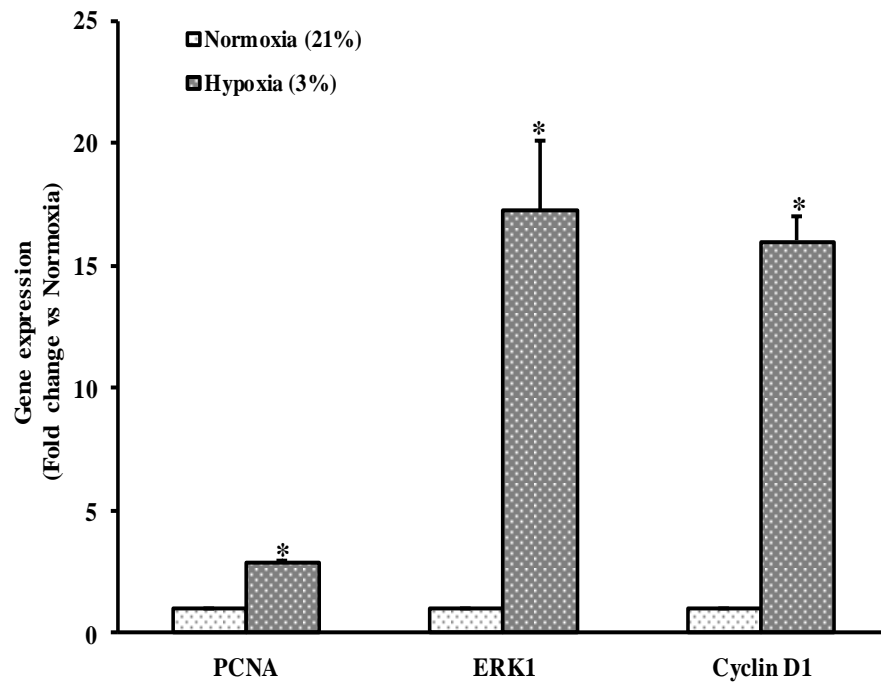


Figure 3.11 The effect of hypoxia (3% O₂) on the proliferative marker genes; PCNA, ERK1 and cyclin D1 expression in serum-stimulated PSMCs. Cells were quiesced for 24 h. 10% serum growing media was added immediately before oxygen incubation time; normoxia (21% oxygen) and hypoxia (3% oxygen) for 24 h. RNA was extracted from the cells. Equal RNA concentrations were used for cDNA sample preparation. Genes were measured using RT-qPCR. Ubiquitin C (UBC) was used as the reference gene for normalization. *p < 0.05 vs. normoxic cells (n=3).

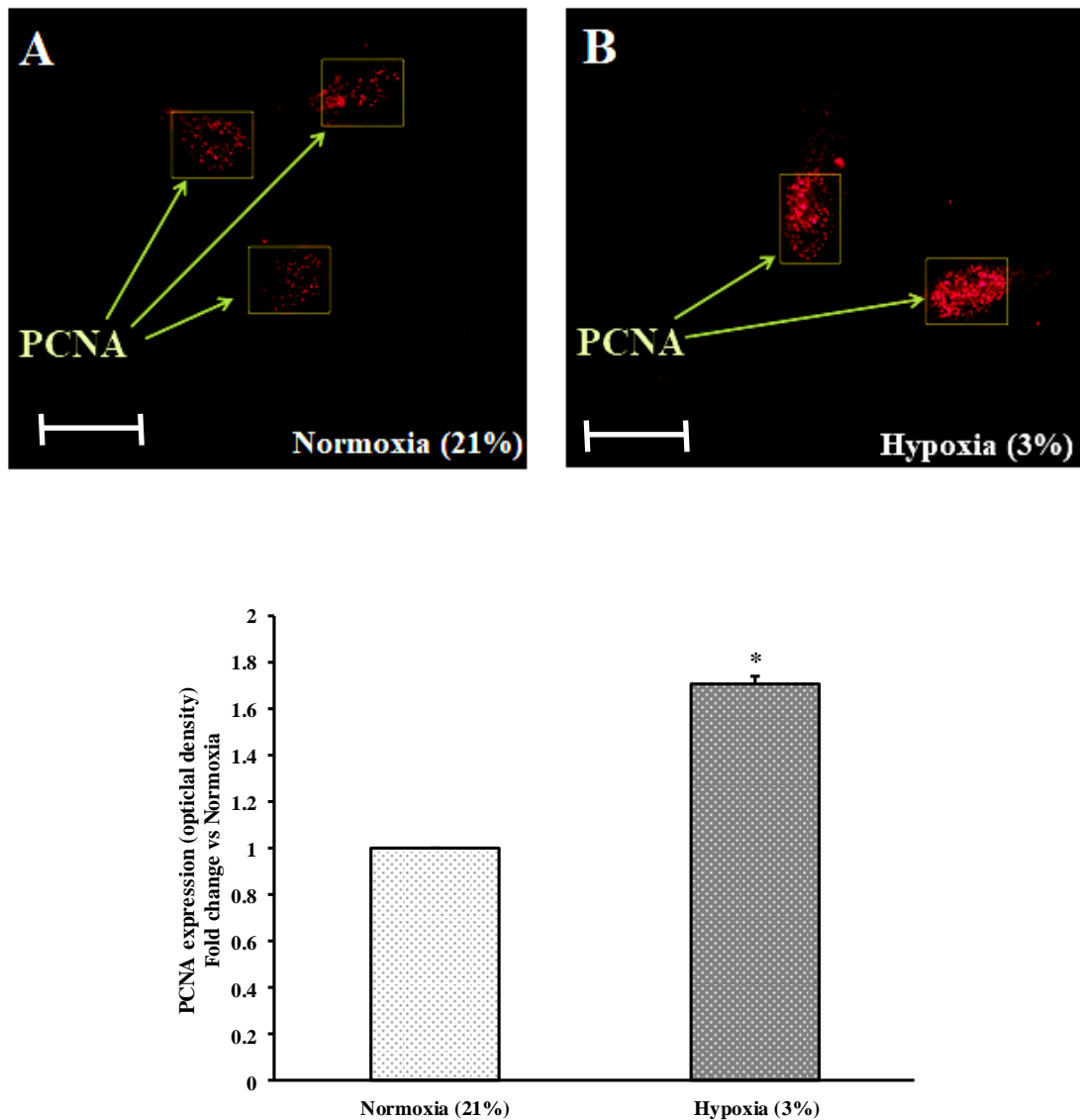


Figure 3.12 The effect of hypoxia (3% O₂) on PCNA expression in serum-stimulated PSMCs. Immunofluorescence (x60) staining of proliferating cell nuclear antigen (PCNA) was shown in cells stimulated with 10% serum under normoxic incubation (21% oxygen) for 24 h as a control (image A) and in cells exposed to hypoxia (3% oxygen) and stimulated with 10% serum for 24 h (image B). The intensity of PCNA positive area was measured using Image J and normalized to control cells (cells with 10% serum normoxic culture). Scale bar is 10 μ m in both images. Each value represents the mean \pm SEM. *p < 0.05 vs. cells cultured in normoxia (n=3).

In addition, cyclin-dependent kinase inhibitor 2A (cdkn2A), which is a cell cycle regulatory gene, was examined. Data show cdkn2A gene expression in hypoxic cells was reduced to 0.18 ± 0.1 fold compared to its level in control cells (Figure 3.13).

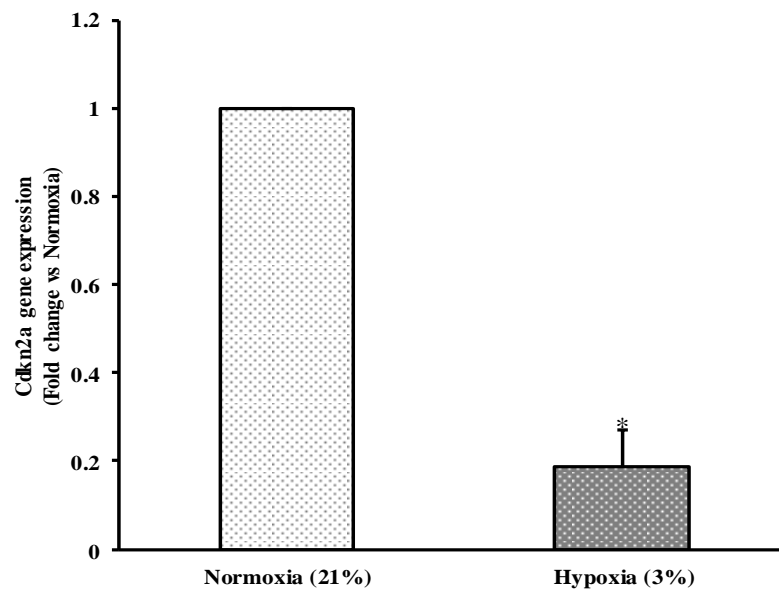
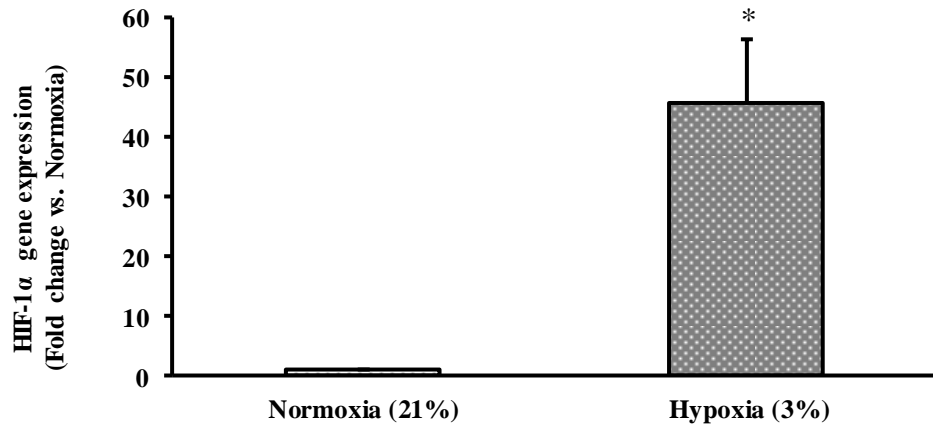


Figure 3.13 The effect of hypoxia (3% O₂) on Cdkn2a gene expression in serum-stimulated PASMCs. Cells were quiesced for 24 h. 10% serum growing media was added immediately before oxygen incubation time; normoxia (21% oxygen) and hypoxia (3% oxygen) for 24 h. RNA was extracted from the cells. Equal RNA concentrations were used for cDNA sample preparation. Cyclin-dependent kinase inhibitor 2A (Cdkn2a) gene was measured using RT-qPCR. Ubiquitin C (UBC) was used as the reference gene for normalization. *p < 0.05 vs. normoxic cells (n=3).

3.13 Hypoxic Marker Genes

To confirm the stressful effect of hypoxia, hypoxia-inducible factor-1 (HIF-1) isoforms: HIF-1 α and HIF-2 α were investigated. Figure 3.14 shows a significant upturn in all hypoxic gene expression (HIF-1 α gene; 45.6 ± 10.6 fold and HIF-2 α gene; 1485 ± 290 fold) in cells exposed to 3% oxygen compared to cells kept at 21% oxygen (control). Finally, arginase-1 gene, a gene that is involved in HIF-2 signalling pathway was also examined. HIF-2 α acts to control nitric oxide homeostasis. This occurs through HIF-2 α regulation of the arginase genes (Branco-Price et al., 2012, Grasemann et al., 2015, Firth et al., 2010). Increased expression of arginase genes is found in pulmonary artery cells derived from PAH lungs and these cells produce lower nitric oxide levels than the non-PAH (control) cells (Xu et al., 2004). The expression of arginase 1 gene in pulmonary endothelium and whole lung samples from mice lacking HIF-2 α is decreased in response to hypoxia (Cowburn et al., 2016). The expression of arginase 1 gene in PASMCs was measured under both normoxic and hypoxic conditions. Data show upregulation of this gene was significant in hypoxic stimulated cells (4.4 ± 0.5 fold, Figure 3.15).

A



B

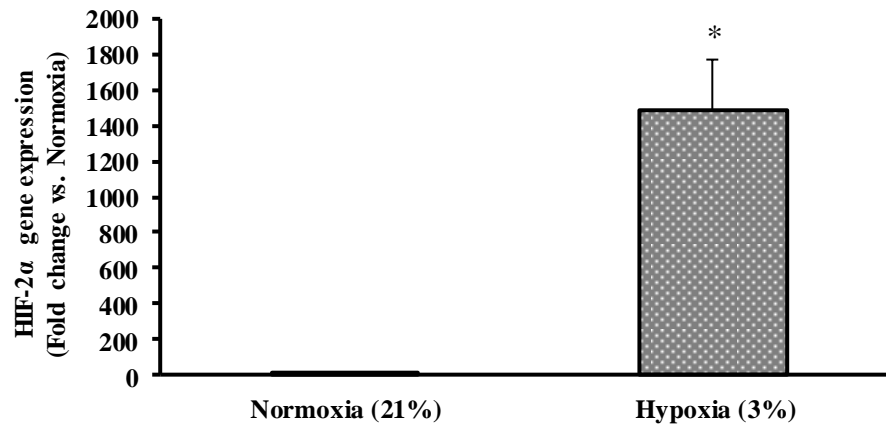


Figure 3.14 Expression of HIF-1 α and HIF-2 α genes in serum-stimulated PSMCs during hypoxia (3% O₂). Cells were quiesced for 24 h. 10% serum growing media was added immediately before oxygen incubation time; normoxia (21% oxygen) and hypoxia (3% oxygen) for 24 h. RNA was extracted from the cells. Equal RNA concentrations were used for cDNA sample preparation. A) HIF-1 α (hypoxia-inducible factor-1 alpha) gene and B) HIF-2 α (hypoxia-inducible factor-2 alpha) gene were measured using RT-qPCR. Ubiquitin C (UBC) was used as the reference gene for normalization. *p < 0.05 vs. normoxic cells (n=3).

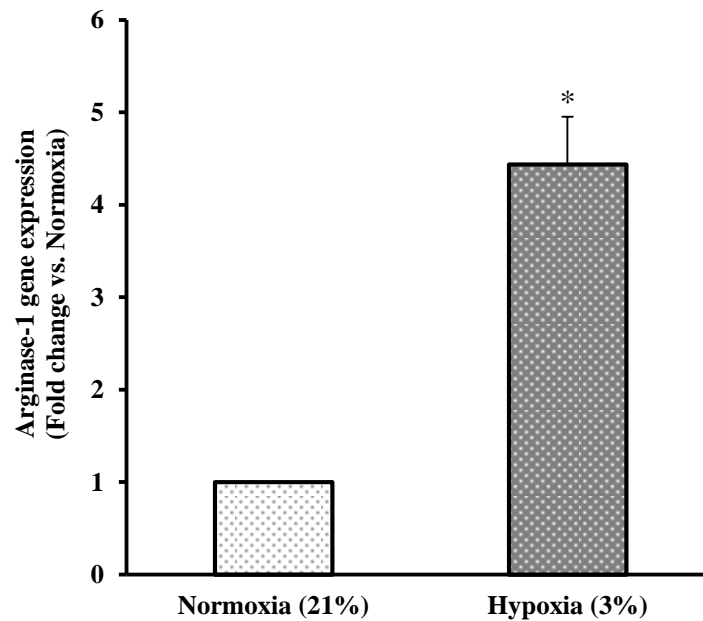


Figure 3.15 The effect of hypoxia (3% O₂) on arginase-1 expression in serum-stimulated PASMCs. Cells were quiesced for 24 h. 10% serum growing media was added immediately before oxygen incubation time; normoxia (21% oxygen) and hypoxia (3% oxygen) for 24 h. RNA was extracted from the cells. Equal RNA concentrations were used for cDNA sample preparation. Arginase-1 gene was measured using RT-qPCR. Ubiquitin C (UBC) was used as the reference gene for normalization. *p < 0.05 vs. normoxic cells (n=3).

3.14 Effect of Hypoxia (3% O₂) on MAPK phosphorylation

Previous data had shown there was no effect of 10% O₂ or 5% O₂, over a 24 h experimental period, with various serum stimulations for 15 minutes, on ERK1/2 phosphorylation in rat PASMCs (Figure 3.7 and Figure 3.9). According to the data presented in Figure 3.10, 3% hypoxic-10% FCS had provided the ability of PASMCs to promote cell proliferation compared to normoxic-10% FCS stimulation. Therefore, in an attempt to understand the mechanism of hypoxia in regulating cell proliferation, Western blotting was undertaken to measure the protein levels of p-ERK1/2, p-p38 MAPK and p-JNK under these conditions (Figure 3.16, Figure 3.17 and Figure 3.18 respectively). A significant increase in the phosphorylation of both ERK1/2 (3.9 ± 0.58 fold) and p38 MAPK (1.8 ± 0.08 fold) was clearly seen in hypoxic cells compared to normoxic cells (Figure 3.16, Figure 3.17). However, hypoxia did not show any change in JNK phosphorylation (Figure 3.18).

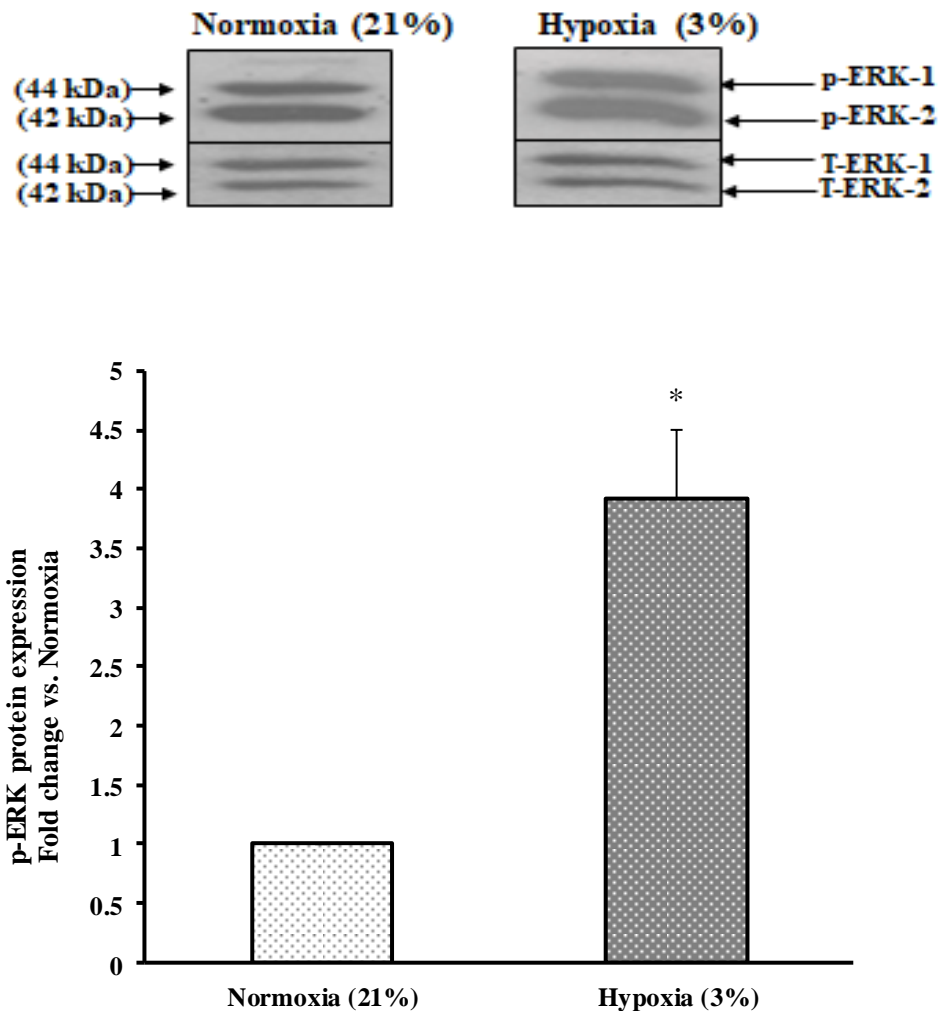


Figure 3.16 The effect of hypoxia (3% O₂) on serum-induced ERK1/2 phosphorylation in PSMCs. Cells were seeded in pairs of 6 well plates. At 70-80% confluence, cells were quiesced for 24 hours. Then, cells were incubated at different oxygen levels; 21% oxygen (normoxia; control) and 3% oxygen (hypoxia; test) for 24 hours and stimulated with 10% FCS for 15 minutes. Blots were assessed by semi-quantitative densitometry and results expressed as fold stimulation relative to control (cells stimulated with 10% FCS under normoxic conditions). Whole cell extracts were prepared and analysed using Western blot for p-ERK1/2 (42-44 kDa) expression and its total (42-44 kDa), which was used as a loading control. Each value represents the mean \pm SEM. * $p < 0.05$ vs. normoxic cells ($n=3$).

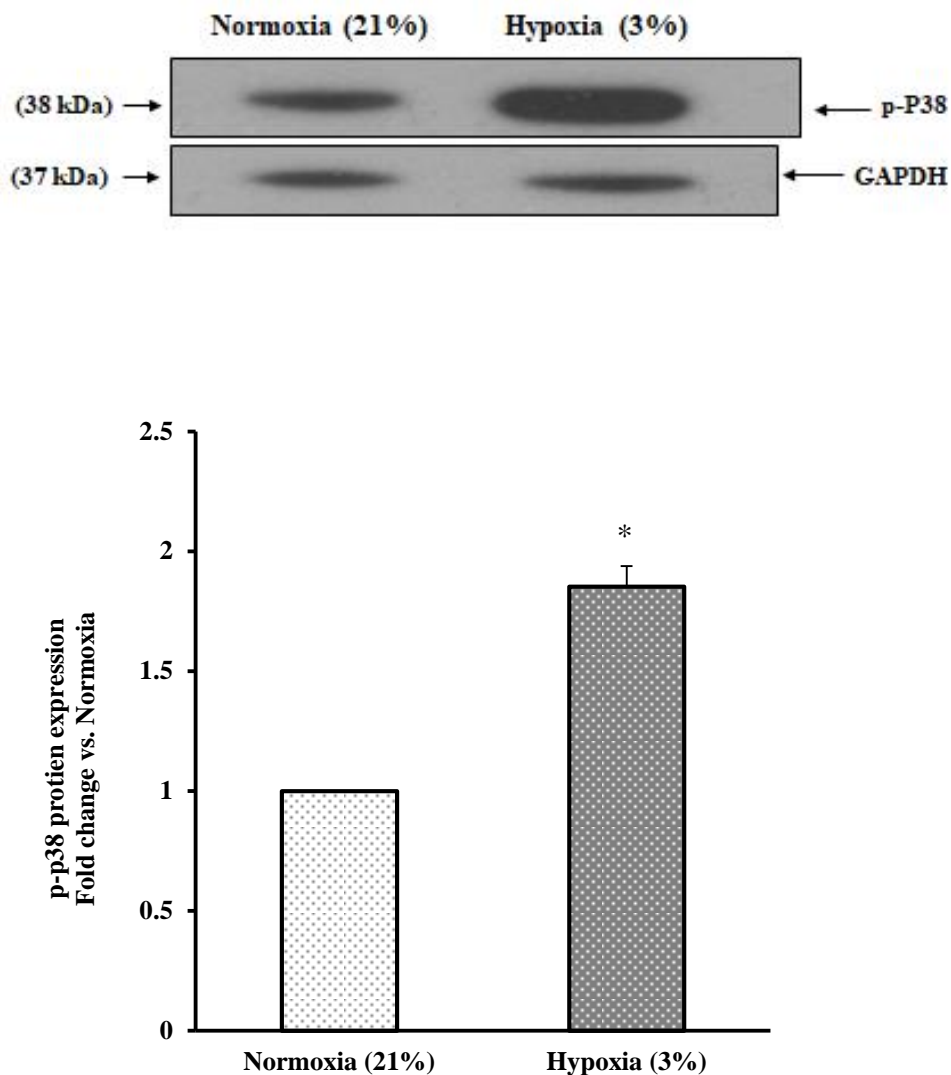


Figure 3.17 The effect of hypoxia (3% O₂) on serum stimulation of p38 MAPK phosphorylation in PASMCs. Cells were seeded in pairs of 6 well plates. At 70-80% confluence, cells were quiesced for 24 hours. Then, cells were incubated at different oxygen levels; 21% oxygen (normoxia; control) and 3% oxygen (hypoxia; test) for 24 hours and were stimulated with 10% FCS for 15 minutes. Blots were assessed by semi-quantitative densitometry and results expressed as fold stimulation relative to control (cells stimulated with 10% FCS under normoxic conditions). Whole cell extracts were prepared and analysed using Western blot for p-p38 MAPK (38 kDa) expression and GAPDH (37 kDa), which was used as a loading control. Each value represents the mean \pm SEM. * $p < 0.05$ vs. normoxic cells (n=3).

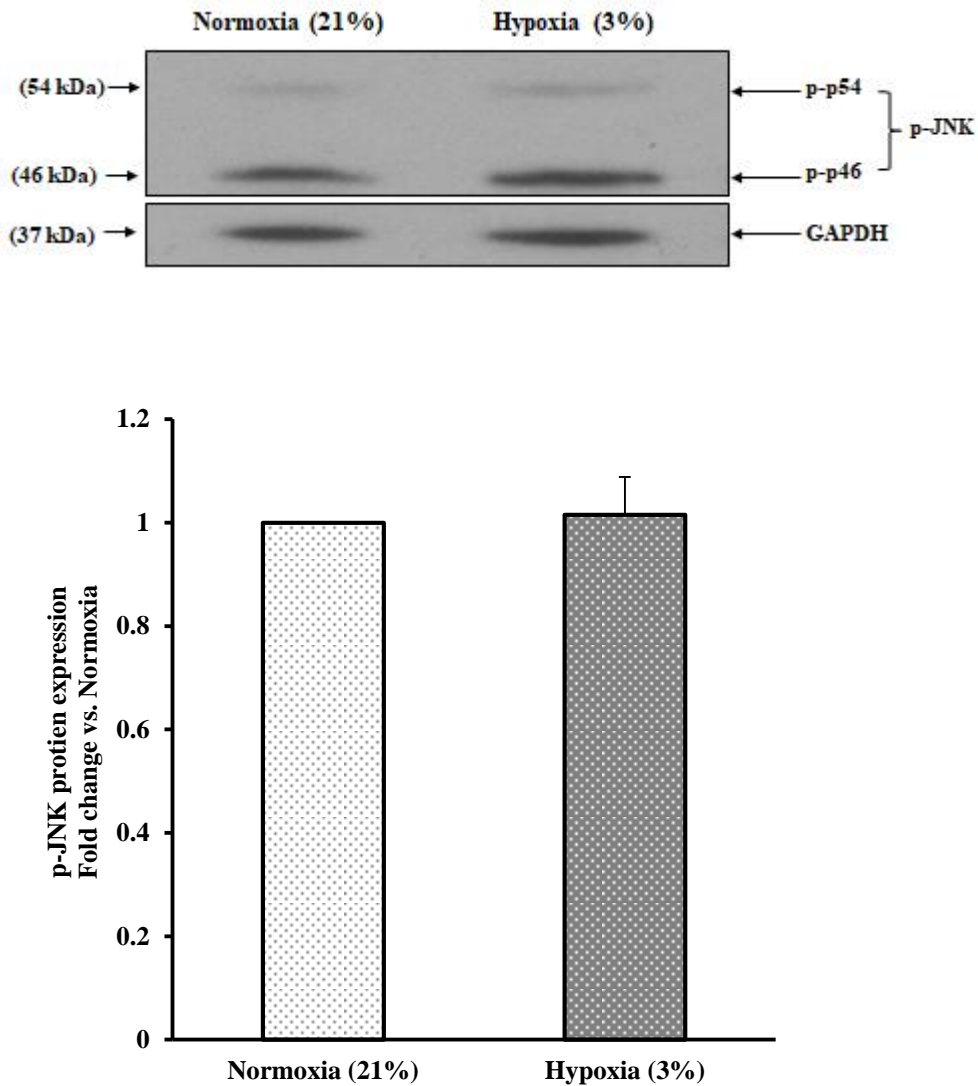


Figure 3.18 The effect of hypoxia (3% O₂) on JNK phosphorylation in PASMCs. Cells were seeded in pairs of 6 well plates. At 70-80% confluence, cells were quiesced for 24 hours. Then, cells were incubated at different oxygen levels; 21% oxygen (normoxia; control) and 3% oxygen (hypoxia; test) for 24 hours and were stimulated with 10% FCS for 15 minutes. Blots were assessed by semi-quantitative densitometry and results expressed as fold stimulation relative to control (cells stimulated with 10% FCS under normoxic conditions). Whole cell extracts were prepared and analysed using Western blot for p-JNK (54/46 kDa) expression and GAPDH (37 kDa), which was used as a loading control. Each value represents the mean \pm SEM (n=3).

3.15 Effect of Hypoxia (3% O₂) on PI3K/mTOR signalling pathway

The involvement of PI3K/mTOR cascade in 10% FCS stimulated cells, that promote cell proliferation following 3% oxygen hypoxia, was examined by measuring PI3K and AKT genes and the downstream signalling genes such as mTORC1 and P70s6K genes (Figure 3.19) using RT-qPCR. Results show a slight increase in PI3K (2 ± 0.4 fold) gene and a significant increase of AKT, mTORC1 and P70s6K genes (3.1 ± 0.5 fold, 3.5 ± 0.4 fold and 25.8 ± 0.49 fold, respectively) in hypoxic cells (Figure 3.19).

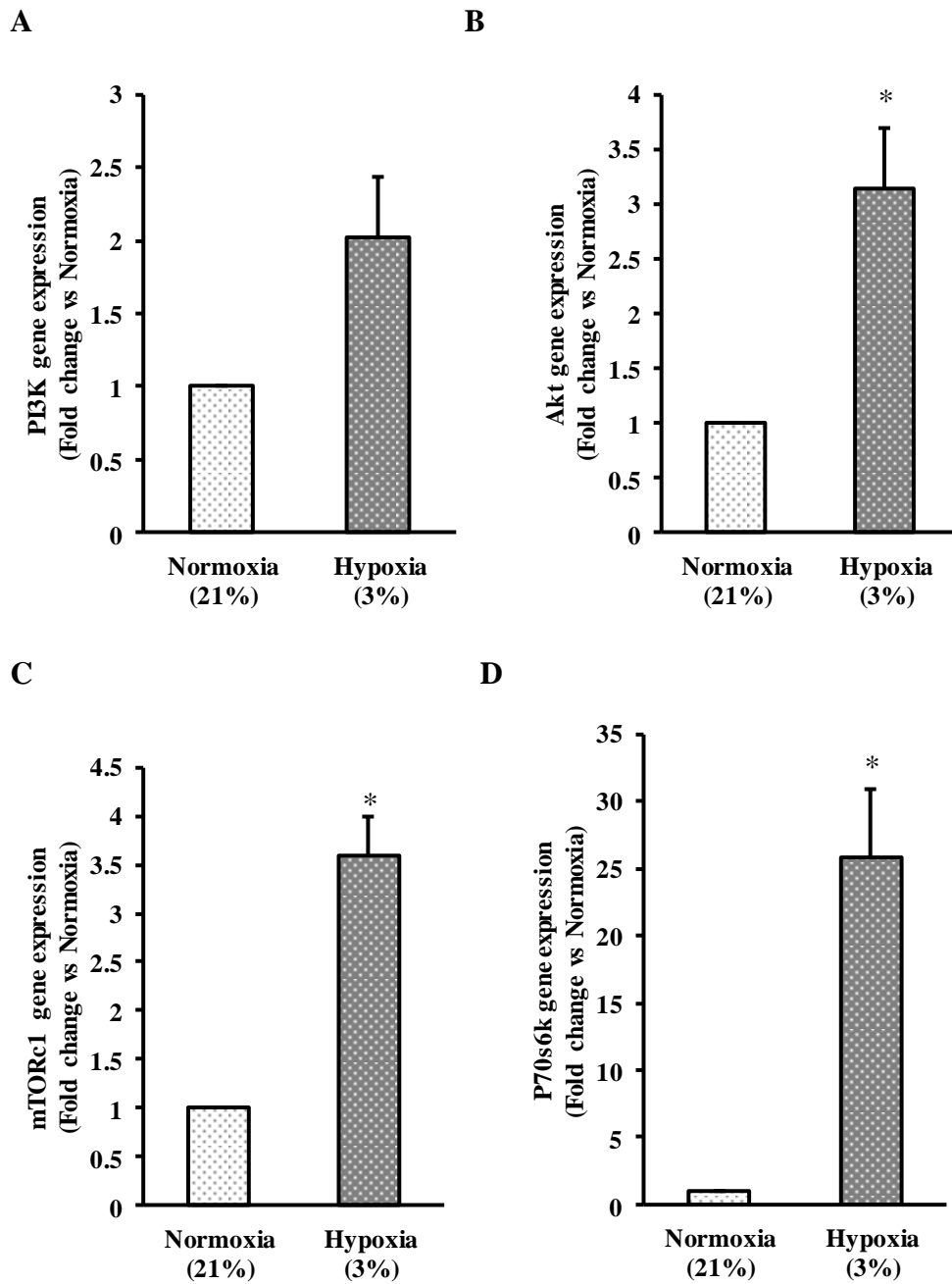


Figure 3.19 The effect of hypoxia (3% O₂) on PI3K/AKT/mTORC1 cascade in serum-stimulated PSMCs. Cells were quiesced for 24 h. 10% FCS was added immediately before normoxia (21% oxygen) and hypoxia (3% oxygen) 24 h incubations. RNA was extracted from the cells. Equal RNA concentrations were used for cDNA sample preparation. PI3K (A), AKT (B), mTORC1 (C) and P70s6k (D) genes were measured using RT-qPCR. Ubiquitin C (UBC) was used as the reference gene for normalization. *p < 0.05 vs. normoxic cells (n=3).

3.16 Discussion

The subject of this chapter covers isolating and characterizing primary PASMCs from rat lung and to establish a proliferative cell model (PASMCs from normal rats, in normoxia and acute hypoxia). The study hypothesized that proliferation of cultured PASMCs could be increased by lowering the oxygen levels (hypoxia). Therefore, this chapter attempts to assess the proliferative responses of the isolated PASMCs to different levels of hypoxia (10%, 5% and 3% O₂) under serum-stimulated conditions. It is believed that hypoxia strongly contributes to PASMC proliferation and pulmonary vascular remodeling (Brock et al., 2014, Chen et al., 2013). However, the mechanisms remain poorly understood. Subsequently, establishing this model will simplify the understanding of hypoxic-dependent proliferation signalling that is involved in the pathophysiology of the disease, particularly in PASMC proliferation. The specific contribution of hypoxia and MAPK/ mTORC1-dependent signalling related to PASMC proliferation is addressed in this chapter. In summary, research to find a reliable *in vitro* hypoxic-proliferative model was necessary to initiate this project.

3.17 The primary isolates of the pulmonary artery

The first aim of this chapter was characterizing the primary isolates of PASMCs from pulmonary arteries. Using the culturing technique described, PASMCs were clearly seen, explanted and started to grow from a rat pulmonary artery. The morphological characteristic “Hill and Valley” was clearly observed (Figure 3.2). The highly expressed specific markers, which exist in the contractile phenotype of SMC, such as myosin heavy chain and α -actin (Figure 3.3) were also of assistance in confirming the cells as smooth muscle cells and positively distinguished them from other adjacent cells found in the pulmonary artery vascular bed. For example, confluent endothelial cells have a distinct cobblestone characteristic appearance which differs from the spindle shape formation of PASMCs.

3.18 Effects of Serum concentration on Cell Proliferation

In this project, [³H] thymidine incorporation experiments were initiated to assess cell proliferation. [³H] Thymidine incorporation is considered as a gold standard measure of DNA synthesis and cell proliferation and it was previously tested and verified in our laboratory. In order to optimize the experiment in this study, the use of incremental serum concentrations to stimulate the cells was assessed (Figure 3.4). The validation of [³H] Thymidine experiments for measuring cell growth will strongly help to assess cell proliferation in experiments in other chapters in this thesis using different stimulants (e.g. PDGF).

3.19 The effect of Acute Hypoxia on PASMC Proliferation

Controversially, there are many studies about the effect of acute hypoxia on cultured PASMCs *in vitro*. It is uncertain if hypoxia directly or indirectly stimulates PASMC proliferation, whether hypoxia pushes the cells to produce autocrine growth factors or whether hypoxia has a strong stimulatory effect on adjacent cells, such as endothelial cells, to secrete factors that promote cellular growth. For example, during acute exposure to hypoxia, endothelial cells are capable of releasing growth factors such as basic fibroblast growth factor (bFGF) and prostaglandins (PGs) that promote smooth muscle cell proliferation (Michiels et al., 1994). On the one hand, many studies have shown that acute hypoxia is an indirect stimulus for PASMC proliferation (Dempsey et al., 1991, Lanner et al., 2005), or it indeed does harm to the cells and causes a reduction in cell proliferation (Eddahibi et al., 1999, Stiebellehner et al., 2003). On the other hand, other studies have demonstrated that acute hypoxia induces PASMC proliferation as a direct stimulant (Benitz et al., 1986, Preston et al., 2006).

The current study shows that rat PASMCs have variable proliferative responses to different hypoxic degrees; 10%, 5% and 3% oxygen. In hypoxia (10% O₂), the DNA synthesis value in hypoxic cells was unaffected in comparison to normoxic control cells in response to 0.1 % FCS (Figure 3.5). At 5% and 3% O₂ in the absence of serum, the growth of PASMCs was enhanced by hypoxia (Figure 3.8 and Figure 3.10, respectively). However, 5% and 3% O₂ exposure failed to induce any significant increase in cell proliferation, suggesting that cells during hypoxia

seem to require more nutrients (growth factors) to promote significant growth following 24 hours incubation. This was seen in hypoxia (3% O₂) as the growth rates of hypoxic cells stimulated with 10% FCS were significantly enhanced (Figure 3.10). Thus, this result, an increase in PASMC proliferation by 3% O₂ level of hypoxia, is the foundation for the following chapter.

3.20 The Effect of Hypoxia (10% and 5% O₂) on ERK1/2 phosphorylation

The mitogen-activated protein kinases (MAPKs) are a group of serine/threonine kinases which are strongly linked with VSMC proliferation (Gennaro et al., 2003, Shen et al., 2014). In particular, it has been reported that in comparison to other MAPK proteins; p38 MAPK and JNK, the phosphorylated form of ERK1/2 protein had a dominant effect on VSMC survival and proliferation in response to PDGF (Zhan et al., 2003). The following chapter goals are therefore to investigate the association between cell proliferation and acute hypoxia in cultured PASMCs and to examine the effect of hypoxia on the MAPK signalling pathway of these cells, assessment of the ERK1/2 phosphorylation at different time points was undertaken in PASMCs. The result highlighted the highest level of ERK1/2 phosphorylation was seen at 15 minutes post stimulation (Figure 3.6). This result is in line with a study by (Zhang et al., 1998) as they found that the MAPK proteins phosphorylation in PASMCs increases at 15 minutes in response to hydrogen peroxide stimulation. Optimization of stimulation time will facilitate the study of all MAPK cascades in PASMCs. For example, in this chapter, investigation of different levels of hypoxia (10%, 5% and 3% O₂) on ERK1/2 phosphorylation was performed using 10% FCS in cells which were cultured for 24 hours under hypoxic conditions and therefore were stimulated with 10% FCS for 15 minutes.

In quiescent cells (cells with 0.1% FCS), Western blot data show hypoxia (10% O₂) did not activate ERK phosphorylation (Figure 3.7). This was correlated with the result of [³H] thymidine incorporation that supports the failure of hypoxia (10% O₂) to be a direct inducer of cell proliferation (Figure 3.5). In hypoxia (5% O₂), an absence of ERK phosphorylation was also observed in quiescent cells (Figure 3.9) whereas [³H] thymidine incorporation results show a slight increase in DNA

synthesis (Figure 3.8), suggesting that ERK1/2 MAPK signalling may not be involved in hypoxic-dependent cell proliferation.

In serum-stimulated cells, Western blot data reinforced that exposure to 10% O₂ (Figure 3.7) or 5% O₂ (Figure 3.9) did not mediate further increase to ERK1/2 phosphorylation. These data were in line with [³H] thymidine incorporation findings (Figure 3.5 and Figure 3.8, respectively) which show that exposure to 10% O₂ or 5% O₂ had no effect on cell proliferation. A suggested explanation for these results is that the acute exposure to 10% O₂ or 5% O₂ had a negative effect on cell proliferation even when cells were stimulated with FCS which may help the hypoxic effect to enhance the cellular growth. It has, however, been reported by (Blaschke et al., 2002) that phosphorylation of ERK1/2 MAPK caused by extracellular hypoxic (1% O₂) stimuli is evidently upregulated in quiescent VSMCs. In addition, the involvement of all MAPK proteins was detected in pulmonary arterial remodeling in response to hypoxia (Jin et al., 2000). Hence, further examination of MAPK signalling proteins and cell proliferation was carried out at a more severe hypoxic level, to clarify the effect of acute hypoxia in both the quiescent and the serum-stimulated PASMCs.

3.21 The Effect of Hypoxia (3% O₂) on PASMC Proliferation

Increased DNA synthesis and proliferation of PASMCs was observed by reducing the oxygen to 3% (Figure 3.10). At 10% serum stimulation, hypoxia (3% O₂) shows a significant increase in cell proliferation (Figure 3.10). This finding supports Schultz and co-workers (2006) study, which reported that hypoxia enhanced the proliferative responses of smooth muscle cells to mitogens in comparison to normoxic controls. To clarify whether there is a substantial effect of hypoxia on cell proliferation, several experiments were performed to investigate the proliferative state by measuring some proteins and genes of signalling pathways, which regulate cell proliferation and may be involved in the hypoxic-dependent mechanism.

Data showed a significant increase in the proliferative genes such as PCNA, cyclin D1 and ERK1 genes (Figure 3.11). An increase of ERK1 gene in the hypoxic group following 10% FCS stimulation was correlated with the Western blot findings

which show a slight increase in its protein expression (Figure 3.16). It has been shown that serotonin (5-HT) and Rho-kinase (ROCK) signalling pathways contribute to hypoxia-induced cell proliferation and pulmonary arterial remodeling (Homma et al., 2007). Serotonin stimulates ERK phosphorylation and therefore, the activated Rho-kinase (ROCK) facilitates the translocation of the phosphorylated ERK into the nucleus, which leads to subsequent activation of nuclear transcription factor cyclin D1 which results in proliferation of PASMC (Mair et al., 2008, Liu et al., 2004). In addition, data showed another correlation between the PCNA gene expression (Figure 3.11) and the fluorescence intensity of PCNA within the PASMCs (Figure 3.12), which both were increased due to the proliferative effect of hypoxia in 10% FCS stimulated cells. These findings are consistent with a study that showed hypoxia activates ROS production which causes elevation of cyclin D1 and PCNA, and subsequently increases PASMC proliferation and remodeling (Adesina et al., 2015). In addition, it has been demonstrated that PCNA positive cells exist in the medial smooth muscle layer of the pulmonary arteries following hypoxic exposure in comparison to normoxic controls (Mizuno et al., 2015).

The result shows a significant reduction of the pro-apoptotic gene in the hypoxic group (*cdkn2a*, Figure 3.13). This finding also supports the hypoxic effect on cell proliferation. It has been reported that an increase in *cdkn2a* expression in human melanoma cells suppressed the proliferation and migration of these cells (Bai et al., 2016).

Data showed the exposure to hypoxia (3% O₂) caused a significant increase in hypoxia-inducible factor-1 (HIF-1 α) gene expression, which is recognised as a key regulator gene of the transcriptional response to hypoxia (Figure 3.14A). This result is consistent with the majority of previously published findings that support the definite relationship between the lack of oxygen in the environment (hypoxia) and the numerous cellular responses (e.g. cell proliferation), which resulted from the transcription factor HIF-1 α . HIF-1 α plays a major role in the pathogenesis of hypoxic pulmonary hypertension particularly in the regulation of PASMC proliferation. For example, the expression of endothelin-1 (ET-1) within the pulmonary vasculature is increased in hypoxic rats (Kim et al., 2015) and the increased expression of HIF-1 α gene in the PASMCs contributes to the ET-1 effect.

This effect includes increased intracellular Ca^{2+} , production of ROS and subsequent ERK1/2 phosphorylation which results in an increase in cell proliferation (Pisarcik et al., 2013). HIF-1 α not only contributes to cell proliferation; but also to the inflammatory mechanisms involved in lung disorders and pulmonary hypertension (Xu et al., 2016).

Additional qPCR findings show an increase in the HIF-2 α gene expression (Figure 3.14B) and in the arginase-1 gene expression (Figure 3.15) in cells that were exposed to hypoxia (3% O_2). These results suggest the vital role of these genes in hypoxia-induced pulmonary hypertension and cell proliferation. Consistent with these results, a study by Elorza and co-workers demonstrated that high levels of HIF-2 α within cancer cells activate the mTORC1 cascade, which enhances cell proliferation (Elorza et al., 2012). Another study by Gordan and co-workers reported that HIF-2 α enhances cell proliferation under hypoxic conditions by increasing c-Myc activity (Gordan et al., 2007). Moreover, it was reported that upregulation of HIF-2 α has strongly contributed to the development of pulmonary hypertension by affecting the pulmonary vascular resistance through arginase-1 dependent mechanisms (Cowburn et al., 2016). This study showed the down-regulation of arginase-1 in isolated lungs from mice lacking HIF-2 α following hypoxic treatment and demonstrated that arginase-1 deletion influenced the development of hypoxic pulmonary hypertension. A rise in pulmonary vascular resistance and the development of pulmonary hypertension are caused by generalized alveolar hypoxia leading to a generalized construction of pulmonary arteries (Weir and Olschewski, 2006). Another study also highlighted the involvement of arginase 1 in hypoxia-induced pulmonary hypertension, which has been involved in decreasing airway nitric oxide and in increasing remodeling and collagen deposition in patients with pulmonary hypertension (Grasemann et al., 2015). Pulmonary arterial hypertension stimulates arginase 1 activity, which promotes the proliferation of vascular smooth muscle cells by increasing the intracellular production of polyamine and L-proline, which in turn stimulate the proliferation of EC and VSM and collagen synthesis, favouring a thick fibrous cap and thus leading to neointima formation and medial thickening of the vascular wall (Wang et al., 2014c, Durante, 2013).

3.22 The Effect of Hypoxia (3% O₂) on p38 MAPK phosphorylation

Several studies have reported the critical role of p38 MAPK in hypoxic pulmonary hypertension pathogenesis and its importance in response to hypoxia (Das et al., 2001, Lu et al., 2004 and Jin et al., 2000). In addition, an activation of p38 MAPK in the pulmonary artery was revealed in both acute and chronic hypoxia (Welsh et al., 2006). In the Western blot experiments conducted in this chapter (Figure 3.17), the data show a significant increase in p38 MAPK phosphorylation was observed in stimulated hypoxic cells, suggesting that the proliferative response of PASMCs due to 3% O₂ appears to be dependent on the constitutive phosphorylation of p38 MAPK. The link between p38 MAPK phosphorylation, HIF-1 α stability and cell proliferation has been shown in hypoxic pulmonary fibroblasts (Pouyssegur et al., 2003).

3.23 The effect of hypoxia (3% O₂) on mTOR signalling pathway

Results show hypoxia (3% oxygen) increases the gene expression of AKT/mTORC1/P70s6k cascade in 10% FCS stimulated cells suggesting that proliferation of PASMCs was enhanced following hypoxic treatment. These findings are correlated with a study which found that activation of the AKT/mTORC1/P70s6k pathway by aldosterone increases proliferation, viability and apoptosis resistance of PASMCs in hypoxic rats (Aghamohammadzadeh et al., 2016).

3.24 Main Findings

The main findings of this chapter are

- PASMCs exposed to 3% O₂ are more likely to show a proliferative response compared to the cells exposed to less hypoxic levels such as 10% O₂ and 5% O₂.
- Acute hypoxia (3% O₂) has a direct proliferative effect on PASMCs and it significantly enhanced the cellular growth in response to 10% FCS stimulation in particular. Therefore, exposure to 3% O₂ as an experimental test model to study the cell signalling involved in PASMC proliferation-induced pulmonary hypertension was successfully achieved.
- The MAPK signalling (particularly ERK1/2 and p38 MAPK) pathway, the intracellular signalling pathway that regulates cell proliferation such as PI3K/ mTORC1 pathway and the cell cycle regulatory gene cyclin D1 appear to contribute to the combined effect of 3% O₂ and 10% serum.

Chapter 4

The Role of Mitochondria in Regulating Pulmonary Artery

Smooth Muscle Cell Proliferation and Migration

4.1 Introduction

One of the main features observed in cardiovascular disease is a reverse phenotypic shift from the normal contractile (quiescent) state to the synthetic phenotype of vascular smooth muscle cells (VSMCs), which promotes cell proliferation and cell migration from the medial layer into the intimal region, which eventually leads to severe narrowing of the vessels (Rudijanto, 2007). As described in chapter 1, excessive proliferation and migration of the PSMCs are the major pathogenic components involved in the development of pulmonary vascular remodeling and pulmonary hypertension, which are aggravated by hypoxia (Marsboom et al., 2012, Schermuly et al., 2005, Luo et al., 2013). Several signalling growth factors/mediators are involved in the aberrant proliferation and migration of smooth muscle cells including platelet-derived growth factor (PDGF), basic fibroblast growth factor (bFGF) and epidermal growth factor (EGF) (Ushio-Fukai et al., 2001, Xin et al., 1994, Yu et al., 2003). PDGF is considered as one of the most potent mitogens in PSMCs, which mediates the conversion to the hyperproliferative/apoptosis-resistant phenotype (Owens et al., 2004). PDGF has also been shown to increase glycolysis and mitochondrial activity in these cells (Moncada et al., 2012) and gene expression has been recognized in response to hypoxia (Voelkel and Tuder, 1995). The mechanisms driving PSMC proliferation and migration in response to PDGF during hypoxia are important as they contribute to the development of pulmonary vascular remodeling (Schermuly et al., 2005). Therefore, identifying signalling proteins associated with the PDGF stimulated cells is necessary as they can provide potential therapeutic targets in pulmonary hypertension. Mitochondria have been suggested to have an important role in the development of pulmonary vascular remodeling. This is probably because of the reversible suppression of the mitochondria involved in the development of cancer, similar to the uncontrolled proliferation of PSMCs in pulmonary hypertension (Dromparis and Michelakis, 2013). The balance between proliferation/apoptosis is mediated by mitochondria and mitochondrial dysfunction could potentially result in either an increase in cell growth/proliferation or an increase in apoptosis (Li et al., 1997). Due to the lack of understanding of the exact mechanisms related to mitochondrial-dependent cell signalling in regulating cell proliferation and

migration, this chapter will focus on identifying the role of mitochondria in PASMCM proliferation and migration.

4.2 Mitochondria and PASMCM proliferation

Mitochondria are motile organelles which are widely known to produce the energy-carrying molecule adenosine triphosphate (ATP), control cell signalling pathways, cell growth and signal apoptosis (Wallace, 2005). Mitochondria have a strong impact on many cell functions including metabolism, ROS generation and mitochondrial dynamics, which all have been shown to be directly associated with hyperproliferative diseases such as pulmonary hypertension and cancer (Archer et al., 2008). Therefore, the study of the role of mitochondria in PASMCM proliferation and migration could explain many unresolved questions in proliferative vascular remodeling. For example, several studies have reported the mitochondria/metabolic theory (the Warburg phenomenon in cancer cells), which is observed in PASMCMs and this contributes to PASMCM over-proliferation and resistance to apoptosis (Dromparis et al., 2010, Paulin and Michelakis, 2014, Sutendra and Michelakis, 2014). In the pulmonary circulation, mitochondria from the PASMCMs are considered as oxygen sensors and during hypoxia, they become hyperpolarized and generate low reactive oxygen species (ROS) levels (Weir et al., 2005). Mitochondria regulate vascular tone through the production of mediators such as H₂O₂ that diffuse to the cell cytoplasm and are involved in the redox state in cells. H₂O₂ is a redox signalling molecule which causes vasodilation and a reduction in cell proliferation (Burke-Wolin and Wolin, 1989, Michelakis et al., 2002). H₂O₂ can alter cell membrane proteins such as K⁺ channels and thus indirectly regulate vascular tone (Paffett and Walker, 2007, Archer et al., 2004). Oxygen and redox-sensitive K⁺ channels have been demonstrated to be the effectors in oxygen sensing in the pulmonary artery (Weir and Archer, 1995). H₂O₂ is released in smooth muscle cells from the electron transport chain in mitochondria (Costa et al., 2016). The physiological level of H₂O₂ is maintained in the cell by several enzymes such as superoxide dismutase-2 (SOD2), also known as manganese superoxide dismutase (MnSOD), an enzyme that converts superoxide (O₂⁻) to H₂O₂ (Wang et al., 2012). A study by Michelakis and co-workers has reported that the pulmonary artery and the systemic artery have different mitochondria. In the hypoxic setting,

mitochondria from the pulmonary artery produce higher expression of SOD2 enzyme and lower expression of electron transport chain components when they are compared with mitochondria from systemic arteries (Michelakis et al., 2002). Consequently, a decrease in mitochondrial ROS generation, H₂O₂ in particular (Figure 4.1), inhibits the redox-sensitive voltage-gated K⁺ channels at the cell membrane, causing depolarization, increasing the intracellular Ca²⁺ levels resulting in activation of the transcription factors nuclear factor of activated T cell (NFAT) and hypoxia-inducible factor-1 (HIF-1), leading to increased proliferation and impaired apoptosis (Yuan et al., 1998, Papandreou et al., 2006, Sutendra et al., 2010, Dromparis et al., 2010).

Moreover, smooth muscle cells in pulmonary hypertension have not only increased rates of glycolysis and altered redox states but also enhanced mitochondrial dynamics (Marsboom et al., 2012). This suggests there is an important link between the morphology of the mitochondria, fission and fusion mitochondrial processes and the proliferative phenotype of the pulmonary artery smooth muscle cell. In patients with PAH, isolated endothelial cells and smooth muscle cells from their lungs showed hyperpolarized and dysmorphic mitochondria associated with a glycolytic shift in the cellular metabolism (Dromparis et al., 2010).

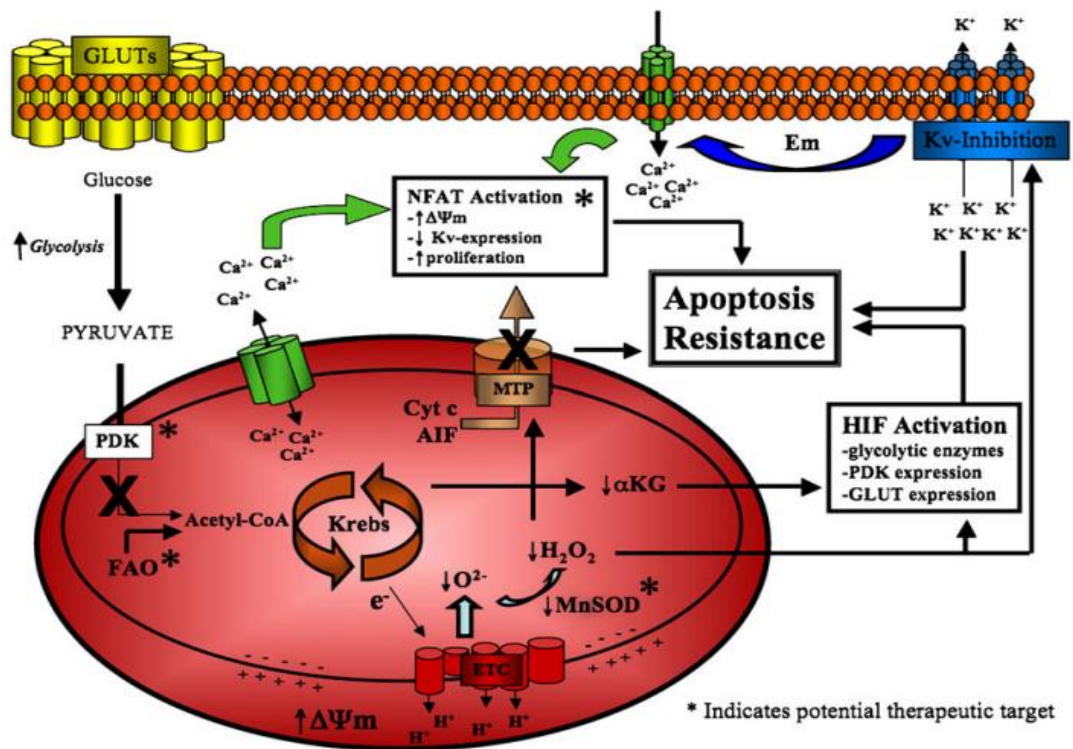


Figure 4.1 The mitochondrial effect on PASM C proliferation/apoptosis balance in PAH. In PASM Cs, mitochondria have decreased pyruvate influx, become hyperpolarized and decreased the activity of Krebs cycle. These changes alter the mitochondrial membrane potential ($\Delta\Psi_m$). As a result, mitochondria are incapable to produce ROS. Impaired mitochondrial ROS leads to the closure of the mitochondria transition pore (MTP), trapping cytochrome c and apoptosis-inducing factor (AIF) in the matrix, resulting in apoptosis resistance. It also inhibits redox-sensitive K^+ channels leading to accumulation of intracellular K^+ and Ca^{2+} , resulting in an increase in contraction and proliferation. Increasing the intracellular Ca^{2+} levels leads to the activation of transcription factors (HIF and NFAT), that further inhibit apoptosis, promote cell proliferation and sustain the PASM C mitochondrial metabolic phenotype. This phenotype is repressed by activating pyruvate dehydrogenase (PDH) by using a pyruvate dehydrogenase kinase inhibitor (e.g. dichloroacetate (DCA), or by inhibiting fatty acid oxidation (FAO) which indirectly stimulates PDH. Restoring mitochondrial ROS (particularly the H_2O_2) by increasing the MnSOD enzyme may also have a beneficial outcome. *Represents potential therapeutic targets predicted by the PASM C mitochondrial metabolic phenotype in PAH. Adapted from (Dromparis et al., 2010).

4.3 Mitochondrial fission protein DRP1 as a potential therapeutic target in pulmonary hypertension

Mitochondria exist in isolation (mitochondrion) or typically in networks that can range from very short fragmented mitochondrial networks to long elongated networks. As mentioned in (Chapter 1, section 1.10), these differences in network lengths are the results of two fundamental processes of mitochondrial movements within the cell known as fission and fusion. Mitochondrial movement is collectively termed mitochondrial dynamics (Suen et al., 2008). Mitochondrial morphology and dynamics are important for maintaining healthy functional mitochondria and regulating the bioenergetic status within the cells (Chen and Chan, 2010). Mitochondrial fission is necessary when the mitochondria are distributed to daughter cells in the case of cell division (Mishra and Chan, 2014). The major protein responsible for mitochondrial fission is the DRP1 protein (Cribbs and Strack, 2009). DRP1 is mainly cytosolic and its recruitment to the mitochondrial surface for fission requires other proteins such as mitochondrial fission 1 (Fis1) and mitochondrial fission factor (Mff) (Gandre-Babbe and van der Bliek, 2008). On the fission sites, DRP1 creates a constriction circle which drives organelle fragmentation (Carlucci et al., 2008). Disruptions in the balance of fission-fusion events are thought to play a role in various pathological conditions such as pulmonary hypertension. For example, dysfunctional mitochondria in pulmonary arterial remodeling, particularly in PSMCs, are due to their oxygen sensing and disordered dynamics (Bonnet et al., 2006). In PSMCs from PAH patients, HIF-1 α is activated, DRP1 expression is increased and the mitochondria are extremely fragmented (Marsboom et al., 2012). Therefore, proteins involved in regulating the processes of mitochondrial fusion/fission are potential targets (Figure 4.2). Recently, the role of DRP1 protein, a protein responsible for mitochondrial fission, has begun to attract attention as a potential therapeutic target in cancer and vascular diseases. Brooks and co-workers have reported increased mitochondrial fission causes an unusual upturn in mitochondrial fragmentation, which leads to an increase in reactive oxygen species (ROS) production, which may increase cell proliferation (Brooks et al., 2009). In addition, Wang et al. (2015) have demonstrated that controlling mitochondrial fission may play a role in preventing cell migration. Moreover, Lim et al. and Marsboom et al. reported that an inhibition

of mitochondrial dynamics prevents mitochondrial fission and slows the proliferation of VSMCs and PASCs, respectively (Lim et al., 2015, Marsboom et al., 2012). These results led to further studies in an attempt to understand the mitochondrial signalling mechanism by inhibiting the fission mediator DRP1 protein.

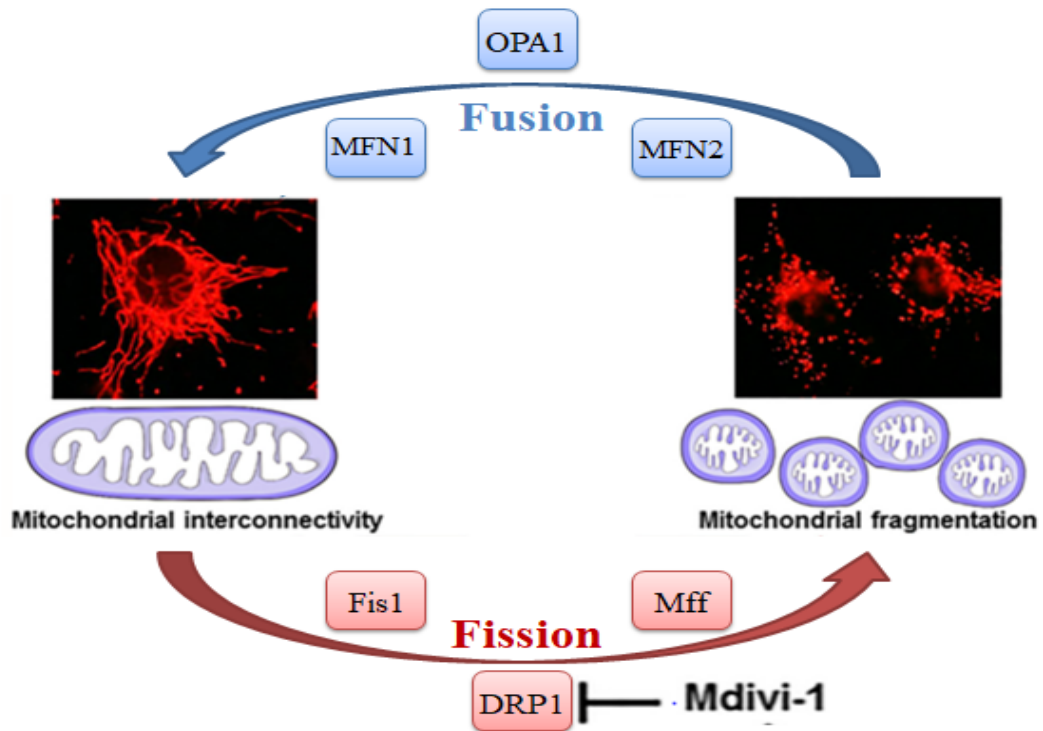


Figure 4.2 Mitochondrial fusion and fission processes and their major mediators. The elongated mitochondrial shape (mitochondrial interconnectivity) is maintained by mitochondrial fusion. This process is mediated by proteins such as mitofusin 1 (MFN1), mitofusin 2 (MFN2) and optic atrophy-1 (OPA1). Mitochondrial fragmentation is maintained by mitochondrial fission which is regulated by proteins such as mitochondrial fission 1 (Fis1), mitochondrial fission factor (Mff) and dynamin-related protein-1 (DRP1). Mdivi-1 suppresses the mitochondrial fission via inhibiting the DRP1 protein. Adapted from (Rosdah et al., 2016).

4.4 Chapter Aims

- To measure the effect of inhibition of mitochondrial fission (using a DRP1 inhibitor, Mdivi-1) on PASC proliferation and migration under normoxic and hypoxic cell culture conditions.
- To examine the bioactivity of the mitochondria following Mdivi-1 treatment under normoxic and hypoxic cell culture conditions.

4.5 Results

4.6 The combined effect of Hypoxia and PDGF on Cell Proliferation

The proliferative response caused by acute hypoxia and PDGF was assessed by [³H]-thymidine incorporation assay in PASMCMs. As previously presented in chapter 3, when quiescent cells were exposed to hypoxia 3% for 24 h, there was an insignificant increase in cellular DNA synthesis. However, in the presence of serum (10% FCS), there was a significant increase (Figure 3.10). In this chapter, [³H] thymidine incorporation experiments were repeated using PDGF in place of serum as a specific mitogen to study its combined effect with hypoxia (3%) on PASMCM proliferation. Initially, increasing PDGF concentrations were used to stimulate PASMCM proliferation under normoxic conditions. As shown in Figure 4.3, the lowest PDGF concentration (5 ng/ml) significantly increases cellular DNA synthesis (5.2 ± 0.36 fold of basal), which was comparable to higher PDGF concentrations; (10 ng/ml = 5.99 ± 0.66 and 20 ng/ml = 5.25 ± 0.29 fold of basal control). Hence, the lowest PDGF concentration (5 ng/ml) was selected to stimulate pulmonary cellular growth under hypoxic (3%) conditions.

Furthermore, the effect of PDGF under acute hypoxic exposure (3% oxygen) was also examined by [³H] thymidine incorporation assay (Figure 4.4). In serum-deprived (0.1% FCS) media, hypoxia increased the rate of DNA synthesis by 1.6 ± 0.4 fold. Following PDGF stimulation, data show that PDGF increased cell proliferation by 4.5 ± 0.5 fold under normoxic conditions. However, exposure of cells to hypoxia significantly enhanced cell growth by 1.59 ± 0.15 fold in comparison to normoxic stimulated cells (Figure 4.4).

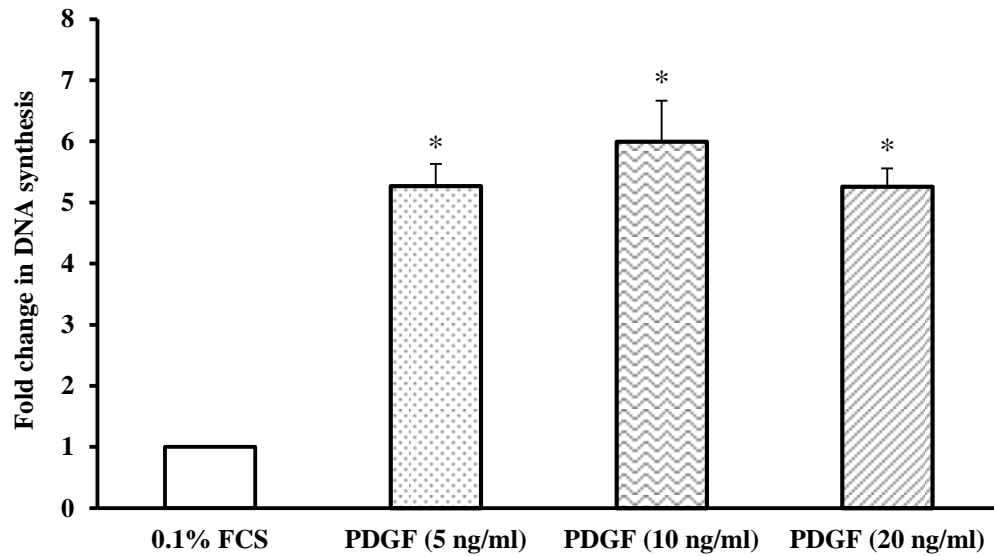


Figure 4.3 The effect of PDGF on pulmonary artery smooth muscle cell proliferation. Cells were quiesced for 24 h in the normoxic incubator. Cells were then stimulated with increasing platelet-derived growth factor (PDGF) concentrations (5, 10 and 20 ng/ml) for 24 h. DNA synthesis was evaluated by [³H]-thymidine incorporation assay. Radioactive counts were measured in disintegrations per minute (DPM) and normalized to DNA synthesis in the control group (quiescent cells, 0.1% FCS). *p <0.05 vs. quiescent cells. Experiments were conducted in quadruplicate (number of wells). Each value represents the mean ± SEM (n=3).

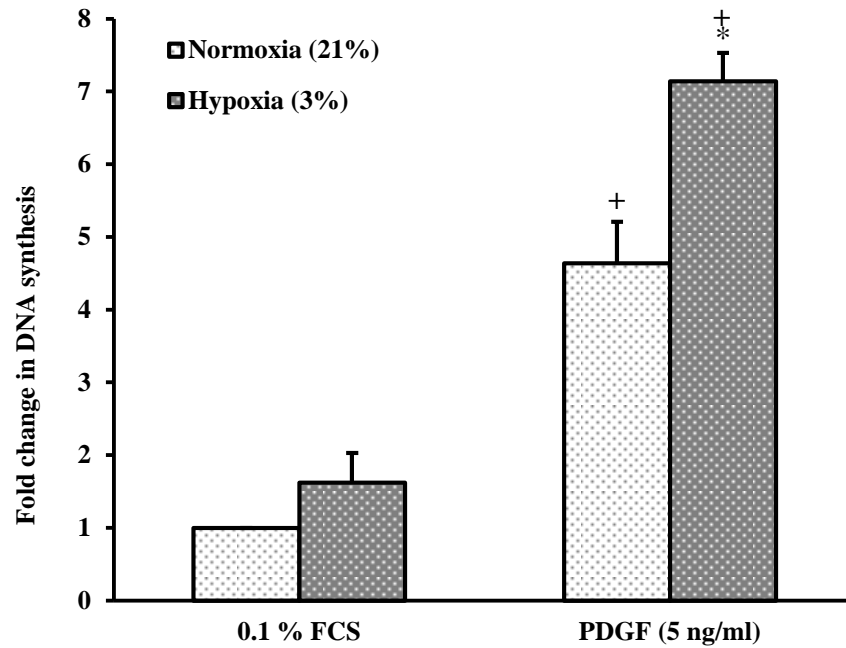


Figure 4.4 The effect of hypoxia on PDGF induced cell proliferation. Cells were quiesced for 24 h under normoxic conditions. Cells were then incubated at different oxygen levels: normoxia (21% oxygen) and hypoxia (3% oxygen) for 24 h. PDGF (5 ng/ml) was added immediately before hypoxic exposure. DNA synthesis was evaluated by [³H]-thymidine incorporation assay. Radioactive counts were measured in disintegrations per minute (DPM) and normalized to DNA synthesis in the control group (quiescent cells, 0.1% FCS). *p <0.05 vs. cells cultured in normoxia. +p <0.05 vs. quiescent cells. Experiments were conducted in quadruplicate (number of wells). Each value represents the mean ± SEM (n=3).

4.7 Effect of Mdivi-1 on Hypoxic-PDGF induced cell Proliferation

In order to assess the effect of Mdivi-1 on PASMCM proliferation under both normoxic (21% oxygen) and hypoxic (3% oxygen) cell culture conditions, DNA synthesis was measured using [³H]-thymidine incorporation assay. Inhibiting mitochondrial fission using 10 μM Mdivi-1 in PDGF stimulated cells resulted in a 27 ± 2.88 % reduction and a 67.5 ± 2.9 % reduction in DNA synthesis under both normoxic and hypoxic conditions, respectively (Figure 4.5). A significant difference in DNA synthesis was detected among Mdivi-1 treatments in hypoxia versus normoxia. Blocking PDGF receptors with 10 μM imatinib was used as a negative control, which reduced the stimulation to near basal levels (Figure 4.5).

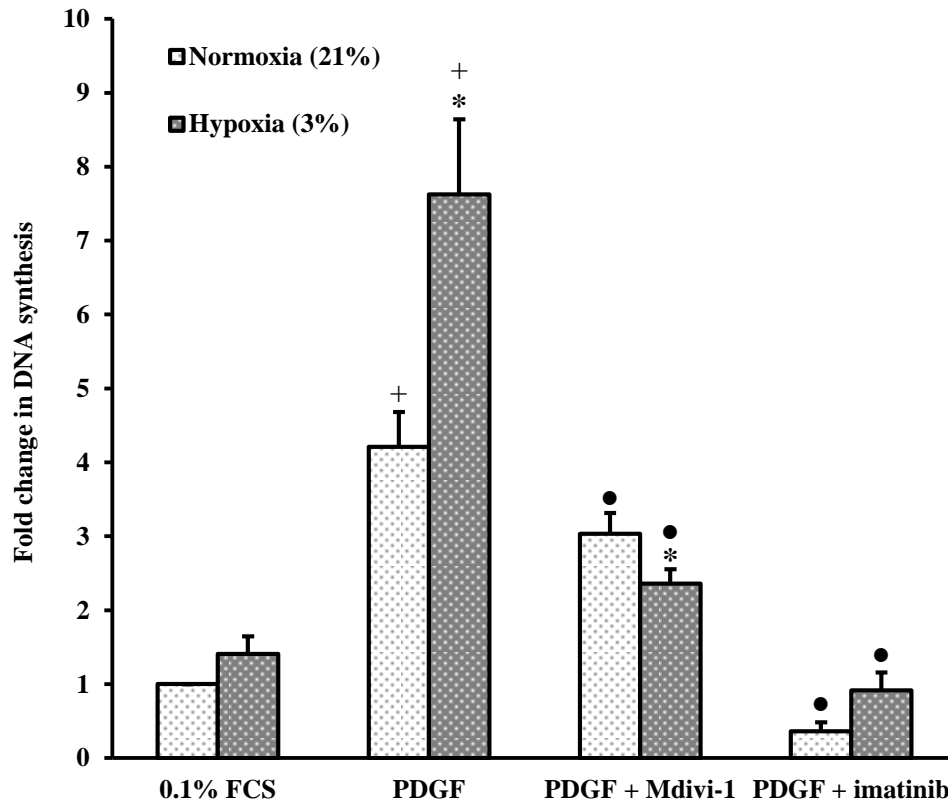


Figure 4.5 The effect of Mdivi-1 on PDGF induced PASC proliferation. Cells were quiesced for 24 h under normoxic conditions. Cells were then stimulated with PDGF (5 ng/ml) and incubated at different oxygen levels: normoxia (21% oxygen) and hypoxia (3% oxygen) for 24 h. Mdivi-1 (10 μ M) or imatinib (10 μ M) were added 30 minutes before stimulation. [3 H]-thymidine incorporation assay was performed for DNA synthesis evaluation. Radioactive counts were measured in disintegrations per minute (DPM) and normalized to DNA synthesis in the PDGF stimulated group. +p <0.05 vs. quiescent cells. *p <0.05 vs. cultured cells in normoxia. •p <0.05 vs. PDGF stimulated cells. Experiments were conducted in quadruplicate (number of wells). Each value represents the mean \pm SEM (n=5).

4.8 Effect of Mdivi-1 on Hypoxic-FCS induced cell Proliferation

As previously reported in chapter 3, at 10% FCS (Figure 3.10), hypoxia (3% O₂) significantly stimulated PASMC proliferation. Therefore, the effect of the DRP1 inhibitor (Mdivi-1) was examined in 10% serum under both normoxic and hypoxic conditions (Figure 4.6). Data show that Mdivi-1 treatment caused a significant reduction in DNA synthesis in response to 10% FCS stimulation (23.1 ± 5.9 %) and the combined stimulatory effects of 10% FCS and hypoxia (3% O₂) (31.4 ± 4.8 %).

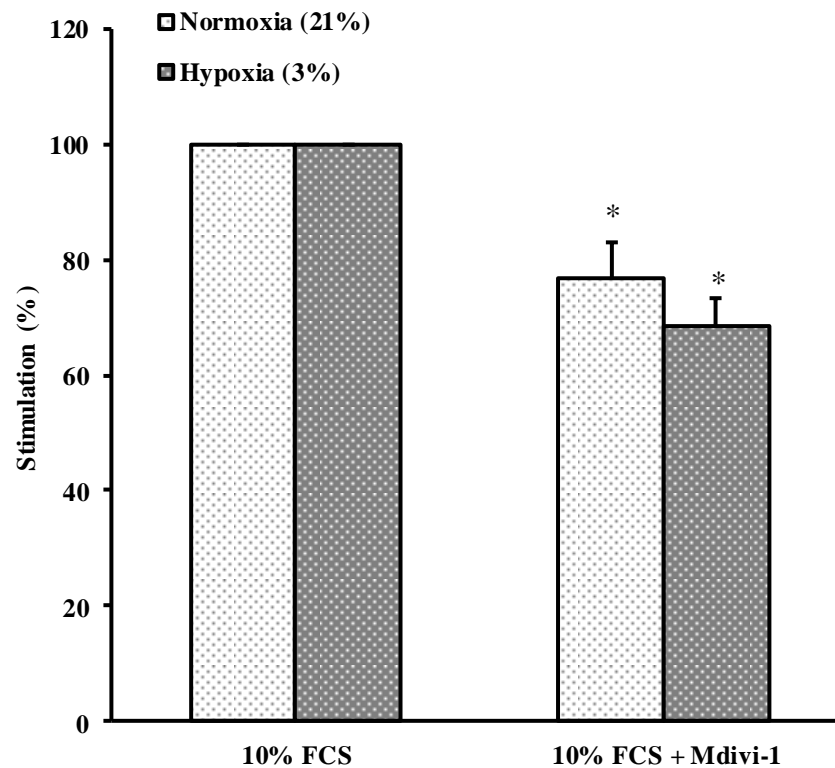
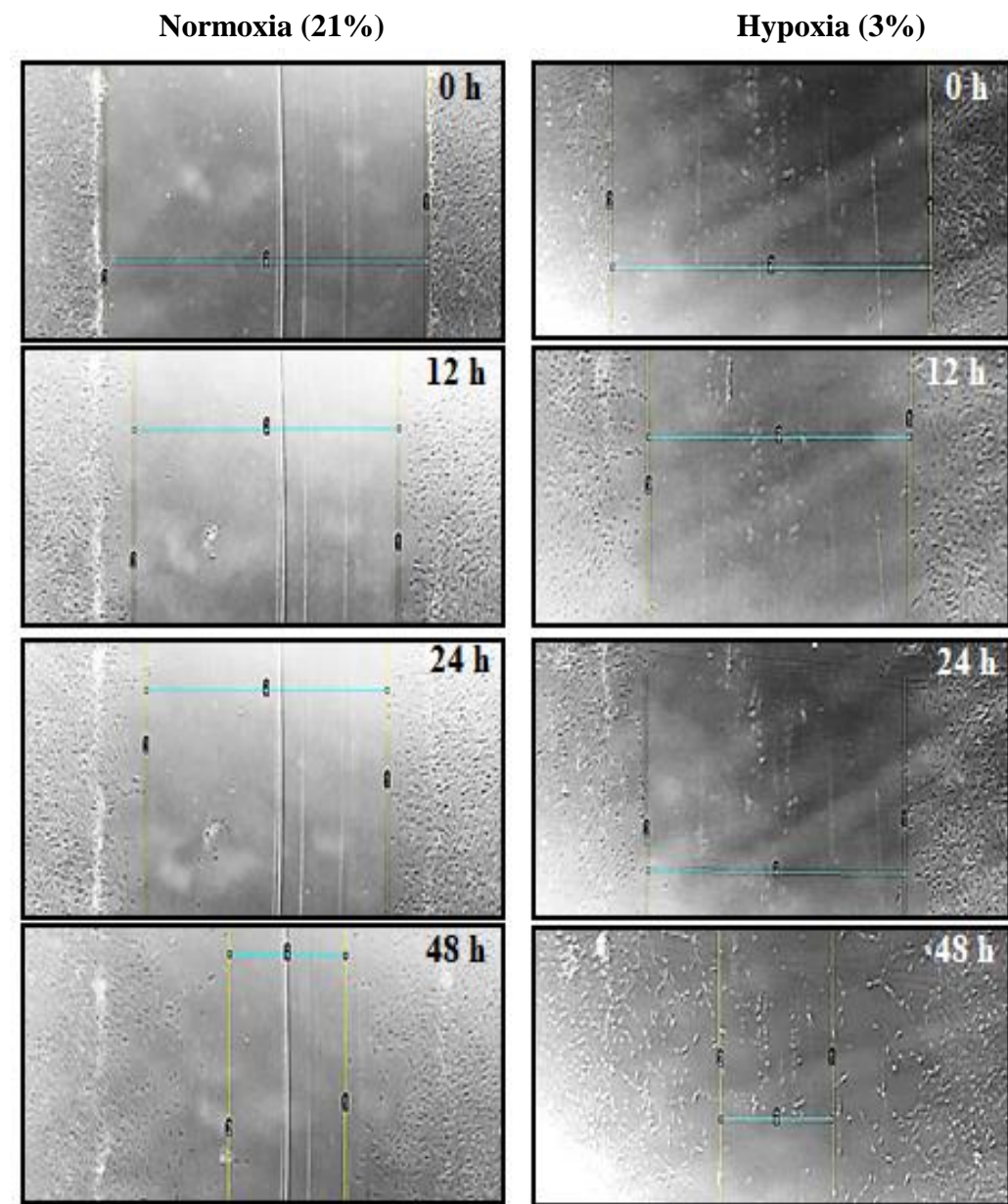


Figure 4.6 The effect of Mdivi-1 on 10% FCS induced PASMCM proliferation. Cells were quiesced for 24 h under normoxic conditions. Cells were then stimulated with 10% FCS and incubated at different oxygen levels: normoxia (21% oxygen) and hypoxia (3% oxygen) for 24 h. Mdivi-1 (10 μ M) was added 30 minutes before stimulation. [3 H]-thymidine incorporation assay was performed for DNA synthesis evaluation. Experiments were conducted in quadruplicate (number of wells). In each oxygen condition, radioactive counts were measured in disintegrations per minute (DPM) and normalized to DNA synthesis in the 10% FCS stimulated cells without Mdivi-1 (control). Results expressed as % stimulation relative to the control (100%). * $p < 0.05$ compared to the corresponding stimulant. Each value represents the mean \pm SEM ($n=4$).

4.9 Effect of Hypoxia on PDGF induced PASMC Migration

Results show PDGF induces PASMC migration in a time-dependent manner in both oxygen incubation levels. PDGF during hypoxia appears to induce more cellular migration but there was no statistical difference in the reduction of scratch distance, or in the PDGF migratory effect, between the control (normoxic) group and the test (hypoxic) group with increasing incubation times (Figure 4.7).

A



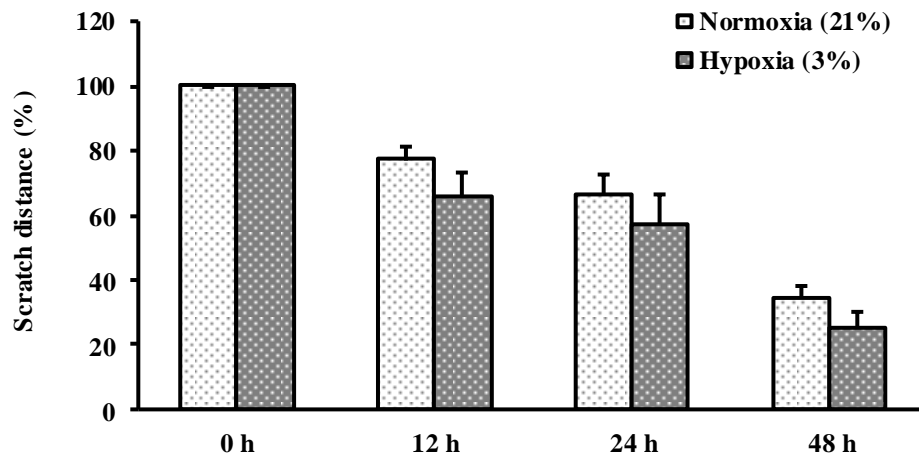
B

Figure 4.7 The effect of hypoxia on PDGF stimulated PASC migration. (A) Microscopic images using x 2 magnification of the scratch migration assay at 0 h, 12 h, 24 h and 48 h. The migratory effect of PDGF (5 ng/ml) was observed at normoxia (21% oxygen) and hypoxia (3% oxygen) of different incubation times: 12 h, 24 h and 48 h compared to 0 h (control, 100%). **(B)** Quantitative data of PASC migration. Each value represents the mean \pm SEM (n=5).

4.10 The effect of Mdivi-1 on PDGF induced PASMC Migration

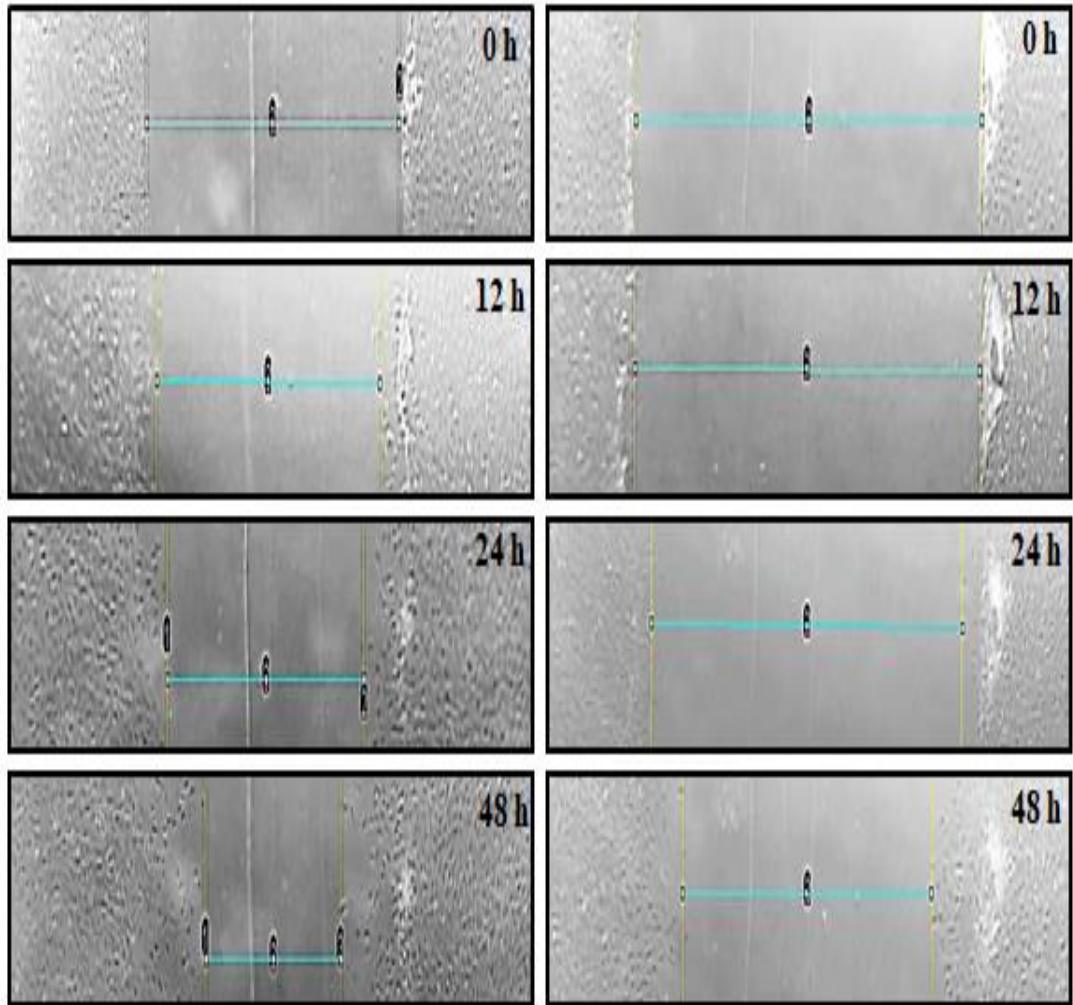
Migration scratch assay experiments were also conducted to assess the influence of mitochondrial fission on PDGF induced PASMC migration. The slowing of the gap closure and inhibition of cell migration by Mdivi-1 was observed in both stimulated normoxic (Figure 4.8) and hypoxic (Figure 4.9) groups over increasing incubation times.

Under normoxic conditions, in comparison to 0 time (control, total scratch distance 100%), the scratch area was reduced by $26.8 \pm 4\%$ in PDGF stimulated cells and only reduced by $10.48 \pm 2.7\%$ after Mdivi-1 treatment at 12 h. This failed to reach statistical significance (Figure 4.8). However, Mdivi-1 significantly inhibited closure of the scratch area at 24 and 48 h. In the absence of Mdivi-1, the scratch area was reduced by $33.3 \pm 6.59\%$ and $54.6 \pm 4.5\%$, respectively. In the presence of Mdivi-1, the scratch area at 24 and 48 h was reduced by $15.9 \pm 2\%$ and $21.3 \pm 3.6\%$, respectively (Figure 4.8).

A

PDGF (Normoxia)

PDGF + Mdivi-1 (Normoxia)



B

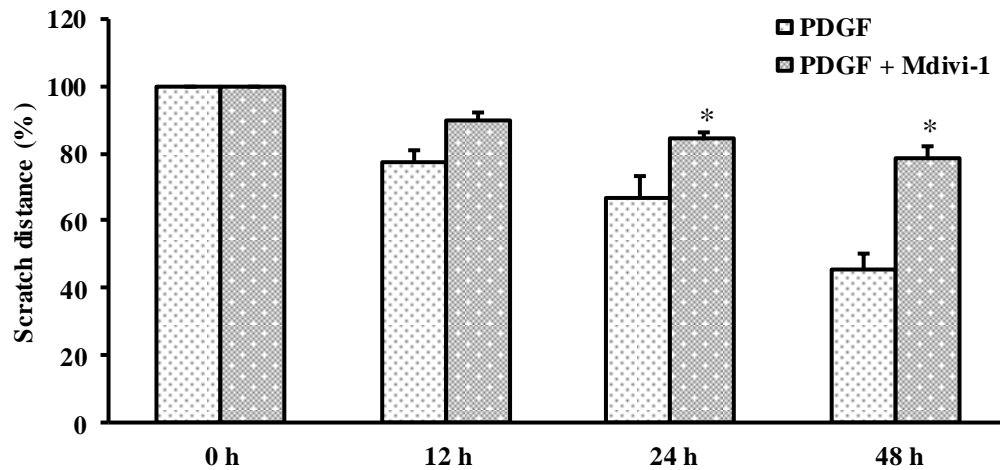
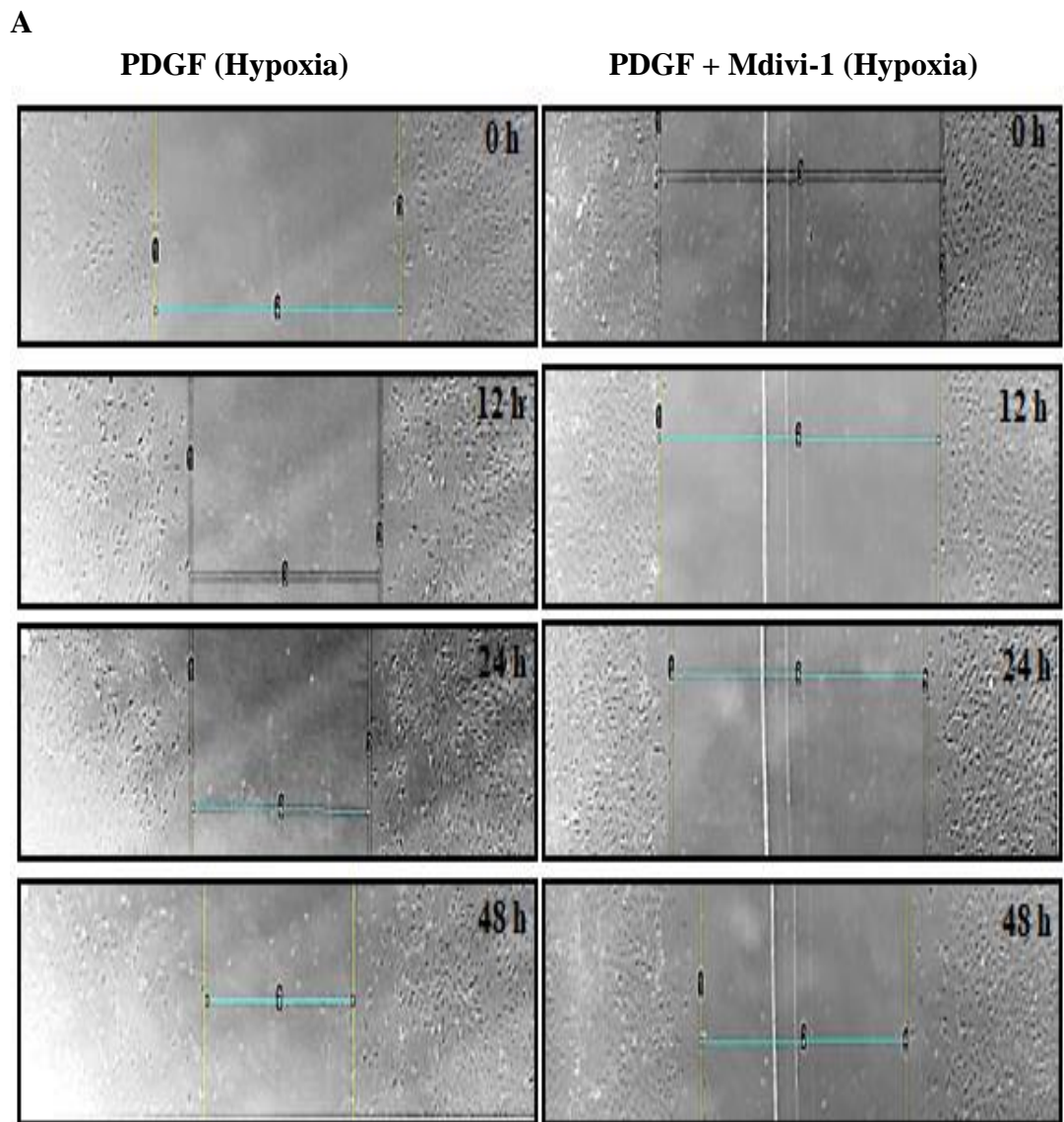


Figure 4.8 The effect of Mdivi-1 on PDGF induced PASMC migration. (A) Microscopic images using x 2 magnification of the scratch migration assay at 0 h, 12 h, 24 h and 48 h. The migratory effect of PDGF was observed with increasing incubation times: 12 h, 24 h and 48 h compared to 0 h (control). Mdivi-1 (10 μ M) was added 30 minutes before stimulation. (B) Quantitative data of PASMC migration. Each value represents the mean \pm SEM (n=5). *p<0.05 compared to compared to PDGF alone.

Under hypoxic conditions, PDGF without Mdivi-1 reduced the scratch area by $48.4 \pm 7.1\%$ at 24 h. However, following addition of Mdivi-1, a significant inhibition of gap closure was observed as the scratch area was only reduced by $23.5 \pm 2.8\%$ (Figure 4.9).



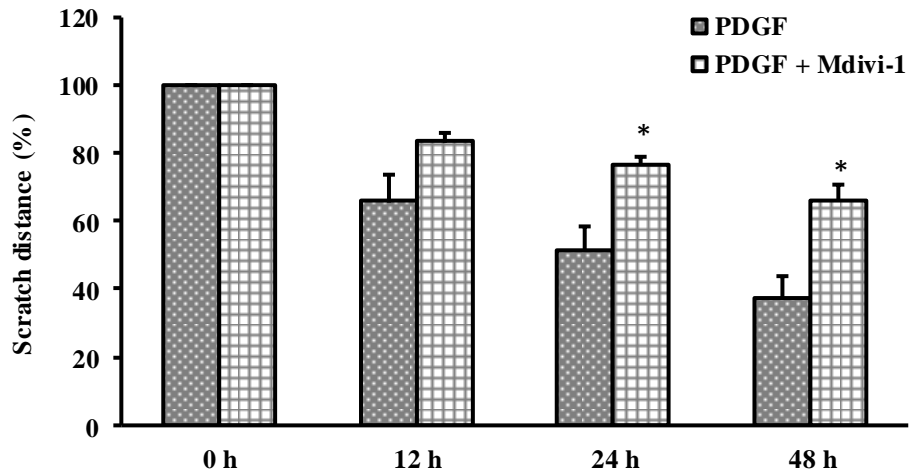
B

Figure 4.9 The effect of Mdivi-1 on PDGF induced PASC migration during hypoxia. (A) Microscopic images of hypoxic cells using x 2 magnification of the scratch migration assay at 0 h, 12 h, 24 h and 48 h. The migratory effect of PDGF was observed with increasing hypoxic (3% oxygen) incubation times: 12 h, 24 h and 48 h compared to 0 h (control). Mdivi-1 (10 μ M) was added 30 minutes before stimulation. (B) Quantitative data of PASC migration. Each value represents the mean \pm SEM (n=5). *p<0.05 compared to PDGF alone.

4.11 Effect of Mdivi-1 on cell cycle progression

In order to assess the effect of the combined effect of PDGF and hypoxia on cell cycle progression and to determine the cell cycle phase at which the mitochondrial drug (Mdivi-1) works, the percentage of PASMCMs in each phase was evaluated by FACs analysis following PDGF incubation of the cells with Mdivi-1 treatment under both normoxic and hypoxic conditions for 72 h (Figure 4.10A).

In the G2 phase, the results in Figure 4.10B showed the percentage of PDGF stimulated cells in response to hypoxia was increased to ($80.7 \pm 2.5\%$) compared with the normoxic control ($65 \pm 1.4\%$). The effect of Mdivi-1 showed different responses in both PDGF normoxic and hypoxic incubations (Figure 4.10B). In normoxia, the percentage of cells following Mdivi-1 treatment was increased to ($80.6 \pm 2.75\%$) compared with the control ($65 \pm 1.4\%$). However, during hypoxia, data showed the percentage of cells following Mdivi-1 treatment was decreased to ($69.5 \pm 1.49\%$) compared with the hypoxic PDGF control ($80.7 \pm 2.5\%$). In the G1 phase, the results in Figure 4.10A showed the percentage of cells in the presence of Mdivi-1 was increased to ($25.8 \pm 1.4\%$) compared with the hypoxic PDGF control ($18 \pm 2.5\%$) but there was no significant change detected.

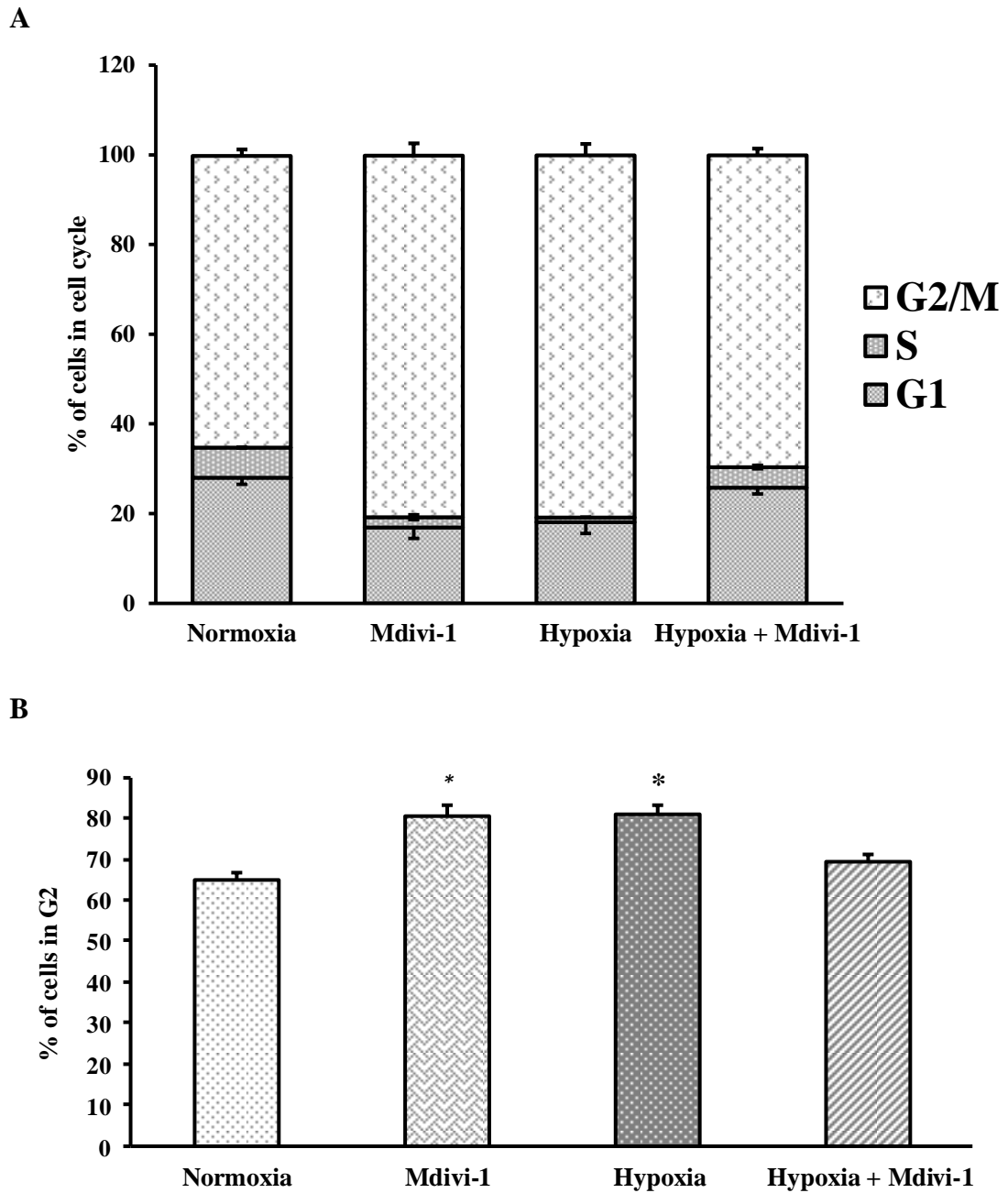


Figure 4.10 The effect of Mdivi-1 on cell cycle progression in PDGF stimulated cells. Figure shows distributions of cells in different phases of the cell cycle (A) and in G2 phase (B) under both normoxic (21% O₂) and hypoxic (3% O₂) conditions following Mdivi-1 treatment. PASMCMs were stimulated with PDGF (5 ng/ml) and treated with Mdivi-1 (10 μM) and incubated in each oxygen condition for 72 h. Total DNA content was determined by the assessment of flow cytometry using propidium iodide (PI). Each value represents the mean ± SEM (n=3). *p < 0.05 vs. PDGF cultured cells in normoxia.

4.12 The effect of Mdivi-1 on cyclin D1 protein expression

To measure the effect of inhibiting mitochondrial fission on cell cycle proteins such as cyclin D1, cyclin D1 was measured by Western blot after stimulating the cells with PDGF following Mdivi-1 treatment under normoxic (control) and hypoxic (test) conditions for 24 h.

Results show there was no difference in cyclin D1 protein expression between the quiescent cells and the PDGF stimulated cells (Figure 4.11). In PDGF stimulated cells, Mdivi-1 caused a slight increase in the protein expression by 1.4 ± 0.3 fold. During hypoxia, quiescent cells exposed to hypoxia for 24 h showed a slight upregulation of the protein expression by 1.4 ± 0.4 fold. PDGF during hypoxia failed to increase cyclin D1 protein level, compared to hypoxic cells without PDGF stimulation. However, an upregulation of the protein by 1.6 ± 0.4 fold was observed by the PDGF effect in hypoxia versus normoxia (Figure 4.11). Moreover, an inhibition of the mitochondrial fission during hypoxia using 10 μ M Mdivi-1 caused a significant reduction by $53.2\% \pm 1.9\%$ in the stimulated cells (Figure 4.11).

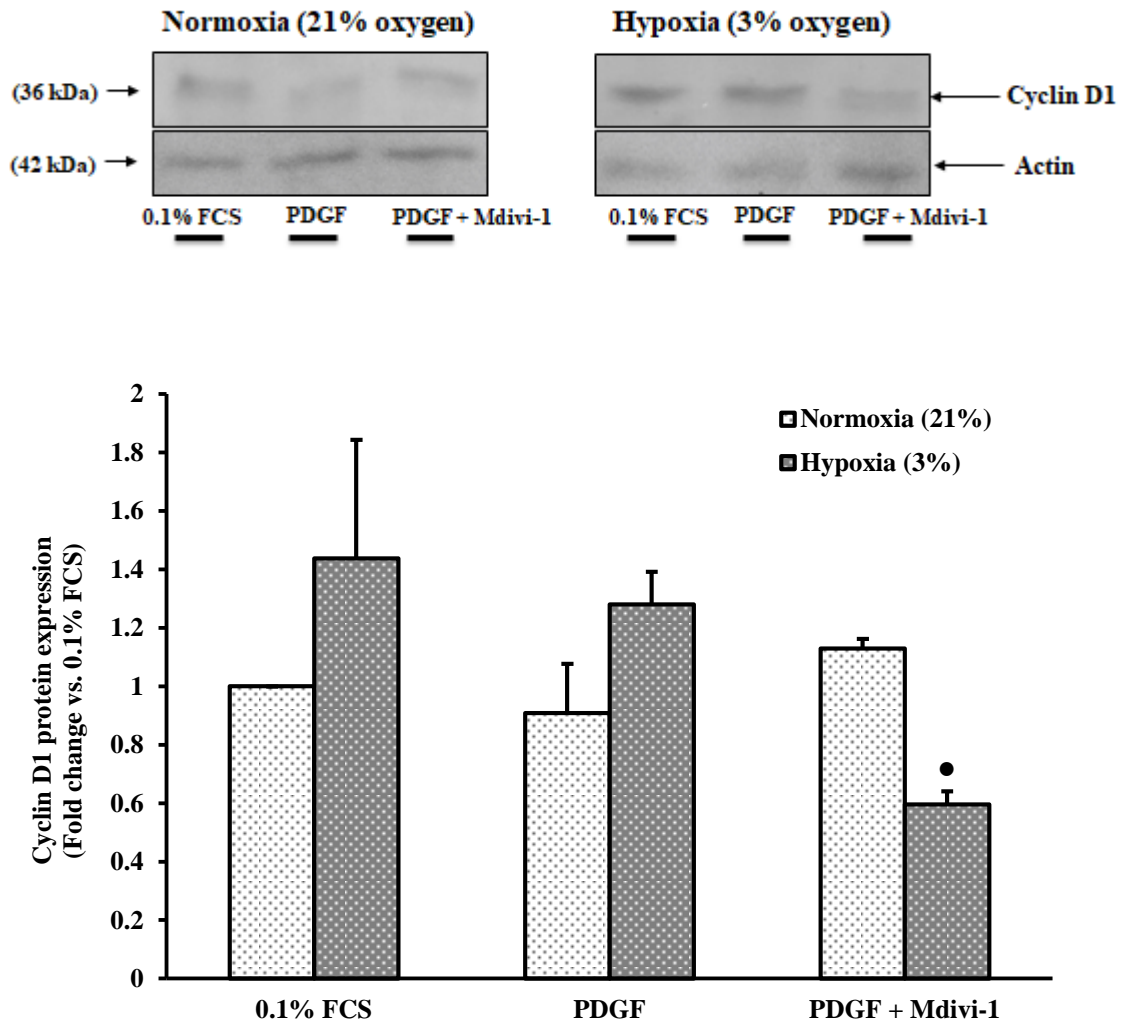


Figure 4.11 The effect of Mdivi-1 on cyclin D1 protein expression in PDGF stimulation during hypoxia. PASMCMs were seeded in pairs of 6 well plates. At 70-80% confluence, cells were quiesced for 24 h. Cells were stimulated with PDGF (5 ng/ml) and incubated at different oxygen levels; 21% oxygen (normoxia) and 3% oxygen (hypoxia) for 24 hours. Mdivi-1 (10 μ M) was added 30 minutes before PDGF stimulation. Whole cell extracts were prepared and analyzed using Western blot for the expression of the cyclin D1 protein (36 kDa) and total actin (42 kDa), which was used as a loading control. Each value represents the mean \pm SEM (n=3). ●p < 0.05 vs. PDGF stimulated cells.

4.13 The effect of Mdivi-1 on cell regulatory gene expression

Genes involved in the cell cycle such as the proliferative gene (cyclin D1) and the tumour suppressor gene (P53) were investigated in PDGF stimulated cells following mitochondrial inhibition under normoxic (control) and hypoxic (test) conditions by RT-qPCR technique.

Data show PDGF caused a significant reduction in cyclin D1 gene expression by $67.7 \pm 5.5\%$, whereas the inhibition of the mitochondria by Mdivi-1 caused a significant increase in the gene expression by 9.8 ± 3 fold (Figure 4.13). Moreover, hypoxia alone induced cyclin D1 expression by 4.46 ± 0.4 fold versus normoxia (Figure 4.13). In addition, PDGF during hypoxia showed an upturn of the expression by 2.6 ± 0.2 fold, compared to cyclin D1 expression in hypoxic background cells (cells quiesced with 0.1% FCS and maintained in 3% O₂). A significant difference in gene expression between hypoxia versus normoxia in the PDGF stimulated cells was detected. The gene expression was increased by 39.1 ± 7.1 fold vs. PDGF effect during normoxia. Mdivi-1 inhibited cyclin D1 gene expression by $66.4 \pm 8.49\%$ in the hypoxic cells (Figure 4.12) and by $99.8 \pm 0.05\%$ in the PDGF stimulated cells during hypoxia (Figure 4.13).

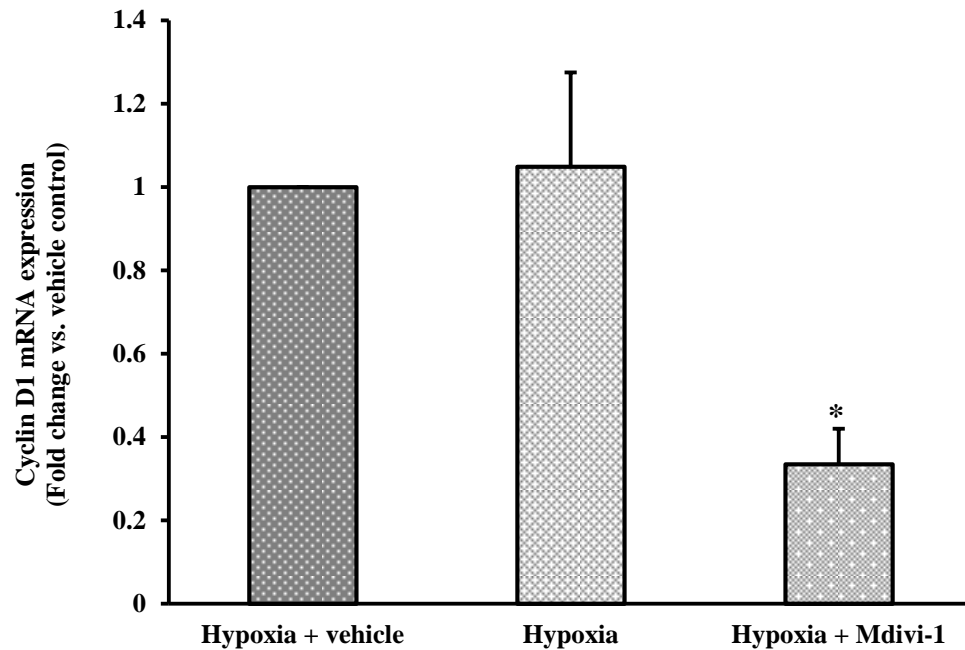


Figure 4.12 The effect of Mdivi-1 on cyclin D1 gene expression in hypoxic cells. Cells were quiesced for 24 h and were then exposed to hypoxia (3% oxygen) for 24 h. Mdivi-1 (10 μ M) was added 30 minutes before hypoxic exposure. RNA was extracted from cells. Equal RNA concentrations were used for cDNA sample preparation. Cyclin D1 gene was measured using RT-qPCR. Ubiquitin C (UBC) was used as the reference gene for normalization. Each value represents the mean \pm SEM (n=3). *p < 0.05 vs. vehicle control cells.

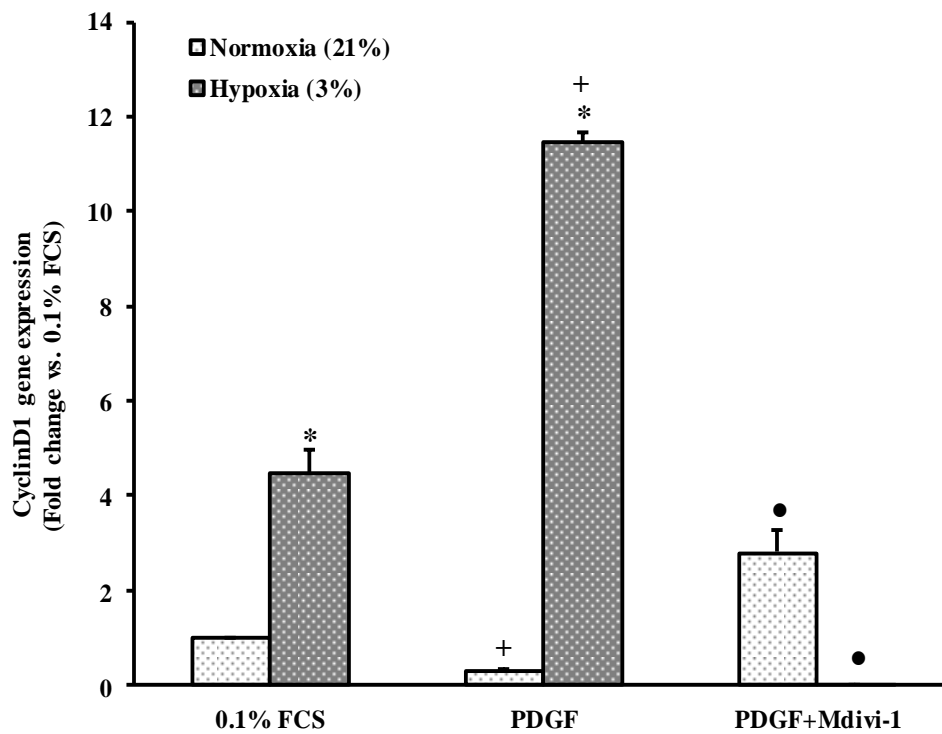


Figure 4.13 The effect of Mdivi-1 on cyclin D1 gene expression in PDGF stimulated cells during hypoxia. Cells were quiesced for 24 h and were then stimulated with PDGF (5 ng/ml) and exposed to different oxygen levels: normoxia (21% oxygen) and hypoxia (3% oxygen) for 24 h. Mdivi-1 (10 μ M) was added 30 minutes before PDGF stimulation. RNA was extracted from cells. Equal RNA concentrations were used for cDNA sample preparation. The expression of cyclin D1 gene was measured using RT-qPCR. Ubiquitin C (UBC) was used as the reference gene for normalization. Each value represents the mean \pm SEM (n=3). +p <0.05 vs. quiescent cells. *p <0.05 vs. cultured cells in normoxia. •p <0.05 vs. PDGF stimulated cells.

Data showed that under normoxic conditions, PDGF upregulated the expression of the P53 gene by 159.8 ± 9.5 fold. However, an inhibition of mitochondrial fission by Mdivi-1 showed a reduction of the gene expression by $65 \pm 4\%$ (Figure 4.14).

In hypoxia, the expression of the P53 gene was reduced by $26.3 \pm 3.6\%$ compared to the normoxic quiescent cells (Figure 4.14). Data also show PDGF enhanced the expression by 37.8 ± 3.9 fold compared to hypoxic background cells (cells quiesced with 0.1% FCS and maintained in 3% O₂). In comparison to PDGF effect in normoxia, the expression of the gene was reduced by $82.6 \pm 1.3\%$. Interestingly, results show Mdivi-1 intervention during hypoxia increased the expression by 4.58 ± 0.3 fold in the PDGF stimulated cells (Figure 4.14).

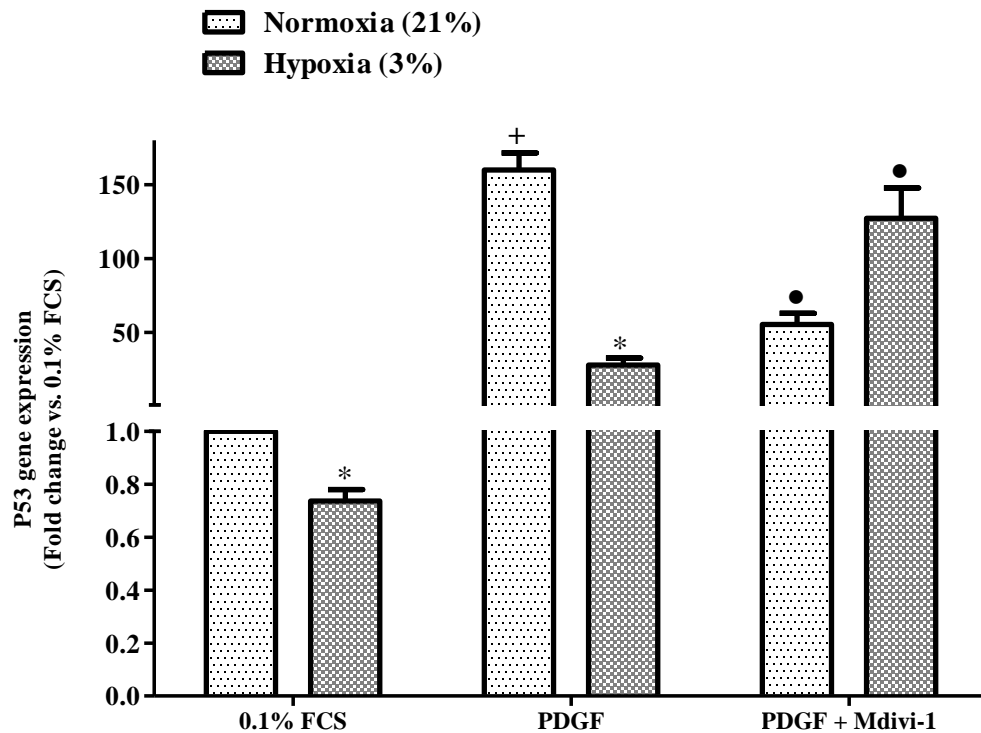


Figure 4.14 The effect of Mdivi-1 on P53 gene expression in PDGF stimulated cells during hypoxia. Cells were quiesced for 24 h and were then stimulated with PDGF (5 ng/ml) and exposed to different oxygen levels: normoxia (21% oxygen) and hypoxia (3% oxygen) for 24 h. Mdivi-1 (10 μ M) was added 30 minutes before PDGF stimulation. RNA was extracted from cells. Equal RNA concentrations were used for cDNA sample preparation. The expression of P53 gene was measured using RT-qPCR. Ubiquitin C (UBC) was used as the reference gene for normalization. Each value represents the mean \pm SEM (n=3). +p <0.05 vs. quiescent cells. *p <0.05 vs. cultured cells in normoxia. •p <0.05 vs. PDGF stimulated cells.

4.14 Mitochondrial functions:

The bioactivity of the mitochondria was examined by measuring ROS activity and ATP turnover in PASMCMs. Superoxide ($O_2^{\cdot-}$) levels in PASMCMs were measured in cells maintained in normoxia and in cells exposed to hypoxia in response to PDGF, and to PDGF following mitochondrial inhibition by Mdivi-1.

4.14.1 Effect of Mdivi-1 on Reactive Oxygen Species (ROS)

Reactive oxygen species (ROS) experiments were performed by the use of dihydroethidium (DHE) compound to measure the superoxide ($O_2^{\cdot-}$) level. This compound was tested on PASMCMs as it significantly enhanced superoxide ($O_2^{\cdot-}$) detection compared to the cells without DHE (Figure 4.15). Moreover, ROS stimulant (angiotensin II) was used as a positive control to confirm the angiotensin II-dependent superoxide effect versus quiescent cells (Figure 4.15). During normoxia, superoxide ($O_2^{\cdot-}$) levels were enhanced by 1.6 ± 0.11 fold in response to PDGF and inhibited by $17.9 \pm 4.5\%$ following Mdivi-1 treatment in PDGF stimulated cells (Figure 4.16).

Data show the generation of superoxide during hypoxia was upregulated by 1.27 ± 0.04 fold compared to the normoxic background cells (Figure 4.16). PDGF during hypoxia increases superoxide ($O_2^{\cdot-}$) production by 1.3 ± 0.08 fold. Moreover, superoxide levels resulted from PDGF during hypoxia did not differ significantly compared to the effect of PDGF during normoxia. Data showed superoxide generated by the combined effects of PDGF and hypoxia was repressed by $21 \pm 5.9\%$ following Mdivi-1 treatment (Figure 4.16).

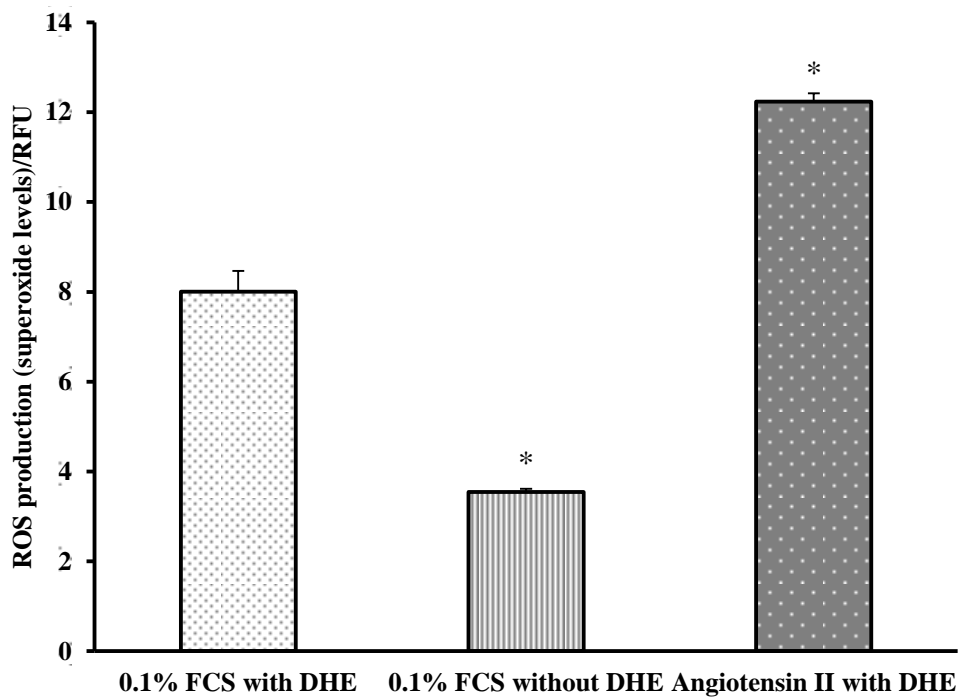


Figure 4.15 Reactive oxygen species (ROS) production (superoxide) in pulmonary artery smooth muscle cells. Superoxide (O_2^-) levels were detected by dihydroethidium (DHE). PASMCs were quiesced with 0.1% FCS for 24 h and were stimulated with angiotensin II (100 nM) for 1 h (n=3). *p <0.05 vs. quiescent cells with DHE. RFU (relative fluorescent units).

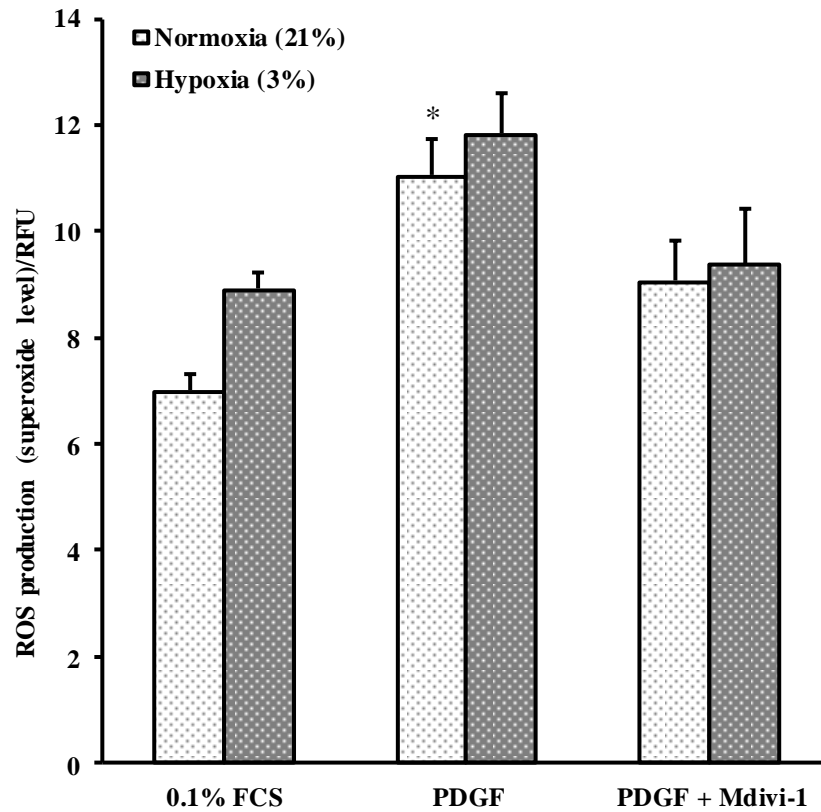


Figure 4.16 The effect of Mdivi-1 on ROS production (superoxide) in PDGF stimulated cells during hypoxia. Superoxide levels were detected by dihydroethidium (DHE) compound. PASM C were incubated at different oxygen levels; 21% oxygen and 3% oxygen for 24 h. Then, cells were stimulated with PDGF (5 ng/ml) for 1 h. Mitochondrial inhibitor Mdivi-1 (10 μ M) was added 30 minutes before stimulation (n=4). *p < 0.05 vs. quiescent cells. RFU (relative fluorescent units).

To further evaluate the redox state in PASMCMs, hydrogen peroxide (H_2O_2) levels were measured in normoxic and hypoxic cells under the effect of PDGF stimulation and Mdivi-1 treatment. Dichlorofluorescein termed 2', 7'-dichlorofluorescein diacetate (DCFH-DA), a cell permeable molecule, is used to detect the intracellular H_2O_2 (Carter et al., 1994). DCFH-DA is cleaved by intracellular esterases to 2', 7'-dichlorofluorescein (DCFH) and is rapidly oxidized by intracellular ROS (H_2O_2) to the highly fluorescent 2', 7'-dichlorofluorescein (DCF) (Dikalov et al., 2007). Results in Figure 4.17A showed a significant increase in H_2O_2 levels when DCF was added in the quiescent cells (cells with 0.1% FCS). In addition, hydrogen peroxide was added in PASMCMs as a positive control to check the stimulatory response of hydrogen peroxide (Figure 4.17B).

H_2O_2 levels were significantly reduced in hypoxic cells versus normoxic cells. Hypoxia caused a reduction of H_2O_2 levels by $45.8 \pm 4.48\%$ and by $37.9 \pm 6.6\%$ in the 0.1% FCS background cells and in PDGF stimulated cells, respectively (Figure 4.18). In addition, PDGF stimulation showed no effect in either normoxic or hypoxic conditions (Figure 4.18). Furthermore, an inhibition of mitochondrial fission by Mdivi-1 exhibited no role in H_2O_2 release in the PDGF stimulated cells in both oxygen conditions (Figure 4.18).

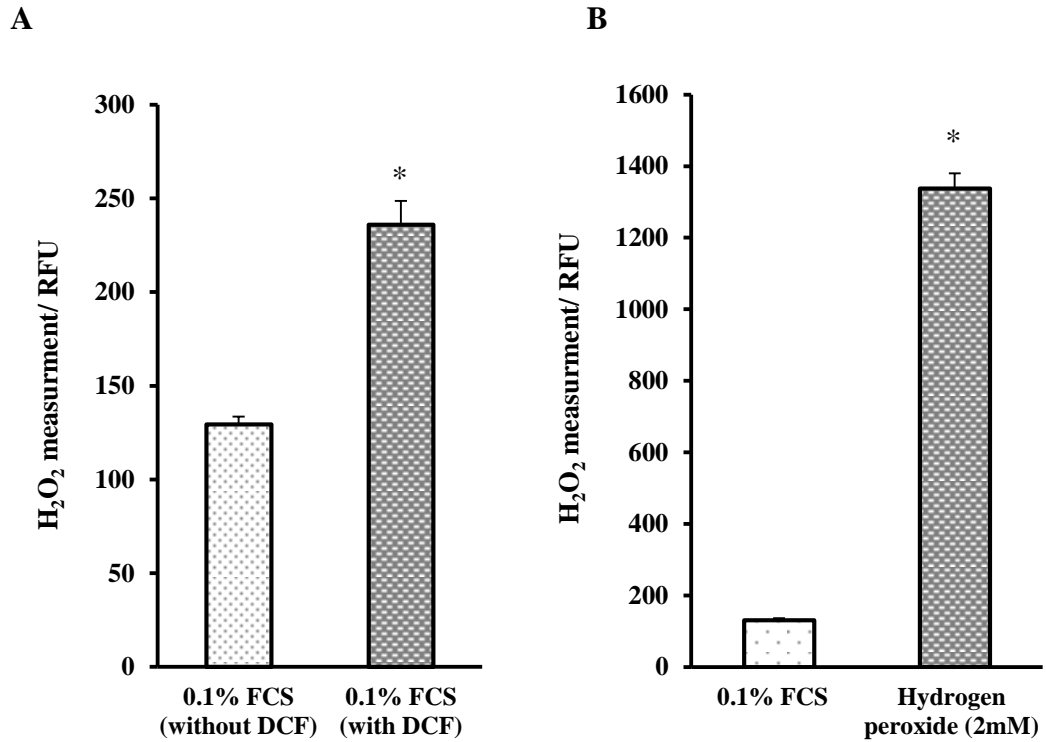


Figure 4.17 H₂O₂ levels in pulmonary artery smooth muscle cells. Cells were quiesced with 0.1% FCS for 24 h. (A) shows 2', 7'-dichlorofluorescein (DCF) caused an increase in the fluorescent intensity (measure of intracellular H₂O₂ release). *p < 0.05 vs. quiescent cells without DCF. (B) shows H₂O₂ levels, that were detected by DCF, after cell stimulation with 2 mM hydrogen peroxide for 1 h. *p < 0.05 vs. quiescent cells (n=3). RFU (relative fluorescent units).

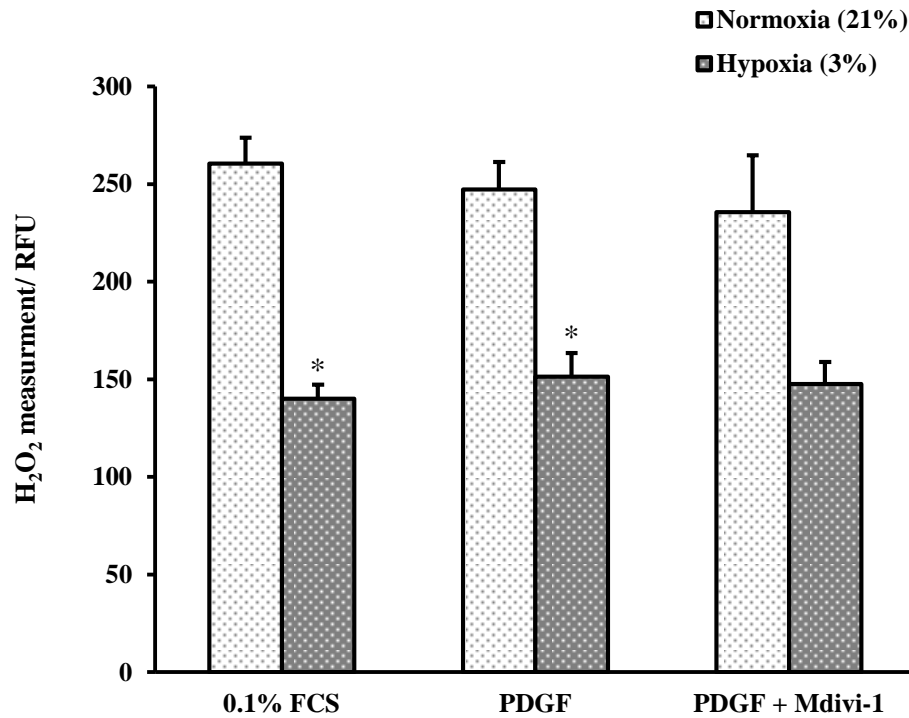


Figure 4.18 The effect of Mdivi-1 on H₂O₂ levels in PDGF stimulated cells during hypoxia. H₂O₂ was detected by 2', 7'-dichlorofluorescein (DCF). PASM Cs were incubated at different oxygen levels; 21% oxygen (normoxia) and 3% oxygen (hypoxia) for 24 h. Then, cells were stimulated with PDGF (5 ng/ml) for 1 h. The mitochondrial inhibitor Mdivi-1 (10 μ M) was added 30 min before stimulation (n=3). *p <0.05 vs. cells cultured in normal oxygen level (21% oxygen). RFU (relative fluorescent units).

4.14.2 Effect of Mdivi-1 on ATP production

Data display a general decrease in ATP production associated with hypoxic cells (Figure 4.19). For example, the production of ATP was significantly decreased by $57.8 \pm 4.2\%$ in the 0.1% FCS cultured hypoxic cells and by $41.2 \pm 2.6\%$ in the PDGF stimulated hypoxic cells in comparison to the 0.1% FCS normoxic cells and the PDGF stimulated cells in normoxia, respectively (Figure 4.19).

In normoxia, results show PDGF enhanced ATP level by 1.7 ± 0.07 fold compared to quiescent cells. Similarly, in hypoxia, PDGF increased ATP production by 2.5 ± 0.1 fold versus quiescent hypoxic cells (Figure 4.19). Results also show a significant reduction in ATP level when PDGF receptors were blocked by imatinib. For example, ATP levels were reduced by $67.9 \pm 0.7\%$ and by $56.8 \pm 1.5\%$ following imatinib treatment in comparison to the PDGF stimulated cells in normoxia and in hypoxia, respectively (Figure 4.19).

Moreover, ATP levels were decreased following Mdivi-1 under both normoxic and hypoxic conditions (Figure 4.19). In normoxia, ATP levels were significantly reduced by $46.2 \pm 3.6\%$ and by $34.6 \pm 7.4\%$ following Mdivi-1 treatment in the quiescent cells and in the PDGF stimulated cells, respectively. During hypoxia, interestingly, Mdivi-1 insignificantly decreased ATP levels by $33 \pm 8.3\%$ in the absence of PDGF and by $23.3 \pm 5.3\%$ in the presence of PDGF (Figure 4.19).

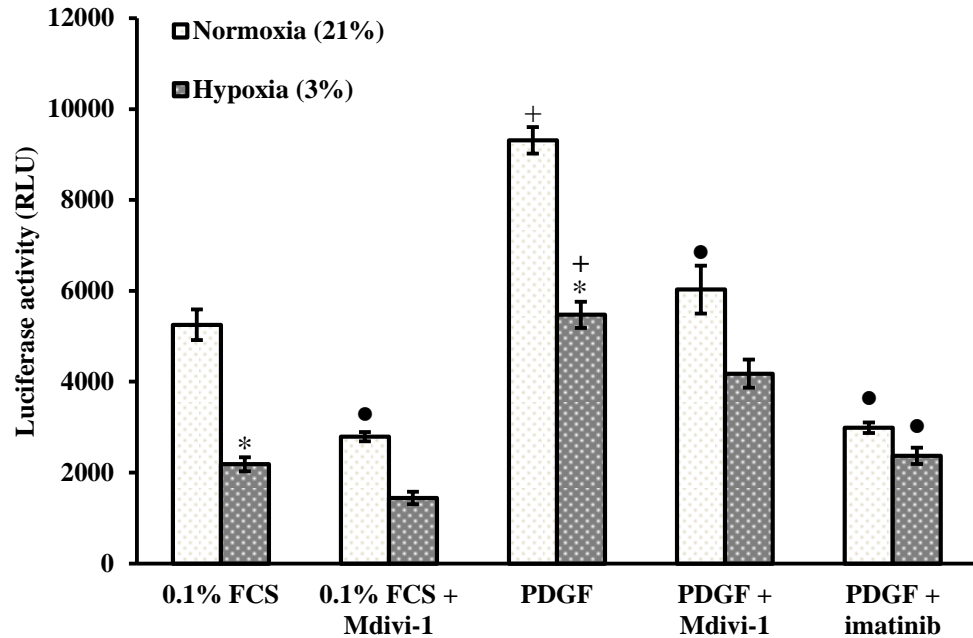


Figure 4.19 The effect of Mdivi-1 on mitochondrial ATP production in PDGF stimulated cells during hypoxia. ATP levels were detected by mitochondrial ToxGlo reagent. PASMCMs were quiesced with 0.1% FCS for 24 h and were then stimulated with PDGF (5 ng/ml) and exposed to different oxygen levels: normoxia (21% O₂) and hypoxia (3% O₂) for 24 h. The DRP1 inhibitor, Mdivi-1 (10 μM) and the positive control imatinib (10 μM) were added 30 minutes before stimulation. ATP levels were measured in quiescent cells, PDGF stimulated cells and Mdivi-1 treated cells with/without PDGF stimulation under both normoxic and hypoxic cell culture conditions (n=3). +p < 0.05 vs. quiescent cells. *p < 0.05 vs. cultured cells in normoxia. •p < 0.05 vs. PDGF stimulated cells. RLU (relative light units).

4.14.3 The effect of Mdivi-1 on mitochondrial ATPase 6 gene expression

To further assess mitochondrial ATP production, a key regulator gene for mitochondrial oxidative phosphorylation (ATPase 6; ATPase subunit 6) was examined in normoxia and hypoxia following PDGF stimulation and Mdivi-1 treatment (Figure 4.20).

In the quiescent cells (cells with 0.1% FCS), the expression of ATPase 6 gene was significantly reduced by $38.9 \pm 5.3\%$ following hypoxic exposure. In addition, PCR data showed that PDGF during normoxia increased ATPase 6 gene expression by 12.6 ± 0.9 fold and Mdivi-1 caused a reduction in the gene expression by $36.29 \pm 10\%$ (Figure 4.20). However, during hypoxia, PDGF had the opposite effect as the expression of ATPase 6 gene was not increased (Figure 4.20). It was significantly decreased by $99 \pm 0.6\%$ compared to hypoxic quiescent cells. Also, Mdivi-1 had a different effect on ATPase 6 gene expression. Following addition of Mdivi-1, a significant difference in ATPase 6 gene expression between hypoxia versus normoxia was detected. Mdivi-1 increased the expression by 7.9 ± 1.6 fold compared to its effect in normoxia (Figure 4.20).

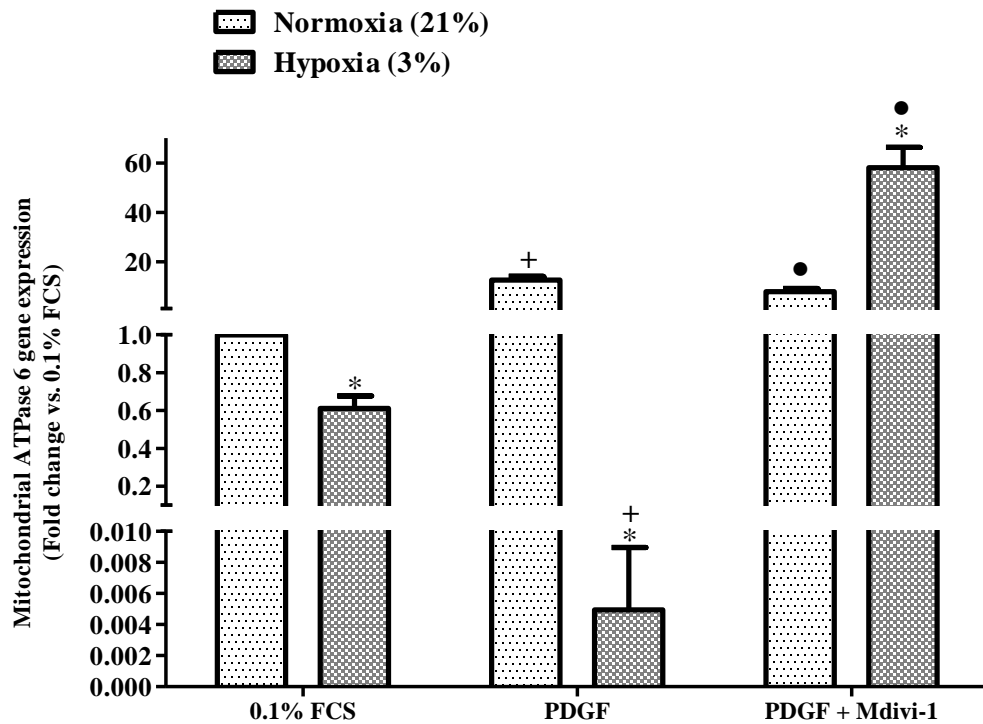


Figure 4.20 The effect of Mdivi-1 on mitochondrial ATPase 6 gene expression in PDGF stimulated cells during hypoxia. Cells were quiesced for 24 h and were then stimulated with PDGF (5 ng/ml) and exposed to different oxygen levels: normoxia (21% oxygen) and hypoxia (3% oxygen) for 24 h. Mdivi-1 (10 μ M) was added 30 minutes before PDGF stimulation. RNA was extracted from cells. Equal RNA concentrations were used for cDNA sample preparation. The expression of ATPase 6 gene was measured using RT-qPCR. Ubiquitin C (UBC) was used as the reference gene for normalization. Each value represents the mean \pm SEM (n=3). +p <0.05 vs. quiescent cells. *p <0.05 vs. cultured cells in normoxia. •p <0.05 vs. PDGF stimulated cells.

4.14.4 Effect of Mdivi-1 on cytochrome c protein expression

The initiation of the apoptotic pathway through the expression of cytochrome c protein was studied by Western blot. Data showed the expression of cytochrome c increased by 3.1 ± 1.6 fold following PDGF stimulation when compared with control cells (cells with 0.1% FCS). This increase failed to reach statistical significance. Mitochondrial inhibition by Mdivi-1 treatment showed no effect in the expression of the protein in the PDGF stimulated cells (Figure 4.21).

In 3% oxygen, data showed hypoxia increased the expression of cytochrome c protein by 10.5 ± 0.6 fold compared to the cells kept under normoxic conditions (Figure 4.21). In addition, the combined effect of hypoxia and PDGF increased the expression by 1.2 ± 0.1 fold compared to hypoxic background cells (cells quiesced with 0.1% FCS and maintained in 3% O₂). Hence, a remarkable difference in cytochrome c protein was clearly observed in hypoxia (10.3 ± 6 fold) versus normoxia following PDGF stimulation (Figure 4.21). Moreover, Mdivi-1 treatment during hypoxia had a similar effect in normoxia as no difference in protein expression was observed in the hypoxic PDGF stimulated cells (Figure 4.21).

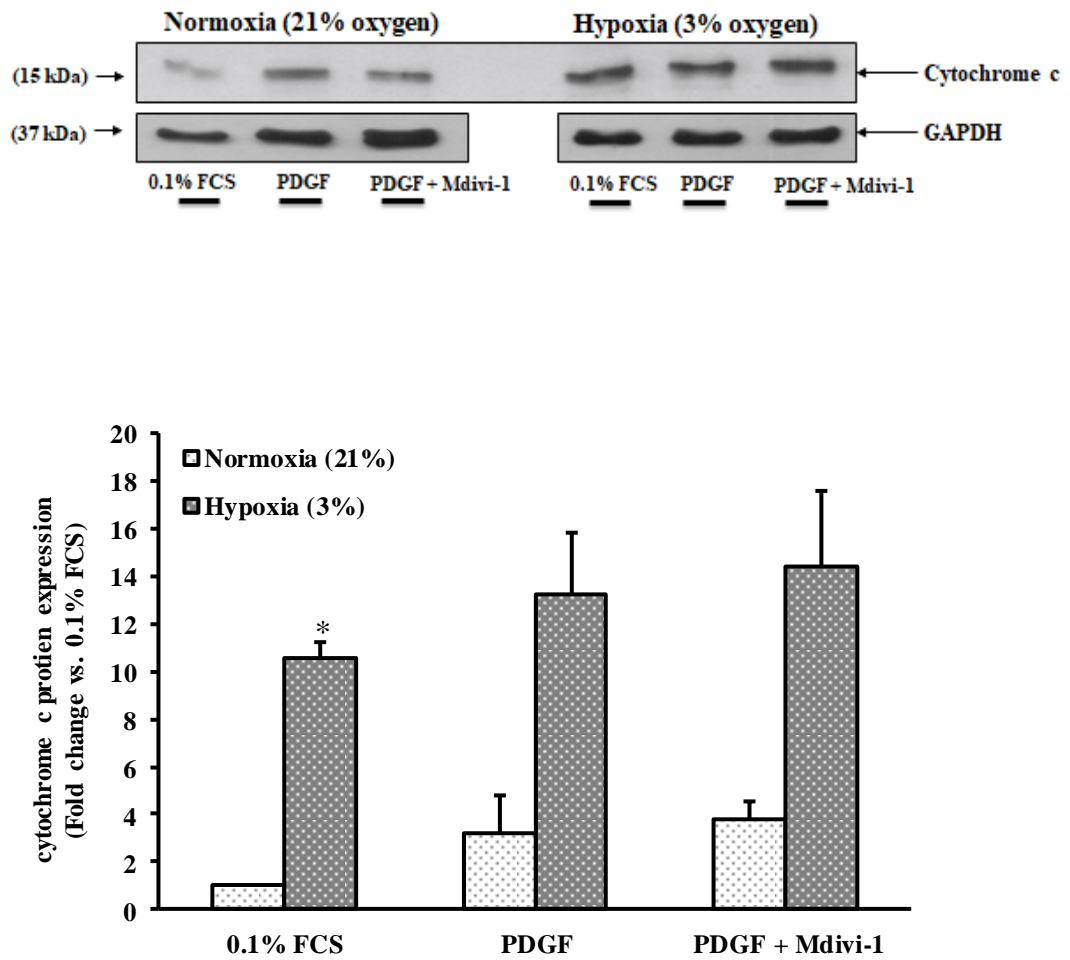


Figure 4.21 The effect Mdivi-1 on cytochrome c protein expression in PDGF stimulation during hypoxia. PSMCMs were seeded in pairs of 6 well plates. At 70-80% confluence, cells were quiesced for 24 h. Cells were stimulated with PDGF (5 ng/ml) and incubated at different oxygen levels; 21% oxygen (normoxia) and 3% oxygen (hypoxia) for 24 hour. Mdivi-1 (10 μ M) was added 30 minutes before PDGF stimulation. Whole cell extracts were prepared and analyzed using Western blot for the expression of cytochrome c (15 kDa) and GAPDH (37 kDa) which was used as a loading control. Each value represents the mean \pm SEM. *p <0.05 vs. cultured cells in normoxia (n=3).

4.14.5 Effect of Mdivi-1 on Cellular Apoptosis (Caspase 3/7 release)

Cellular apoptosis was assessed by measuring the release of caspase 3/7 in PASMCMs in response to PDGF following Mdivi-1 treatment under both normoxic and hypoxic conditions. Data showed hypoxia significantly reduced caspase 3/7 release by $33.6 \pm 1.5\%$ in quiescent cells (cells with 0.1% FCS). PDGF reduced the release of caspase 3/7 by $69 \pm 1.1\%$ in the normoxic conditions and by $64.6 \pm 2.4\%$ in the hypoxic conditions. In addition, the reduction of caspase 3/7 release was significant in hypoxia versus normoxia ($24.2 \pm 5.5\%$) in PDGF stimulated cells (Figure 4.22).

In quiescent cells (0.1% FCS), the release of caspase 3/7 was reduced by $58.9 \pm 1.5\%$ following Mdivi-1 treatment. However, the release of caspase 3/7 was not changed significantly during hypoxia following Mdivi-1 treatment as a slight decrease in caspase 3/7 release ($23.9 \pm 14.4\%$) was observed (Figure 4.22).

In PDGF stimulated cells, Mdivi-1 caused a significant decrease in caspase 3/7 release by $46.9 \pm 3.8\%$ in normoxia whereas it caused a small but insignificant decrease in caspase 3/7 release ($17.9 \pm 7.8\%$) in hypoxia. Paclitaxel was added to the PDGF stimulated cells under normoxic and hypoxic conditions as a positive control which shows a significant increase in caspase 3/7 release in both groups (Figure 4.22).

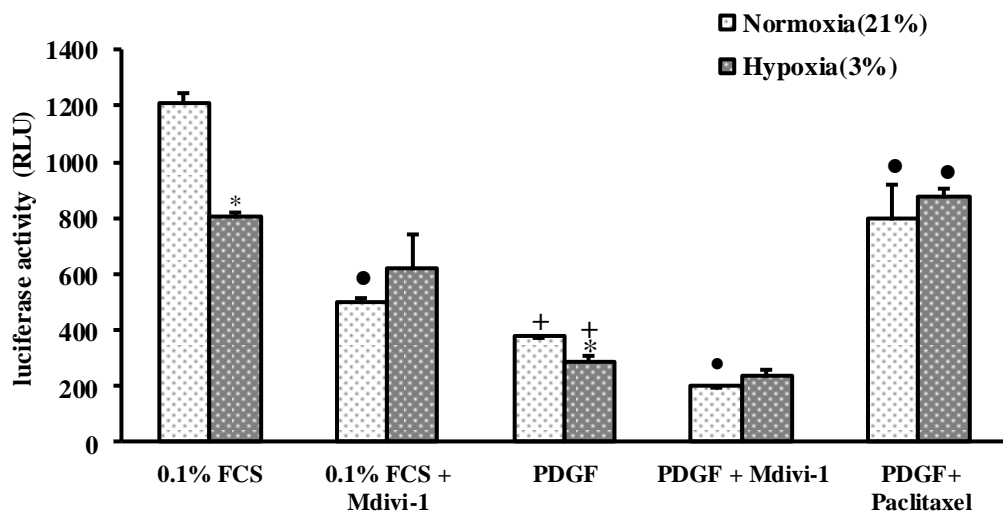


Figure 4.22 The effect of Mdivi-1 on apoptotic activity in PDGF stimulated cells during hypoxia. The release of caspase 3/7 within the cells was detected by ApoTox-Glo reagent. PASMCMs were quiesced with 0.1% FCS for 24 h and were then stimulated with PDGF (5 ng/ml) and exposed to different oxygen levels: normoxia (21% O₂) and hypoxia (3% O₂) for 24 h. The DRP1 inhibitor, Mdivi-1 (10 μ M) and the positive control Paclitaxel (1 μ M) were added 30 minutes before stimulation. Caspase 3/7 release was measured in quiescent cells (cells with 0.1% FCS), PDGF stimulated cells and Mdivi-1 treated cells in the absence or presence of PDGF under both normoxic and hypoxic cell culture conditions (n=3). +p <0.05 vs. quiescent cells. *p <0.05 vs. cultured cells in normoxia. •p <0.05 vs. PDGF stimulated cells.

4.15 The effect of Mdivi-1 on mitochondrial marker gene expression

The involvement of mitochondrial dysfunction associated with hypoxic PASMCMs and the influence of the mitochondrial fission inhibitor on the mitochondrial status within the PASMCMs was assessed by measuring mitochondrial marker genes such as dynamin-related protein-1 (DRP1) gene, mitochondrial transcription factor A (TFAM) and mitochondrial cytochrome c oxidase II in the normoxic (control) cells and in the hypoxic (test) cells in response to PDGF stimulation and Mdivi-1 treatment. Gene expression was measured in the background cells (cells with 0.1% FCS), PDGF stimulated cells and in PDGF stimulated cells treated with Mdivi-1 under both normoxic and hypoxic condition.

4.15.1 The effect of Mdivi-1 on DRP1 gene expression

In normoxia, Figure 4.23 showed PDGF dependent DRP1 response was clearly observed as PDGF significantly increased the expression of DRP1 gene by 33.9 ± 4.7 fold. In addition, treating the stimulated cells with the DRP1 inhibitor (Mdivi-1) showed an inhibition of the expression by $60.1 \pm 3.9\%$. In comparison to normoxic quiescent cells, hypoxia (3% O₂) significantly increased the expression of the DRP1 gene by 46.1 ± 4.7 fold (Figure 4.23). DRP1 gene expression was significantly reduced by $46.5 \pm 8.5\%$ in response to PDGF during hypoxia. Furthermore, the PDGF-DRP1 effect was also reduced during hypoxia in comparison with its effect in normoxia ($26.5 \pm 10.3\%$) but no statistical difference was detected. Mdivi-1 during hypoxia reduced DRP1 gene expression by $51.2 \pm 6.7\%$ in the PDGF stimulated cells (Figure 4.23).

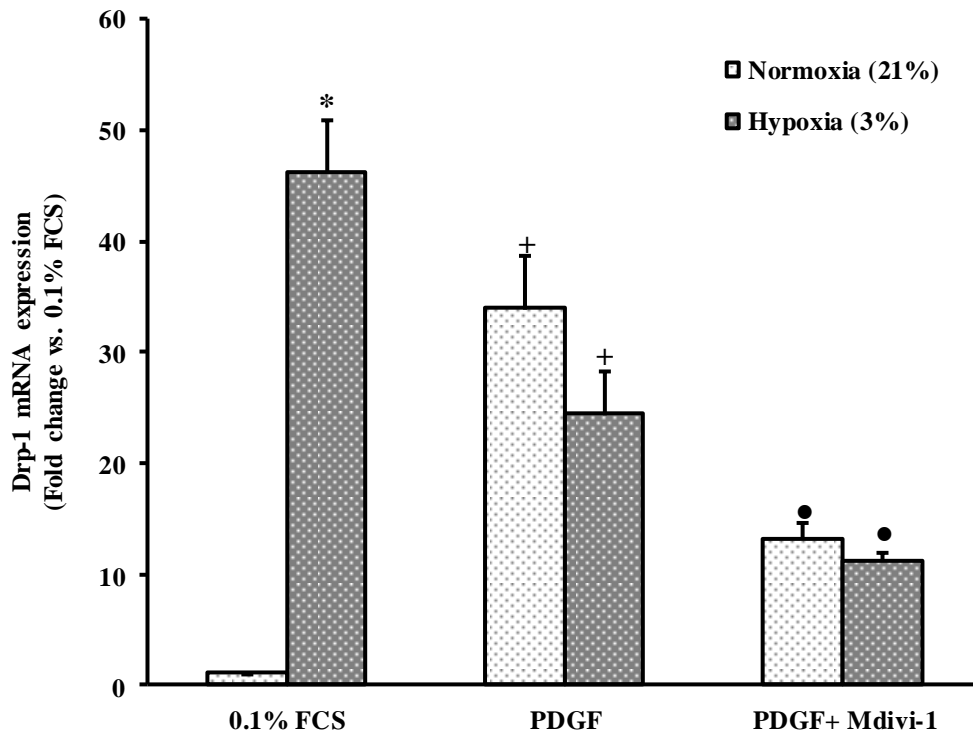


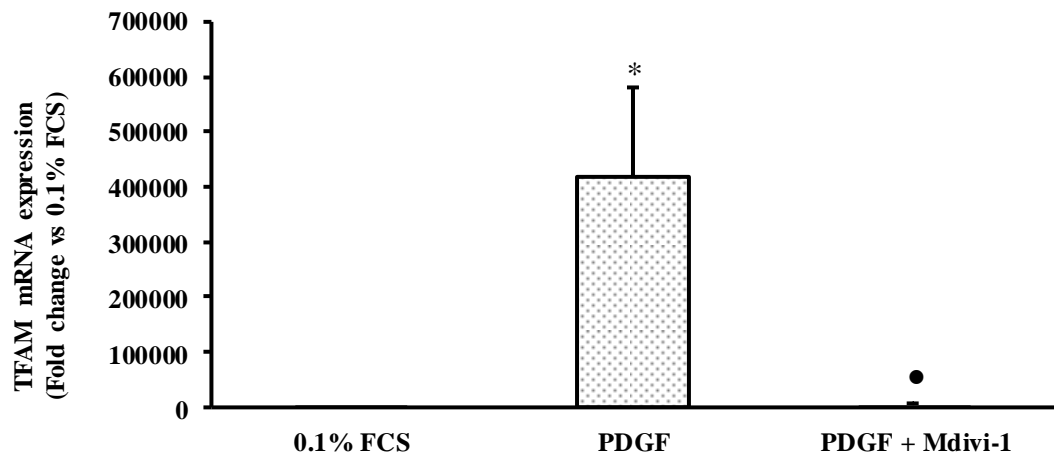
Figure 4.23 The effect of Mdivi-1 on DRP1 gene expression in PDGF stimulated cells during hypoxia. Cells were quiesced for 24 h and were then stimulated with PDGF (5 ng/ml) and exposed to different oxygen levels: normoxia (21% oxygen) and hypoxia (3% oxygen) for 24 h. Mdivi-1 (10 μ M) was added 30 minutes before PDGF stimulation. RNA was extracted from cells. Equal RNA concentrations were used for cDNA sample preparation. The expression of DRP1 gene was measured using RT-qPCR. Ubiquitin C (UBC) was used as the reference gene for normalization. Each value represents the mean \pm SEM (n=3). +p <0.05 vs. quiescent cells. *p <0.05 vs. cultured cells in normoxia. ●p <0.05 vs. PDGF stimulated cells.

4.15.2 The effect of Mdivi-1 on TFAM gene expression

A mitochondrial biogenesis marker gene which is called mitochondrial transcription factor A (TFAM) was examined using RT-qPCR. Data showed in PASMCMs maintained at normoxic incubation, the expression of TFAM gene was significantly enhanced by 418287.5 ± 160362.2 fold following PDGF stimulation while Mdivi-1 treatment caused a significant reduction of the gene expression by $98.5 \pm 0.47\%$ in the PDGF stimulated cells (Figure 4.24A).

In hypoxia, the expression of TFAM was significantly higher (24390.3 ± 4908.5 fold) in comparison with its expression in the normoxic quiescent cells (Figure 4.25A). However, it was reduced following PDGF stimulation by $72.9 \pm 12.6\%$ (Figure 4.24B). In comparison to the PDGF effect in normoxia, TFAM gene expression was significantly decreased by $97.9 \pm 0.8\%$ during hypoxia (Figure 4.25B). The DRP1 inhibitor (Mdivi-1) showed no effect on TFAM gene expression in the PDGF stimulated cells during hypoxia (Figure 4.24B).

A



B

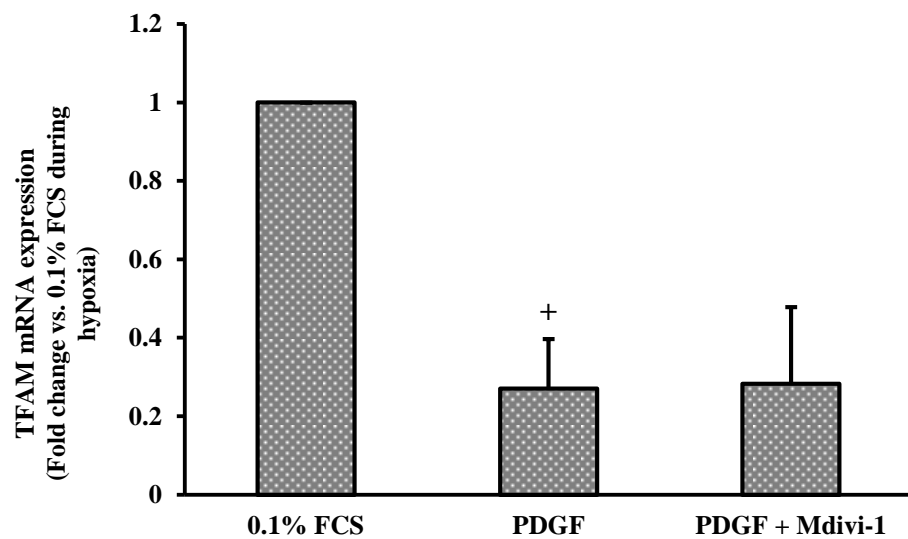
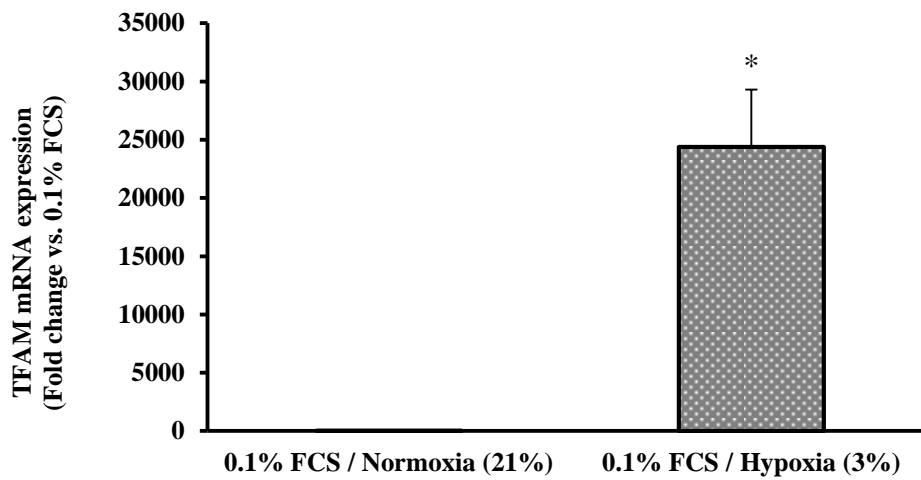


Figure 4.24 The effect of Mdivi-1 on TFAM gene expression in PDGF stimulated cells. Cells were quiesced for 24 h and were then stimulated with PDGF (5 ng/ml) and exposed to different oxygen levels: **A**) Normoxia (21% oxygen) and **B**) Hypoxia (3% oxygen) for 24 h. Mdivi-1 (10 μ M) was added 30 minutes before PDGF stimulation. RNA was extracted from cells. Equal RNA concentrations were used for cDNA sample preparation. The expression of mitochondrial transcription factor A (TFAM) gene was measured using RT-qPCR. Ubiquitin C (UBC) was used as the reference gene for normalization. Each value represents the mean \pm SEM (n=3). *p <0.05 vs. quiescent cells in normoxia. •p <0.05 vs. PDGF stimulated cells. +p <0.05 vs. quiescent cells in hypoxia.

A



B

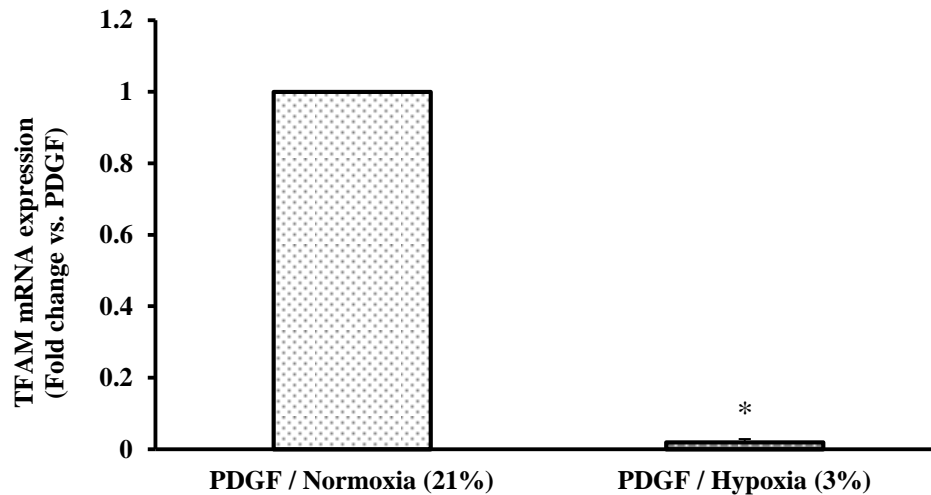


Figure 4.25 Data extracted from Figure 4.24 A and B to highlight the effect of hypoxia on mitochondrial TFAM gene expression in (A) quiescent cells and in (B) PDGF stimulated cells. Cells were quiesced for 24 h and were exposed to hypoxia (3% oxygen) for 24 h. PDGF (5 ng/ml) was added before hypoxic exposure. RNA was extracted from cells. Equal RNA concentrations were used for cDNA sample preparation. The expression of mitochondrial transcription factor A (TFAM) gene was measured using RT-qPCR. Ubiquitin C (UBC) was used as the reference gene for normalization. Each value represents the mean \pm SEM (n=3). *p < 0.05 vs. cultured cells in normoxia.

4.15.3 The effect of Mdivi-1 on COX-II gene expression

Another mitochondrial marker gene is cytochrome c oxidase subunit 2 (COX-II), which is the second subunit of the mitochondrial respiratory chain component (complex IV). It was also investigated following Mdivi-1 treatment.

Mdivi-1 increased COX-II gene expression by 6.5 ± 1.1 fold in the hypoxic cells with 0.1% FCS (Figure 4.26). Figure 4.27 shows the expression of cytochrome c oxidase II (COX-II) gene was upregulated by 8.6 ± 0.8 fold in response to PDGF. In addition, the expression of the COX-II gene was inhibited by $54.6 \pm 6\%$ following Mdivi-1 treatment. However, COX-II expression was increased by 3.2 ± 0.5 fold after 24 h hypoxic exposure. PDGF during hypoxia showed a different effect on COX-II expression as the gene expression following PDGF stimulation was slightly reduced in comparison with its expression in hypoxic background cells. Therefore, in comparison to the PDGF normoxic effect, the expression of the COX-II gene during hypoxia in the PDGF stimulated cells was significantly decreased by $65.7 \pm 2.4\%$. Moreover, data showed an inhibition of DRP1 by Mdivi-1 during hypoxia increased COX-II gene expression by 2.3 ± 0.1 fold in the PDGF stimulated cells (Figure 4.27).

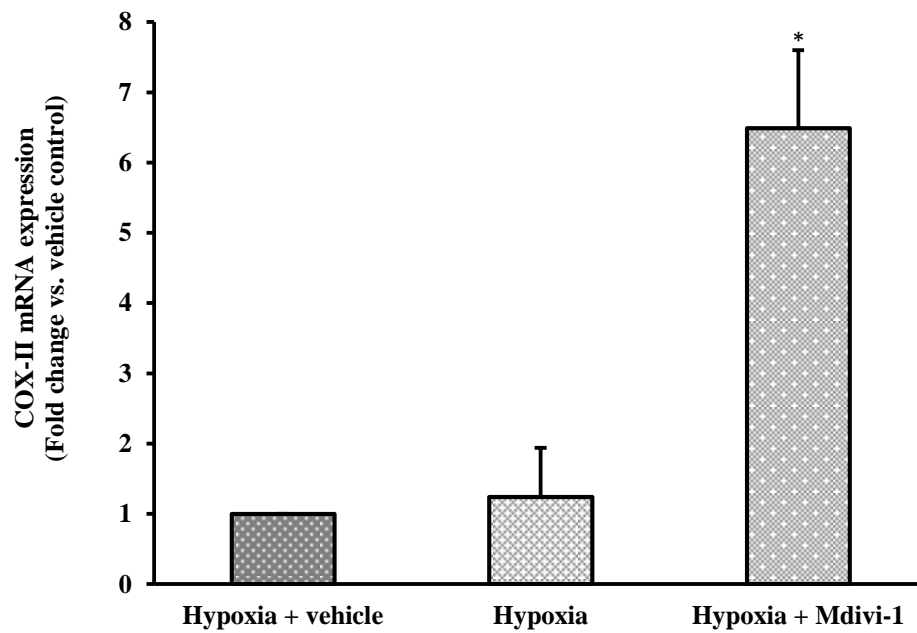


Figure 4.26 The effect of Mdivi-1 on mitochondrial COX-II gene expression in quiescent hypoxic cells. Cells were quiesced for 24 h and were then exposed to hypoxia (3% oxygen) for 24 h. Mdivi-1 (10 μ M) was added 30 minutes before hypoxic exposure. RNA was extracted from cells. Equal RNA concentrations were used for cDNA sample preparation. Cytochrome c oxidase II (COX-II) gene was measured using RT-qPCR. Ubiquitin C (UBC) was used as the reference gene for normalization. Each value represents the mean \pm SEM (n=3). *p <0.05 vs. vehicle control cells.

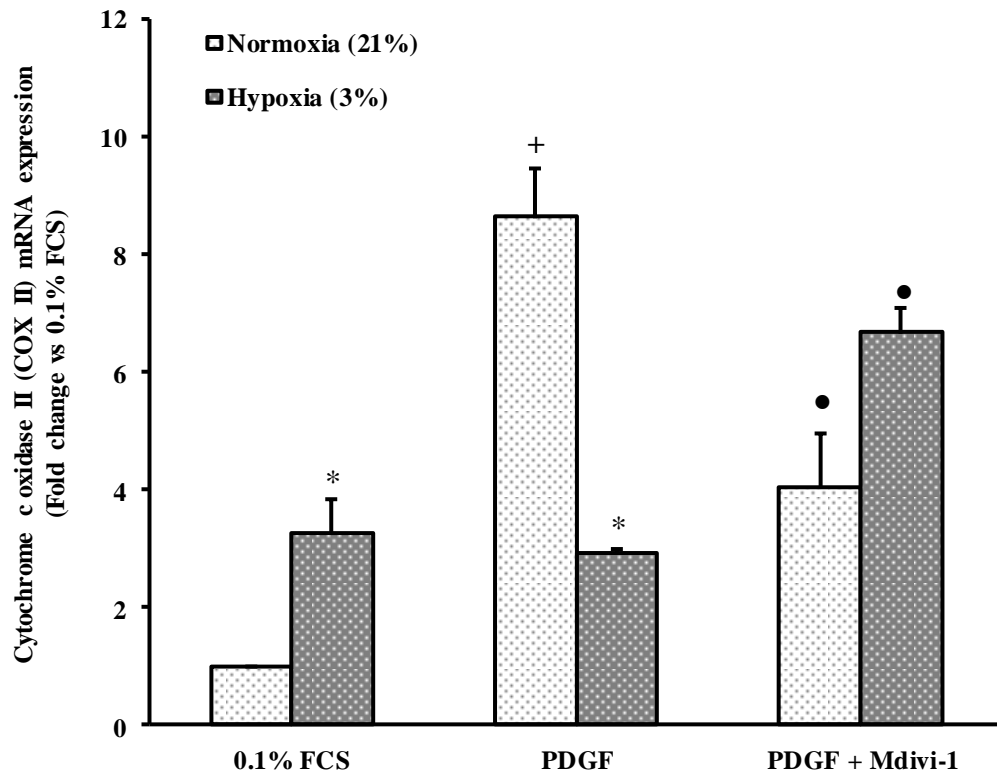


Figure 4.27 The effect of Mdivi-1 on mitochondrial COX-II gene expression in PDGF stimulated cells during hypoxia. Cells were quiesced for 24 h and were then stimulated with PDGF (5 ng/ml) and exposed to different oxygen levels: normoxia (21% oxygen) and hypoxia (3% oxygen) for 24 h. Mdivi-1 (10 μ M) was added 30 minutes before PDGF stimulation. RNA was extracted from cells. Equal RNA concentrations were used for cDNA sample preparation. The expression of cytochrome c oxidase II (COX-II) gene was measured using RT-qPCR. Ubiquitin C (UBC) was used as the reference gene for normalization. Each value represents the mean \pm SEM (n=3). ⁺p <0.05 vs. quiescent cells. *p <0.05 vs. cultured cells in normoxia. [•]p <0.05 vs. PDGF stimulated cells.

4.16 The effect of Mdivi-1 on Mitochondrial Morphology

The mitochondrial morphology, density and localization within the PASMCMs were identified by the use of MitoTracker dye. The distribution of the mitochondria in the cytoplasm was visualized following 24 h incubations by epi-fluorescence microscope in response to different oxygen experimental conditions.

In normoxia, the mitochondria were elongated and fused (135 ± 8.2 Pixels, Figure 4.29) following 24 h nutrient starvation (background cells, Figure 4.28A). However, stimulation of the cells with 5 ng/ml PDGF caused a substantial shift in the mitochondrial dynamics to the fission state (Figure 4.28B) as the mitochondria were fragmented around the nuclei and became shorter in size (8 ± 0.9 Pixels, Figure 4.29). Treating the stimulated cells with mitochondrial fission inhibitor (Mdivi-1) had a strong effect on the mitochondrial morphology as elongated mitochondria were observed (Figure 4.28C). The length of the mitochondria in the treated cells was 25.9 ± 2.9 Pixels (Figure 4.29).

Hypoxia caused a significant decrease in the mitochondrial length as it was decreased to 12.1 ± 0.8 Pixels compared with the quiescent cells under normoxia (135 ± 8.2 Pixels, Figure 4.29). A microscopic image in Figure 4.28D shows fragmented mitochondria that were observed in quiescent cells (cells with 0.1% FCS) following hypoxic exposure (3% O₂). The combined effect of PDGF and hypoxia caused an elongation of the mitochondria (Figure 4.28E) as the mitochondrial length was increased to 81.7 ± 6.1 Pixels compared with the hypoxic quiescent cells (12.1 ± 0.8 Pixels). This effect increased the mitochondrial length by 10.8 ± 1.7 fold versus the PDGF effect during normoxia (Figure 4.29). Moreover, the length of the mitochondria in the hypoxic PDGF stimulated cells was increased to 117.15 ± 9.7 Pixels following Mdivi-1 treatment (Figure 4.29) and the mitochondrial network formation was clearly observed (Figure 4.28F).

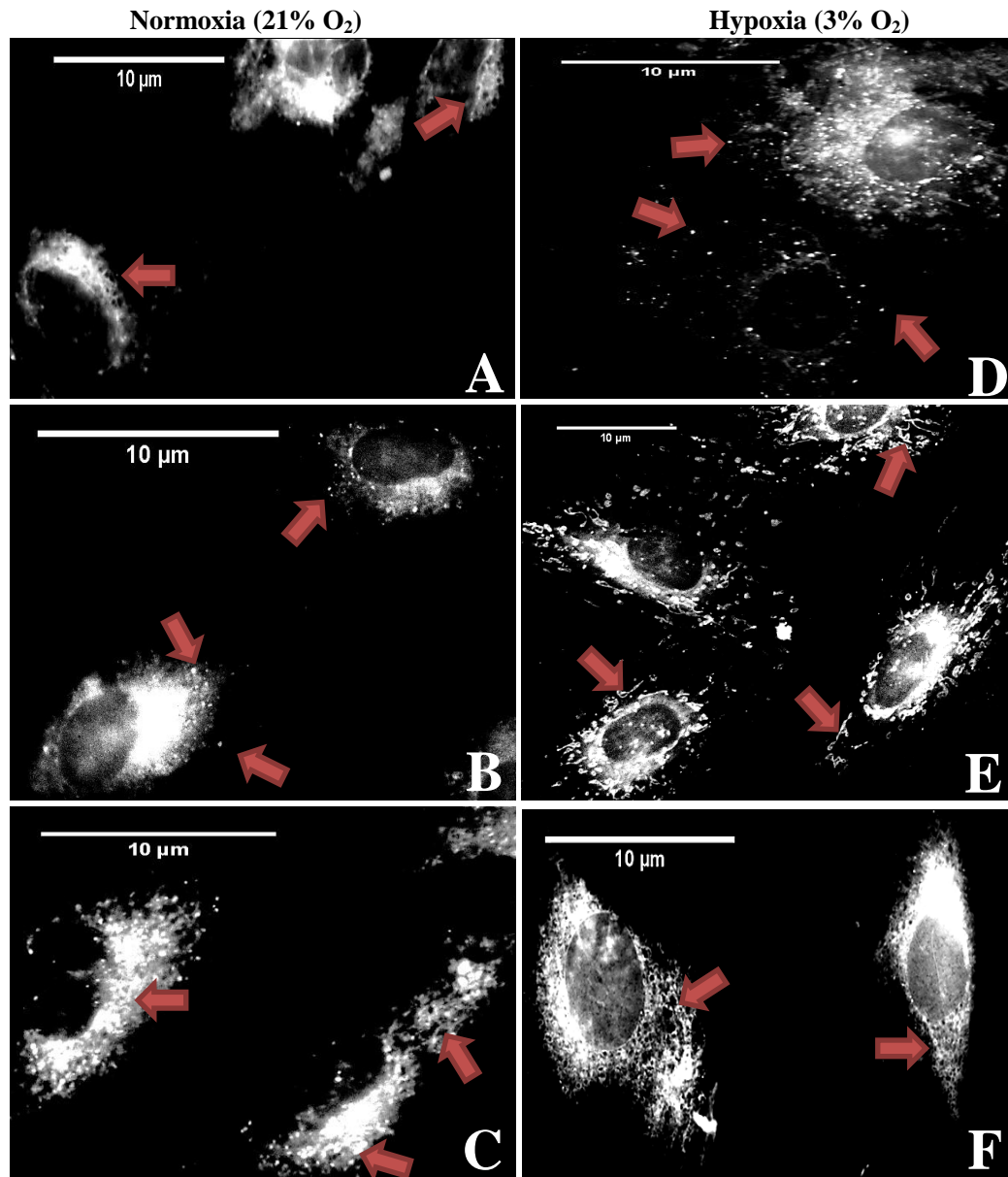


Figure 4.28 Representative images show mitochondrial morphology in the quiescent cells and after stimulating the cells with PDGF following Mdivi-1 treatment during normoxia and hypoxia. PASMCMs were quiesced with 0.1% FCS for 24 h and were immediately stimulated with PDGF (5 ng/ml) and exposed to different oxygen levels: normoxia (21% O₂) and hypoxia (3% O₂) for 24 h. Mdivi-1 (10 μM) was added 30 minutes before stimulation. Cells were stained with MitoTracker red fluorescence for 30 minutes and were imaged by epi-fluorescence microscope (x60 magnification, scale bar is 10 μm in all images). Mitochondria are represented by the red arrows in all images. Under normoxic conditions (1st column), elongated mitochondria were observed in the quiescent cells (control, image A) while they were fragmented following PDGF stimulation (image B). In the presence of Mdivi-1, the mitochondria were elongated in the PDGF stimulated cells (image C). Under hypoxic conditions (2nd column), fragmented mitochondria were observed in quiescent cells (cells with 0.1% FCS, image D) while the mitochondria were longer after PDGF stimulation (image E). Mdivi-1 induced mitochondrial network formation (fusion) in the PDGF stimulated cells (image F).

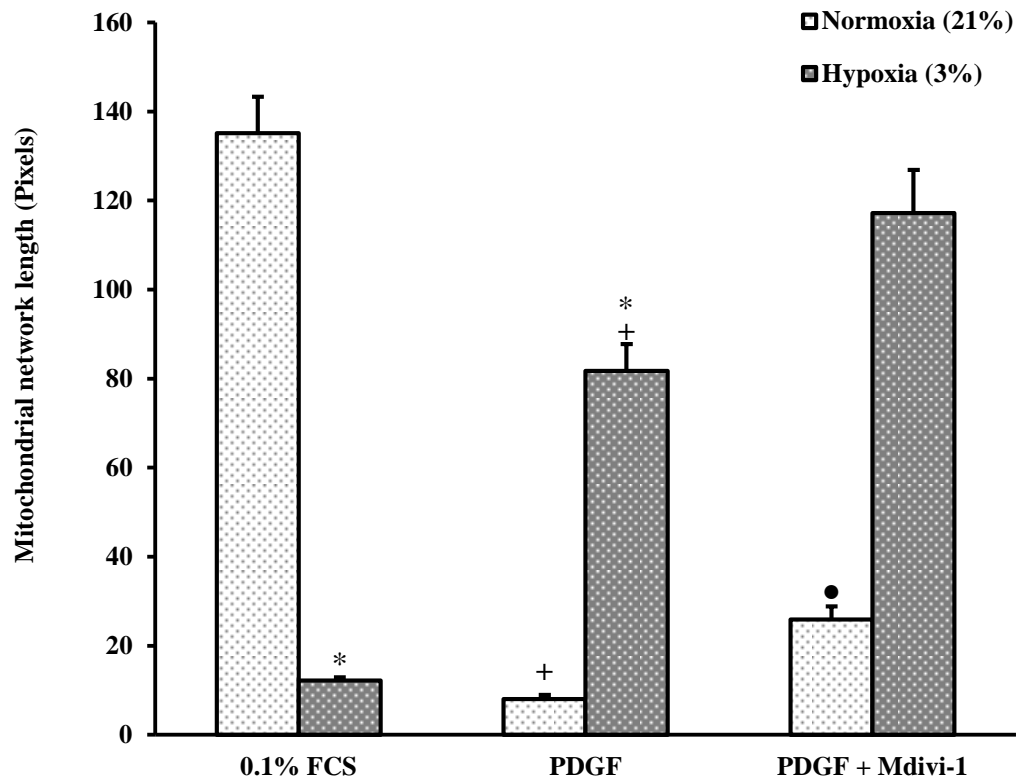


Figure 4.29 The mitochondrial length in the quiescent cells, PDGF stimulated cells and stimulated cells following Mdivi-1 treatment during normoxia and hypoxia. Cells were quiesced for 24 h and were then immediately stimulated with PDGF (5 ng/ml) and exposed to different oxygen levels: normoxia (21% oxygen) and hypoxia (3% oxygen) for 24 h. Mdivi-1 (10 μ M) was added 30 minutes before PDGF stimulation. PASM C s were stained with MitoTracker red fluorescence for 30 minutes and were imaged using an epi-fluorescence microscope (x60 magnification). Image J was used for mitochondrial length measurements. Each value represents the mean \pm SEM (n=3). +p < 0.05 vs. quiescent cells. *p < 0.05 vs. cultured cells in normoxia. •p < 0.05 vs. PDGF stimulated cells.

4.17 The effect of Mdivi-1 on mitochondrial morphology and localization in FCS stimulated cells during hypoxia

The mitochondrial morphology within the PASMCMs was also examined in response to 10% serum stimulation during hypoxia following Mdivi-1 treatment.

Figure 4.30A shows 10% serum caused mitochondrial fragmentation with a shorter size. However, during hypoxia, the mitochondria were elongated following 10% serum stimulation (Figure 4.30C). The mitochondrial length was increased to 85.1 ± 12.1 Pixels in comparison to serum stimulation in normoxia (19.4 ± 2.9 Pixels, Figure 4.31).

During normoxia, data showed that 10 μ M Mdivi-1 caused a significant increase in the mitochondrial length in the stimulated cells (5.5 ± 1.1 fold, Figure 4.31). Similarly, during hypoxia, it enhanced the mitochondrial length of the serum-stimulated cells by 1.4 ± 0.3 fold (Figure 4.31). Images obtained using epifluorescence microscopy and the mitochondrial dye MitoTracker show mitochondrial length in serum-stimulated cells was longer following the addition of Mdivi-1 under both normoxic (Figure 4.30B) and hypoxic (Figure 4.30D) conditions.

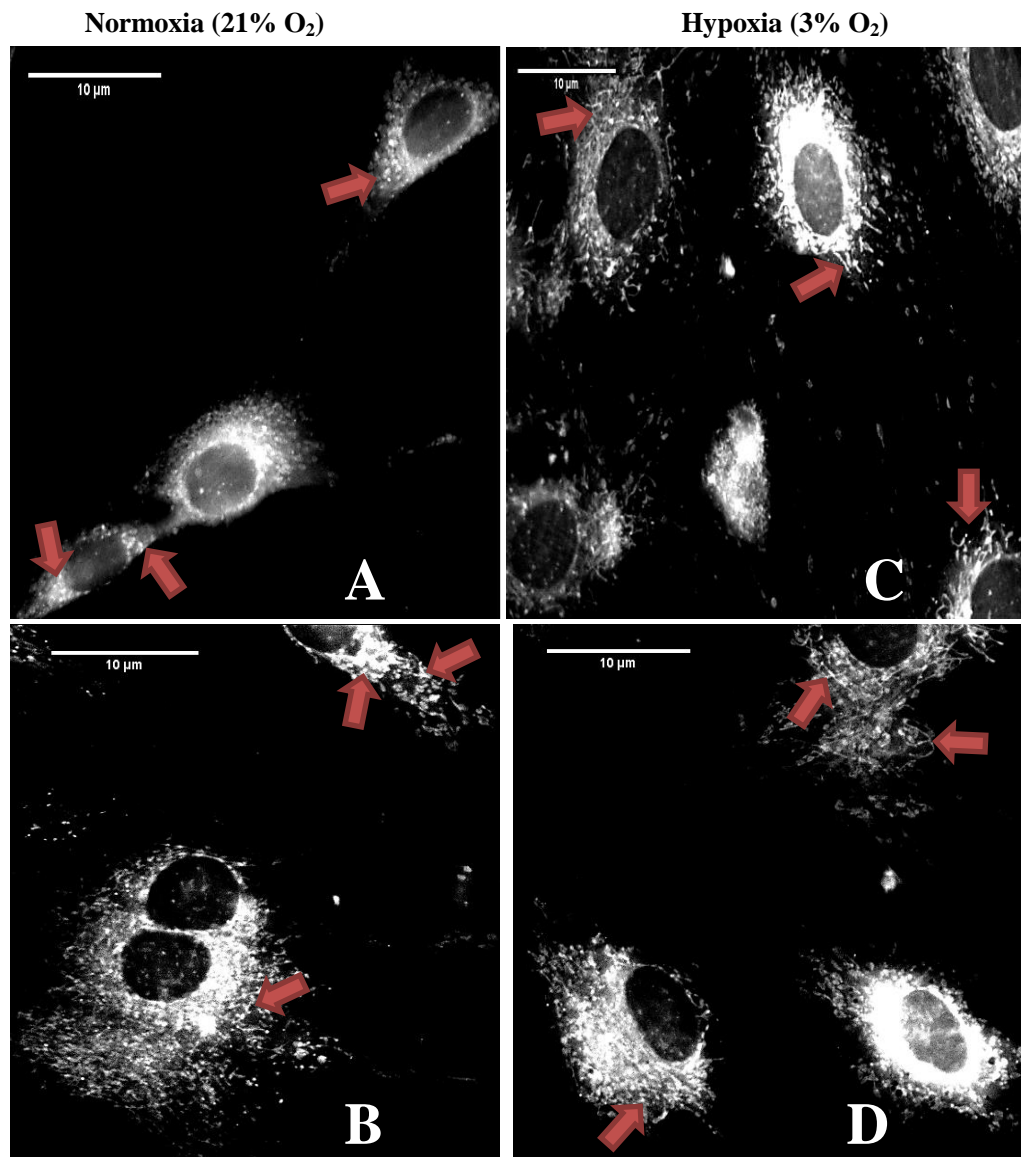


Figure 4.30 Representative images show mitochondrial morphology in 10% serum stimulated cells and stimulated cells with Mdivi-1 during normoxia and hypoxia. PASMCs were quiesced for 24 h and were immediately stimulated with 10% FCS and exposed to different oxygen levels: normoxia (21% O₂) and hypoxia (3% O₂) for 24 h. Mdivi-1 (10 μM) was added 30 minutes before 10% FCS stimulation. Cells were stained with MitoTracker red fluorescence for 30 minutes and were imaged by epi-fluorescence microscope (x60 magnification, scale bar is 10 μm in all images). Mitochondria are represented by the red arrows in all images. Under normoxic conditions (1st column), mitochondria were fragmented following 10% FCS stimulation (image A) and became shorter in size compared to the quiescent cells (control, Figure 4.28A). The mitochondria were longer following the addition of Mdivi-1 (image B). Under hypoxic conditions (2nd column), 10% FCS caused an elongation of the mitochondria (image C) in comparison to control cells (cells quiesced with 0.1% FCS and maintained in 3% O₂, Figure 4.28D). Mdivi-1 caused an increase in the mitochondrial network formation (fusion) in the 10% FCS stimulated cells (image D).

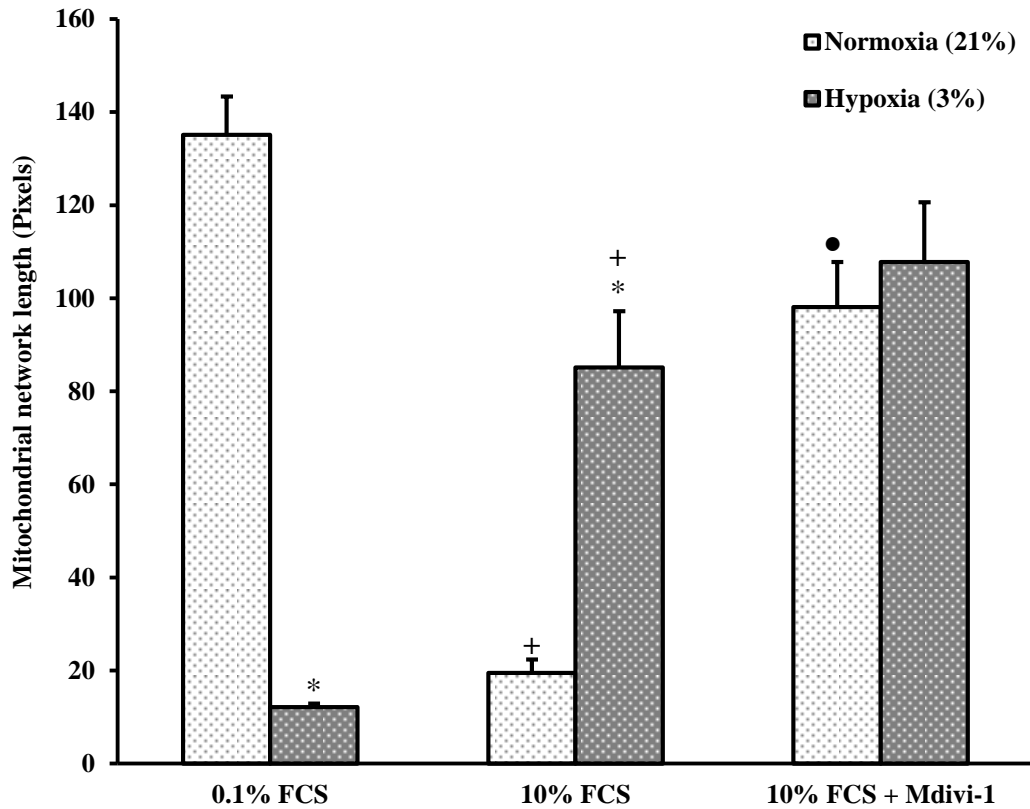


Figure 4.31 The mitochondrial length in the quiescent cells, 10% serum stimulated cells and stimulated cells with Mdivi-1 treatment during normoxia and hypoxia. Cells were quiesced for 24 h and were immediately stimulated with 10% FCS and exposed to different oxygen levels: normoxia (21% oxygen) and hypoxia (3% oxygen) for 24 h. Mdivi-1 (10 μ M) was added 30 minutes before serum stimulation. PASM C s were stained with MitoTracker red fluorescence for 30 minutes and were imaged using epi-fluorescence microscope (x60 magnification). Image J was used for mitochondrial length measurements. Each value represents the mean \pm SEM (n=3). +p <0.05 vs. quiescent cells. *p <0.05 vs. cultured cells in normoxia. •p <0.05 vs. 10%FCS stimulated cells.

4.18 Generation of Mitochondrial-depleted cells (Rho cells)

As described in Methods Section 2.14, Rho cells were generated by culturing the PASMCMs with ethidium bromide for 21 days in order to inhibit the mitochondria non-pharmacologically. Cells treated with ethidium bromide result in the depletion of their mitochondrial DNA, which causes morphological and functional changes in mitochondria, including a loss in the assembly of oxidative phosphorylation (OXPHOS) subunits, and impaired mitochondrial respiration (DiMauro and Schon, 2003, Grimwood and Wagner, 1976). Lacking functional electron transport chain, Rho cells cannot normally regulate the redox state and their mitochondria generate fewer ROS (Chandel and Schumacker, 1999). In addition, dysfunction of the OXPHOS complexes leads to depolarisation of the mitochondrial membrane potential ($\Delta\Psi_m$) (Green et al., 2011). PCR was performed to measure the expression of mitochondrial marker genes (COX-II and TFAM gene) and to assess the mitochondrial function at the end of 21 day incubation. Results showed the expression of COX-II gene was almost repressed in the rho cells. Moreover, TFAM gene expression was reduced to the half in the rho cells versus its normal gene expression in cultured cells without ethidium bromide (Figure 4.32).

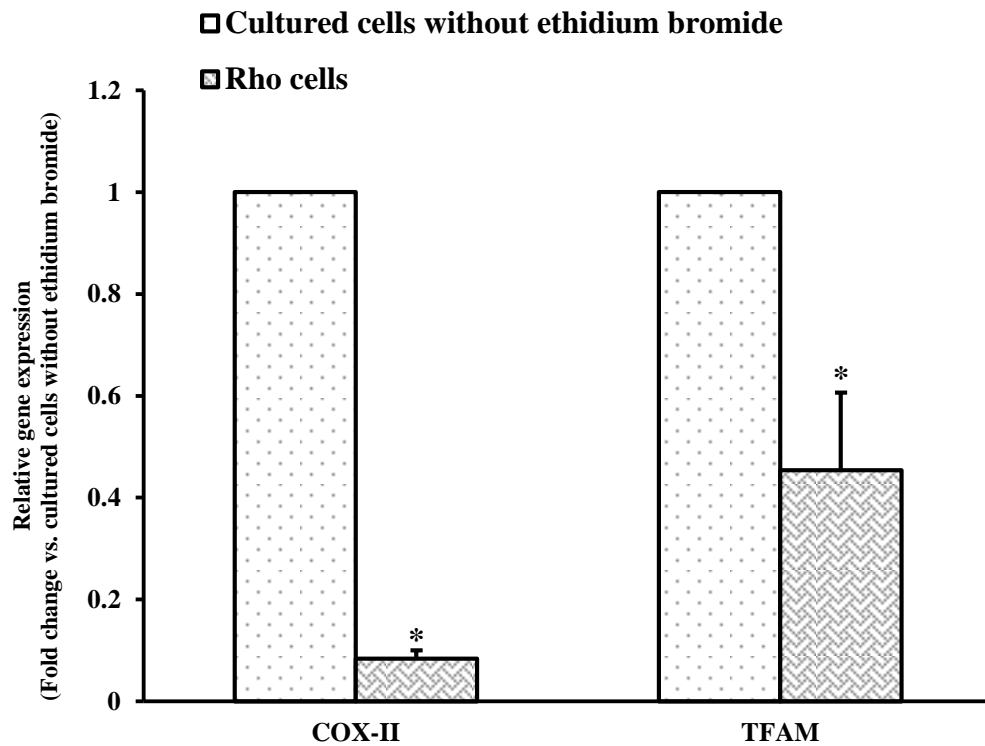


Figure 4.32 The loss of mitochondrial marker genes in the mitochondrial-depleted Rho cells. Rho cells were generated by culturing the cells with 10% FCS media containing 50 ng/ml ethidium bromide, 50 ng uridine and 1 mM sodium pyruvate for 21 days at normal incubation. Control cells were cultured with 10% FCS media for 21 days at normal incubation. RNA was extracted from cells and cDNA sample were prepared. Mitochondrial marker genes; cytochrome c oxidase II (COX-II) and mitochondrial transcription factor A (TFAM) were measured in cultured cells and rho cells at the end of the 21 day incubation by RT-qPCR. Ubiquitin C (UBC) was used as the reference gene for normalization (n=3). *p < 0.05 vs. cultured cells without ethidium bromide.

4.19 The effect of PDGF on Mito-depleted Rho cell Proliferation

The [³H]-thymidine incorporation assay was used to investigate the effect of PDGF on the cellular proliferation (DNA synthesis) during normoxia and hypoxia in mito-depleted Rho cells and the 21 days cultured cells. Cells were quiesced with 0.1% FCS for 24 h and were then stimulated with PDGF for 24 h in both oxygen conditions (normoxia and hypoxia).

During normoxia, Figure 4.33 shows Rho cells incubated with 0.1% FCS had a significant reduction in DNA synthesis ($43.8 \pm 11.3\%$ versus cells with 0.1% FCS, control). PDGF increased DNA synthesis by 1.8 ± 0.13 fold. However, in the mito-depleted Rho cells, PDGF showed no effect.

Data also showed that hypoxia increased the DNA synthesis level by 1.6 ± 0.26 fold compared to the normoxic cells with 0.1% serum (control). However, this effect failed to induce DNA synthesis in the hypoxic Rho cells as the DNA synthesis values caused by hypoxia returned to the basal DNA synthesis level (Figure 4.33). Moreover, PDGF during hypoxia increased DNA synthesis by 1.65 ± 0.08 fold compared to the hypoxic cells and by 1.46 ± 0.13 fold compared to the PDGF stimulated cells in normoxia. In the hypoxic Rho cells, DNA synthesis values caused by PDGF were not decreased and were slightly higher in comparison to the values in the hypoxic Rho cells without PDGF (1.26 ± 0.21 fold). However, the proliferative response resulting from the combined effects of hypoxia and PDGF was significantly decreased by $60 \pm 1.5\%$ in the hypoxic Rho cells (Figure 4.33).

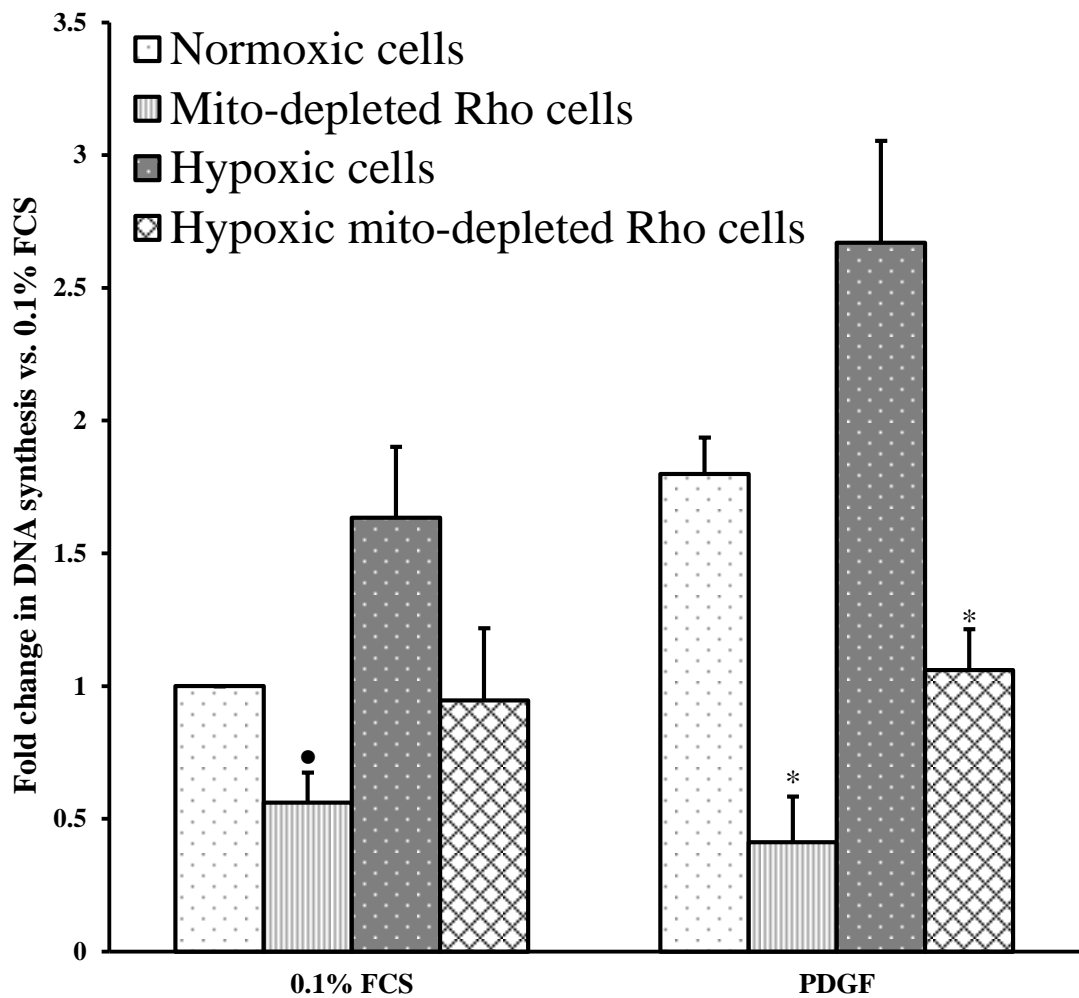


Figure 4.33 The effect of PDGF stimulation on the proliferative response of mito-depleted Rho cells under normoxic and hypoxic conditions. Cells were cultured for 21 days (control group) in parallel with Mito-depleted Rho cells (test group). After mito-depleted Rho cells generation, both cell groups were quiesced for 24 h and were stimulated with PDGF (5 ng/ml) and incubated at different oxygen levels; 21% oxygen (normoxia) and 3% oxygen (hypoxia) for 24 hours. Incorporation of [³H]-thymidine assay was used for DNA synthesis evaluation. Radioactive counts were measured in disintegrations per minute (DPM) and normalized to DNA synthesis in the control group (quiescent cells, 0.1% FCS). Experiments were conducted in quadruplicate (number of wells). Each value represents the mean \pm SEM (n=3). *p<0.05 vs. PDGF stimulated cells. •p <0.05 vs. normal cells cultured with 0.1% FCS (control).

4.20 Discussion

The work presented in chapter 3 has characterized a feature of the hypoxic PASMC behaviour. In particular, cells have been shown to proliferate when they are exposed to hypoxia (3% O₂). In this study, a cell based model (PASMCs isolated from rat pulmonary arteries and cultured in hypoxia, as identified in Chapter 3) was established. Platelet-derived growth factor (PDGF) was selected to stimulate the cells instead of serum. Techniques to evaluate cell proliferation and migration were carried out and the effects of mitochondrial inhibition on PASMC proliferation and migration during normoxia (21% oxygen) and hypoxia (3% oxygen) were determined. The mitochondrial function in response to the mitochondrial DRP1 inhibitor (Mdivi-1) was also examined. The main findings of this chapter are that inhibiting the mitochondrial fission protein DRP1 with Mdivi-1 in PASMCs leads to a decrease in cell proliferation and migration and causes an increase in mitochondrial network formation under both normoxic and hypoxic conditions. Mdivi-1 decreased proliferation as measured by decreased incorporation of [³H]-thymidine and its action was confirmed by measuring gene expression of DRP1. During normoxia, Mdivi-1 produced a shift in cell cycle towards a G2/M phase arrest. This shift in the cell cycle appears to be through inhibiting the expression of P53 gene and upregulating the expression of cyclin D1 gene. The reduction in cell proliferation and migration in the presence of Mdivi-1 was correlated with a decrease in the mitochondrial function (ATP levels). It was also correlated with a reduction in the expression level of mitochondrial marker genes including COX-II, TFAM and ATPase 6. Conversely, during hypoxia, Mdivi-1 produced a shift in cell cycle towards a G1 phase arrest. This shift in the cell cycle seems to be through upregulating the expression of P53 gene and inhibiting the expression of cyclin D1 gene. The inhibitory effect of Mdivi-1 on cell proliferation and migration was associated with the reversal of the mitochondrial function through upregulating the mitochondrial COX-II, ATPase 6 and P53 gene expression.

4.21 The study of PDGF signalling in pulmonary hypertension

It is well-known that FCS contains various growth factors, such as insulin-like growth factor-1 (IGF-1), EGF, PDGF and fibroblast growth factor (FGF), which promote multiple effects. These effects include Ca²⁺ mobilization, inositol-

phosphate formation and cAMP/cGMP formation which caused by growth factors signalling (Van Langendonck et al., 1997, Rubin et al., 1980, Sagirkaya et al., 2007). The initial signal, which resulted from the ligand-receptor complex can transform into more widespread and general effectors that leads to the initiation of multiple intracellular changes required for DNA replication and cell division (Dulbecco and Elkington, 1975). Therefore, in order to overcome the intracellular interactions due to the effects of various growth factors in FCS and to be more specific, PDGF was used to stimulate the cells instead of FCS.

Several lines of evidence have extensively shown the involvement of PDGF signalling in the pulmonary vasculature, remodeling and in pulmonary hypertension pathobiology (Yang et al., 2009, Barst, 2005). It has been shown that PDGF influences the mitochondrial morphology, energetics, ROS generation and causes mitochondrial shortening/fission through increasing the DRP1 level, which eventually increases smooth muscle cell migration and intimal hypertrophy (Wang et al., 2015b). The PDGF dependent DRP1/mitochondrial fission effect has also been shown to play an important role in chronic hypoxic PASMCM proliferation (Marsboom et al., 2012). Blocking PDGF signalling by a receptor kinase inhibitor (imatinib) was shown to regress pulmonary vascular remodeling and to improve the survival of animal models of pulmonary hypertension (Schermyly et al., 2005). These studies underline the importance of mitochondrial fission and metabolism in the PDGF pathway involved in pulmonary hypertension pathobiology. However, some side effects associated with imatinib therapy such as cardiotoxicity have been reported. Thus, extensive pharmacological research is needed to find a more specific mitochondrial target in the PDGF transduction pathway. A PDGF induced model of a highly proliferative cell phenotype associated with mitochondrial fragmentation has been previously demonstrated in VSMC (Salabei and Hill, 2013, Perez et al., 2010). Therefore, using PDGF during normoxia in our study as a positive control group will provide a better understanding of the series of biological and mitochondrial changes in terms of PASMCM proliferation and migration in response to acute hypoxia (test group). Hence, knowing the main intracellular signal transduction pathways of PDGF during normoxia will clarify the impact of mitochondrial signalling on the PDGF-hypoxic interaction during cell proliferation and migration. This was accomplished by determining the exact mechanism of

dynamamin-related protein-1 (DRP1) during both normoxic and hypoxic conditions using the mitochondrial fission inhibitor (Mdivi-1) as a promising approach to attenuate pulmonary vascular remodeling, specifically PASMC proliferation and migration.

In order to study signalling pathways that contribute to the proliferation of vascular smooth muscle cells, previously published studies have used 10 ng/ml concentration of PDGF to stimulate these cells (Yang et al., 2015, Li et al., 2017, Zhan et al., 2003). Therefore, in this study, three different concentrations of PDGF; 5 ng/ml, 10 ng/ml and 20 ng/ml were initially tested on the PASMCs (Figure 4.3). The low concentration (5 ng/ml) was selected because it approximately showed a similar proliferative response in DNA synthesis compared to other concentrations (10 ng/ml and 20 ng/ml). As there is no concentration-dependent effect on PASMC proliferation among PDGF concentrations (Figure 4.3), lower concentrations of PDGF (such as 1 ng/ml) should be considered. However, it has been reported in a previous study that 1 ng/ml and 10 ng/ml concentrations of PDGF have the same responses in PASMC proliferation (DNA synthesis values) during both normoxia and hypoxia (Goncharova et al., 2012).

4.22 Effect of mitochondrial inhibition on PASMC proliferation

To inhibit the mitochondrial-fission process pharmacologically and to investigate the effects of inducing mitochondrial fusion (reducing DRP1 levels) on PASMC proliferation and migration during hypoxia, the mitochondrial division inhibitor-1 (Mdivi-1), which is a DRP1 inhibitor molecule, was used.

In the current study, [³H]-thymidine incorporation assay (Figure 4.4) shows PDGF stimulated PASMCs have a higher proliferative capacity when they are exposed to hypoxia, which is in line with the previous chapters' findings when 10% serum was used to stimulate the cells during hypoxia (Figure 3.10). This finding has been confirmed by other investigators. Schultz and colleagues (2006) found that moderate hypoxia (5% oxygen) enhanced PASMC proliferation in response to several growth factors such as PDGF, FGF and EGF in comparison to their normoxic control (21% oxygen). Another study by ten Freyhaus and co-workers

(2011) found PASCs proliferated faster in response to hypoxia (1% oxygen) when the cells were stimulated with PDGF.

Results show following mitochondrial-fission inhibition, both the PDGF-dependent proliferation (Figure 4.5) and the FCS-dependent proliferation (Figure 4.6) of cells during both normoxic and hypoxic conditions were significantly decreased. It is noticeable that the inhibitory effects of Mdivi-1 in the cells with PDGF (Figure 4.5) during hypoxia were considerably higher than the Mdivi-1 inhibitory effects during normoxia, suggesting that the existence of the mitochondrial fission process, particularly mitochondrial DRP1, is highly required in PDGF induced-PASC proliferation during hypoxia in particular. To identify the exact mechanism of Mdivi-1 under hypoxia, signalling pathways involved in regulating PASC proliferation (such as MAPKs) will be investigated in the next chapter.

4.23 Mitochondrial DRP1 role in cell proliferation during normoxia

The measures of cell proliferation in response to addition of PDGF are dependent on mitochondrial activity/fission. There was a correlation of mitochondrial gene expression and cell proliferation. PCR results showed that mitochondrial fission gene DRP1 and other mitochondrial genes including TFAM, COX-II and ATPase 6 gene were upregulated in the PDGF stimulated cells and downregulated when the mitochondria were inhibited by the mitochondrial fission inhibitor Mdivi-1 (Figure 4.23, Figure 4.24A, Figure 4.27, Figure 4.20). As expected, the results in Figure 4.23 did confirm that Mdivi-1 has a role in the inhibition of mitochondrial DRP1 gene. Mdivi-1 has previously been reported to be a selective inhibitor of the mitochondrial DRP1 and this effect leads to inhibition of the mitochondrial fission (Cassidy-Stone et al., 2008, Tanaka and Youle, 2008). Similarly, it has been reported that Mdivi-1 inhibited mitochondrial fission and reduced proliferation of other cells such as VSMCs (Chalmers et al., 2012, Torres et al., 2016), fibroblasts (Tian et al., 2018) and cancer cells (Rehman et al., 2012).

In quiescent cells (cells with 0.1% FCS), the loss of mitochondrial fission and the increase of tubulated mitochondria were clearly observed (Figure 4.28A). A significant increase of mitochondrial-fission marker (DRP1) gene by PDGF,

compared to quiescent cells (Figure 4.23), is consistent with the increase of the fragmented mitochondria seen by epifluorescence microscope in the PDGF stimulated cells (Figure 4.28B). Moreover, the measurement of mitochondrial length in cells stimulated with PDGF was significantly smaller compared to quiescent cells (Figure 4.29). These results agree with findings of other studies that found that the mitochondria in unstimulated control VSMCs are showing networks of long filaments (fusion) while the mitochondria are showing fragmented and short (fission) when the cells are stimulated with PDGF (Wang et al., 2015b, Salabei and Hill, 2013). This highlights the importance of the DRP1 gene in PDGF-dependent proliferation. This suggestion was confirmed by the use of a DRP1 inhibitor (Mdivi-1). The reduction of PSMC proliferation by inhibiting this gene via Mdivi-1 was associated with the loss of mitochondrial fragmentation and the increase of mitochondrial length which were observed in the Mdivi-1 treated cells (Figure 4.28C and Figure 4.29). These findings are consistent with Wang et al and Salabei and Hill studies which both reported that inhibiting mitochondrial fission via inhibiting the DRP1 protein promotes an increase in mitochondrial length in VSMCs. DRP1 inhibition can also prevent PDGF induced cell proliferation and mitochondrial bioenergetics (Wang et al., 2015b, Salabei and Hill, 2013). This change in the mitochondrial length is also observed in senescent human umbilical vein endothelial cells (HUVECs) and is correlated with the inhibition of mitochondrial DRP1 (Mai et al., 2010).

In addition, another mitochondrial marker gene, the mitochondrial transcription factor A (TFAM) gene, was also upregulated following PDGF stimulation and the expression of the gene was decreased when Mdivi-1 was added (Figure 4.24A), suggesting that there is a strong link between DRP1 activity, TFAM expression and PSMC proliferation induced by PDGF. A linear-correlation of TFAM gene expression and the mitochondrial DNA levels has been previously identified, indicating that the TFAM gene plays an essential role in regulating the abundance of mitochondrial DNA (Kang et al., 2007). Furthermore, the loss of mitochondrial DNA and the reduction of mitochondrial respiration resulting from preventing the fission process through DRP1 inhibition has been previously verified (Parone et al., 2008). These PCR results agreed with a previous study that showed that the

increase in the expression of TFAM gene and the number of mitochondria in VSMCs was correlated with an increase in cell proliferation (Yoshida et al., 2005).

Moreover, the results show cytochrome c oxidase II (COX-II) (another mitochondrial gene marker) was upregulated by PDGF and downregulated following mitochondrial fission inhibition (Figure 4.27) and this suggests the need of the mitochondrial respiration process (including ATP aerobic production) for PSMCs to proliferate in response to PDGF. This result is consistent with the ATP assay finding in this study as PDGF significantly increased ATP levels and a reduction of ATP levels was seen when inhibiting PDGF receptors by imatinib or when inhibiting mitochondrial fission with Mdivi-1 (Figure 4.19). Moreover, other findings which support these results show the upregulation of ATPase 6 gene, a key regulatory gene for the mitochondrial oxidative phosphorylation process, when cells were stimulated with PDGF and the gene was significantly decreased following Mdivi-1 treatment (Figure 4.20). A positive correlation between the mitochondrial cytochrome c oxidase (complex IV) subunit, the content of ATP through the oxidative phosphorylation (OXPHOS) and the expression of COX-II has been previously demonstrated (Bragina et al., 2015). Taken together, increased ATP level and mitochondrial respiration is essential in PDGF induced cell proliferation and migration under normoxic conditions. This finding was previously reported in rat aortic VSMCs (Perez et al., 2010).

Furthermore, another assessment of the mitochondrial activity was also performed by measuring the cellular reactive oxygen species (ROS). It has been previously known that excessive ROS production is linked to PSMC proliferation (Wedgwood et al., 2001). Data in Figure 4.16 show superoxide ($O_2^{\cdot-}$) was significantly upregulated by PDGF while lower levels were produced by PDGF with Mdivi-1 treatment. This suggests ROS (particularly superoxide) may play a major role in PDGF dependent proliferation through DRP1 triggering mechanism. It has demonstrated that PDGF activates the mitochondrial energetics, mitochondrial fission and ROS levels in VSMCs and the deficiency of DRP1 is proportional with the reduction in mitochondrial respiration coupling efficiency (Wang et al., 2015b). Hence, this suggests Mdivi-1 seems to have a direct inhibitory effect on the

respiratory coupling of the mitochondria by decreasing ROS production and by diminishing the increase in cellular ATP.

The above findings conclude that PDGF increases DRP1 expression, promotes mitochondrial fission, and increases cell proliferation and mitochondrial bioenergetics. Further confirmation of the mitochondrial role in PDGF-dependent proliferation during normoxia was performed by inhibiting the mitochondria non-pharmacologically through mito-depleted Rho cell generation. Following 24 h PDGF stimulation, proliferation of Rho cells was measured using [³H]-thymidine incorporation assay and compared to the control (21 days cultured cells without ethidium bromide). It can be seen that data obtained from [³H]-thymidine incorporation assay (Figure 4.33) that non-pharmacological inhibition of mitochondria caused a reduction in DNA synthesis of PASMCMs induced by PDGF or by low serum-condition (0.1% FCS).

Taken together, both the pharmacological inhibition of the mitochondria by preventing the fission process by Mdivi-1 and the non-pharmacological inhibition of the mitochondria by generating Rho cells showed a reduction in PASMCM proliferation during normoxia thereby confirming the necessity of the mitochondria in PDGF-dependent cell proliferation.

4.24 Mitochondrial DRP1 role in cell proliferation during hypoxia

In the current study, PDGF stimulation during both oxygen incubations: normoxia or hypoxia led to an increase in cell proliferation and migration (Figure 4.4 and Figure 4.7). However, cell signalling responses to PDGF seem to be different among hypoxic exposure. For example, in normoxia, PDGF caused a significant increase in mitochondrial fission DRP1 gene expression and caused mitochondrial fragmentation in comparison to quiescent cells (Figure 4.23 and Figure 4.28B, respectively). However, during hypoxia, there was a significant reduction in the mitochondrial fission DRP1 gene expression in cells treated with PDGF in comparison to hypoxic background cells (cells quiesced with 0.1% FCS and maintained in 3% O₂), suggesting that the mitochondrial fission process may not be involved in cell proliferation (Figure 4.23). This finding was in line with the

morphological shape of the mitochondria which in these cells were fused instead of being fragmented after PDGF stimulation (Figure 4.28E). Many studies have reported that the increase of the mitochondrial length could be due to the inhibition of DRP1 expression (Ong et al., 2010, Sharp et al., 2014). However, to date there is no evidence regarding the effect of PDGF on the expression of mitochondrial DRP1 which may lead to an increase in mitochondrial length in the proliferative PASMCMs under hypoxic conditions.

For further investigation, the proliferative cells were treated with a DRP1 inhibitor, Mdivi-1. Data show further inhibition of the mitochondrial fission process caused a decrease in cell proliferation (Figure 4.5), migration (Figure 4.9) and DRP1 gene expression (Figure 4.23). This suggests that despite the reduction in mitochondrial DRP1 gene, the loss of fragmented mitochondria, and the increase of fused mitochondria (Figure 4.23, Figure 4.28E and Figure 4.29) resulting from the combined effect of PDGF and hypoxia, the low expression of mitochondrial DRP1 still seems to be essential in PDGF induced cell proliferation and migration during hypoxia. Data also show the length of mitochondrial network in the proliferative cells was increased following Mdivi-1 treatment (Figure 4.29 and Figure 4.28F). Taken together, these data agreed with the findings of other studies, which reported that the inhibition of mitochondrial fission protein DRP1 with Mdivi-1 induces an increase in mitochondrial length and inhibits the proliferation of PASMCMs during hypoxia (Marsboom et al., 2012, Parra et al., 2017). Ryan and co-workers have also found similar finding which showed that knockdown of DRP1 by siRNA results in elongated mitochondrial network in PAH PASMCMs (Ryan et al., 2015).

Other mitochondrial genes; COX-II and ATPase 6 were also measured in PDGF stimulated cells following Mdivi-1 treatment. Mdivi-1 significantly upregulates COX-II gene, which suggests cell proliferation and migration were inhibited when Mdivi-1 attempted to improve the mitochondrial function specifically by increasing the mitochondrial oxidative phosphorylation process (Figure 4.27). This finding was consistent with the Mdivi-1 effect on the mitochondrial ATPase 6 gene (a gene involved in ATP synthesis process and ATP production) as Mdivi-1 significantly activates its expression (Figure 4.20). The increase of this gene by Mdivi-1 may explain why its inhibitory effect on the ATP level during hypoxia was not effective

and not as significant as its inhibition on the ATP level during normoxia (Figure 4.19). Taken together, the presence of mitochondrial DRP1 during hypoxia could have an important role in controlling the mitochondrial function specifically by decreasing the mitochondrial oxidative phosphorylation process and ATP production in cell proliferation during hypoxia as the PDGF stimulated-hypoxic cells seem to be more dependent on the metabolic Warburg shift (glycolytic shift) instead of mitochondrial ATP generation and the TCA cycle activity. In agreement with this, the study by Parra and co-authors has reported that Mdivi-1 inhibits the proliferation of PASMCMs and the mitochondrial dysfunction caused by hypoxia. They found that, by inhibiting mitochondrial fission protein DRP1 with Mdivi-1, the mitochondrial fission, the glycolytic shift and the increases of glycolytic marker genes hexokinase 2 (HK2), phosphofruktokinase 2 (PFKFB2) and glucose transporter 1 (GLUT1) were also inhibited. They also found Mdivi-1 prevents the reduction in both mitochondrial membrane potential and oxygen consumption in the hypoxic PASMCMs (Parra et al., 2017). Moreover, a recent study has found that the increase in mitochondrial networking and the reversal of the glycolytic shift are associated with the inhibition of DRP1 by Mdivi-1 in microglia (Nair et al., 2019).

To confirm the role of Mdivi-1 in inhibiting cell proliferation during hypoxia by the reversal of mitochondrial function, the expression of P53 gene was measured (Figure 4.14). As P53 antagonizes the Warburg effect through decreasing GLUT expression and the glycolytic shift and stimulating mitochondrial TCA cycle activity, its inhibition serves to promote the Warburg effect (Maddocks and Vousden, 2011, Vousden and Ryan, 2009). A recent study has found knock-down of P53 using siRNA in PASMCMs resulted in a metabolic shift toward glycolysis, an inhibition of mitochondrial respiration including the TCA cycle and a reduction in ATP production (Wakasugi et al., 2019). Mitochondrial-dependant cell proliferation (PDGF stimulated cells during normoxia), shows the expression of P53 gene was significantly higher than its expression during hypoxia. Moreover, data also show inhibiting the mitochondria by Mdivi-1 significantly inhibits P53 gene during normoxia while significantly upregulating P53 gene expression during hypoxia, which confirms that inhibiting DRP1 may have a potential role in improving the mitochondrial activity to inhibit cell proliferation during hypoxia.

The non-pharmacological inhibition of the mitochondria by generating Rho cells also confirmed the need for the glycolytic shift in cell proliferation during hypoxia. Following PDGF and hypoxia stimulation, the proliferation of Rho cells was decreased compared to 21 days cultured cells but DNA synthesis values were only returned to the normal background DNA synthesis level, which suggests even the mitochondria (particularly mitochondrial metabolism) were inhibited, PASM Cs could maintain their growth and proliferate by increasing mitochondrial dysfunction and glycolytic metabolism.

4.25 The effect of Mdivi-1 on cell cycle progression

Data show Mdivi-1 increased the G2 phase of the cell cycle in PDGF stimulated cells, suggesting Mdivi-1 could diminish PASM C proliferation by causing cell cycle arrest at G2/M phase (Figure 4.10B). This finding agreed with the findings of Rehman et al and Marsboom et al who determined that mitochondrial fission inhibition by Mdivi-1 prevents the cell cycle progression causing G2/M arrest in lung cancer and PASM Cs, respectively (Rehman et al., 2012, Marsboom et al., 2012). Another study by Sun and co-workers also showed a reduction of cell proliferation is linked with the G2/M phase cell cycle arrest in PASM Cs (Sun et al., 2017). In PAH PASM Cs, Marsboom et al found that Mdivi-1 prevents the inactivation of cyclin-dependent kinase 1 (CDK1). CDK1 degrades cyclin B1 levels leads to stop cell cycle progression from G2 to mitosis. This leads to a consequence of activation of checkpoint proteins and changes in cyclin levels which suggests that Mdivi-1 may interact at this stage causing a reduction of PASM C proliferation (Marsboom et al., 2012).

CDK1 is involved in the modulation of the centrosome cycle including centrosome duplication, chromosome condensation and separation (Hochegger et al., 2007, Crasta et al., 2006, Abe et al., 2011, Robellet et al., 2015). It has been reported that Mdivi-1 induced misalignment of mitotic chromosomes and caused a G2/M arrest in cancer cells (Wang et al., 2015a). Activation of cyclin B1/CDK1 complex partly increases the mitochondrial respiration thus providing sufficient energy to the cells for the G2/M transition which reduces the overall cell cycle time (Wang et al., 2014d). Data in Figure 4.19, Figure 4.27, and Figure 4.20 show that inhibiting

DRP1 by Mdivi-1 caused a reduction in ATP levels and in expression of mitochondrial COX-II and ATPase 6 genes, respectively. These data suggest that Mdivi-1 inhibits mitochondrial respiratory chain function and decreases the required amount of ATP for cell cycle progression which leads to cell cycle arrest at G2/M phase and slows cell proliferation.

The reduction of cell proliferation by the drug may be via increasing the apoptotic effect (through its ability to push the cells toward the apoptotic mechanism which leads to cell death) or via the DNA damage effect of the drug (through slowing the division process of the cells where the cells accumulate at G2/M phase resulting in slowing the proliferative rate of the cells) (DiPaola, 2002). It has been reported that fused mitochondria or the prevention of mitochondrial fission can lead to increased cell survival or induces cell apoptosis as fission process plays an important role in regulating two different processes: cell apoptosis and cellular mitosis (Brooks et al., 2009, Taguchi et al., 2007). A study by Szabadkai et al reported that increased DRP1 expression can inhibit the apoptotic response induced by stimuli such as C₂ ceramide (Szabadkai et al., 2004). In contrast, other studies demonstrated that a DRP1 inhibitor, Mdivi-1, can inhibit cell apoptosis and promote cell proliferation (Mitra et al., 2009, Cassidy-Stone et al., 2008). Hence, in order to identify the fate of the cells following G2/M arrest caused by Mdivi-1, some cell cycle regulatory components such as cyclin D1, P53 were assessed.

Under normoxic conditions, data obtained from Western blot (Figure 4.11) show a slight increase in cyclin D1 protein by Mdivi-1 pre-treatment. In line with this observation, PCR data show Mdivi-1 caused a significant increase in cyclin D1 gene expression (Figure 4.13). These findings contradict the findings in the study of Salabei and Hill (2013). They showed that inhibition of DRP1 by Mdivi-1 can inhibit PDGF induced cell proliferation and overexpression of cyclin D1 in aortic VSMCs (Salabei and Hill, 2013). It has been reported that cyclin D1 serves as an important regulator of the continuing cell cycle progression (Stacey, 2003). An accumulation of cyclin D1 proteins suggests Mdivi-1 slows the proliferation rate by extending the duration of PASMCMs at G2/M phase, which indicates the DNA damaging effect of Mdivi-1 could encourage the cells toward the repairing mechanism before entering mitosis. In addition to the above findings, data show

mitochondrial functions and genes were inhibited following Mdivi-1 treatment suggesting that there is a negative correlation between cyclin D1 expression and mitochondrial function. Many studies showed that cyclin D1 can repress the mitochondrial function, ATP production, oxidative phosphorylation process and gluconeogenesis (Wang et al., 2006, Bhalla et al., 2014, Lee et al., 2014, Tchakarska et al., 2011). Taken together, these findings suggest that inhibiting mitochondrial function with Mdivi-1 could be through increasing cyclin D1 expression, thereby inhibiting the mitochondrial function. This suggestion could highlight that PSMCs (not aortic VSMCs) during G2/M phase could compensate an inhibitory effect of Mdivi-1 on the mitochondria via shifting from OXPHOS metabolism toward the cytosolic glycolysis as these cells resemble the behaviour of cancer cell metabolism.

This suggestion was confirmed though measuring the cell cycle inhibitor gene; P53 following Mdivi-1 treatment (Figure 4.14). It is known that the G2 arrest is not affected by the expression of P53 gene (Kastan et al., 1991). Data show Mdivi-1 caused a reduction in P53 gene expression which may support the effect of Mdivi-1 during normoxia as it arrested the cells at the G2/M phase via its DNA damaging effect. This result agrees with findings of Wang et al study. They found that in cancer cells P53 is not required for the mitotic arrest caused by Mdivi-1. They further demonstrated Mdivi-1 induced an accumulation of M phase cells in both P53 knockout and wild-type cells (Wang et al., 2015a). The restriction of PSMCs at G2/M phase by Mdivi-1 could also explain why the inhibitory effect of Mdivi-1 on cell proliferation during normoxia was not potent enough compared to its powerful effect during hypoxia (Figure 4.5). Taken together, these findings may elucidate effect of Mdivi-1 on mitochondrial-dependent mechanism. Specifically, on the progression of cell cycle targeting the G2/M phase and may result in the accumulation of cyclin D1 gene and the reduction of the P53 gene.

During hypoxia, data show an increase of cells at G1 phase following Mdivi-1 treatment (Figure 4.10A). This result contradicts what was observed during normoxia which suggests the progression of cell cycle could be modulated by the cellular responses to hypoxia (such as mitochondrial dysfunction). For example, the G1/S transition is affected by the metabolic status of the cells (Mandal et al., 2010).

Mitochondrial dysfunction can activate two signals to enforce the cell cycle checkpoint particularly between the G1 and S phase. This associated with the downregulation of cyclin E protein levels and the increased mitochondrial ROS (Owusu-Ansah et al., 2008). There is a study which demonstrated that Mdivi-1 decreased cell proliferation and induced G1 cell cycle arrest (Chalmers et al., 2012). However, this study examined the effect of Mdivi-1 in cerebral artery smooth muscle cells under normoxic conditions. To date there is no evidence regarding the effect of Mdivi-1 on cell cycle progression in the PASMCs under hypoxic conditions. Data suggest an accumulation of cells at the G1 phase by Mdivi-1 is possibly due to low cyclin D1 level. Cyclin D1 is required in the progression of the cell cycle and when it is inhibited, cells were arrested at the G1 phase (Morgan, 1995). Thus, measuring cyclin D1 proteins and gene expression was performed. Western blot data confirmed the FACS finding as cyclin D1 protein was significantly decreased following Mdivi-1 treatment (Figure 4.11). Recent evidence by Gu and co-workers showed similar findings in the airway smooth muscle cells following PDGF stimulation. They found Mdivi-1 caused a significant decrease in cell proliferation and cyclin D1 proteins but did not arrest the cells at G2/M phase (Gu et al., 2019). Indeed, PCR data confirm the Western blot result and also show Mdivi-1 directly caused an inhibition of cyclin D1 gene expression (Figure 4.12 and Figure 4.13, respectively). Data display that Mdivi-1 caused a significant increase in tumor suppressor P53 suggesting that P53 upregulation is associated with the G1 cell cycle arrest in response to Mdivi-1 (Figure 4.14). Taken together, these data agreed with the finding of Arora and co-workers in cancer cells, that documented that downregulating cyclin D1 arrested cell cycle at G1 phase and upregulating P53 induced early apoptosis, resulted in decreased cell proliferation (Arora et al., 2017). Many studies have found that P53 upregulation is related to G1 cell cycle arrest. It activates p21, a protein that acts as an inhibitor of the cyclin-dependent kinases (CDKs), which eventually caused repression of the cyclin E-CDK2 complex leading to G1 arrest (Jones et al., 2005, Waldman et al., 1995, el-Deiry et al., 1994). Moreover, Wei et al found that inhibiting PDGF-induced PASMC proliferation was associated with the G1 cell cycle arrest and decreased gene expression levels of cyclin D1, cyclin E and CDK2 (Wei et al., 2016). Taken together, inhibiting mitochondrial fission during hypoxia seems to accelerate cell apoptotic signalling

pathways which leads to an inhibition of cell proliferation through the accumulation of cells at the G1 phase.

4.26 The effect of Mdivi-1 on PASC MC Migration

The current study found the migratory capacity of PASC MCs was enhanced following chemotactic stimulation in a time-dependent manner (Figure 4.7). PDGF stimulation is associated with the release of specific cytokines and extracellular matrix components which may trigger some signalling pathways to promote cell migration. It has been reported that PDGF directly activates DRP1 phosphorylation at serine 616 which enhances DRP1 binding with the mitochondria and activates mitochondrial fission (Wang et al., 2015b). Data showed Mdivi-1 reduces cell migration in normoxia (Figure 4.8). These findings suggest that the effect of PDGF on cell migration was accompanied by changes in DRP1 activity and mitochondrial fission/ fusion status (network formation). Previous studies demonstrated that cell migration could be affected by altering the mitochondrial shape. In metastatic breast cancer cells, it has been shown mitochondrial fragmentation is associated with an increase in cell migration, whereas mitochondrial elongation caused a reduction in cell migration (Zhao et al., 2013). Moreover, the same finding was reported in lymphocytes (Campello et al., 2006). These studies correlate with the migratory effect of PDGF stimulation during normoxia which was shown to promote mitochondrial fission and cell migration. In addition, data in Figure 4.7 showed PDGF stimulation during hypoxia increased cell migration. This was consistent with a study which showed rat PASC MCs in response to hypoxia either at 4% oxygen or 1% oxygen had an increase in the migration rate (Walker et al., 2016). Moreover, data show that despite the reduced DRP1 level and the presence of elongated mitochondria due to the combined effects of PDGF and hypoxia, further inhibition of DRP1 by Mdivi-1 leads to hyper-fusion of the mitochondria and reduces cell migration (Figure 4.9), which suggests not only hypoxia but also minor levels of DRP1 are necessary to promote cell migration. This result is consistent with a study that showed that Mdivi-1 inhibits cell migration induced by hypoxia in human glioblastoma U251 cells (Wan et al., 2014).

Potentially PASMCMs could also proliferate after creating the scratch within the well when they were stimulated with PDGF, this might limit the findings of this study. Ideally, the measurement of cell proliferation should be assessed in parallel to the cell migration assay. For example, cell counting using the haemocytometer or immuno-fluorescence staining for the proliferative markers such as PCNA should be undertaken when images were taken at 0 h and at different stimulation times: 12 h, 24 h and 48 h.

4.27 Effect of Mdivi-1 on Cell apoptosis

Results show the significant reduction of caspase 3/7 release was observed in response to Mdivi-1 during normoxia (Figure 4.22). This result suggests Mdivi-1 had no role in activating the apoptotic pathway via caspase signalling during normoxia. This finding is consistent with the FACS finding. The effect of the drug to slow the proliferation rate during cell arrest at G2 was not through inducing cell apoptosis (G1 phase). Moreover, measuring cytochrome c protein level by Western blot also supported that as there was a small insignificant decrease in cytochrome c protein level following Mdivi-1 treatment (Figure 4.21).

However, during hypoxia, the apoptotic activity (caspase 3/7 release) was not statistically decreased by Mdivi-1 treatment and a small insignificant increase of cytochrome c protein expression was notable following Mdivi-1 treatment (Figure 4.21). These data suggest the Mdivi-1 during hypoxia is more likely to initiate cell apoptosis, as its effect on cell cycle progression showed the cell cycle was arrested at the G1 phase.

4.28 Summary of Results

The experimental findings presented in this chapter show that mitochondrial inhibition has a marked inhibitory effect on pulmonary artery smooth muscle cell proliferation and migration. The effect of Mdivi-1 has been characterised in normoxia and in hypoxia. The results in this chapter concluded that:-

- Chemotactic stimulation of normal PASMCMs by PDGF leads to an increase in mitochondrial fragmentation and bioenergetics, ROS production

(particularly superoxide) and eventually promotes PASMC proliferation and migration.

- Mitochondrial hyperactivity, shortness of the mitochondria and mitochondrial-fission shift play a crucial role in PASMC proliferation induced by PDGF as when the mitochondrial fission is inhibited by Mdivi-1, the cells arrest in the G2/M phase of the cell cycle, therefore, slowing proliferation.
- Inhibiting the mitochondria with Mdivi-1 is more likely to slow PASMC proliferation through inhibiting the P53 gene and through increasing the gene expression of cyclin D1.
- Mitochondrial dysfunction, the decrease in mitochondrial fragmentation, and the increase in mitochondria elongation play a vital role in PDGF induced cell proliferation during hypoxia. However, the existence of mitochondrial dynamic DRP1 protein is largely required.
- Inhibiting mitochondrial fission with Mdivi-1 during hypoxia seems to diminish PASMC proliferation and migration through inhibiting the cyclin D1 expression and increasing the expression of P53 and mitochondrial genes (COX-II and ATPase 6).
- Inhibition of mitochondrial fission in PDGF induced cell proliferation and migration during hypoxia with Mdivi-1 seems to target the glycolytic shift (Warburg effect) within the cells by improving the activity and the function of the mitochondria.
- Non-pharmacological inhibition of the mitochondria, through generating Rho cells, abolished and reduced PASMC proliferation during normoxia and hypoxia, respectively.

Chapter 5

**The Mechanism of Mdivi-1-Dependent Inhibition of
PASMC Proliferation and Migration under Hypoxia**

5.1 Introduction

The results in chapter 4 demonstrated the potential for blocking mitochondrial fission by a DRP1 inhibitor; Mdivi-1 to attenuate proliferation and migration of PSMCs. In particular, a significant reduction in DNA synthesis in the PDGF stimulated cells by Mdivi-1 was observed under hypoxic conditions compared to the normoxic conditions (Figure 4.5). This highlights the importance of mitochondrial fission protein DRP1 in the regulation of PSMC proliferation under hypoxic conditions. It has been reported that the HIF1 α activation induces mitochondrial fragmentation in PSMCs from PAH patients versus control PSMCs (without PAH) and the blocking of the mitochondrial fission through inhibiting the DRP1 reduces cell proliferation which may have a therapeutic potential (Marsboom et al., 2012). However, the specific mechanisms associated with DRP1 inhibition in the proliferation and migration of PSMCs during hypoxia are poorly defined.

Multiple intracellular signalling cascades involved in the regulation of cell proliferation and migration can contribute to the development of pulmonary vascular remodeling and pulmonary hypertension (Chen et al., 2014, Morrell et al., 2009). One of these signalling cascades is the mTOR signalling pathway which plays a key role in cell proliferation, mitochondrial biogenesis and energy equilibrium (Antico Arciuch et al., 2012). mTOR signalling is involved in the stimulation of PSMC proliferation and migration (ten Freyhaus et al., 2011). HIF-1 α is involved in hypoxia-induced protein tyrosine phosphatase (PTP) down-regulation in PAH and specifically PSMCs. PTPs dephosphorylate the activated PDGF receptor and thus a decrease in expression and activity of PTPs leads to increased phosphorylation of the PDGF receptor. Consequently, this results in an increase in downstream intracellular signalling and PSMC proliferation and migration (ten Freyhaus et al., 2011). However, the full picture of mTOR signalling mechanism including the presence of mitochondrial fission protein DRP1 leading to cell proliferation and the re-programming of mitochondrial function are not fully understood.

Another signalling pathway involved in the proliferation of PSMCs in PAH is the MAPK signalling pathway. A study by Wilson and co-workers showed the expression of phosphorylated MAPKs (including ERK1/2, p38 MAPK and JNK) is significantly higher in PAH PSMCs compared to the control PSMCs (Wilson et al., 2015). Various studies showed the MAPK pathway is involved in the PDGF induced progression of cell cycle and cell proliferation (Stawowy et al., 2002, Li et al., 2006, Finlay et al., 2005). However, the link between the mitochondrial DRP1 and the MAPK signalling in regulating PSMC proliferation and migration remains unclear. One study by Lim et al showed that inhibiting mitochondrial DRP1 by siRNA leads to a significant decrease in proliferation and migration of VSMCs. They found a positive correlation between the mitochondrial DRP1 and the ERK1/2 proteins as DRP1 inhibition is correlated with the inhibition of the phosphorylated MEK1/2 and ERK1/2 (Lim et al., 2015). However, the molecular mechanism related to DRP1 has not been investigated in PSMCs.

Therefore, a better understanding of the complex signalling cascades (including the signalling cascade of hypoxia, MAPK and the mTOR) within the PSMCs and their influence on the mitochondrial DRP1 dependent proliferation and migration is merited. This will identify whether these pathways are potential therapeutic targets for treatment of PAH. This chapter focuses on the participation of the mitochondrial fission protein DRP1 in the hypoxia, MAPK, and mTOR signalling pathways.

5.2 Chapter Aims

This chapter aims to identify signalling pathways involved in mitochondrial-dependent cell proliferation and migration during hypoxia.

5.3 Results

5.4 The effect of PDGF on HIF-1 α gene expression

The RT-qPCR experiment which was carried out in Chapter 3 (Figure 3.14A) displayed the existence of HIF-1 α gene in hypoxic PASMCMs stimulated with serum in comparison to cells stimulated with serum during normoxia. In this chapter, to investigate the role of PDGF under the influence of hypoxia, a similar approach was adopted in assessing HIF-1 α gene expression at different oxygen levels: normoxia (21% oxygen) and hypoxia (3% oxygen) in cells without stimulation and in cells stimulated with PDGF (Figure 5.1).

Data show a significant increase in HIF-1 α gene expression (22.35 ± 1.8 fold) in quiescent hypoxic cells compared to normoxic quiescent cells (Figure 5.1). During hypoxia, PDGF reduced this gene expression by $96\% \pm 1.3\%$ in comparison to quiescent hypoxic cells. In addition, in normoxia, the reduction of this gene by PDGF was also observed ($99.95\% \pm 0.02\%$) compared to quiescent cells (Figure 5.1). However, in comparison to normoxic cells stimulated with PDGF (control group), HIF-1 α gene expression remains significantly higher (209.9 ± 48.9 fold) in PDGF stimulated cells during hypoxia (Figure 5.1).

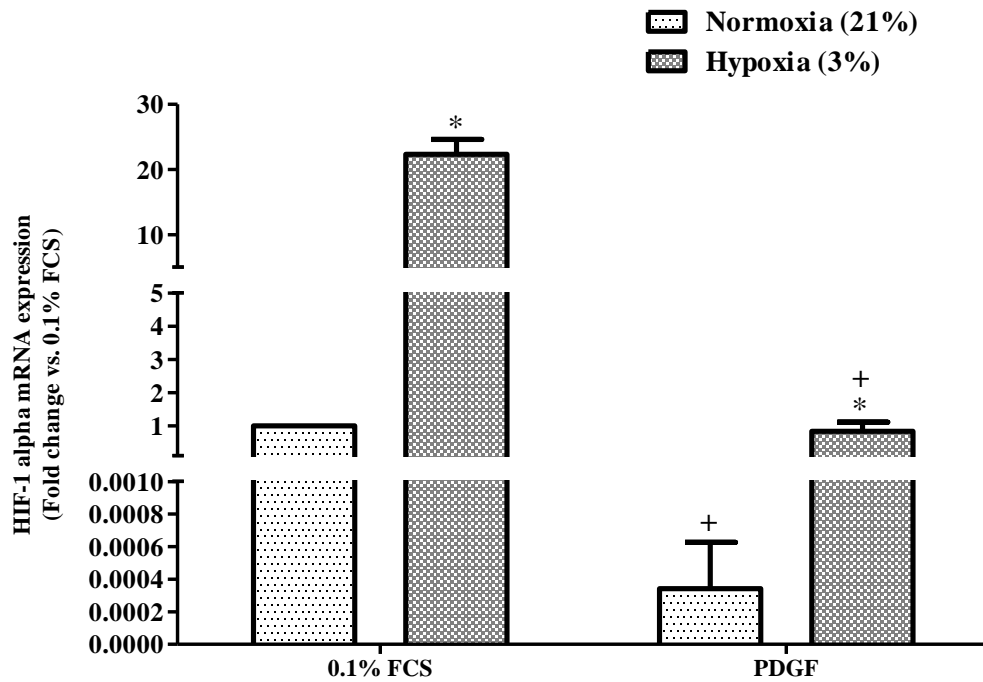


Figure 5.1 The effect of PDGF on HIF-1 α gene expression during hypoxia. Cells were quiesced with 0.1% FCS for 24 h and subsequently exposed to different oxygen levels: normoxia (21% oxygen) and hypoxia (3% oxygen) for 24 h. PDGF (5 ng/ml) was added before oxygen incubation time for 24 h. RNA was extracted from cells. Equal RNA concentrations were used for cDNA sample preparation. Hypoxia-inducible factor-1 alpha (HIF-1 α) gene was measured in quiescent and stimulated groups using RT-qPCR. Ubiquitin C (UBC) was used as the reference gene for normalization. Each value represents the mean \pm SEM (n=3). *p < 0.05 vs. normoxic cells. +p < 0.05 vs. quiescent cells in each oxygen condition.

5.5 The effect of PDGF receptor antagonist on HIF-1 α protein expression in hypoxic-PDGF stimulated cells

In hypoxia, in order to support the result obtained above (Figure 5.1), which shows the inhibitory effect of PDGF on HIF-1 α gene expression, Western blot was accomplished for measuring HIF-1 α proteins in cells exposed to hypoxia stimulated with PDGF for 24 h following imatinib treatment. Blocking of PDGF receptors was performed prior to PDGF stimulation and hypoxic exposure. The result shows HIF-1 α protein was significantly upregulated by 1.3 ± 0.06 fold in the presence of imatinib (Figure 5.2).

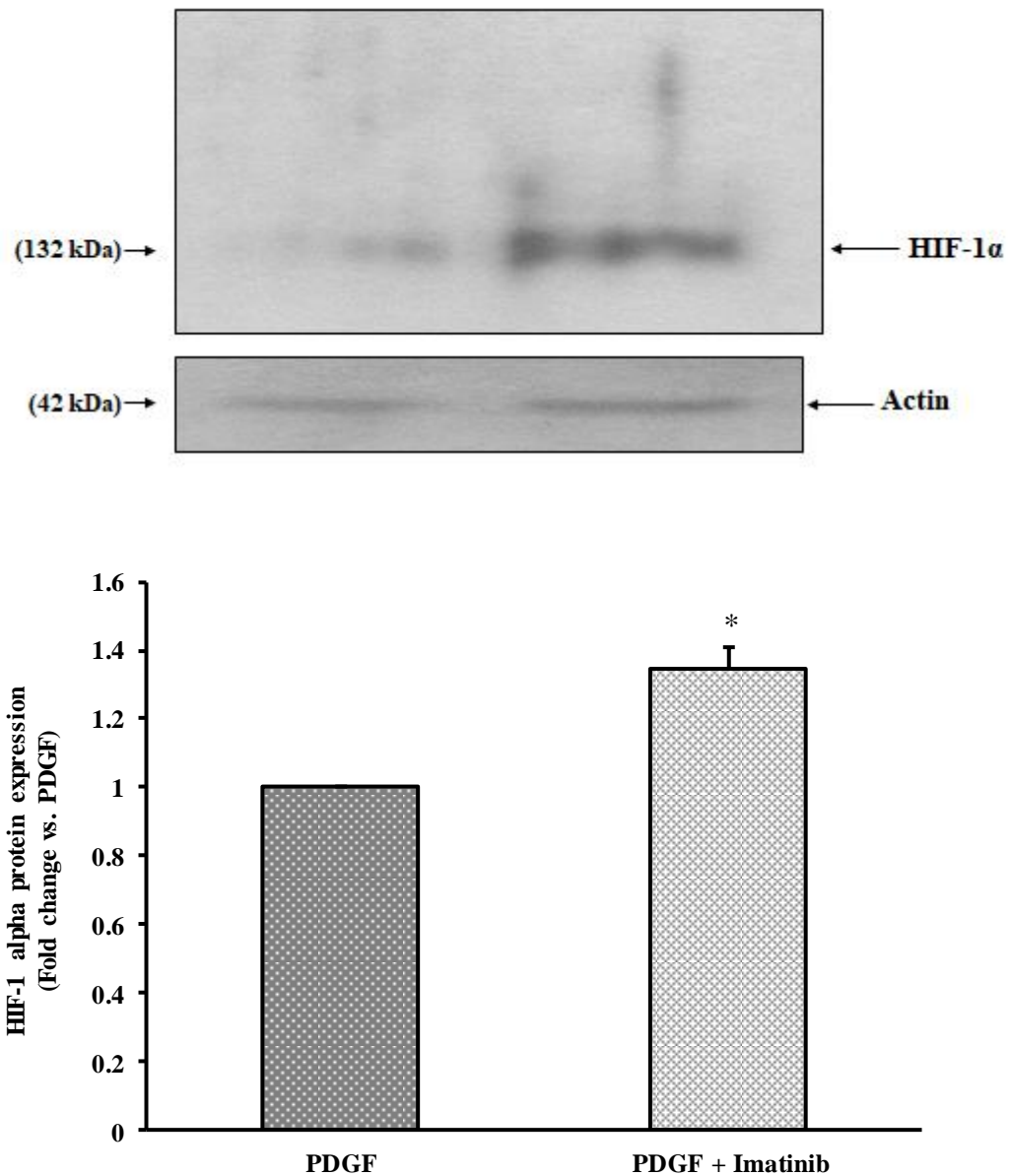


Figure 5.2 The effect of PDGF receptor antagonist on HIF-1 α protein expression in PDGF stimulated cells during hypoxia. PASMCs were stimulated with PDGF (5 ng/ml) and incubated in the hypoxic incubator for 24 h. Imatinib (10 μ M) was added 30 minutes before stimulation. Whole cell extracts were prepared and analyzed using Western blot for expression of HIF-1 α protein (132 kDa). Total actin (42 kDa) was used as a loading control. Each value represents the mean \pm SEM (n=3). *p <0.05 vs. PDGF stimulated cells without imatinib.

5.6 The effect of Mdivi-1 on HIF-1 α gene expression in PDGF stimulated cells during hypoxia

The effect of Mdivi-1 on HIF-1 α gene expression was investigated in cells stimulated with PDGF under normoxic (control) and hypoxic (test) conditions. It was also examined in hypoxic background cells (cells quiesced with 0.1% FCS and maintained in 3% O₂).

In normoxic cells stimulated with PDGF, Mdivi-1 upregulates HIF-1 α gene expression by 175 ± 46 fold (Figure 5.3, control group). In hypoxic background cells, data show Mdivi-1 causes an increase in HIF-1 α gene expression by 5.2 ± 0.5 fold (Figure 5.4 A). However, it downregulates the HIF-1 α gene by $99.3 \pm 0.19\%$ after PDGF stimulation (Figure 5.4 B, test group).

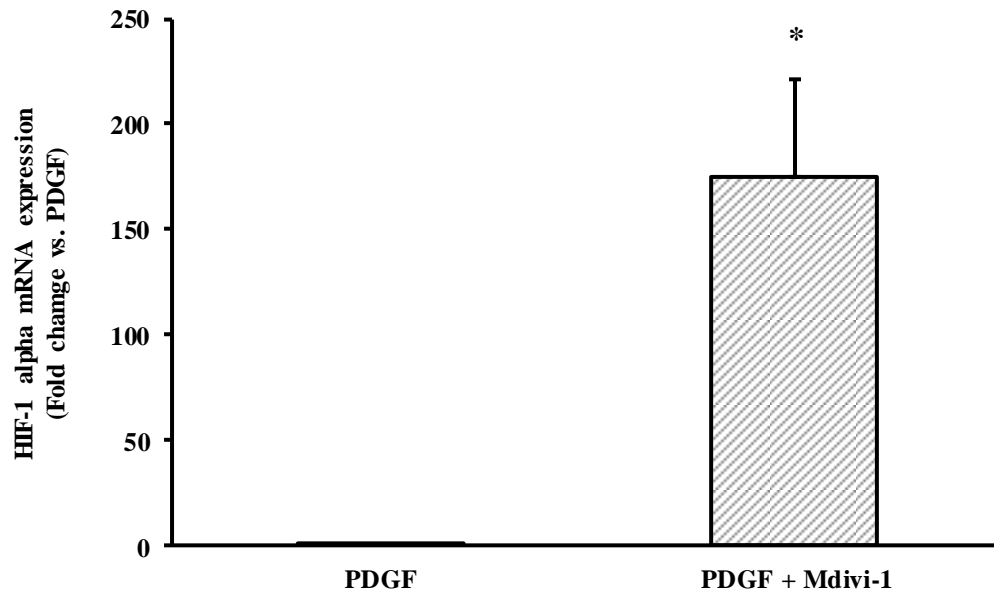
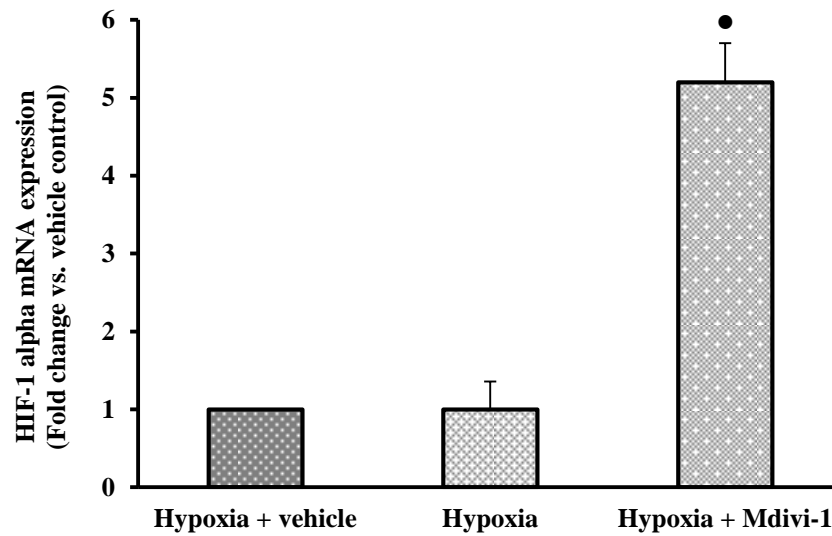


Figure 5.3 The effect of Mdivi-1 on HIF-1 α expression in cells stimulated with PDGF. Cells were stimulated with PDGF (5 ng/ml) for 24 h. Mdivi-1 (10 μ M) was added 30 minutes before stimulation. RNA was extracted from cells and equal RNA concentrations were used for cDNA sample preparation. Hypoxia-inducible factor-1 alpha (HIF-1 α) gene was measured in stimulated and treated groups using RT-qPCR. Ubiquitin C (UBC) was used as the reference gene for normalization. * $p < 0.05$ vs. stimulated cells (n=3).

A



B

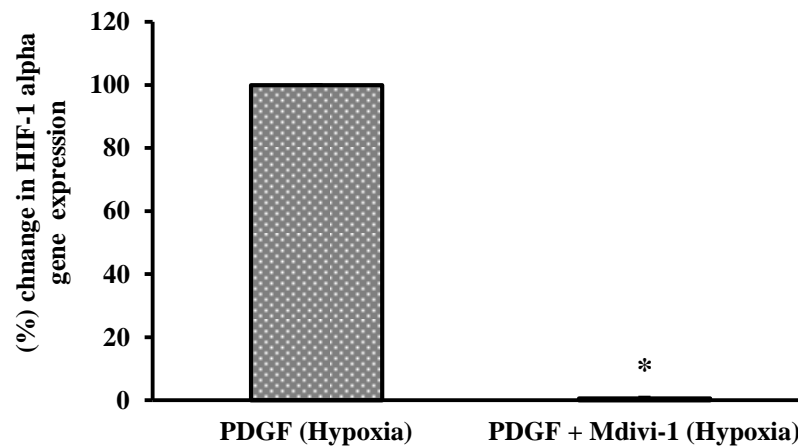


Figure 5.4 The effect of Mdivi-1 on HIF-1 α gene expression in (A) quiescent and (B) PDGF stimulated cells during hypoxia. Cells were quiesced for 24 h. For quiescent cells (A), cells were exposed to hypoxia (3% oxygen) for 24 h. For stimulated cells (B), cells were stimulated with PDGF (5 ng/ml) and incubated in hypoxia (3% oxygen) for 24 h. Mdivi-1 (10 μ M) was added 30 minutes before hypoxic exposure and PDGF stimulation. RNA was extracted from cells. Equal RNA concentrations were used for cDNA sample preparation. Hypoxia-inducible factor-1 alpha (HIF-1 α) gene was measured using RT-qPCR. Ubiquitin C (UBC) was used as the reference gene for normalization. ●p <0.05 vs. vehicle control cells. *p <0.05 vs. PDGF stimulated cells (n=3).

5.7 The effect of Mdivi-1 on FIH-1 gene expression in PDGF stimulated cells during hypoxia

As described in Chapter 1 (Figure 1.7), an oxygen-dependent enzyme called Factor-inhibiting HIF1- α (FIH-1) has been known to control the transcriptional activity of HIF-1 α . The influence of mitochondria on this enzyme was investigated in PSMCs using RT-qPCR technique. The effect of hypoxia (Figure 5.6) and the effect of Mdivi-1 in hypoxic cells (Figure 5.5) on FIH-1 gene expression were examined. Then, gene expression was investigated in cells stimulated with PDGF following Mdivi-1 treatment in normoxic (control) and in hypoxic (test) cells.

Data show the expression of FIH-1 gene was increased by the effect of hypoxia to 2.1 ± 0.3 fold (Figure 5.6) and was upregulated by 216.7 ± 27.2 fold after Mdivi-1 treatment (Figure 5.5). In normoxia, the expression of FIH-1 gene was increased by PDGF to 8.7 ± 1.3 fold and it was reduced by $93.2 \pm 0.1\%$ after Mdivi-1 treatment (Figure 5.6). However, during hypoxia, the FIH-1 gene expression level was decreased by $64.17 \pm 2.4\%$ following PDGF stimulation. It was increased by 3.4 ± 0.5 fold when the stimulated cells were treated with Mdivi-1 (Figure 5.6).

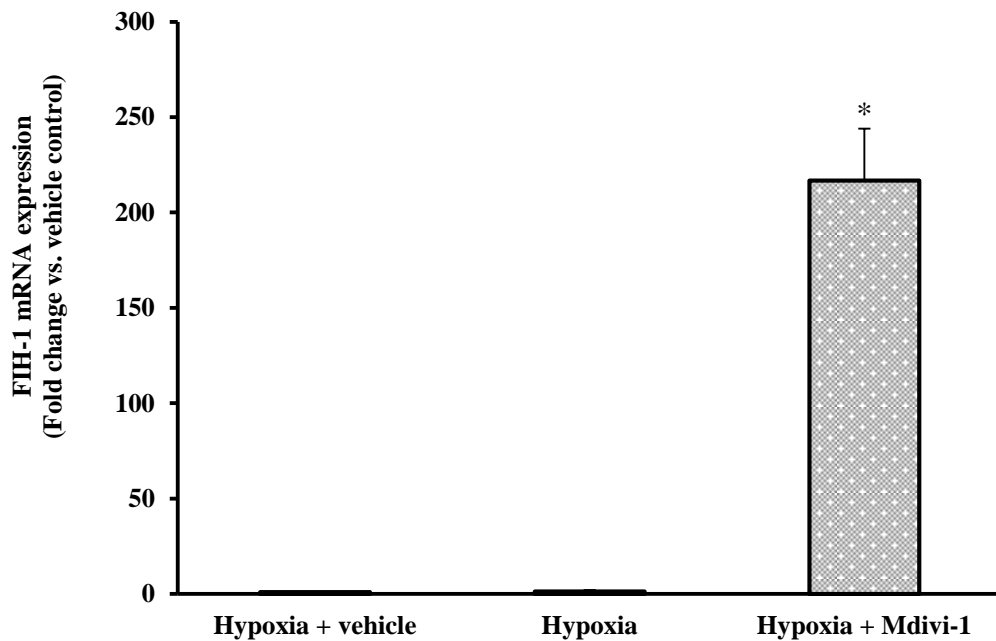


Figure 5.5 The effect of Mdivi-1 on FIH-1 gene expression in hypoxic cells. Cells were quiesced for 24 h and were then exposed to hypoxia (3% oxygen) for 24 h. Mdivi-1 (10 μ M) was added 30 minutes before hypoxic exposure. RNA was extracted from cells. Equal RNA concentrations were used for cDNA sample preparation. Factor inhibiting HIF-1 α (FIH-1) gene was measured using RT-qPCR. Ubiquitin C (UBC) was used as the reference gene for normalization. * $p < 0.05$ vs. vehicle control cells (n=3).

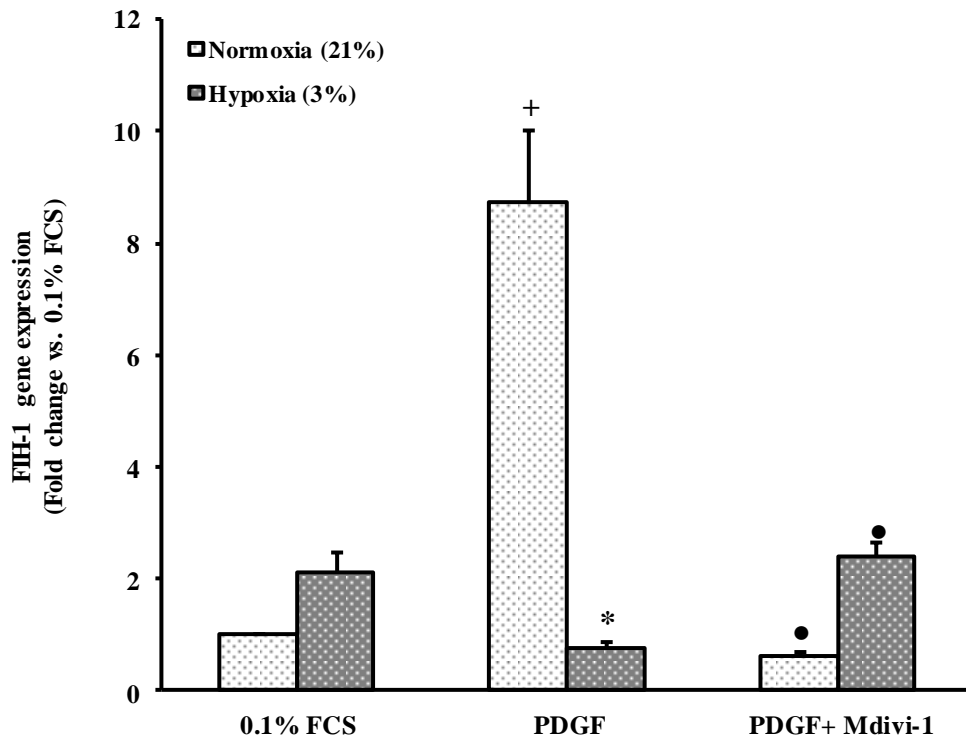


Figure 5.6 The effect of Mdivi-1 on FIH-1 gene expression in PDGF stimulated cells during hypoxia. Cells were quiesced for 24 h and were then stimulated with PDGF (5 ng/ml) and exposed to different oxygen levels: normoxia (21% oxygen) and hypoxia (3% oxygen) for 24 h. Mdivi-1 (10 μ M) was added 30 minutes before PDGF stimulation. RNA was extracted from cells. Equal RNA concentrations were used for cDNA sample preparation. Factor inhibiting HIF-1 α (FIH-1) gene was measured using RT-qPCR. Ubiquitin C (UBC) was used as the reference gene for normalization. Each value represents the mean \pm SEM (n=3). +p <0.05 vs. quiescent cells. *p <0.05 vs. cells cultured in normoxia. •p <0.05 vs. PDGF stimulated cells (n=3).

5.8 Effect of Mdivi-1 on MAPK pathways in PDGF stimulated cells during hypoxia

To study the effect of inhibiting mitochondrial fission by the use of Mdivi-1 on the MAPK signalling pathway, the phosphorylation of ERK1/2, p38 MAPK and JNK proteins was measured by Western blot after stimulating the cells with PDGF following Mdivi-1 treatment under normoxic (control) and hypoxic (test) conditions.

5.8.1 Effect of Mdivi-1 on ERK1/2 phosphorylation

Figure 5.7 exhibits that PDGF induced ERK1/2 phosphorylation by 9.4 ± 1.65 fold. Following Mdivi-1 treatment, this phosphorylation was increased by 1.7 ± 0.35 fold. Data also show hypoxia did not increase ERK1/2 phosphorylation compared to quiescent cells maintained under normoxic conditions. PDGF in hypoxia showed higher ERK1/2 phosphorylation (3.7 ± 0.9 fold) than the PDGF effect in normoxia. Treatment with Mdivi-1 during hypoxia showed no difference in ERK1/2 phosphorylation in PDGF stimulation.

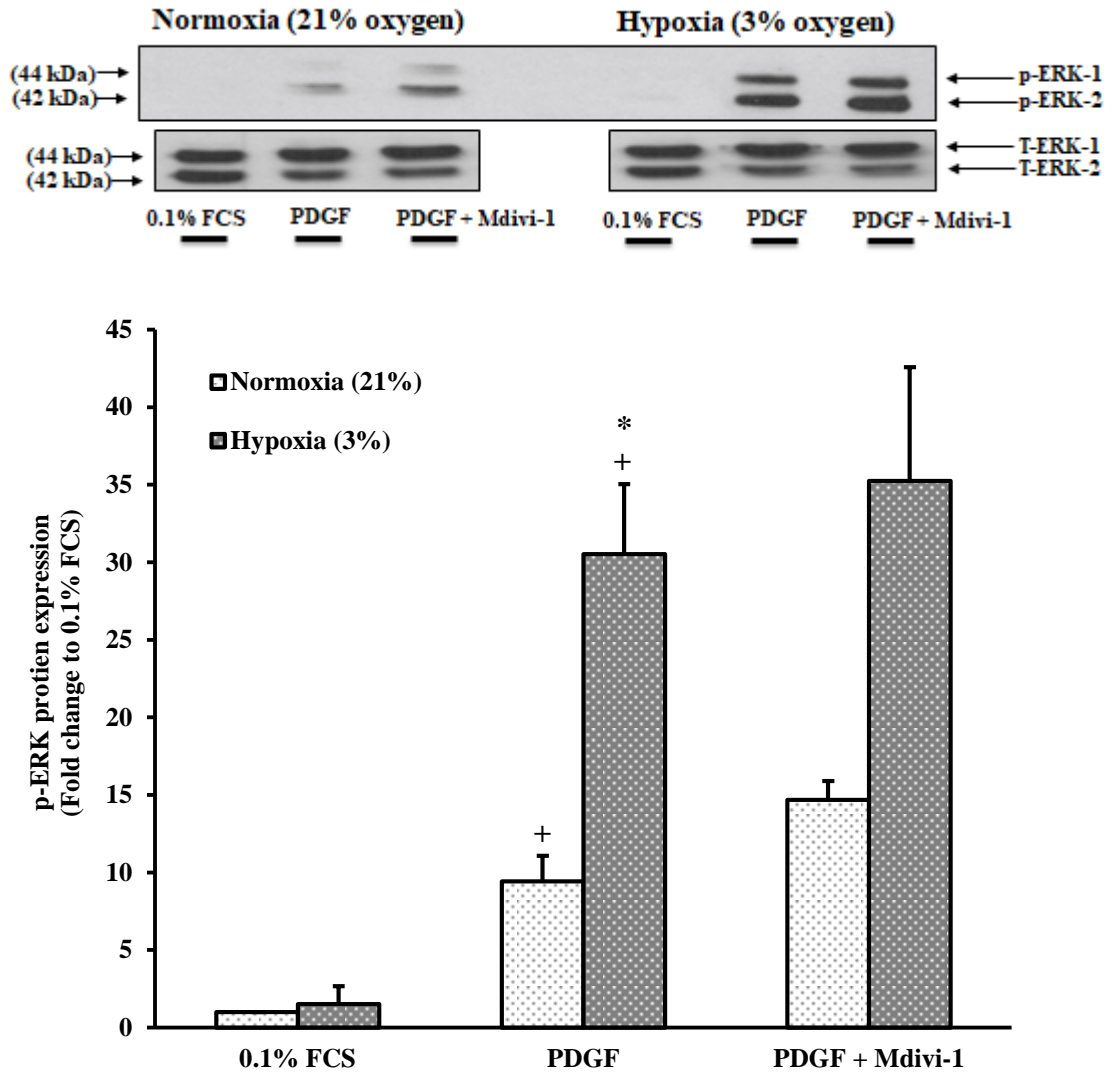


Figure 5.7 The effect of Mdivi-1 on ERK1/2 phosphorylation in PDGF stimulation during hypoxia. PASM Cs were seeded in pairs of 6 well plates. At 70-80% confluence, cells were quiesced for 24 h. Cells were then incubated at different oxygen levels; 21% oxygen (normoxia) and 3% oxygen (hypoxia) for 24 h and were stimulated with PDGF (5 ng/ml) for 15 minutes. The mitochondrial inhibitor (Mdivi-1, 10 μ M) was added 30 minutes before PDGF stimulation. Whole cell extract were prepared and analyzed using Western blot for p-ERK1 (42-44 kDa) expression and its total (42-44 kDa), which was used as a loading control. Each value represents the mean \pm SEM (n=3). *p <0.05 vs. cells cultured in normoxia. +p <0.05 vs. quiescent cells in each oxygen condition.

5.8.2 Effect of Mdivi-1 on p38 MAPK phosphorylation

Western blot data show PDGF stimulates p38 MAPK phosphorylation by 2.6 ± 0.7 fold. Following mitochondrial treatment (Mdivi-1), p38 MAPK phosphorylation was increased by 5.1 ± 1.7 fold in comparison to quiescent cells (Figure 5.8).

Results also show hypoxia in cells with 0.1% FCS failed to increase p38 MAPK phosphorylation compared to normoxia. PDGF during hypoxia significantly enhanced p38 phosphorylation above the normal PDGF effect by 1.3 ± 0.3 fold and caused further increase in p-p38 MAPK protein level by 1.4 ± 0.3 fold in Mdivi-1 treated cells.

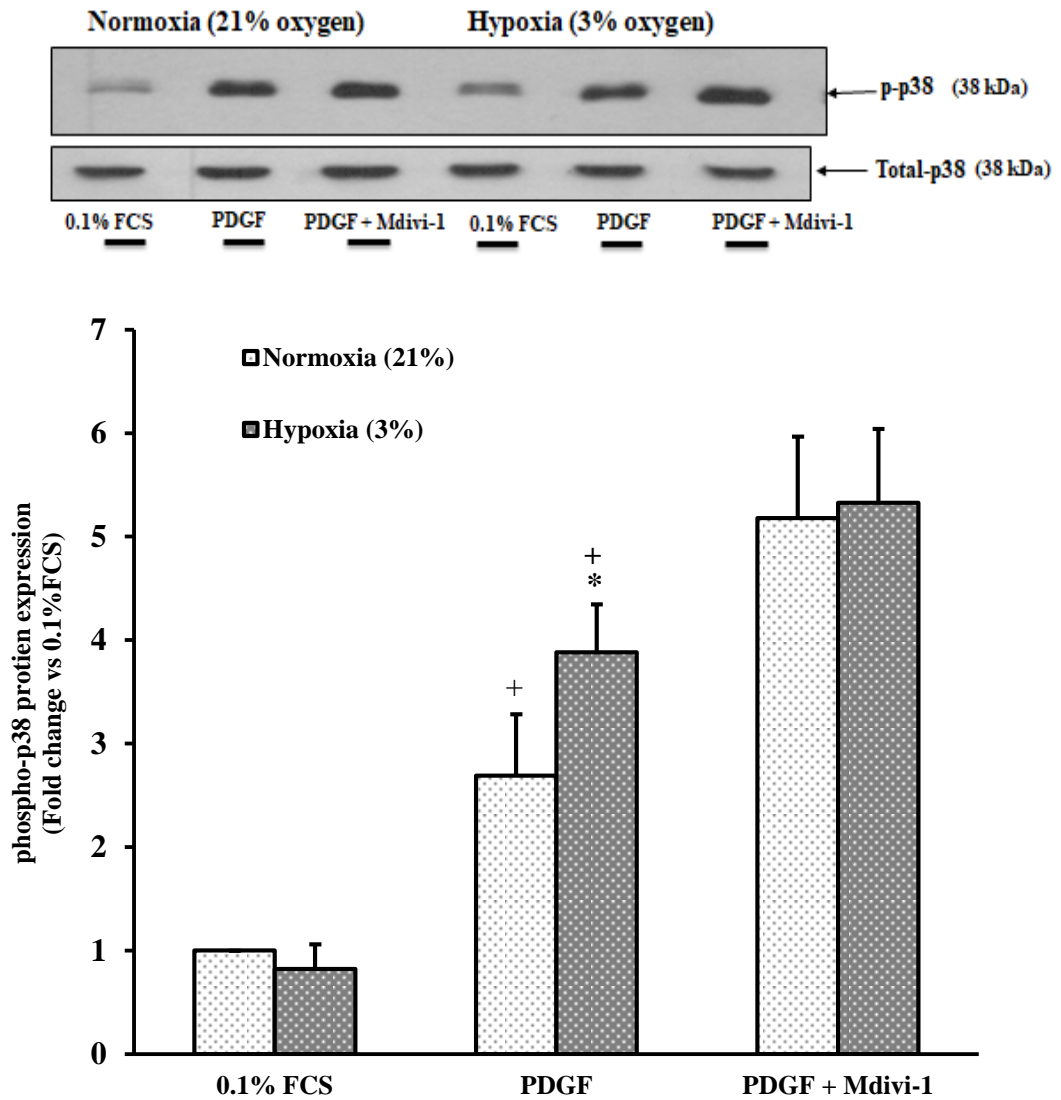


Figure 5.8 The effect of Mdivi-1 on p38 MAPK phosphorylation in PDGF stimulation during hypoxia. PASMCs were seeded in pairs of 6 well plates. At 70-80% confluence, cells were quiesced for 24 h. Cells were then incubated at different oxygen levels; 21% oxygen (normoxia) and 3% oxygen (hypoxia) for 24 h and were stimulated with PDGF (5 ng/ml) for 15 minutes. Mdivi-1 (10 μ M) was added 30 minutes before PDGF stimulation. Whole cell extracts were prepared and analyzed using Western blot for p-p38 (38 kDa) and its total (38 kDa), which was used as a loading control. Each value represents the mean \pm SEM (n=3). *p <0.05 vs. cells cultured in normoxia. +p <0.05 vs. quiescent cells in each oxygen condition.

5.8.3 Effect of Mdivi-1 on JNK phosphorylation

Figure 5.9 showed PDGF increased p-JNK protein level by 1.3 ± 0.1 fold while Mdivi-1 showed no effect. In cells with 0.1% FCS, hypoxia significantly increased JNK phosphorylation by 1.7 ± 0.2 fold.

Under hypoxic conditions, PDGF had the opposite effect from its effect under normoxic conditions as the protein level of p-JNK was decreased by $14.9 \pm 4.7\%$ after PDGF stimulation (Figure 5.9). However, hypoxia did not show any significant difference in JNK phosphorylation in the PDGF stimulated cells compared to normoxia. Treating the hypoxic stimulated cells with Mdivi-1 increased the protein level of p-JNK by 1.3 ± 0.2 fold but there was no statistical difference detected (Figure 5.9).

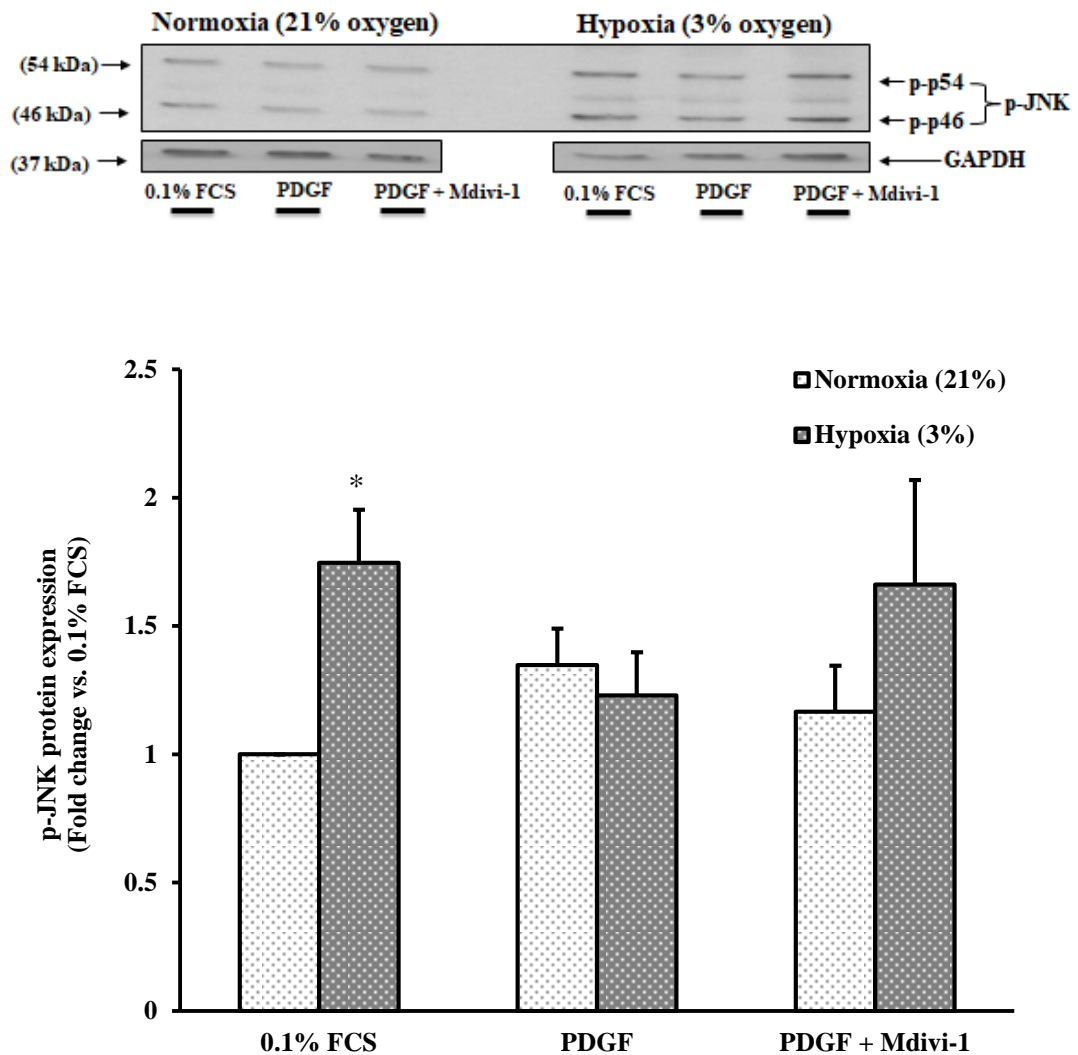


Figure 5.9 The effect Mdivi-1 on JNK phosphorylation in PDGF stimulation during hypoxia. PSMCs were seeded in pairs of 6 well plates. At 70-80% confluence, cells were quiesced for 24 h. Cells were then incubated at different oxygen levels; 21% oxygen (normoxia) and 3% oxygen (hypoxia) for 24 h and were stimulated with PDGF (5 ng/ml) for 15 minutes. Mdivi-1 (10 μ M) was added 30 minutes before PDGF stimulation. Whole cell extracts were prepared and analyzed using Western blot for p-JNK (54/46 kDa) and GAPDH (37 kDa), which was used as a loading control. Each value represents the mean \pm SEM (n=3). *p < 0.05 vs. cells cultured in normoxia.

5.9 Effect of Mdivi-1 on PI3K/mTOR signalling pathway in PDGF stimulated cells during hypoxia

The effect of hypoxia alone, PDGF stimulation and the effect of mitochondrial inhibition on the PI3K/mTOR signalling pathway under both normoxic (control) and hypoxic (test) conditions was assessed by evaluating genes and proteins of this pathway.

5.9.1 The effect of Mdivi-1 on PI3K gene expression

Figure 5.10 shows that Mdivi-1 upregulated PI3K gene expression by 34.6 ± 3.8 fold in cells with 0.1% FCS maintained in 3% O₂ for 24 h. Figure 5.11 shows hypoxia stimulated PI3K gene expression by 17.6 ± 4.9 fold after 24 h incubation. In addition, Figure 5.11 shows that PI3K gene expression was increased following stimulation with both PDGF in normoxia (130.9 ± 21.5 fold) and PDGF in hypoxia (84.9 ± 10.48 fold) in comparison to PI3K gene expression in quiescent cells. PDGF in hypoxia reduced the expression of this gene by $32.9 \pm 4.9\%$ compared to its normal effect. Moreover, Mdivi-1 significantly repressed PI3K gene expression by $70.8 \pm 8.11\%$ in normoxia and showed no change in the gene expression during hypoxia in the PDGF stimulated cells (Figure 5.11).

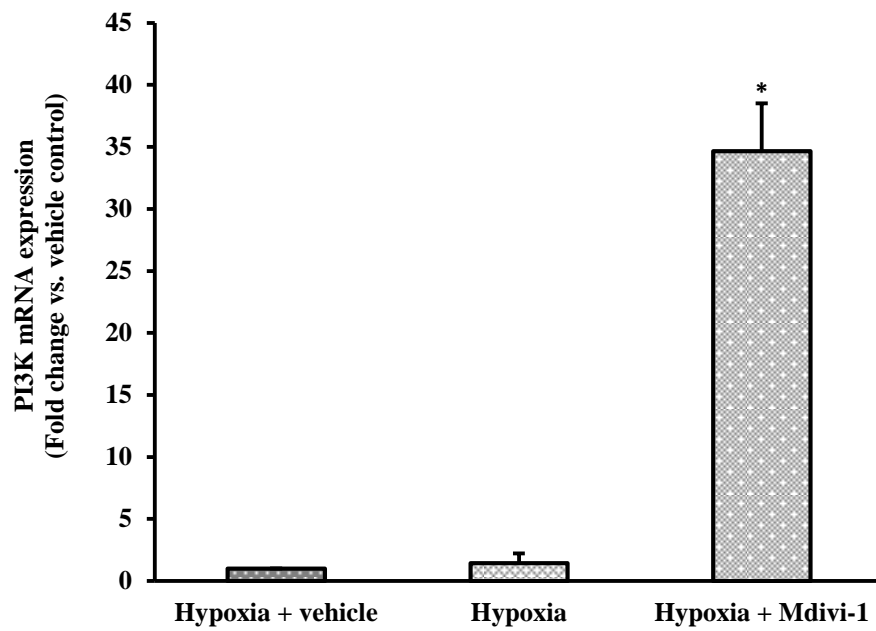


Figure 5.10 The effect of Mdivi-1 on PI3K gene expression in quiescent hypoxic cells. Cells were quiesced for 24 h and were then exposed to hypoxia (3% oxygen) for 24 h. Mdivi-1 (10 μ M) was added 30 minutes before hypoxic exposure. RNA was extracted from cells. Equal RNA concentrations were used for cDNA sample preparation. PI3K gene was measured using RT-qPCR. Ubiquitin C (UBC) was used as the reference gene for normalization. Each value represents the mean \pm SEM (n=3). *p <0.05 vs. vehicle control cells.

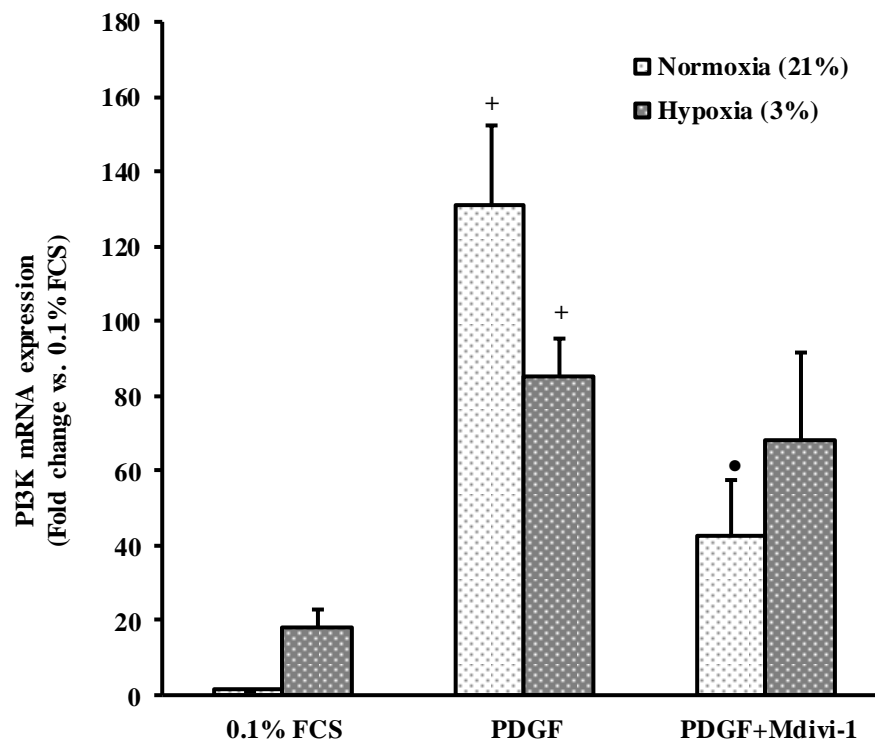


Figure 5.11 The effect of Mdivi-1 on PI3K gene expression in PDGF stimulated cells during hypoxia. Cells were quiesced for 24 h and were then stimulated with PDGF (5 ng/ml) and exposed to different oxygen levels: normoxia (21% oxygen) and hypoxia (3% oxygen) for 24 h. Mdivi-1 (10 μ M) was added 30 minutes before PDGF stimulation. RNA was extracted from cells. Equal RNA concentrations were used for cDNA sample preparation. PI3K gene was measured using RT-qPCR. Ubiquitin C (UBC) was used as the reference gene for normalization. Each value represents the mean \pm SEM (n=3). + p <0.05 vs. quiescent cells. • p <0.05 vs. PDGF stimulated cells.

5.9.2 The effect of Mdivi-1 on PTEN gene expression

A negative regulator of the intracellular PI3K level, the PTEN gene was assessed in response to PDGF stimulation and mitochondrial inhibition under normoxic and hypoxic conditions using the RT-PCR technique (Figure 5.12).

In normoxia, PDGF caused a slight increase in the PTEN gene expression level by 1.75 ± 0.47 fold whereas mitochondrial treatment with Mdivi-1 significantly downregulated this gene by $80.2 \pm 1\%$ (Figure 5.12). The result shows 24 h hypoxia exposure reduced PTEN gene expression in PSMCs as PTEN gene expression was decreased by $80.2 \pm 3.8\%$ in 0.1% FCS quiescent cells and by $82.1 \pm 3.7\%$ in PDGF stimulated cells compared to the corresponding cells in normoxia (Figure 5.12).

In hypoxia, an increase in PTEN gene expression was not significant following PDGF stimulation. It was increased by 1.5 ± 0.3 fold in comparison to hypoxic background cells (cells quiesced with 0.1% FCS and maintained in 3% O₂). However, following Mdivi-1 treatment, PTEN gene expression in the PDGF stimulated cells was decreased by $42.9 \pm 5.3\%$ (Figure 5.12).

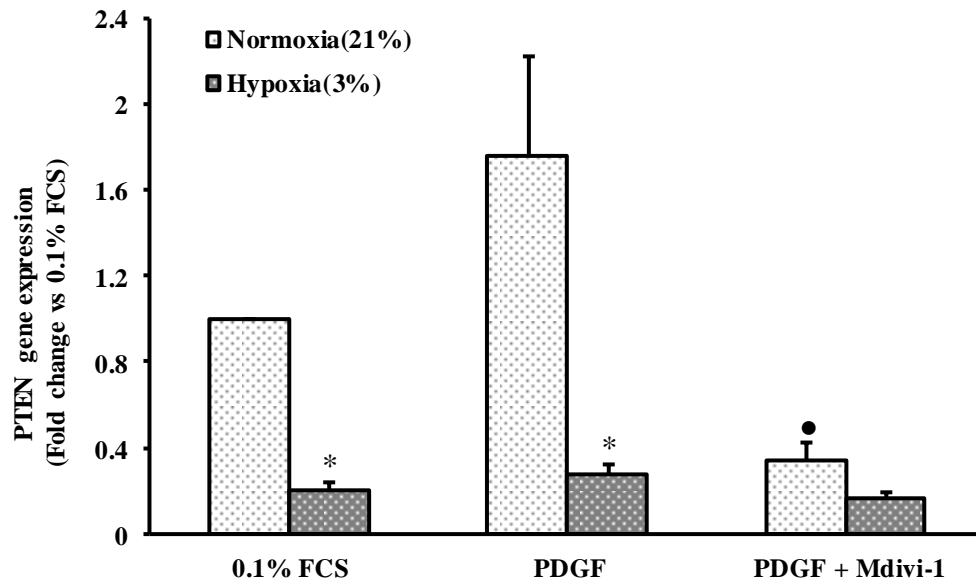


Figure 5.12 The effect of Mdivi-1 on PTEN gene expression in PDGF stimulated cells during hypoxia. Cells were quiesced for 24 h and were then stimulated with PDGF (5 ng/ml) and exposed to different oxygen levels: normoxia (21% oxygen) and hypoxia (3% oxygen) for 24 h. Mdivi-1 (10 μ M) was added 30 minutes before PDGF stimulation. RNA was extracted from cells. Equal RNA concentrations were used for cDNA sample preparation. PTEN gene was measured using RT-qPCR. Ubiquitin C (UBC) was used as the reference gene for normalization. Each value represents the mean \pm SEM (n=3). *p < 0.05 vs. cultured cells in normoxia. ●p < 0.05 vs. PDGF stimulated cells.

5.9.3 The effect of Mdivi-1 on PDK-1 phosphorylation

The effect of hypoxia, PDGF stimulation and mitochondrial inhibition on PDK-1 phosphorylation was assessed using Western blot (Figure 5.13). In normoxia, an increase in PDK-1 phosphorylation was not significant following PDGF stimulation (1.2 ± 0.1 fold). Mitochondrial fission treatment (Mdivi-1) showed an inhibition of PDK-1 phosphorylation by $33 \pm 6.3\%$.

In hypoxia, phosphorylation of PDK-1 was increased by 1.6 ± 0.1 fold versus quiescent cells that were kept under normoxic conditions. PDGF stimulation shows no effect in comparison to quiescent cells under hypoxic conditions. Mdivi-1 inhibited PDK-1 phosphorylation by $39.4 \pm 3.5\%$ in the PDGF stimulated cells (Figure 5.13).

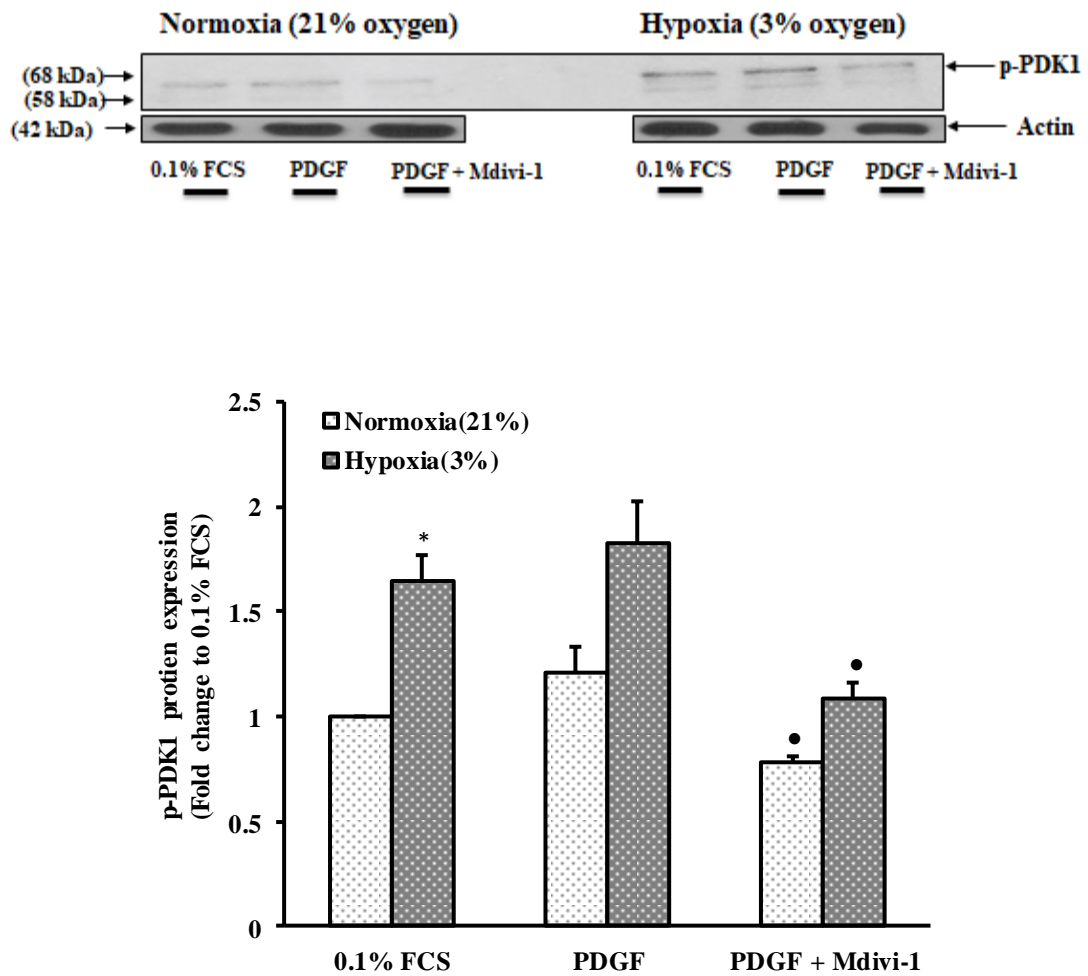


Figure 5.13 The effect of Mdivi-1 on PDK1 phosphorylation in PDGF stimulation during hypoxia. PASMCs were seeded in pairs of 6 well plates. At 70-80% confluence, cells were quiesced for 24 h. Cells were stimulated with PDGF (5 ng/ml) and incubated at different oxygen levels; 21% oxygen (normoxia) and 3% oxygen (hypoxia) for 24 hours. Mdivi-1 (10 μ M) was added 30 minutes before PDGF stimulation. Whole cell extracts were prepared and analyzed using Western blot for p-PDK1 (68-58 kDa) and actin (42 kDa), which was used as a loading control. Each value represents the mean \pm SEM (n=3). *p < 0.05 vs. cultured cells in normoxia. •p < 0.05 vs. PDGF stimulated cells.

5.9.4 The effect of Mdivi-1 on AKT gene expression

In order to investigate the role of mitochondrial fission using the mitochondrial DRP1 inhibitor (Mdivi-1) after 24 h hypoxia exposure and after 24 h PDGF stimulation of PSMCs under normoxic (control) and hypoxic (test) conditions on AKT gene expression, RNA was extracted from PSMCs and RT-qPCR was performed to measure the gene expression.

Figure 5.14 shows 10 μ M Mdivi-1 caused upregulation of AKT gene expression by 4 ± 0.7 fold in hypoxic cells. In normoxia, the expression of AKT was increased by 13.2 ± 2.1 fold in the PDGF stimulated cells compared to the quiescent cells and increased by 2.3 ± 0.45 in the Mdivi-1 treated cells compared to the PDGF stimulated cells (Figure 5.15). In hypoxia, the expression of AKT in PSMCs was greater by 2.8 ± 0.8 fold than normoxia. Moreover, PDGF in hypoxia increased AKT expression by 4.3 ± 1.2 fold compared to its expression in the hypoxic cells. However, PDGF activation of this gene in hypoxia was reduced by $23.3 \pm 3.9\%$ in comparison to PDGF activation in normoxia. Similarly, upregulation of AKT gene caused by Mdivi-1 treatment was also observed in hypoxia (2.4 ± 0.1 fold) when the cells were stimulated with PDGF (Figure 5.15).

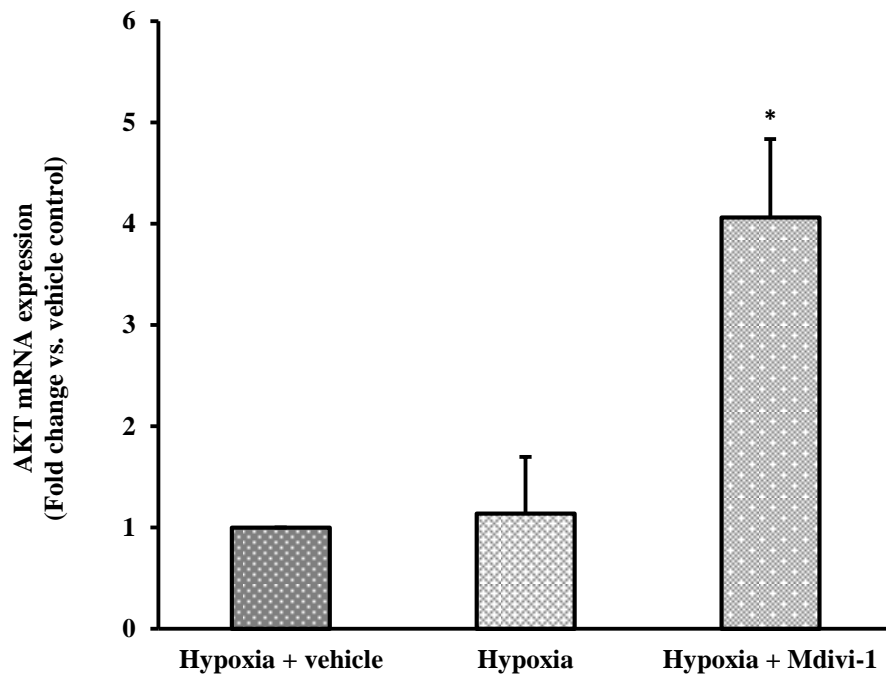


Figure 5.14 The effect of Mdivi-1 on AKT gene expression in quiescent hypoxic cells. Cells were quiesced for 24 h and were then exposed to hypoxia (3% oxygen) for 24 h. Mdivi-1 (10 μ M) was added 30 minutes before hypoxic exposure. RNA was extracted from cells. Equal RNA concentrations were used for cDNA sample preparation. AKT gene was measured using RT-qPCR. Ubiquitin C (UBC) was used as the reference gene for normalization. Each value represents the mean \pm SEM (n=3). *p <0.05 vs. vehicle control cells.

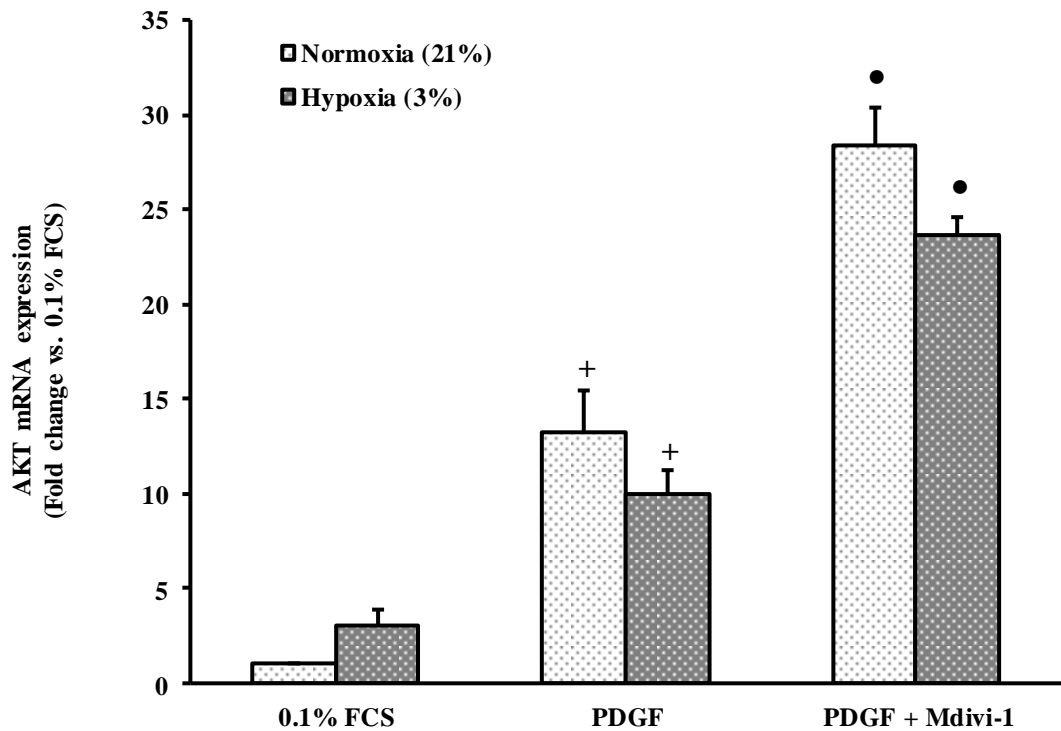


Figure 5.15 The effect of Mdivi-1 on AKT gene expression in PDGF stimulated cells during hypoxia. Cells were quiesced for 24 h and were then stimulated with PDGF (5 ng/ml) and exposed to different oxygen levels: normoxia (21% oxygen) and hypoxia (3% oxygen) for 24 h. Mdivi-1 (10 μ M) was added 30 minutes before PDGF stimulation. RNA was extracted from cells. Equal RNA concentrations were used for cDNA sample preparation. AKT gene was measured using RT-qPCR. Ubiquitin C (UBC) was used as the reference gene for normalization. Each value represents the mean \pm SEM (n=3). +p < 0.05 vs. quiescent cells. •p < 0.05 vs. PDGF stimulated cells.

5.9.5 The effect of Mdivi-1 on mTORC1 gene expression

The role of mTORC1 in hypoxia was examined by RT-qPCR to measure its expression in quiescent cells, cells stimulated with PDGF under normoxic (control) and hypoxic (test) conditions. In addition, the effect of Mdivi-1 on mTORC1 gene expression was also investigated in hypoxic cells (Figure 5.16) and in PDGF stimulated cells in both normoxia and hypoxia (Figure 5.17).

In normoxia, the expression of the mTORC1 gene was reduced by $89.8 \pm 3\%$ in the presence of PDGF and upregulated by 6.9 ± 2.7 fold in response to Mdivi-1 treatment. Furthermore, result shows there was no difference in the gene expression under hypoxia. However, a significant increase in mTORC1 gene was detected following the combined effects of PDGF and hypoxia as the gene expression was increased by 3.1 ± 0.7 fold compared to quiescent hypoxic cells and by 25 ± 4.4 fold compared to cells stimulated with PDGF in normoxia (Figure 5.17). Mdivi-1 caused a significant reduction in the gene expression by $97.9 \pm 0.7\%$ and by $99.9 \pm 0.003\%$ in the hypoxic cells with/without PDGF (Figure 5.17 and, Figure 5.16, respectively).

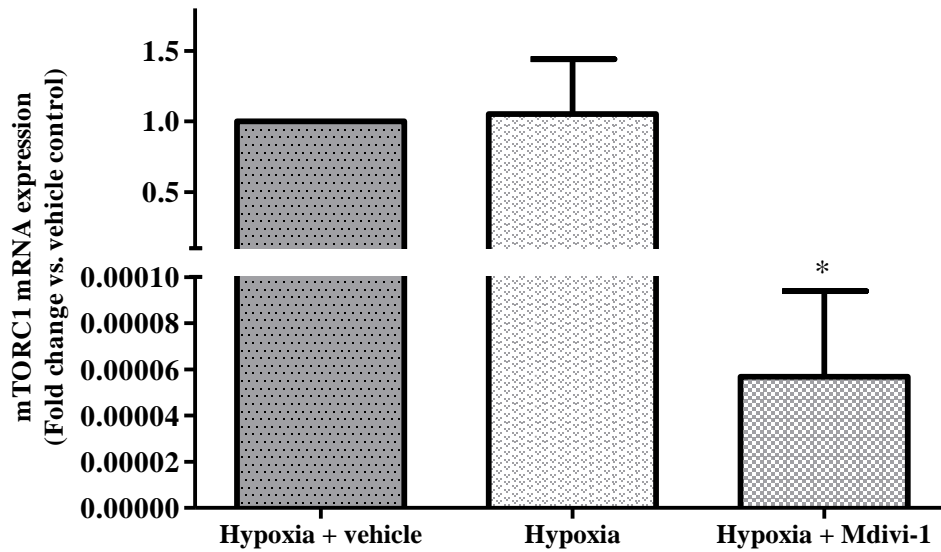


Figure 5.16 The effect of Mdivi-1 on mTORC1 gene expression in quiescent hypoxic cells. Cells were quiesced for 24 h and were then exposed to hypoxia (3% oxygen) for 24 h. Mdivi-1 (10 μ M) was added 30 minutes before hypoxic exposure. RNA was extracted from cells. Equal RNA concentrations were used for cDNA sample preparation. mTORC1 gene was measured using RT-qPCR. Ubiquitin C (UBC) was used as the reference gene for normalization. Each value represents the mean \pm SEM (n=3). *p <0.05 vs. vehicle control cells.

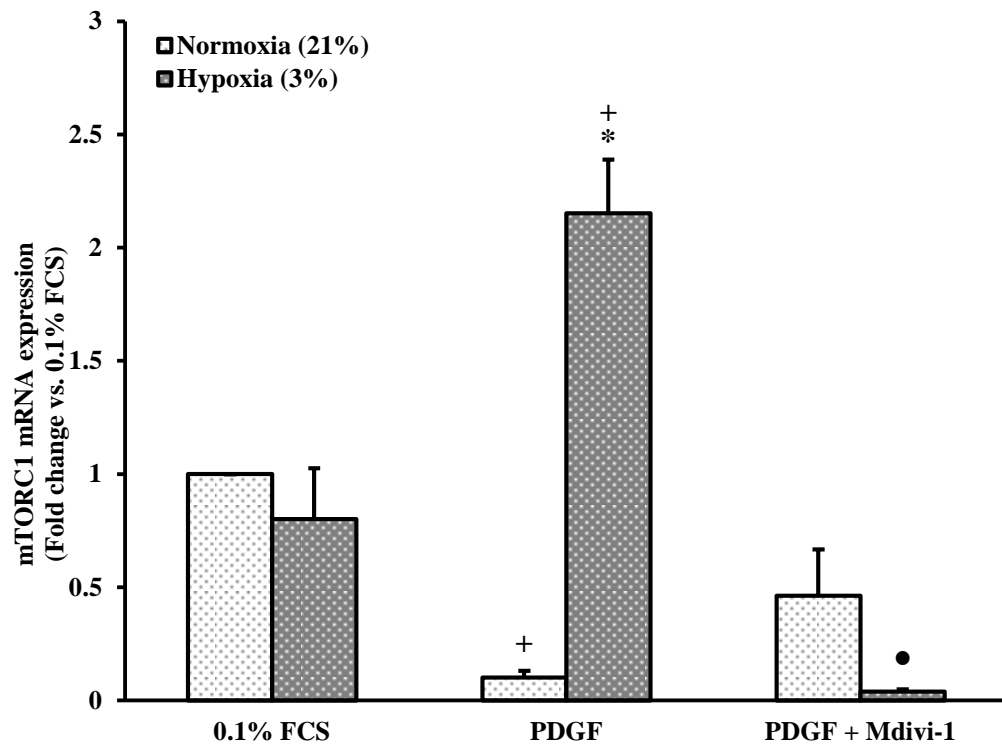


Figure 5.17 The effect of Mdivi-1 on mTORC1 gene expression in PDGF stimulated cells during hypoxia. Cells were quiesced for 24 h and were then stimulated with PDGF (5 ng/ml) and exposed to different oxygen levels: normoxia (21% oxygen) and hypoxia (3% oxygen) for 24 h. Mdivi-1 (10 μ M) was added 30 minutes before PDGF stimulation. RNA was extracted from cells. Equal RNA concentrations were used for cDNA sample preparation. The expression of mTORC1 gene was measured using RT-qPCR. Ubiquitin C (UBC) was used as the reference gene for normalization. Each value represents the mean \pm SEM (n=3). +p < 0.05 vs. quiescent cells. *p < 0.05 vs. cultured cells in normoxia. •p < 0.05 vs. PDGF stimulated cells.

5.9.6 The effect of Mdivi-1 on 4EBP1 gene expression

The downstream mTORC1 gene (4EBP1) was also examined. PCR data showed a significant increase in the expression of 4EBP1 gene by 87.7 ± 13.2 fold following PDGF stimulation and a significant reduction by $98.7 \pm 0.4\%$ in response to Mdivi-1 (Figure 5.18). In cells with 0.1% FCS, hypoxia enhanced 4EBP1 gene expression by 51 ± 9.18 fold compared to the normoxic cells.

Figure 5.18 showed the expression of the gene was reduced by $96.5 \pm 0.7\%$ under the hypoxic PDGF stimulation compared to the gene expression in hypoxic background cells. As a result, a significant difference in 4EBP1 gene expression among PDGF effects between hypoxia versus normoxia was detected as the gene expression during hypoxia was reduced by $97.5 \pm 0.8\%$. Mitochondrial inhibition by the use of Mdivi-1 showed a slight increase in 4EBP1 gene expression by 17.2 ± 4.2 fold in hypoxic PDGF stimulated cells (Figure 5.18).

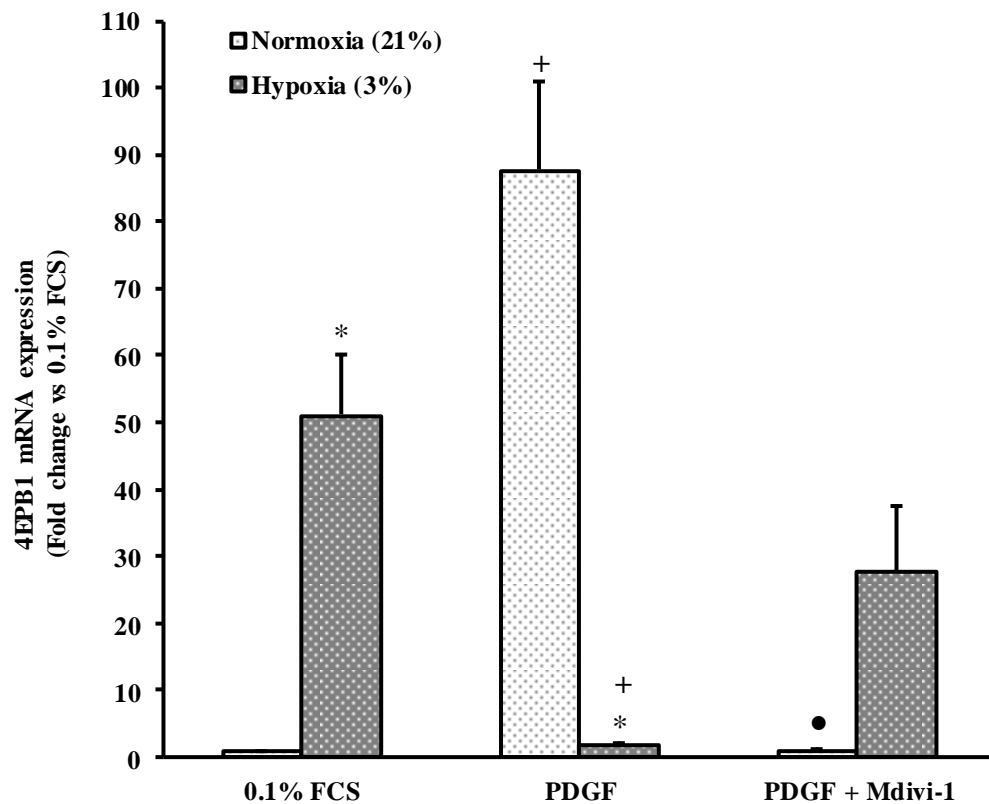


Figure 5.18 The effect of Mdivi-1 on 4EPB1 gene expression in PDGF stimulated cells during hypoxia. Cells were quiesced for 24 h and were then stimulated with PDGF (5 ng/ml) and exposed to different oxygen levels: normoxia (21% oxygen) and hypoxia (3% oxygen) for 24 h. Mdivi-1 (10 μ M) was added 30 minutes before PDGF stimulation. RNA was extracted from cells. Equal RNA concentrations were used for cDNA sample preparation. The expression of 4EPB1 gene was measured using RT-qPCR. Ubiquitin C (UBC) was used as the reference gene for normalization. Each value represents the mean \pm SEM (n=3). +p <0.05 vs. quiescent cells. *p <0.05 vs. cultured cells in normoxia. •p <0.05 vs. PDGF stimulated cells.

5.9.7 The effect of Mdivi-1 on P70s6k gene expression

Another downstream gene of the PI3K/mTORC1 signalling cascade which was also investigated is P70s6K gene (Figure 5.19). In comparison to the P70s6k gene expression level in quiescent cells, data show the expression of the gene was inhibited by $86.8 \pm 8.7\%$ in response to PDGF stimulation. Following Mdivi-1 treatment, P70s6k gene expression was upregulated by 21.3 ± 3.3 fold in the PDGF stimulated cells. Moreover, results indicate that acute hypoxia caused a significant increase in P70s6k gene expression by 64.8 ± 7.9 fold versus normoxia. PDGF caused an opposite effect during hypoxia as it caused a further increase in P70s6k gene beyond its expression in the hypoxic cells by 1.62 ± 0.09 fold. Furthermore, the DRP1 inhibitor (Mdivi-1) showed a significant inhibition of this gene expression by $42.3 \pm 2.3\%$ in cells that were stimulated with PDGF and exposed to hypoxia for 24 h (Figure 5.19).

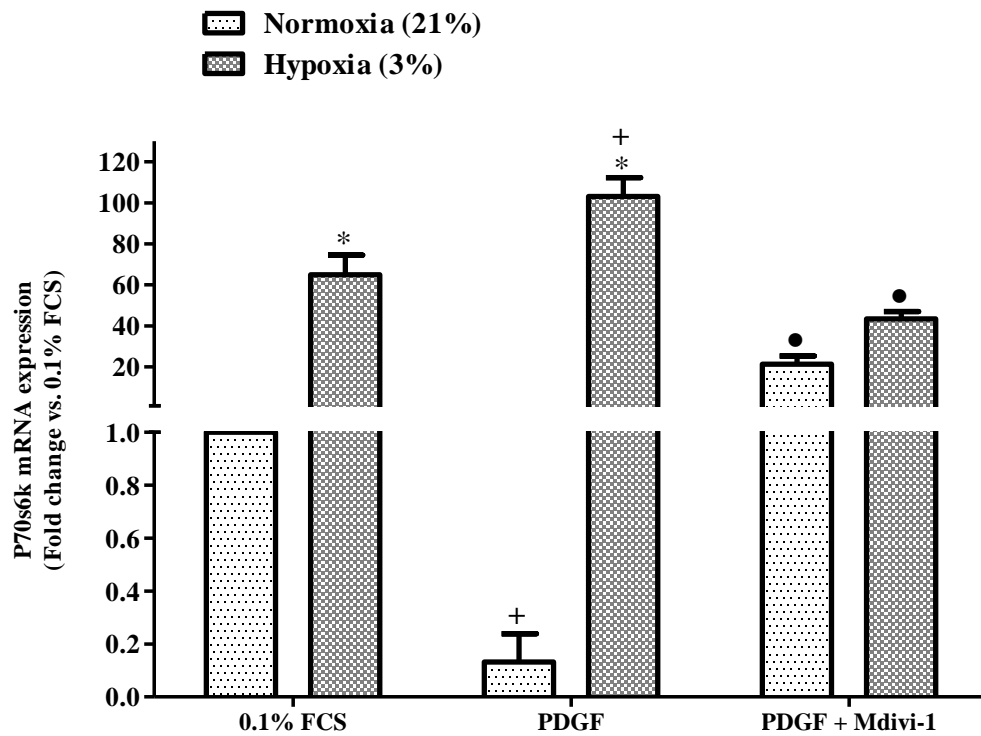


Figure 5.19 The effect of Mdivi-1 on P70s6K gene expression in PDGF stimulated cells during hypoxia. Cells were quiesced for 24 h and were then stimulated with PDGF (5 ng/ml) and exposed to different oxygen levels: normoxia (21% oxygen) and hypoxia (3% oxygen) for 24 h. Mdivi-1 (10 μ M) was added 30 minutes before PDGF stimulation. RNA was extracted from cells. Equal RNA concentrations were used for cDNA sample preparation. The expression of P70s6K gene was measured using RT-qPCR. Ubiquitin C (UBC) was used as the reference gene for normalization. Each value represents the mean \pm SEM (n=3). +p <0.05 vs. quiescent cells. *p <0.05 vs. cultured cells in normoxia. •p <0.05 vs. PDGF stimulated cells.

5.10 The effect of mTORC1 knockdown alone and with Mdivi-1 on PDGF-induced cell proliferation during hypoxia

Previous results showed that increased mTORC1 gene expression was correlated with increased cell proliferation in PSMCs following PDGF stimulation during hypoxia (3% O₂) (Figure 5.17 and Figure 4.4) and both mTORC1 expression and cell proliferation were reduced by inhibiting the mitochondria using Mdivi-1 (Figure 5.17 and Figure 4.5), suggesting that mTORC1 may play a major role in controlling the mitochondrial DRP1, cell growth and proliferation. To investigate this, cell proliferation following mTORC1 knockdown alone, and with Mdivi-1 treatment was assessed (Figure 5.21).

5.10.1 The transfection efficacy of mTORC1 siRNA

The transfection was performed using different concentrations of mTORC1 siRNA as follows; 25 nM, 50 nM and 75 nM. Figure 5.20 shows all mTORC1 siRNA concentrations significantly decreased the level of mTORC1 gene expression. The inhibition of the mTORC1 gene expression was increased to more than 99% at the maximum mTORC1 siRNA concentration (75 nM) without compromising cellular integrity (this was checked by examining the morphology and appearance of the cell using the microscope). Thus, this concentration was chosen for assessing cell proliferation, DRP1 expression and hypoxic genes levels (HIF-1 α and FIH-1), which all may contribute to mediating cell proliferation.

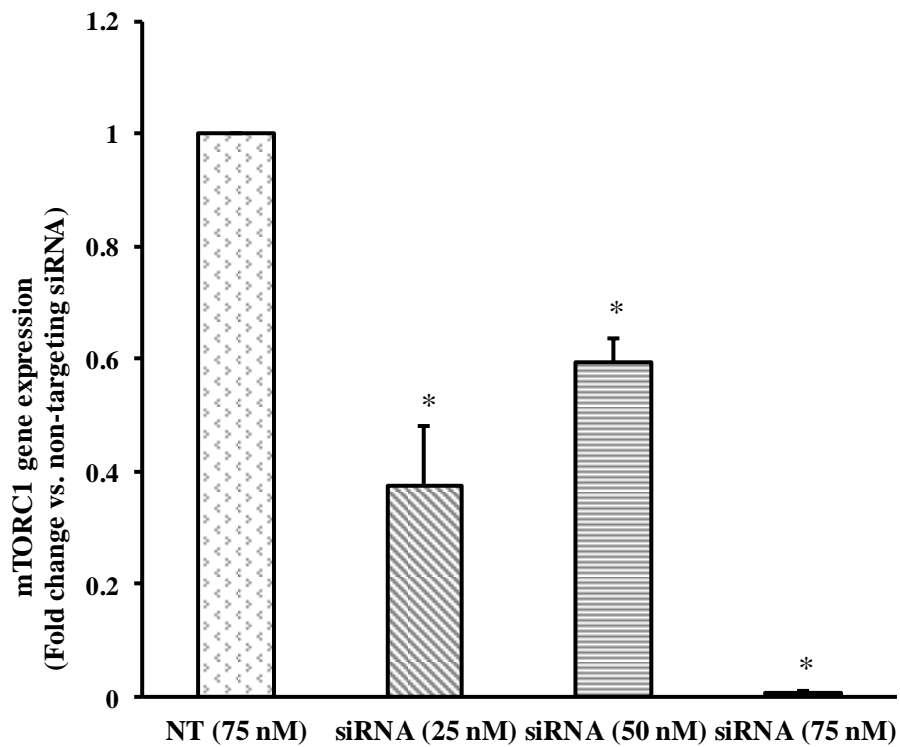
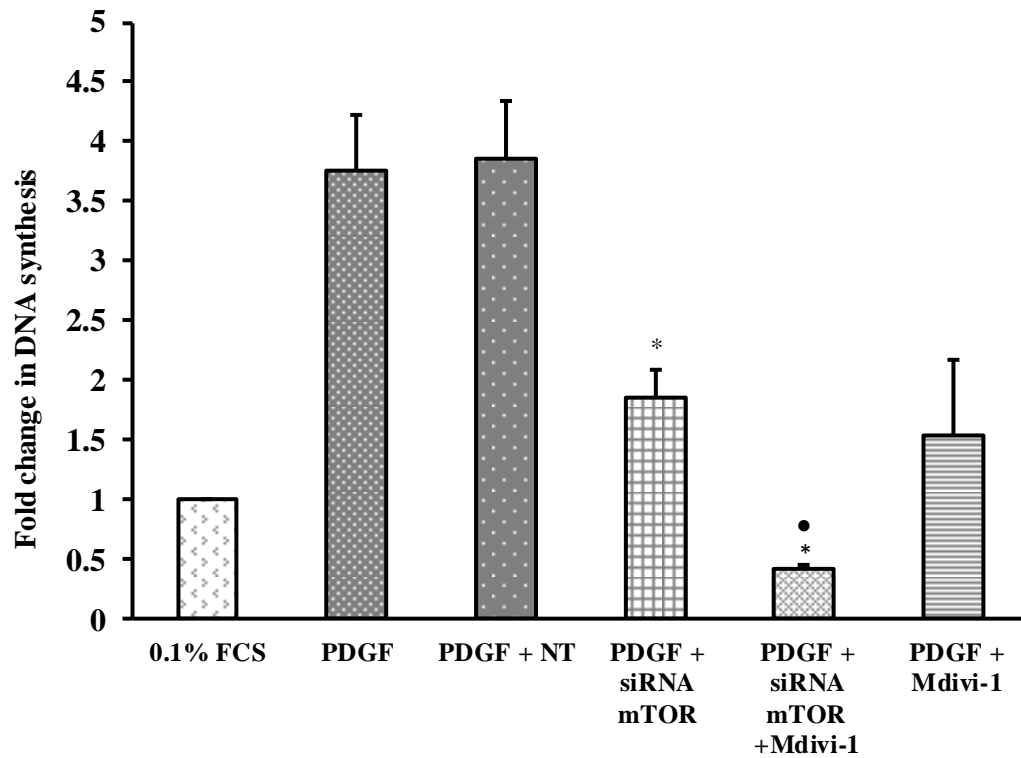


Figure 5.20 The transfection efficacy of siRNA for mTORC1 in PASMCs. Cells were transfected with a scrambled or non-targeting siRNA 75 nM (NT), different concentrations of siRNA for mTORC1; 25 nM, 50 nM and 75 nM for 72 h prior to stimulation with PDGF (5 ng/ml) under hypoxia for 24 h. RNA was extracted from the cells. Equal RNA concentrations were used for cDNA sample preparation. The expression of mTORC1 gene was measured using RT-qPCR. Ubiquitin C (UBC) was used as the reference gene for normalization. Each value represents the mean \pm SEM. * $p < 0.05$ vs. cells transfected with non-targeting siRNA (n=3).

5.10.2 The effect of mTORC1 knockdown alone and with Mdivi-1 on Cell Proliferation

Chapter 3 demonstrated a significant increase in mTORC1 expression and in cell proliferation in response to 10% FCS during hypoxia (Figure 3.19C and Figure 3.10, respectively). In this chapter, using a specific growth factor (PDGF), a significant increase in cell proliferation and mTORC1 was also seen during hypoxia (Figure 4.4 and Figure 5.17, respectively). This suggests mTORC1 could be essential during hypoxia to increase cell proliferation.

To confirm these results, cell proliferation in PSMCs was assessed following mTORC1 knockdown using the [³H]-thymidine incorporation assay. Data show cell proliferation in cells treated with siRNA against mTORC1 was significantly reduced by $51.9 \pm 0.26\%$ in comparison to the agonist control. Interestingly, the combined effect of mTORC1 knockdown and DRP1 inhibition by Mdivi-1 caused a further reduction in DNA synthesis level by $88.4 \pm 2.4\%$ in comparison to the agonist control, and by $75.9 \pm 5.1\%$ in comparison to the cells treated with siRNA against mTORC1 (Figure 5.21).



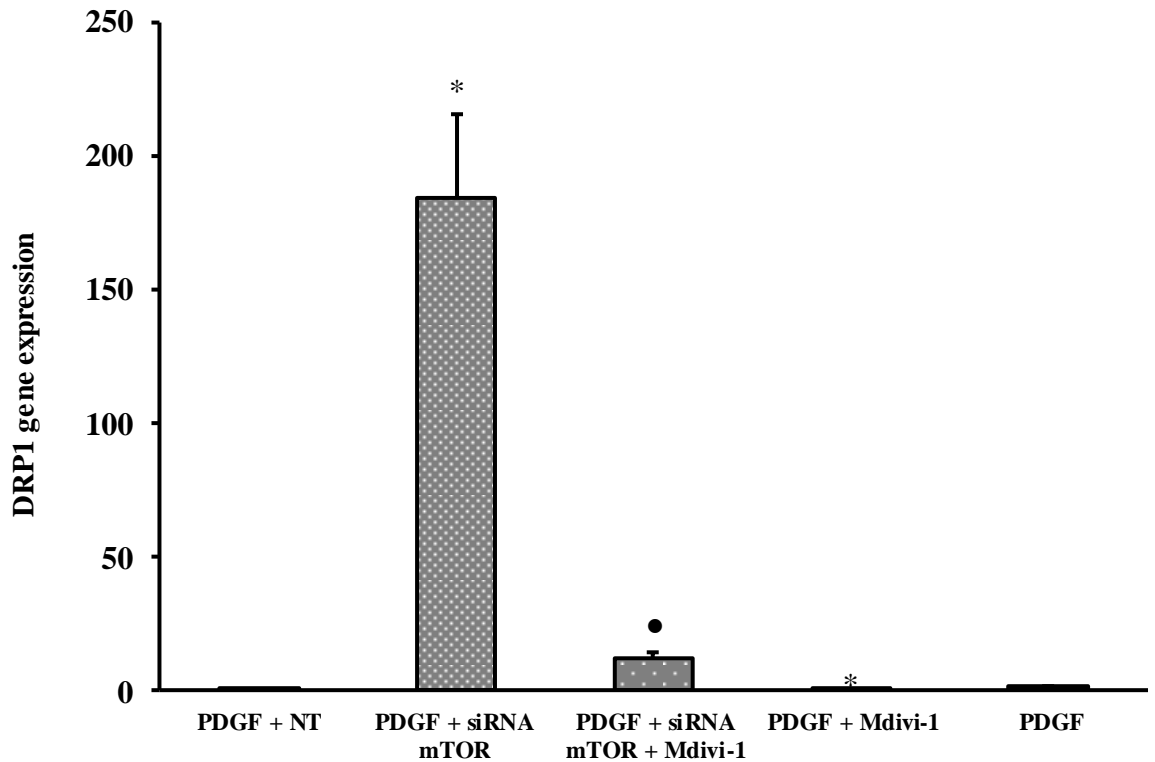
PDGF		+	+	+	+	+
mTORC1 siRNA				+	+	
NT			+			
Mdivi-1					+	+

Figure 5.21 The effect of siRNA mTORC1 alone and with Mdivi-1 on PDGF-induced cell proliferation during hypoxia. PASMCMs were transfected with a scrambled or non-targeting (NT) siRNA (75 nM), mTORC1 siRNA (75 nM) for 72 h prior to stimulation. Cells were quiesced for 24 h and were then stimulated with PDGF (5 ng/ml) and exposed to hypoxia (3% O₂) for 24 h. Mdivi-1 (10 μM) was added 30 minutes before stimulation. DNA synthesis was evaluated by [³H]-thymidine incorporation assay. Radioactive counts were measured in disintegrations per minute (DPM) and normalized to DNA synthesis in the control group (quiescent cells, 0.1% FCS). *p < 0.05 vs. agonist-stimulated control. ●p < 0.05 vs. cells treated with siRNA against mTORC1. Experiments were conducted in quadruplicate (number of wells). Each value represents the mean ± SEM (n=4).

5.10.3 The effect of mTORC1 knockdown alone and with Mdivi-1 on mitochondrial DRP1 gene expression

Previous data showed that PDGF under hypoxic conditions caused an increase in mTORC1 gene expression (Figure 5.17) and a decrease in mitochondrial DRP1 gene expression (Figure 4.23), suggesting that mTORC1 is involved in the regulation of PASMC proliferation during hypoxia and the PDGF-induced mTORC1 could inhibit the formation of mitochondrial fission gene DRP1. To investigate whether mTORC1 is able to control DRP1 expression, the DRP1 gene was measured following mTORC1 knockdown in PDGF induced cell proliferation during hypoxia. Data show the DRP1 gene was increased by 184.1 ± 31.7 fold following mTORC1 knockdown (Figure 5.22).

The results of previous experiments showed inhibiting DRP1 by Mdivi-1 in cells stimulated with PDGF during hypoxia causes a significant decrease in cell proliferation (Figure 4.5) and in mTORC1 gene expression (Figure 5.17) which suggests that both mTORC1 and DRP1 genes seems to be essential for cell proliferation. The direct inhibitory effect of Mdivi-1 on DRP1 was clearly seen in the cells treated with siRNA against mTORC1 as DRP1 gene was significantly inhibited by $92.7 \pm 1.67\%$ (Figure 5.22).

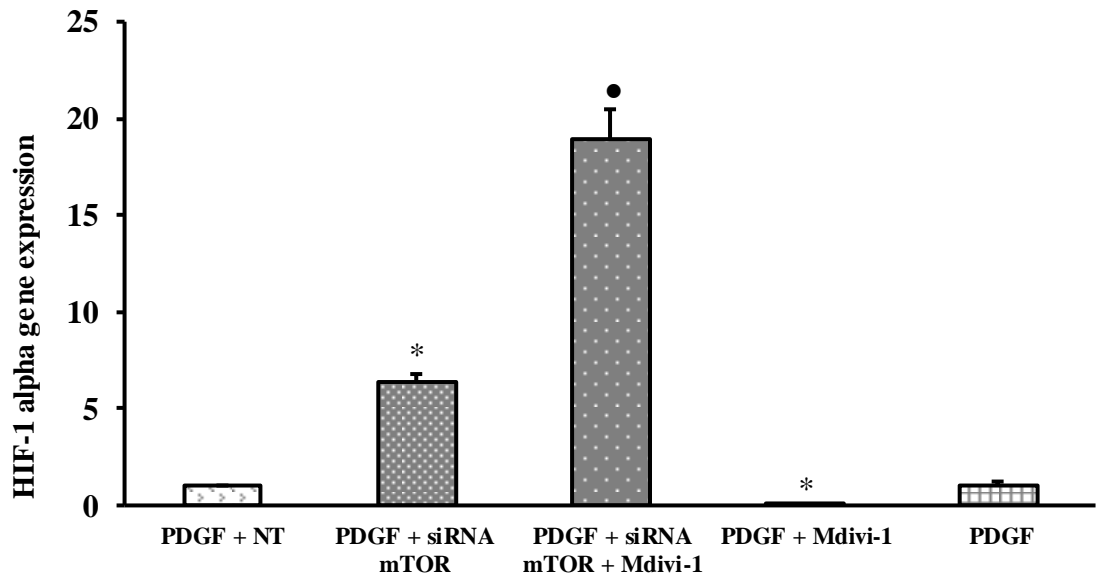


PDGF	+	+	+	+	+
mTORC1 siRNA		+	+		
NT	+				
Mdivi-1			+	+	

Figure 5.22 The effect of siRNA mTORC1 alone and with Mdivi-1 on DRP1 gene expression upon PDGF stimulated cells during hypoxia. PASMCs were transfected with a scrambled or non-targeting (NT) siRNA (75 nM), mTORC1 siRNA (75 nM) for 72 h prior to stimulation. Cells were quiesced for 24 h and were then stimulated with PDGF (5 ng/ml) and exposed to hypoxia (3% O₂) for 24 h. Mdivi-1 (10 μM) was added 30 minutes before stimulation. RNA was extracted from the cells. Equal RNA concentrations were used for cDNA sample preparation. The expression of DRP1 gene was measured using RT-qPCR. Ubiquitin C (UBC) was used as the reference gene for normalization. Each value represents the mean ± SEM. *p<0.05 vs. agonist-stimulated control. ●p<0.05 vs. cells treated with siRNA against mTORC1 (n=3).

5.10.4 The effect of mTORC1 knockdown alone and with Mdivi-1 on HIF-1 α gene expression

During hypoxia, results also show HIF-1 α gene expression was significantly reduced by PDGF (Figure 5.1) suggesting that PDGF induced cell proliferation through controlling not only mitochondrial fission DRP1 gene but also HIF-1 α expression. The Western blot experiment was performed to measure HIF-1 α protein expression in response to imatinib treatment in PDGF stimulated cells during hypoxia. A significant increase in protein expression was observed when PDGF receptors were blocked by imatinib (Figure 5.2). Taken together, both findings suggest PDGF activates mTORC1 and mitochondrial fusion, promotes cell proliferation and is more likely to negatively regulate HIF-1 α component. To confirm this, HIF-1 α expression following mTORC1 knockdown was performed. Data show a significant increase in HIF-1 α expression by 6.4 ± 0.4 fold when mTORC1 was knocked down. Surprisingly, following Mdivi-1, the HIF-1 α gene was further significantly increased by 3 ± 0.35 fold in the cells treated with siRNA against mTORC1 (Figure 5.23).

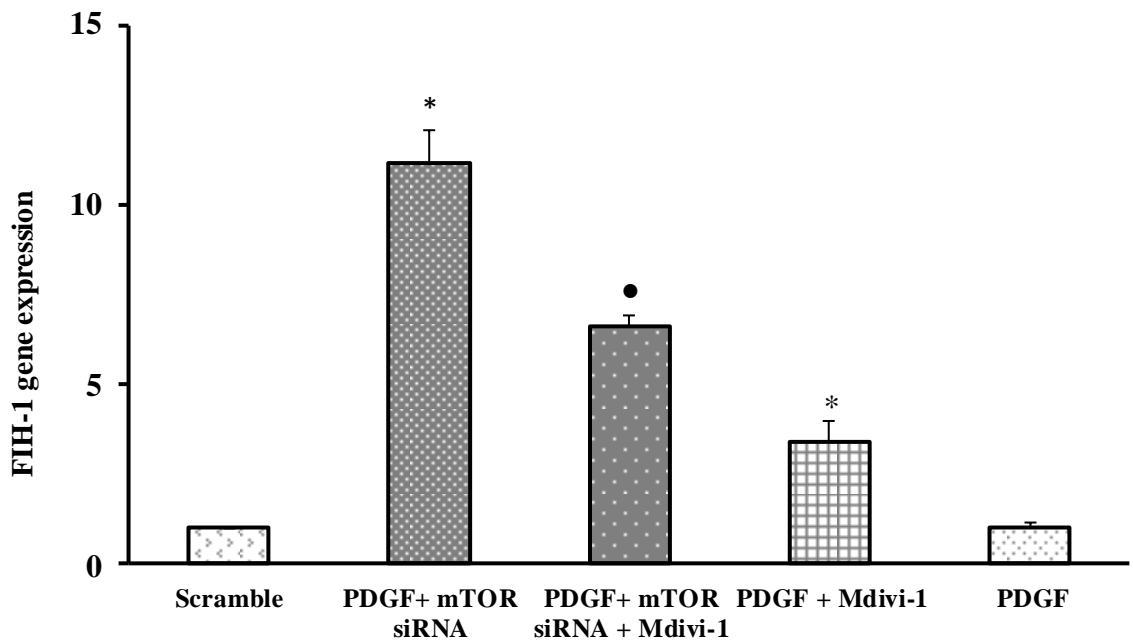


PDGF	+	+	+	+	+
mTORC1 siRNA		+	+		
NT	+				
Mdivi-1			+	+	

Figure 5.23 The effect of siRNA mTORC1 alone and with Mdivi-1 on HIF-1 α gene expression upon PDGF stimulated cells during hypoxia. PASM Cs were transfected with non-targeting (NT) siRNA (75 nM), mTORC1 siRNA (75 nM) for 72 h prior to stimulation. Cells were quiesced for 24 h and were then stimulated with PDGF (5 ng/ml) and exposed to hypoxia (3% O₂) for 24 h. Mdivi-1 (10 μ M) was added 30 minutes before stimulation. RNA was extracted from the cells. Equal RNA concentrations were used for cDNA sample preparation. The expression of HIF-1 α gene was measured using RT-qPCR. Ubiquitin C (UBC) was used as the reference gene for normalization. Each value represents the mean \pm SEM. *p<0.05 vs. agonist-stimulated control. ●p<0.05 vs. cells treated with siRNA against mTORC1 (n=3).

5.10.5 The effect of mTORC1 knockdown alone and with Mdivi-1 on FIH-1 gene expression

To investigate whether the reduction of FIH-1 gene expression that was caused by PDGF during hypoxia (Figure 5.6) is due to mTORC1 expression; FIH-1 gene expression was measured following mTORC1 knockdown (Figure 5.24). In PDGF stimulated cells, data show FIH-1 gene expression was increased by 11.16 ± 0.91 fold when mTORC1 was knocked down. In addition, following the effect of mTORC1 silencing, inhibiting the mitochondria using Mdivi-1 caused a significant decrease in FIH-1 gene expression ($39.39 \pm 5.21\%$, Figure 5.24). Taken together, these data suggest that mTORC1 drives cell proliferation through not only the negative regulatory effect on HIF-1 α and DRP1 genes but also on the FIH-1 gene.



PDGF	+	+	+	+	+
mTORC1 siRNA		+	+		
NT	+				
Mdivi-1			+	+	

Figure 5.24 The effect of siRNA mTORC1 alone and with Mdivi-1 on FIH-1 gene expression upon PDGF stimulated cells during hypoxia. PASM Cs were transfected with non-targeting (NT) siRNA (75 nM), mTOR siRNA (75 nM) for 72 h prior to stimulation. Cells were quiesced for 24 h and were then stimulated with PDGF (5 ng/ml) and exposed to hypoxia (3% O₂) for 24 h. Mdivi-1 (10 μM) was added 30 minutes before stimulation. RNA was extracted from the cells. Equal RNA concentrations were used for cDNA sample preparation. The expression of FIH-1 gene was measured using RT-qPCR. Ubiquitin C (UBC) was used as the reference gene for normalization. Each value represents the mean ± SEM. *p<0.05 vs. agonist-stimulated control. ●p<0.05 vs. cells treated with siRNA against mTORC1 (n=3).

5.11 Discussion

The aim of this chapter was to investigate whether the signalling pathway of hypoxia, MAPKs and mTOR can participate in the mechanism of inhibiting PASM proliferation and migration by inhibiting the mitochondrial DRP1 using Mdivi-1 under hypoxic conditions. The main finding in this chapter is that the inhibition of PASM proliferation by Mdivi-1 is associated with the upregulation of FIH-1 gene expression that caused by the inhibitory effect of Mdivi-1 on the mTORC1 gene which leads to suppression of the HIF-1 α gene expression.

5.12 The involvement of HIF-1 α gene in mitochondrial-dependent proliferation of PSMs

Data showed a significant increase in HIF-1 α gene expression following hypoxic exposure in PDGF stimulated cells (Figure 5.1) and a significant reduction of the gene following Mdivi-1 treatment (Figure 5.4B). The result of [³H] thymidine incorporation experiment in chapter 4 showed PDGF increased DNA synthesis under hypoxic conditions and Mdivi-1 treatment caused a significant reduction in DNA synthesis (Figure 4.5). Taken together, these findings suggest that the PDGF induced cell proliferation during hypoxia is associated with the increase in the expression of HIF-1 α that could regulate the proliferation of PSMs. Similar results found in a study by Marsboom and co-authors showed that HIF-1 α activation increases proliferation of the PAH PSMs in comparison with the non-PAH PSMs and inhibiting the mitochondrial fission using Mdivi-1 leads to a decrease in PASM proliferation. They found that the inhibition of HIF-1 α by chetomin, a small molecule that inhibits HIF-1 α gene transcription, caused a significant reduction in PASM proliferation. They also reported that the HIF-1 α activation causes a glycolytic shift when PSMs proliferate (Marsboom et al., 2012). This suggests that the inhibition of cell proliferation by Mdivi-1 does possibly inhibit the glycolytic shift and improve the mitochondrial function by inhibiting the expression of HIF-1 α gene. This suggestion is supported by the PCR results in chapter 4 as the expression of the mitochondrial marker genes such as COX-II (Figure 4.27), ATPase 6 (Figure 4.20) and P53 (Figure 4.14) were all significantly increased following Mdivi-1 treatment. This supports the suggestion

that the proliferation of PSMCs seems to be dependent on the glycolytic shift (the Warburg effect) rather than the mitochondrial metabolism, which closely resembles the behaviour of cancer cells (Archer et al., 2013).

5.13 MAPK phosphorylation following mitochondrial inhibition

The MAPK signalling pathway is commonly recognized as being involved in VSMC proliferation (Sprague and Khalil, 2009). The Western blot data showed no significant difference in ERK1/2, p38 MAPK and JNK during both normoxia and hypoxia following mitochondrial fission inhibition (Figure 5.7, Figure 5.8 and Figure 5.9, respectively). These findings suggest that the mitochondria could enhance PSMC proliferation during normoxia and hypoxia through other signalling pathways apart from MAPK signalling cascades.

5.14 The participation of the mitochondrial fission protein DRP1 in the mTOR signalling pathway

The PI3K signalling axis has been shown to be activated in PDGF-dependent PSMC proliferation (Goncharova et al., 2002). Perez and co-workers reported that PDGF plays a major role in enhancing cell glycolysis and cell proliferation in a PI3K dependent mechanism (Perez et al., 2010). In the current study, the inhibition of cell proliferation using Mdivi-1 during normoxic PDGF stimulation is consistent with the reduction in PI3K/PTEN signalling genes which are considered as the head substrates for mTORC1 signalling pathway. Furthermore, in PDGF stimulated cells, the results showed that Mdivi-1 prevents the phosphorylation of PDK1 suggesting that Mdivi-1 slows cell proliferation via the inhibition of PDK1 phosphorylation. In addition, the expression of the downstream mTORC1 gene (4EBP1) was also decreased with the anti-proliferative effect of Mdivi-1. It has been reported that 4EBP1 plays an important role in regulating the activity of the mitochondria and mitochondrial biogenesis (Morita et al., 2013). Taken together, these findings highlight the inhibition of the mitochondrial fission results in inhibiting PSMC proliferation through suppressing the mitochondrial function (including mitochondrial biogenesis and the oxidative phosphorylation process) and inhibiting the PI3K/PTEN/PDK1 signalling axis.

The PI3K/AKT/PDK1 signalling cascade was also investigated during hypoxia in order to identify mitochondrial cell signalling genes and proteins that are involved in cell proliferation and migration. Contrary to normoxic condition findings, Mdivi-1 showed no significant role for PI3K and PTEN genes during hypoxia (Figure 5.11 and Figure 5.12) suggesting that these genes are not involved in regulating cell proliferation and mitochondrial dysfunction via DRP1 function during hypoxia. Moreover, the Western blot data show phosphorylation of PDK1 during hypoxia was higher than during normoxia in the PDGF stimulated cells and inhibiting DRP1 by Mdivi-1 caused a significant decrease in PDK1 phosphorylation in both oxygen conditions (Figure 5.13). The results in chapter 4 showed that inhibiting mitochondrial fission using Mdivi-1 in PDGF stimulated cells resulted in a reduction in DNA synthesis under both normoxic and hypoxic conditions (Figure 4.5). Taken together, these data suggest Mdivi-1 reduces cell proliferation via the inhibition of PDK1 phosphorylation. It has been demonstrated that the knockdown of PDK1 limits hypoxia induced PAH in a mouse model (Di et al., 2019) and significantly inhibits the proliferation of lung cancer cells (Ye et al., 2015) and renal cell carcinoma (Zhou et al., 2019).

The results obtained within this thesis show that the distribution of fused/elongated mitochondria instead of fragmented mitochondria (Figure 4.28E and Figure 4.30C), increased mTORC1 expression (Figure 5.17 and Figure 3.19C) and cell proliferation (Figure 4.4 and Figure 3.10) were observed in PSMCs during hypoxia in response to PDGF and 10% FCS, respectively. The increase in mitochondrial length in PDGF and in 10% FCS induced proliferation during hypoxia was significantly increased in comparison to the corresponding stimulant during normoxia and to the corresponding hypoxic background (Figure 4.29 and Figure 4.31, respectively). Also, both fission gene DRP1 and the mitochondrial biogenesis marker gene TFAM were significantly reduced in cells stimulated with PDGF during hypoxia in comparison to the hypoxia background (Figure 4.23 and Figure 4.24B, respectively). Taken together, the results confirmed that PDGF during hypoxia is more likely to enhance cell proliferation through increasing mTORC1 expression and reducing mitochondrial DRP1 expression.

In the hypoxic PDGF stimulated cells, both cell proliferation and mTORC1 gene expression were significantly increased (Figure 4.4 and Figure 5.17, respectively), whereas inhibiting the mitochondria with a DRP1 inhibitor (Mdivi-1) reduced cell proliferation (Figure 4.5) and showed an inhibition of the gene expression (Figure 5.17). The direct inhibitory effect of Mdivi-1 on mTORC1 was also observed in the hypoxic background cells (Figure 5.16). These findings suggest Mdivi-1 directly targeted the mTORC1 and this gene may have a role in PDGF hypoxic-dependent cell proliferation. It has been reported that mTORC1 has a potential role in hypoxia-induced PASMC proliferation and pulmonary hypertension (Wang et al., 2014b). To confirm the mTORC1 role, the assessment of PDGF induced cell proliferation during hypoxia following mTORC1 knockdown was performed. Results show mTORC1 knockdown inhibits cell proliferation (Figure 5.21). Taken together, these data suggest PASMC proliferation during hypoxia seems to be dependent on the mTORC1 gene as the cell growth was significantly decreased when the mTORC1 gene was silenced (siRNA). Similarly both proliferation and expression of mTORC1 gene was significantly reduced by Mdivi-1.

Therefore, this study sought to measure mitochondrial DRP1 expression following mTORC1 knockdown. Results show the mitochondrial fission marker gene DRP1 was significantly upregulated following mTORC1 knockdown (Figure 5.22). This may suggest there is an inverse relationship between mTORC1 and the mitochondrial fission process as an upregulation of mTORC1 gene during hypoxia by PDGF, which particularly enhanced cell proliferation, could explain why mitochondrial DRP1 expression was decreased and why the mitochondria shape becomes fused or tubulated which could be due to the negative regulatory effect of mTORC1 (Figure 4.28E). This supports the suggestion that mTORC1 plays an important role in controlling mitochondrial fission/ fusion state via the DRP1 gene expression.

This finding also suggests the over-expression of the DRP1 gene and increased mitochondrial fission are not involved in mediating cell proliferation in response to the combined effect of PDGF and hypoxia. To investigate this, the effect of DRP1 inhibitor (Mdivi-1) on mTORC1 expression and PASMC proliferation was examined in the mTORC1 gene silencing study. The result shows Mdivi-1 caused a

further reduction in cell proliferation in cells treated with siRNA against mTORC1 (Figure 5.21). Taken together, these findings suggest both mTORC1 and DRP1 (only at low expression) appear to be essential in PDGF induced cell proliferation during hypoxia.

5.15 The effect of Mdivi-1 on PASMC Migration

The results in chapter 4 showed that inhibiting mitochondrial fission with Mdivi-1 reduces PASMC migration under both normoxic (Figure 4.7) and hypoxic (Figure 4.8) conditions. In this chapter, signalling pathways that may be involved in mitochondrial dependent migration of PASMCs were examined. Data showed ERK1/2 was phosphorylated by PDGF stimulation during normoxia and hypoxia (Figure 5.7) and it was previously known that the phosphorylation of ERK1/2 is linked with the phenotypic switching in VSMCs (Carrillo-Sepulveda and Barreto-Chaves, 2010). It has been reported that an increase in ERK1/2 phosphorylation is associated with PDGF induced cell proliferation in cultured PASMCs (Yamboliev and Gerthoffer, 2001). ERK1/2 activates DRP1 at serine 616 which results in increased mitochondrial fission (Yu et al., 2011). However, our findings showed that mitochondrial fission inhibition in PDGF induced cell migration had no role on the phosphorylation of ERK1/2 protein (Figure 5.7), suggesting that the migratory effect resulting from DRP1 activation and mitochondrial morphological changes is not through the ERK1/2 MAPK signalling pathway. In addition, data show Mdivi-1 caused a significant inhibition of PDK1 phosphorylation in both oxygen conditions suggesting that phosphorylated PDK1 may play a major role in mitochondrial DRP1 mechanism in regulating cell migration. Weber and co-workers noted that activation of PDGF receptors induced an increase in the intracellular levels of ROS which led to VSMC migration. They found that the PDK1 activated by PDGF is a significant ROS-sensitive mediator of VSMC migration (Weber et al., 2004).

Another signalling pathway which may contribute to the PDGF-induced migratory effect is the PI3K/mTORC1 pathway. It has previously been reported that PI3K is an essential component that promotes PASMC migration following PDGF stimulation (Yamboliev et al., 2001). A similar result which was seen in our lab highlights the significant increase in PI3K gene expression during normoxia and

hypoxia conditions (Figure 5.11). The inhibitory effect of mitochondria by Mdivi-1 was only seen during normoxia, suggesting that the mitochondria (mainly mitochondrial fission) have an important role in mediating PI3K signalling axis during normoxia as the inhibition of PI3K gene expression could contribute to the reduction of PASM C migration. However, during hypoxia, data show PI3K component seems to be not participating in the PDGF-induced migratory effect. The PCR results show that during hypoxia, both HIF-1 α and mTORC1 gene expression levels were significantly decreased following Mdivi-1 treatment (Figure 5.4 B and Figure 5.17, respectively). This highlights the chance of these genes being involved in a mitochondrial role in mediating cell migration as it has been demonstrated that the HIF-1 α /mTORC1 axis is required in mediating cell migration during hypoxia (Lee et al., 2015). Similarly, another study by Wan and co-workers found hypoxia increases DRP1 expression and inhibiting HIF-1 α using echinomycin, a HIF-1 α inhibitor, leads to an inhibition of DRP1 expression. This suggests that hypoxia may induce cell migration through the upregulation of DRP1 via HIF-1 α (Wan et al., 2014).

Although Mdivi-1 is believed to produce a selective inhibition of mitochondrial DRP1 protein and inhibit mitochondrial fission, it is not completely targeted to the mitochondria as a variety of different cellular effects appear to be considerable in response to Mdivi-1. For example, in cardiomyocytes Mdivi-1 performs DRP1-independent action as it directly inhibits the rapidly activating delayed-rectifier and acetylcholine-activated K⁺ channels, and this is not as a consequence of its inhibition of mitochondrial fission (So et al., 2012). Inhibiting some types of K⁺ channels may regulate cell proliferation and migration (Cidad et al., 2010). In addition, a change in mitochondrial outer membrane permeabilization (MOMP) was reported following Mdivi-1 treatment due to its DRP1-independent effect (Kushnareva et al., 2012). This change and other mitochondrial dysfunctions may regulate cell migration via ROS (Ma et al., 2013, Tochwang et al., 2013). A somewhat debated study related to the effect of Mdivi-1 on the mitochondrial fission was published in 2017 by Bordt and co-workers. They reported that Mdivi-1 does not specifically target the mitochondrial DRP1 but instead inhibits the mitochondrial complex 1 in the electron transport chain in neuronal cells (Bordt et al., 2017). Therefore, an off-target effect of Mdivi-1 should be considered and

further investigation is required. Preferably, in order to elucidate the role of DRP1 in PASMC proliferation and migration, parallel experiments should be conducted in future work to validate the findings presented in this thesis such as the use of molecular tools to block the mitochondrial fission function including knockdown of DRP1 gene. The use of adenoviral vectors coding for a dominant negative form of DRP1 (DRP1 K38A) in PASMCs is also recommended (Parra et al., 2017).

5.16 The mechanism of Mdivi-1 on hypoxic genes

Results in Figure 4.5 and Figure 5.3 showed that Mdivi-1 treatment in PDGF stimulated cells during normoxia slowed cell proliferation and increased HIF-1 α . In hypoxic background cells, Mdivi-1 significantly enhanced HIF-1 α (Figure 5.4A). These data suggest inhibiting DRP1 is correlated with increased HIF-1 α . Surprisingly, Mdivi-1 caused a significant reduction in HIF-1 α gene expression in PDGF stimulated cells during hypoxia (Figure 5.4B). Taken together, these results suggest that Mdivi-1 does not directly inhibit HIF-1 α and the inhibition of HIF-1 α in PASMCs stimulated with PDGF during hypoxia might be through a change in a particular gene involved in PDGF/hypoxia signalling in response to Mdivi-1 treatment.

The current study sought to whether the inhibition of HIF-1 α gene by Mdivi-1 is related to its inhibitory effect on mTORC1, therefore, HIF-1 α gene was measured following the combined effects of mTORC1 knockdown and Mdivi-1 in PDGF stimulated cells under hypoxia. Mdivi-1 increased HIF-1 α gene expression after mTORC1 knockdown (Figure 5.23). Despite the role of mTORC1 in controlling HIF-1 alpha expression, this finding confirms the inhibitory effect of Mdivi-1 on HIF-1 α gene expression in cells with PDGF during hypoxia is not through mTORC1. Therefore, Mdivi-1 has a direct increasing effect on HIF-1 alpha and the inhibition of HIF-1 α by Mdivi-1 in cells with PDGF and hypoxia was due to the effect of Mdivi-1 on other proteins and genes involved in PDGF signalling or hypoxia signalling apart from mTORC1, which could inhibit or degrade the HIF-1 α activity.

Therefore, the study sought to measure gene expression of FIH-1, the enzyme that suppresses the activity of HIF-1 α . It has been reported that FIH-1 knockdown in LM8 osteosarcoma did not affect the tumor growth while over-expression of FIH-1

caused an increase in the tumor growth and promoted the pericytes of the tumor vasculature (Aguado et al., 2013). The same study highlighted the strong correlation between PDGF, vessel maturation and this enzyme. Aguado and colleagues (2013) reported an increase in PDGF in the tumor was associated with vessel maturation and when inhibiting PDGF in FIH-1 overexpressing tumor cells this leads to decreased pericyte recruitment and tumor growth. This finding which is in line with our finding shows the role of PDGF in increasing FIH-1 gene expression during normoxia, which leads to cell proliferation while inhibiting the mitochondria leading to slow cell proliferation and decrease FIH-1 gene expression. During hypoxia, a significant reduction of FIH-1 expression in PDGF stimulated cells (Figure 5.6) which suggests this could be due to mTORC1 over-expression which may control the expression of this gene. Following an investigation, data show the expression of FIH-1 gene was significantly increased in cells treated with siRNA against mTORC1 (Figure 5.24) which confirms that mTORC1 negatively regulates the FIH-1 gene expression and the increase of this gene may contribute to the inhibition of cell proliferation during hypoxia.

The PCR data show that FIH-1 gene expression was significantly increased following Mdivi-1 treatment in both hypoxia background cells (Figure 5.5) and cells with PDGF during hypoxia (Figure 5.6) suggesting that inhibiting fission by Mdivi-1 during hypoxia leads to an increase in FIH-1 which eventually could contribute not only to degrading the HIF-1 α but also in inhibiting PASM C proliferation.

To investigate if the inhibitory effect of Mdivi-1 on the mTORC1 expression is related to FIH-1 over-expression, both cell proliferation and FIH-1 expression were assessed in mTORC1 knock-down cells following Mdivi-1 treatment. Mdivi-1 caused a significant decrease in cell proliferation (Figure 5.21) and FIH-1 expression (Figure 5.24) in comparison to cells treated with siRNA against mTORC1 that were without Mdivi-1 treatment, which suggests the increasing effect of Mdivi-1 on FIH-1 expression was prevented in response to the absence of mTORC1 in PDGF stimulated cells during hypoxia. These data conclude that Mdivi-1 increased FIH-1 through its inhibitory effect on mTORC1 leading to further inhibition of cell proliferation. This highlights mitochondrial fission function, particularly DRP1, during hypoxia which plays a key role in promoting

the mitochondrial dysfunction and the glycolytic shift in PASMC proliferation through increasing mTORC1 that controls FIH-1 which in turn maintains the transcriptional activity of HIF1- α .

The knockdown of mTORC1 gene using siRNA was confirmed by the RT-qPCR. However, knockdown of mTORC1 should have been further confirmed by Western blot analysis which would be a part of future work using antibodies for Western blot against mTORC1 and downstream proteins of the mTOR signalling pathways (such as P70s6K). Such experiments would support the key findings in this thesis.

5.17 Summary of Results

The results in this chapter concluded that:-

- In hypoxic cell model, activation of HIF1 α during a 24 h acute hypoxic period is appropriate to enhance DRP1 activity which causes fragmented mitochondria with an increase in PASMC proliferation.
- Inhibiting the mitochondria with Mdivi-1 is more likely to slow PASMC proliferation through inhibiting the mTORC1 signalling (the upstream cascade PI3K/PTEN/PDK1 genes and the downstream 4EPB1 gene) and the FIH-1 gene and through increasing the gene expression of AKT and P70s6k.
- PDGF-dependent PASMC proliferation is substantially increased by acute hypoxia (3% oxygen) which mainly depends on mTORC1 gene expression.
- Inhibiting mitochondrial fission with Mdivi-1 during hypoxia seems to diminish PASMC proliferation and migration through inhibiting the expression of HIF-1 α , PDK1, mTORC1 and its downstream P70S6K and increasing the expression of FIH-1 and AKT genes.
- Mdivi-1 increased FIH-1 gene expression by inhibiting mTORC1 gene leads to suppression of HIF-1 α gene expression and inhibition of PASMC proliferation.

Chapter 6

General discussion

6.1 General Discussion

Mitochondrial dynamics and metabolism are essential to maintain cell function and play an important role in cardiovascular/hyperproliferative diseases including pulmonary hypertension. In pulmonary hypertension, aberrant PASMCM proliferation is driven by hypoxia, which leads to remodeling of the pulmonary arteries resulting in right ventricular failure. The general aim of this study was to determine the role of mitochondria in the PASMCM hyperproliferative/apoptotic resistant phenotype and its relationship to hypoxia, which may provide new therapeutic strategies for PAH through targeting mitochondrial dysfunction needed for the proliferative and migratory PASMCM phenotype.

The work presented in this thesis was able to validate the hypoxic cell culture model to induce cell proliferation. Therefore, by using this model, the influence of mitochondrial inhibition on cell proliferation and migration was studied through down-regulation of mitochondrial DRP1. This was part of a longer-term objective to explore mitochondrial DRP1, a protein involved in mitochondrial fission process, as a possible therapeutic intervention for the use in hypoxic/hyperproliferative diseases such as pulmonary hypertension.

The present work reinforces previous studies which highlight the importance of hypoxia, altered mitochondrial dynamics, and the presence of DRP1 in mediating proliferation and migration of smooth muscle cells (Marsboom et al., 2012, Salabei and Hill, 2013) and identifies new mitochondrial signalling acquired from the combined effects of hypoxia and PDGF via down-regulation of mitochondrial DRP1 which strongly contributes to PASMCM proliferation, migration and pulmonary hypertension pathophysiology. This work found that Mdivi-1 not only inhibited proliferation and migration of PASMCMs during hypoxia, but also reversed the hypoxic-induced glycolytic mitochondrial-metabolic phenotype.

6.2 Cell signalling in a hypoxic cell model

The results in Chapter 3 concluded that among three different hypoxic levels; 10%, 5% and 3% oxygen, acute exposure of hypoxia (3% O₂) was sufficient to stimulate cellular growth and proliferation of PASMCMs, which was successfully achieved as a

cell model to study the cell signalling pathways involved in PASMCM proliferation enhanced by hypoxia.

The effect of hypoxia (3% O₂) on cell proliferation was investigated not only in growth factor-mediated cell proliferation but also in low-serum culture conditions (cells with 0.1% FCS). The data in Chapter 4 found that PASMCMs exposed to hypoxia were significantly resistant to apoptosis and were able to proliferate and adapt with a glycolytic shift in metabolism. In addition, the mitochondrial alteration in dynamics (the shift to fission and the increase in DRP1 expression) and the loss of mitochondrial function (a decrease in mitochondrial ATP production, ROS (H₂O₂ levels) and cell apoptosis) were observed following acute hypoxia treatment. Data also showed the expression of the HIF-1 α and the proliferative gene cyclin D1 was significantly increased after hypoxic exposure. Taken together, these data confirmed the proliferative/impaired apoptotic phenotype of PASMCMs, which are consistent with previously published findings that showed the phenotypic change in PASMCMs in PAH. Bonnet and co-workers found the increase in HIF-1 α activity, the excessive DRP1 expression, the fragmentation of the mitochondrial network and the aerobic glycolysis/Warburg phenomenon were strongly linked with the proliferative phenotype of PAH-PASMCMs (Bonnet et al., 2006). In addition, data showed enhanced mitochondrial DRP1 gene expression in hypoxic PASMCMs was correlated with the distribution of fragmented mitochondria and the decrease in mitochondrial length (promotes fission). Marsboom and co-workers (2012) have confirmed this demonstrating HIF-1 α activation in normal PASMCMs is enough to enhance DRP1 induced mitochondrial network fragmentation (promotes fission).

In tumor cells, it has been reported that low ROS (H₂O₂ levels) leads to an increase in cell proliferation and cyclin D1 expression (Antico Arciuch et al., 2012). This finding is consistent with the findings of the current study. A decrease in H₂O₂ levels and an increase in DNA synthesis and cyclin D1 gene expression were observed in PASMCMs with 0.1% FCS after exposure to hypoxia. A reduction in mitochondrial ROS levels (H₂O₂ levels) is one of the abnormal changes observed in both PAH-PASMCMs and cancer cells (Archer et al., 2008). Other findings presented in this thesis demonstrate that hypoxia-induced an increase in mitochondrial fission, a decrease in mitochondrial function (ATP production) and a reduction of both

PTEN and P53 gene expression, suggesting that there is a shift to the Warburg/glycolytic metabolism as these findings are correlated with the abnormalities in the mitochondrial dynamics and the cell metabolism that are found in cancer cells (Wang et al., 2014a). Deletion of PTEN in smooth muscle cells exposed to hypoxia has been shown to promote irreversible progression of pulmonary hypertension due to increased proliferation, recruitment of inflammatory cells resulting in severe pulmonary arterial remodeling (Horita et al., 2013).

In addition, data showed there was a significant increase in JNK phosphorylation in hypoxic cells, which suggests JNK phosphorylation is mediated by low oxygen stress. JNK is an important mediator of signals in response to environmental stress such as UV light, oxidative stress and hypoxia (Force et al., 1996, Woodgett et al., 1995). This finding supports the finding in another study of hypoxia-induced pulmonary arterial remodeling which showed that phosphorylation of JNK peaks at day 1 of the hypoxic exposure in the pulmonary arteries (Jin et al., 2000).

On the basis of these results, the validity of the hypoxic culture work is confirmed as the proliferative phenotype of PASMCs was clearly seen in a model of hypoxia. Figure 6.1 summarises the main findings of the influence of acute hypoxic treatment (3% oxygen) on PASMC signalling related to cell proliferation and mitochondrial dynamics.

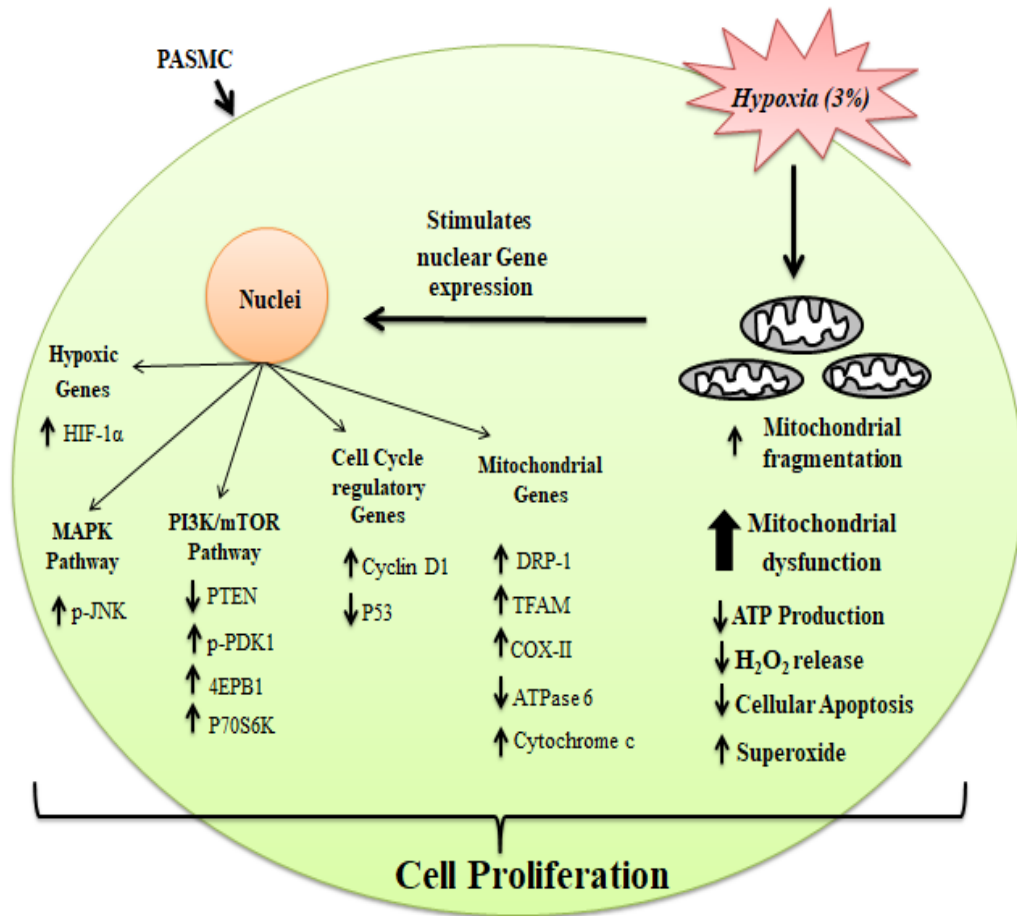


Figure 6.1 Schematic diagram summarises the main findings in the established hypoxia cell model. The diagram shows the effect of acute hypoxia (3% oxygen) on PASMC proliferation. A minor increase in cell proliferation by hypoxia was associated with increased mitochondrial fragmentation, increased superoxide production and the loss of mitochondrial function (a decrease in mitochondrial ATP production, ROS (H₂O₂ levels) and cell apoptosis were observed). Figure shows the most important proteins and genes that are involved in the hypoxic cell model that may promote cell proliferation. Arrows represents the changes in cells with 0.1% FCS during hypoxia vs. background cells (0.1% FCS) during normoxia.

6.3 DRP1 Role in cell Proliferation and Migration during Hypoxia

Until recently, there had been no study of mitochondrial DRP1 inhibition on PASMCM proliferation and migration in response to PDGF under hypoxia. Hence, the present study has challenged, for the first time, the primary cultures of rat PASMCMs with two stimulators (hypoxia and PDGF) following the DRP1 inhibitor (Mdivi-1) treatment as the mitochondrial fission mechanisms/pathways are not understood.

The present work has reported the form and bioenergetics of mitochondria (including mitochondrial network fragmentation, function and metabolism) is crucial mediator of cell proliferation and migration during normoxia. When the mitochondria were extensively active following PDGF; there was a significant increase in DRP1 expression and mitochondrial fragmentation. Therefore, inhibiting the mitochondria, DRP1 in particular by Mdivi-1, slows cell proliferation at G2/M via down-regulation of FIH-1, COX-II and ATPase 6 gene expression, inhibition of PDK1 phosphorylation and up-regulation of HIF1 α , p70s6k and cyclin D1 gene expression suggesting that PASMCMs are dependent on the mitochondrial fragmentation, function and metabolism to proliferate through the change in these genes. This indicates following addition of Mdivi-1 and DRP1 inhibition, cells may take on an apoptotic resistant phenotype, thus favouring a cell proliferative status. Following Mdivi-1 treatment, both dysfunctional mitochondria and the reduction in cellular apoptosis were observed which are linked with these genes. This may provide a clear picture of the important genes or proteins that may contribute to the defective mitochondria, the switch to glycolytic metabolism, the elongated shape of the mitochondria and the apoptotic-resistance feature of the PASMCMs observed when the DRP1 level was inhibited by Mdivi-1.

Data show acute hypoxic exposure in the presence of PDGF switched the phenotype of PASMCMs to hyperproliferative/apoptotic-resistant phenotype as the loss of mitochondrial function (including a decrease in ATP, ROS (H₂O₂), cell apoptosis, and the expression of the mitochondrial genes; DRP1, TFAM, COX-II and ATPase 6 in comparison to PDGF stimulation during normoxia) was observed. This was associated with an increase in mTORC1, P70S6K and cyclin D1 gene

expression levels and a decrease in DRP1, HIF1 α and FIH-1 gene expression levels in comparison to the hypoxic background cells. This suggests, therefore, that all these changes are more likely to enhance proliferation of PSMCs and appear to contribute to the upsurge of mitochondria dysfunction, the decrease in mitochondrial fission, the increase of elongated mitochondria and the increase in glycolic metabolism. These results also support the role of DRP1 in regulating cell proliferation during mitochondrial inhibition, as most genes that were affected by decreasing DRP1 function by Mdivi-1 in PDGF stimulated cells during normoxia were also affected after decreasing DRP1 function by PDGF treatment during hypoxia.

The present work highlighted that the over-expression of mTORC1 could control DRP1 and FIH-1 genes and could be crucial in regulating the distribution of elongated mitochondria and the proliferation of PSMCs during hypoxia. Inhibiting cell proliferation under hypoxic conditions by the DRP1 inhibitor (Mdivi-1) causes hyper-fused mitochondria around the nuclei and reverses mitochondrial function via inhibition of mTORC1 gene expression, which leads to an increase in FIH-1 gene expression. Increased FIH-1 gene expression in turn could suppress the HIF1 α activity. Improving the mitochondrial function by Mdivi-1 could be through over-expression of COX-II and ATPase 6 genes while inhibiting the Warburg shift by Mdivi-1 could be by down-regulation of HIF1 α activity. The inhibition of PDK1 phosphorylation, P70s6k gene expression and cyclin D1 gene expression also appear to be involved in recovering the mitochondrial function. These results suggest that maintaining a certain level of DRP1 is still crucial to enhancing cell proliferation during hypoxia and inhibiting this level by Mdivi-1 has a potent effect in reversing the mitochondrial function, mediating mitochondrial hyper-fusion and inhibiting cell proliferation under hypoxic conditions. A schematic representation of the main findings presented in this thesis is provided in Figure 6.2.

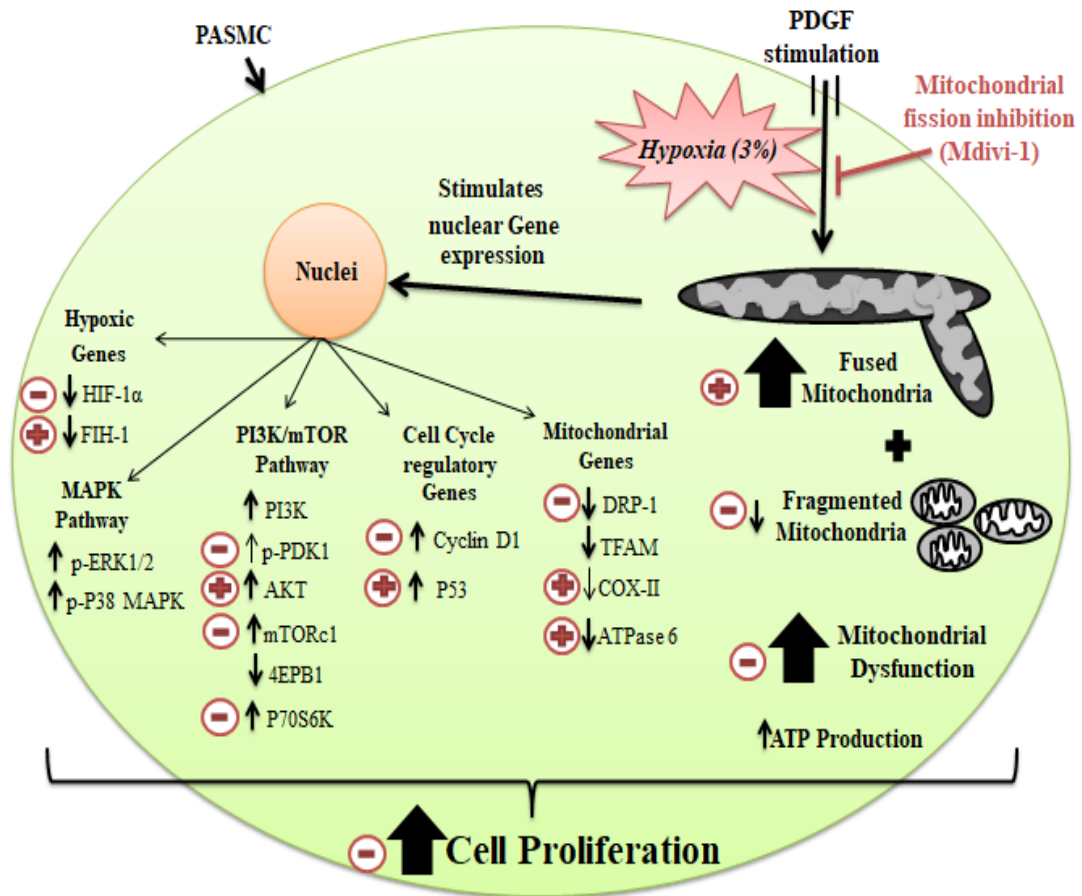


Figure 6.2 The mitochondrial role in Hypoxic-PDGF induced cell proliferation (Schematic summary). The diagram shows the effect of PDGF during hypoxia (3% oxygen) following Mdivi-1 treatment. PDGF during hypoxia caused a significant decrease in mitochondrial fission DRP1 gene, TFAM gene and ATPase 6 gene which all contributed to mitochondrial dysfunction. Elongated mitochondria and the increase in ATP levels by PDGF were clearly observed. PDGF induces cell proliferation by increasing MAPK (ERK1/2 and p38 MAPK), PI3K/mTORC1/P70s6k signalling and cell cycle regulatory genes (cyclin D1 and P53) and by decreasing hypoxic genes (HIF1 α and FIH-1). Cell proliferation was inhibited by Mdivi-1 via its inhibitory mechanism on mTORC1 and its downstream P70s6k, PDK1 and cyclin D1. Mdivi-1 significantly forced HIF1 α degradation by increasing the FIH-1 gene through its direct inhibitory effect on mTORC1. Bold arrows represent the significant changes in cells with PDGF during hypoxia vs. background hypoxic cells (0.1% FCS). The red circle represents the significant changes following mitochondrial DRP1 inhibition by Mdivi-1.

6.4 Study Limitations and Future Work

In chapter 3, the effect of different hypoxic levels on smooth muscle cells obtained from rat pulmonary arteries was studied in order to determine the effect of hypoxia on PASMC proliferation in an *in vitro* setting. This was necessary to achieve a positive correlation between acute hypoxia and cell proliferation. There are a number of issues to be considered in stabilising a cell model of hypoxia in order to drive cell growth which may explain the contradictory findings that are found in relation to many other *in vitro* studies.

For example, the degree/severity of hypoxia could play a role in the contradictory findings. Several studies have reported there is a decrease in cell proliferation when PASMCs are exposed to severe hypoxia or anoxia (Hassoun et al., 1989, Cooper and Beasley, 1999). Therefore, this was considered in the current study where moderate levels of hypoxia were applied. Another important issue to be considered is the seeding density of cells in culture plates. Several studies have reported that acute hypoxia causes a decrease in proliferation of PASMC when cells are seeded at a density of $> 10 \times 10^3$ cells $\cdot \text{cm}^{-2}$ (Eddahibi et al., 1999, Stiebellehner et al., 2003). Therefore, lower seeding densities were performed in the current study.

Moreover, another issue to be considered in hypoxic *in vitro* studies is the difference in the source of the PASMCs selected for the study. Experiments which derive the cells from the same part of the pulmonary artery could provide conflicting data. For example, Howard and co-workers found PASMC from the distal part did not proliferate following hypoxic treatment (Howard et al., 2012). However, Stotz and colleagues found the distal PASMCs proliferate faster in response to acute hypoxia by 10% increase in comparison to the proliferative rate of the control cells (Stotz et al., 2004). The differences in findings were also found in the proximal PASMCs (Dempsey et al., 1991, Ambalavanan et al., 1999).

The findings of the current study are only linked to the cell-based work and this may be a weakness when considering the application of these findings in an *in vivo* setting. For example, the immune systems in the body including the inflammatory processes are essential pathogenic components of pulmonary arterial remodeling

and this was not taken into account following hypoxic stress. Therefore, the reported responses in our hypoxic cell culture model might differ from the responses in an *in vivo* setting. Thus, the application of this work is needed to move to a whole animal model. Moreover, the dominant changes in pulmonary vascular remodeling occur at the distal part of the pulmonary arteries while the PASMCs that were used in the current study were obtained from the proximal arteries which may also differ when considering the application of the present findings in an *in vivo* setting. Also, chronic exposure to hypoxia has been well-accepted to enhance cell proliferation as both histological and morphological examinations of pulmonary arteries of animal models following chronic hypoxia show a significant thickening of the smooth muscle layers (Angelini et al., 2013, Girgis et al., 2007). The results of the current study showed proliferative PASMC signalling responses following acute hypoxia, which might differ following chronic hypoxic exposure. However, an advantage of the cell culture model of acute hypoxia is that it provides the potential of rapid screen mitochondrial signalling pathways in regulating cell proliferation and migration using an appropriate concentration of molecules (including growth factors or drugs). This would permit future experiments to be considered using different settings e.g. chronic hypoxia or human cells/ tissue.

6.5 Conclusion

The present study concludes that mitochondrial DRP1 plays an important role in cell proliferation and migration during hypoxia. It is more likely to be linked with increased mTORC1 and decreased FIH-1 hypoxic enzyme as the down-regulation of mTORC1 by inhibiting DRP1 function increases FIH-1 expression and inhibits cell proliferation during hypoxia. Consequently, because Mdivi-1 is now the only commercially available small-molecule inhibitor of mitochondrial fission, the assessment of cell proliferation, the measurements of FIH-1, HIF-1 α and mTORC1 proteins, and the assessment of mitochondrial shape and function should be performed following the knockdown of DRP1 gene. Also, the development of another inhibitor will be needed to confirm the specificity of the key findings in this thesis.

References

- AARONSON, P. I., ROBERTSON, T. P. & WARD, J. P. 2002. Endothelium-derived mediators and hypoxic pulmonary vasoconstriction. *Respir Physiol Neurobiol*, 132, 107-20.
- ABE, K., TOBA, M., ALZOUBI, A., ITO, M., FAGAN, K. A., COOL, C. D., VOELKEL, N. F., MCMURTRY, I. F. & OKA, M. 2010. Formation of plexiform lesions in experimental severe pulmonary arterial hypertension. *Circulation*, 121, 2747-54.
- ABE, S., NAGASAKA, K., HIRAYAMA, Y., KOZUKA-HATA, H., OYAMA, M., AOYAGI, Y., OBUSE, C. & HIROTA, T. 2011. The initial phase of chromosome condensation requires Cdk1-mediated phosphorylation of the CAP-D3 subunit of condensin II. *Genes Dev*, 25, 863-74.
- ADESINA, S. E., KANG, B. Y., BIJLI, K. M., MA, J., CHENG, J., MURPHY, T. C., MICHAEL HART, C. & SUTLIFF, R. L. 2015. Targeting mitochondrial reactive oxygen species to modulate hypoxia-induced pulmonary hypertension. *Free Radic Biol Med*, 87, 36-47.
- AGHAMOHAMMADZADEH, R., ZHANG, Y. Y., STEPHENS, T. E., ARONS, E., ZAMAN, P., POLACH, K. J., MATAR, M., YUNG, L. M., YU, P. B., BOWMAN, F. P., OPOTOWSKY, A. R., WAXMAN, A. B., LOSCALZO, J., LEOPOLD, J. A. & MARON, B. A. 2016. Up-regulation of the mammalian target of rapamycin complex 1 subunit Raptor by aldosterone induces abnormal pulmonary artery smooth muscle cell survival patterns to promote pulmonary arterial hypertension. *Faseb j*, 30, 2511-27.
- AGUADO, A., GALAN, M., ZHENYUKH, O., WIGGERS, G. A., ROQUE, F. R., REDONDO, S., PECANHA, F., MARTIN, A., FORTUNO, A., CACHOFEIRO, V., TEJERINA, T., SALAICES, M. & BRIONES, A. M. 2013. Mercury induces proliferation and reduces cell size in vascular smooth muscle cells through MAPK, oxidative stress and cyclooxygenase-2 pathways. *Toxicol Appl Pharmacol*, 268, 188-200.
- AHN, N. G., SEGER, R., BRATLIEN, R. L. & KREBS, E. G. 1992. Growth factor-stimulated phosphorylation cascades: activation of growth factor-stimulated MAP kinase. *Ciba Found Symp*, 164, 113-26; discussion 126-31.
- AMBALAVANAN, N., MARIANI, G., BULGER, A. & PHILIPS, I. J. 1999. Role of nitric oxide in regulating neonatal porcine pulmonary artery smooth muscle cell proliferation. *Biol Neonate*, 76, 291-300.
- ANDERSON, H. C., CHACKO, S., ABBOTT, J. & HOLTZER, H. 1970. The loss of phenotypic traits by differentiated cells in vitro. VII. Effects of 5-bromodeoxyuridine and prolonged culturing on fine structure of chondrocytes. *Am J Pathol*, 60, 289-312.
- ANDREADI, C., NOBLE, C., PATEL, B., JIN, H., AGUILAR HERNANDEZ, M. M., BALMANN, K., COOK, S. J. & PRITCHARD, C. 2012. Regulation of MEK/ERK pathway output by subcellular localization of B-Raf. *Biochem Soc Trans*, 40, 67-72.
- ANGELINI, D. J., SU, Q., YAMAJI-KEGAN, K., FAN, C., SKINNER, J. T., POLOCZEK, A., EL-HADDAD, H., CHEADLE, C. & JOHNS, R. A. 2013. Hypoxia-induced mitogenic factor (HIMF/FIZZ1/RELMalpha) in chronic hypoxia- and antigen-mediated pulmonary vascular remodeling. *Respir Res*, 14, 1.

- ANTICO ARCIUCH, V. G., ELGUERO, M. E., PODEROSO, J. J. & CARRERAS, M. C. 2012. Mitochondrial regulation of cell cycle and proliferation. *Antioxid Redox Signal*, 16, 1150-80.
- ARCHER, S. L., FANG, Y. H., RYAN, J. J. & PIAO, L. 2013. Metabolism and bioenergetics in the right ventricle and pulmonary vasculature in pulmonary hypertension. *Pulm Circ*, 3, 144-52.
- ARCHER, S. L., GOMBERG-MAITLAND, M., MAITLAND, M. L., RICH, S., GARCIA, J. G. & WEIR, E. K. 2008. Mitochondrial metabolism, redox signaling, and fusion: a mitochondria-ROS-HIF-1 α -Kv1.5 O₂-sensing pathway at the intersection of pulmonary hypertension and cancer. *Am J Physiol Heart Circ Physiol*, 294, H570-8.
- ARCHER, S. L., WEIR, E. K. & WILKINS, M. R. 2010. Basic science of pulmonary arterial hypertension for clinicians: new concepts and experimental therapies. *Circulation*, 121, 2045-66.
- ARCHER, S. L., WU, X. C., THEBAUD, B., MOUDGIL, R., HASHIMOTO, K. & MICHELAKIS, E. D. 2004. O₂ sensing in the human ductus arteriosus: redox-sensitive K⁺ channels are regulated by mitochondria-derived hydrogen peroxide. *Biol Chem*, 385, 205-16.
- ARORA, R., BHARTI, V., GAUR, P., AGGARWAL, S., MITTAL, M. & DAS, S. N. 2017. Operculina turpethum extract inhibits growth and proliferation by inhibiting NF-kappaB, COX-2 and cyclin D1 and induces apoptosis by up regulating P53 in oral cancer cells. *Arch Oral Biol*, 80, 1-9.
- ARSHAM, A. M., HOWELL, J. J. & SIMON, M. C. 2003. A novel hypoxia-inducible factor-independent hypoxic response regulating mammalian target of rapamycin and its targets. *J Biol Chem*, 278, 29655-60.
- BADESCH, D. B., CHAMPION, H. C., SANCHEZ, M. A., HOEPER, M. M., LOYD, J. E., MANES, A., MCGOON, M., NAEIJE, R., OLSCHESKI, H., OUDIZ, R. J. & TORBICKI, A. 2009. Diagnosis and assessment of pulmonary arterial hypertension. *J Am Coll Cardiol*, 54, S55-66.
- BAI, M., YU, N. Z., LONG, F., FENG, C. & WANG, X. J. 2016. Effects of CDKN2A (p16INK4A/p14ARF) Over-Expression on Proliferation and Migration of Human Melanoma A375 Cells. *Cell Physiol Biochem*, 40, 1367-1376.
- BARST, R. J. 2005. PDGF signaling in pulmonary arterial hypertension. *J Clin Invest*, 115, 2691-4.
- BENITZ, W. E., COULSON, J. D., LESSLER, D. S. & BERNFIELD, M. 1986. Hypoxia inhibits proliferation of fetal pulmonary arterial smooth muscle cells in vitro. *Pediatr Res*, 20, 966-72.
- BHALLA, K., LIU, W. J., THOMPSON, K., ANDERS, L., DEVARAKONDA, S., DEWI, R., BUCKLEY, S., HWANG, B. J., POLSTER, B., DORSEY, S. G., SUN, Y., SICINSKI, P. & GIRNUN, G. D. 2014. Cyclin D1 represses gluconeogenesis via inhibition of the transcriptional coactivator PGC1 α . *Diabetes*, 63, 3266-78.
- BLASCHKE, F., STAWOWY, P., GOETZE, S., HINTZ, O., GRAFE, M., KINTSCHER, U., FLECK, E. & GRAF, K. 2002. Hypoxia activates beta(1)-integrin via ERK 1/2 and p38 MAP kinase in human vascular smooth muscle cells. *Biochem Biophys Res Commun*, 296, 890-6.
- BOCHATON-PIALLAT, M. L. & GABBIANI, G. 2005. Modulation of smooth muscle cell proliferation and migration: role of smooth muscle cell heterogeneity. *Handb Exp Pharmacol*, 645-63.

- BONNET, S., MICHELAKIS, E. D., PORTER, C. J., ANDRADE-NAVARRO, M. A., THEBAUD, B., BONNET, S., HAROMY, A., HARRY, G., MOUDGIL, R., MCMURTRY, M. S., WEIR, E. K. & ARCHER, S. L. 2006. An abnormal mitochondrial-hypoxia inducible factor-1alpha-Kv channel pathway disrupts oxygen sensing and triggers pulmonary arterial hypertension in fawn hooded rats: similarities to human pulmonary arterial hypertension. *Circulation*, 113, 2630-41.
- BORDT, E. A., CLERC, P., ROELOFS, B. A., SALADINO, A. J., TRETTER, L., ADAM-VIZI, V., CHEROK, E., KHALIL, A., YADAVA, N., GE, S. X., FRANCIS, T. C., KENNEDY, N. W., PICTON, L. K., KUMAR, T., UPPULURI, S., MILLER, A. M., ITOH, K., KARBOWSKI, M., SESAKI, H., HILL, R. B. & POLSTER, B. M. 2017. The Putative Drp1 Inhibitor mdivi-1 Is a Reversible Mitochondrial Complex I Inhibitor that Modulates Reactive Oxygen Species. *Dev Cell*, 40, 583-594.e6.
- BOUALLEGUE, A., DAOU, G. B. & SRIVASTAVA, A. K. 2007. Endothelin-1-induced signaling pathways in vascular smooth muscle cells. *Curr Vasc Pharmacol*, 5, 45-52.
- BRAGINA, O., GURJANOVA, K., KRISHTAL, J., KULP, M., KARRO, N., TOUGU, V. & PALUMAA, P. 2015. Metallothionein 2A affects the cell respiration by suppressing the expression of mitochondrial protein cytochrome c oxidase subunit II. *J Bioenerg Biomembr*, 47, 209-16.
- BRANCO-PRICE, C., ZHANG, N., SCHNELLE, M., EVANS, C., KATSCHINSKI, D. M., LIAO, D., ELLIES, L. & JOHNSON, R. S. 2012. Endothelial cell HIF-1alpha and HIF-2alpha differentially regulate metastatic success. *Cancer Cell*, 21, 52-65.
- BRENNAN, L. A., STEINHORN, R. H., WEDGWOOD, S., MATA-GREENWOOD, E., ROARK, E. A., RUSSELL, J. A. & BLACK, S. M. 2003. Increased superoxide generation is associated with pulmonary hypertension in fetal lambs: a role for NADPH oxidase. *Circ Res*, 92, 683-91.
- BROCK, M., SAMILLAN, V. J., TRENKMANN, M., SCHWARZWALD, C., ULRICH, S., GAY, R. E., GASSMANN, M., OSTERGAARD, L., GAY, S., SPEICH, R. & HUBER, L. C. 2014. AntagomiR directed against miR-20a restores functional BMPR2 signalling and prevents vascular remodelling in hypoxia-induced pulmonary hypertension. *Eur Heart J*, 35, 3203-11.
- BROOKS, C., WEI, Q., CHO, S. G. & DONG, Z. 2009. Regulation of mitochondrial dynamics in acute kidney injury in cell culture and rodent models. *J Clin Invest*, 119, 1275-85.
- BROWN, M. D. & SACKS, D. B. 2008. Compartmentalised MAPK pathways. *Handb Exp Pharmacol*, 205-35.
- BURKE-WOLIN, T. & WOLIN, M. S. 1989. H₂O₂ and cGMP may function as an O₂ sensor in the pulmonary artery. *J Appl Physiol (1985)*, 66, 167-70.
- CAMPELLO, S., LACALLE, R. A., BETTELLA, M., MANES, S., SCORRANO, L. & VIOLA, A. 2006. Orchestration of lymphocyte chemotaxis by mitochondrial dynamics. *J Exp Med*, 203, 2879-86.
- CARGNELLO, M., TCHERKEZIAN, J. & ROUX, P. P. 2015. The expanding role of mTOR in cancer cell growth and proliferation. *Mutagenesis*, 30, 169-76.

- CARLUCCI, A., LIGNITTO, L. & FELICIELLO, A. 2008. Control of mitochondria dynamics and oxidative metabolism by cAMP, AKAPs and the proteasome. *Trends Cell Biol*, 18, 604-13.
- CARRILLO-SEPULVEDA, M. A. & BARRETO-CHAVES, M. L. 2010. Phenotypic modulation of cultured vascular smooth muscle cells: a functional analysis focusing on MLC and ERK1/2 phosphorylation. *Mol Cell Biochem*, 341, 279-89.
- CARTER, W. O., NARAYANAN, P. K. & ROBINSON, J. P. 1994. Intracellular hydrogen peroxide and superoxide anion detection in endothelial cells. *J Leukoc Biol*, 55, 253-8.
- CASSIDY-STONE, A., CHIPUK, J. E., INGERMAN, E., SONG, C., YOO, C., KUWANA, T., KURTH, M. J., SHAW, J. T., HINSHAW, J. E., GREEN, D. R. & NUNNARI, J. 2008. Chemical inhibition of the mitochondrial division dynamin reveals its role in Bax/Bak-dependent mitochondrial outer membrane permeabilization. *Dev Cell*, 14, 193-204.
- CHALMERS, S., SAUNTER, C., WILSON, C., COATS, P., GIRKIN, J. M. & MCCARRON, J. G. 2012. Mitochondrial motility and vascular smooth muscle proliferation. *Arterioscler Thromb Vasc Biol*, 32, 3000-11.
- CHANDEL, N. S. 2010. Mitochondrial regulation of oxygen sensing. *Adv Exp Med Biol*, 661, 339-54.
- CHANDEL, N. S. & SCHUMACKER, P. T. 1999. Cells depleted of mitochondrial DNA (rho0) yield insight into physiological mechanisms. *FEBS Lett*, 454, 173-6.
- CHANG, C. R. & BLACKSTONE, C. 2007. Cyclic AMP-dependent protein kinase phosphorylation of Drp1 regulates its GTPase activity and mitochondrial morphology. *J Biol Chem*, 282, 21583-7.
- CHARDIN, P., CAMONIS, J. H., GALE, N. W., VAN AELST, L., SCHLESSINGER, J., WIGLER, M. H. & BAR-SAGI, D. 1993. Human Sos1: a guanine nucleotide exchange factor for Ras that binds to GRB2. *Science*, 260, 1338-43.
- CHEN, B., NELIN, V. E., LOCY, M. L., JIN, Y. & TIPPLE, T. E. 2013. Thioredoxin-1 mediates hypoxia-induced pulmonary artery smooth muscle cell proliferation. *Am J Physiol Lung Cell Mol Physiol*, 305, L389-95.
- CHEN, H. & CHAN, D. C. 2010. Physiological functions of mitochondrial fusion. *Ann N Y Acad Sci*, 1201, 21-5.
- CHEN, J., TANG, H., SYSOL, J. R., MORENO-VINASCO, L., SHIOURA, K. M., CHEN, T., GORSHKOVA, I., WANG, L., HUANG, L. S., USATYUK, P. V., SAMMANI, S., ZHOU, G., RAJ, J. U., GARCIA, J. G., BERDYSHEV, E., YUAN, J. X., NATARAJAN, V. & MACHADO, R. F. 2014. The sphingosine kinase 1/sphingosine-1-phosphate pathway in pulmonary arterial hypertension. *Am J Respir Crit Care Med*, 190, 1032-43.
- CHEN, R. H., SARNECKI, C. & BLENIS, J. 1992. Nuclear localization and regulation of erk- and rsk-encoded protein kinases. *Mol Cell Biol*, 12, 915-27.
- CHRISTMAN, B. W., MCPHERSON, C. D., NEWMAN, J. H., KING, G. A., BERNARD, G. R., GROVES, B. M. & LOYD, J. E. 1992. An imbalance between the excretion of thromboxane and prostacyclin metabolites in pulmonary hypertension. *N Engl J Med*, 327, 70-5.
- CIDAD, P., MORENO-DOMINGUEZ, A., NOVENSA, L., ROQUE, M., BARQUIN, L., HERAS, M., PEREZ-GARCIA, M. T. & LOPEZ-LOPEZ,

- J. R. 2010. Characterization of ion channels involved in the proliferative response of femoral artery smooth muscle cells. *Arterioscler Thromb Vasc Biol*, 30, 1203-11.
- COLEMAN, M. L. & RATCLIFFE, P. J. 2009. Signalling cross talk of the HIF system: involvement of the FIH protein. *Curr Pharm Des*, 15, 3904-7.
- COOL, C. D., GROSHONG, S. D., OAKEY, J. & VOELKEL, N. F. 2005. Pulmonary hypertension: cellular and molecular mechanisms. *Chest*, 128, 565s-571s.
- COOPER, A. L. & BEASLEY, D. 1999. Hypoxia stimulates proliferation and interleukin-1alpha production in human vascular smooth muscle cells. *Am J Physiol*, 277, H1326-37.
- CORBIN, J. D., BEASLEY, A., BLOUNT, M. A. & FRANCIS, S. H. 2005. High lung PDE5: a strong basis for treating pulmonary hypertension with PDE5 inhibitors. *Biochem Biophys Res Commun*, 334, 930-8.
- COSTA, R. M., FILGUEIRA, F. P., TOSTES, R. C., CARVALHO, M. H., AKAMINE, E. H. & LOBATO, N. S. 2016. H₂O₂ generated from mitochondrial electron transport chain in thoracic perivascular adipose tissue is crucial for modulation of vascular smooth muscle contraction. *Vascul Pharmacol*, 84, 28-37.
- COTTRILL, K. A. & CHAN, S. Y. 2013. Metabolic dysfunction in pulmonary hypertension: the expanding relevance of the Warburg effect. *Eur J Clin Invest*, 43, 855-65.
- COWAN, K. N., JONES, P. L. & RABINOVITCH, M. 2000. Elastase and matrix metalloproteinase inhibitors induce regression, and tenascin-C antisense prevents progression, of vascular disease. *J Clin Invest*, 105, 21-34.
- COWBURN, A. S., CROSBY, A., MACIAS, D., BRANCO, C., COLACO, R. D., SOUTHWOOD, M., TOSHNER, M., CROTTY ALEXANDER, L. E., MORRELL, N. W., CHILVERS, E. R. & JOHNSON, R. S. 2016. HIF2alpha-arginase axis is essential for the development of pulmonary hypertension. *Proc Natl Acad Sci U S A*, 113, 8801-6.
- CRASTA, K., HUANG, P., MORGAN, G., WINEY, M. & SURANA, U. 2006. Cdk1 regulates centrosome separation by restraining proteolysis of microtubule-associated proteins. *Embo j*, 25, 2551-63.
- CRIBBS, J. T. & STRACK, S. 2009. Functional characterization of phosphorylation sites in dynamin-related protein 1. *Methods Enzymol*, 457, 231-53.
- CROSSWHITE, P. & SUN, Z. 2014. Molecular mechanisms of pulmonary arterial remodeling. *Mol Med*, 20, 191-201.
- CUENDA, A. & ROUSSEAU, S. 2007. p38 MAP-kinases pathway regulation, function and role in human diseases. *Biochim Biophys Acta*, 1773, 1358-75.
- CUMMINS, E. P., BERRA, E., COMERFORD, K. M., GINOUVES, A., FITZGERALD, K. T., SEEBALLUCK, F., GODSON, C., NIELSEN, J. E., MOYNAGH, P., POUYSSEGUR, J. & TAYLOR, C. T. 2006. Prolyl hydroxylase-1 negatively regulates I κ B kinase-beta, giving insight into hypoxia-induced NF κ B activity. *Proc Natl Acad Sci U S A*, 103, 18154-9.
- D'ALONZO, G. E., BARST, R. J., AYRES, S. M., BERGOFSKY, E. H., BRUNDAGE, B. H., DETRE, K. M., FISHMAN, A. P., GOLDRING, R. M., GROVES, B. M., KERNIS, J. T. & ET AL. 1991. Survival in patients

- with primary pulmonary hypertension. Results from a national prospective registry. *Ann Intern Med*, 115, 343-9.
- DAVIE, N., HALEEN, S. J., UPTON, P. D., POLAK, J. M., YACOUB, M. H., MORRELL, N. W. & WHARTON, J. 2002. ET(A) and ET(B) receptors modulate the proliferation of human pulmonary artery smooth muscle cells. *Am J Respir Crit Care Med*, 165, 398-405.
- DAVIE, N. J., CROSSNO, J. T., JR., FRID, M. G., HOFMEISTER, S. E., REEVES, J. T., HYDE, D. M., CARPENTER, T. C., BRUNETTI, J. A., MCNIECE, I. K. & STENMARK, K. R. 2004. Hypoxia-induced pulmonary artery adventitial remodeling and neovascularization: contribution of progenitor cells. *Am J Physiol Lung Cell Mol Physiol*, 286, L668-78.
- DEMPSEY, E. C., MCMURTRY, I. F. & O'BRIEN, R. F. 1991. Protein kinase C activation allows pulmonary artery smooth muscle cells to proliferate to hypoxia. *Am J Physiol*, 260, L136-45.
- DERIJARD, B., HIBI, M., WU, I. H., BARRETT, T., SU, B., DENG, T., KARIN, M. & DAVIS, R. J. 1994. JNK1: a protein kinase stimulated by UV light and Ha-Ras that binds and phosphorylates the c-Jun activation domain. *Cell*, 76, 1025-37.
- DEYOUNG, M. P., HORAK, P., SOFER, A., SGROI, D. & ELLISEN, L. W. 2008. Hypoxia regulates TSC1/2-mTOR signaling and tumor suppression through REDD1-mediated 14-3-3 shuttling. *Genes Dev*, 22, 239-51.
- DI MISE, A., WANG, Y. X. & ZHENG, Y. M. 2017. Role of Transcription Factors in Pulmonary Artery Smooth Muscle Cells: An Important Link to Hypoxic Pulmonary Hypertension. *Adv Exp Med Biol*, 967, 13-32.
- DI, R., YANG, Z., XU, P. & XU, Y. 2019. Silencing PDK1 limits hypoxia-induced pulmonary arterial hypertension in mice via the Akt/p70S6K signaling pathway. *Exp Ther Med*, 18, 699-704.
- DIBBLE, C. C. & CANTLEY, L. C. 2015. Regulation of mTORC1 by PI3K signaling. *Trends Cell Biol*, 25, 545-55.
- DIKALOV, S., GRIENGLING, K. K. & HARRISON, D. G. 2007. Measurement of reactive oxygen species in cardiovascular studies. *Hypertension*, 49, 717-27.
- DIMAURO, S. & SCHON, E. A. 2003. Mitochondrial respiratory-chain diseases. *N Engl J Med*, 348, 2656-68.
- DIPAOLA, R. S. 2002. To arrest or not to G(2)-M Cell-cycle arrest : commentary re: A. K. Tyagi et al., Silibinin strongly synergizes human prostate carcinoma DU145 cells to doxorubicin-induced growth inhibition, G(2)-M arrest, and apoptosis. *Clin. cancer res.*, 8: 3512-3519, 2002. *Clin Cancer Res*, 8, 3311-4.
- DORFMULLER, P., ZARKA, V., DURAND-GASSELIN, I., MONTI, G., BALABANIAN, K., GARCIA, G., CAPRON, F., COULOMB-LHERMINE, A., MARFAING-KOKA, A., SIMONNEAU, G., EMILIE, D. & HUMBERT, M. 2002. Chemokine RANTES in severe pulmonary arterial hypertension. *Am J Respir Crit Care Med*, 165, 534-9.
- DROMPARIS, P. & MICHELAKIS, E. D. 2013. Mitochondria in vascular health and disease. *Annu Rev Physiol*, 75, 95-126.
- DROMPARIS, P., PAULIN, R., SUTENDRA, G., QI, A. C., BONNET, S. & MICHELAKIS, E. D. 2013. Uncoupling protein 2 deficiency mimics the effects of hypoxia and endoplasmic reticulum stress on mitochondria and triggers pseudohypoxic pulmonary vascular remodeling and pulmonary hypertension. *Circ Res*, 113, 126-36.

- DROMPARIS, P., SUTENDRA, G. & MICHELAKIS, E. D. 2010. The role of mitochondria in pulmonary vascular remodeling. *J Mol Med (Berl)*, 88, 1003-10.
- DULBECCO, R. & ELKINGTON, J. 1975. Induction of growth in resting fibroblastic cell cultures by Ca⁺⁺. *Proc Natl Acad Sci U S A*, 72, 1584-8.
- DUNN, C., WILTSHIRE, C., MACLAREN, A. & GILLESPIE, D. A. 2002. Molecular mechanism and biological functions of c-Jun N-terminal kinase signalling via the c-Jun transcription factor. *Cell Signal*, 14, 585-93.
- DURANTE, W. 2013. Role of arginase in vessel wall remodeling. *Front Immunol*, 4, 111.
- EDDAHIBI, S., FABRE, V., BONI, C., MARTRES, M. P., RAFFESTIN, B., HAMON, M. & ADNOT, S. 1999. Induction of serotonin transporter by hypoxia in pulmonary vascular smooth muscle cells. Relationship with the mitogenic action of serotonin. *Circ Res*, 84, 329-36.
- EDDAHIBI, S., HUMBERT, M., FADEL, E., RAFFESTIN, B., DARMON, M., CAPRON, F., SIMONNEAU, G., DARTEVELLE, P., HAMON, M. & ADNOT, S. 2001. Serotonin transporter overexpression is responsible for pulmonary artery smooth muscle hyperplasia in primary pulmonary hypertension. *J Clin Invest*, 108, 1141-50.
- EGAN, S. E., GIDDINGS, B. W., BROOKS, M. W., BUDAY, L., SIZELAND, A. M. & WEINBERG, R. A. 1993. Association of Sos Ras exchange protein with Grb2 is implicated in tyrosine kinase signal transduction and transformation. *Nature*, 363, 45-51.
- EL-DEIRY, W. S., HARPER, J. W., O'CONNOR, P. M., VELCULESCU, V. E., CANMAN, C. E., JACKMAN, J., PIETENPOL, J. A., BURRELL, M., HILL, D. E., WANG, Y. & ET AL. 1994. WAF1/CIP1 is induced in p53-mediated G1 arrest and apoptosis. *Cancer Res*, 54, 1169-74.
- ELORZA, A., SORO-ARNAIZ, I., MELENDEZ-RODRIGUEZ, F., RODRIGUEZ-VAELLO, V., MARSBOOM, G., DE CARCER, G., ACOSTA-IBORRA, B., ALBACETE-ALBACETE, L., ORDONEZ, A., SERRANO-OVIEDO, L., GIMENEZ-BACHS, J. M., VARA-VEGA, A., SALINAS, A., SANCHEZ-PRIETO, R., MARTIN DEL RIO, R., SANCHEZ-MADRID, F., MALUMBRES, M., LANDAZURI, M. O. & ARAGONES, J. 2012. HIF2alpha acts as an mTORC1 activator through the amino acid carrier SLC7A5. *Mol Cell*, 48, 681-91.
- FAGAN, K. A., TYLER, R. C., SATO, K., FOUTY, B. W., MORRIS, K. G., JR., HUANG, P. L., MCMURTRY, I. F. & RODMAN, D. M. 1999. Relative contributions of endothelial, inducible, and neuronal NOS to tone in the murine pulmonary circulation. *Am J Physiol*, 277, L472-8.
- FARBER, H. W. & LOSCALZO, J. 2004. Pulmonary arterial hypertension. *N Engl J Med*, 351, 1655-65.
- FIKE, C. D. & KAPLOWITZ, M. R. 1996. Chronic hypoxia alters nitric oxide-dependent pulmonary vascular responses in lungs of newborn pigs. *J Appl Physiol (1985)*, 81, 2078-87.
- FINKEL, T. 2011. Signal transduction by reactive oxygen species. *J Cell Biol*, 194, 7-15.
- FINLAY, G. A., THANNICKAL, V. J., FANBURG, B. L. & KWIATKOWSKI, D. J. 2005. Platelet-derived growth factor-induced p42/44 mitogen-activated protein kinase activation and cellular growth is mediated by reactive oxygen species in the absence of TSC2/tuberin. *Cancer Res*, 65, 10881-90.

- FIRTH, A. L., YAO, W., REMILLARD, C. V., OGAWA, A. & YUAN, J. X. 2010. Upregulation of Oct-4 isoforms in pulmonary artery smooth muscle cells from patients with pulmonary arterial hypertension. *Am J Physiol Lung Cell Mol Physiol*, 298, L548-57.
- FIRTH, J. D. & RATCLIFFE, P. J. 1992. Organ distribution of the three rat endothelin messenger RNAs and the effects of ischemia on renal gene expression. *J Clin Invest*, 90, 1023-31.
- FLIPPO, K. H. & STRACK, S. 2017. Mitochondrial dynamics in neuronal injury, development and plasticity. *J Cell Sci*, 130, 671-681.
- FORCE, T., POMBO, C. M., AVRUCH, J. A., BONVENTRE, J. V. & KYRIAKIS, J. M. 1996. Stress-activated protein kinases in cardiovascular disease. *Circ Res*, 78, 947-53.
- FRID, M. G., DEMPSEY, E. C., DURMOWICZ, A. G. & STENMARK, K. R. 1997. Smooth muscle cell heterogeneity in pulmonary and systemic vessels. Importance in vascular disease. *Arterioscler Thromb Vasc Biol*, 17, 1203-9.
- FRID, M. G., KALE, V. A. & STENMARK, K. R. 2002. Mature vascular endothelium can give rise to smooth muscle cells via endothelial-mesenchymal transdifferentiation: in vitro analysis. *Circ Res*, 90, 1189-96.
- FROHMAN, M. A. 2010. Mitochondria as integrators of signal transduction and energy production in cardiac physiology and disease. *J Mol Med (Berl)*, 88, 967-70.
- FROST, A. E., BARST, R. J., HOEPER, M. M., CHANG, H. J., FRANTZ, R. P., FUKUMOTO, Y., GALIE, N., HASSOUN, P. M., KLOSE, H., MATSUBARA, H., MORRELL, N. W., PEACOCK, A. J., PFEIFER, M., SIMONNEAU, G., TAPSON, V. F., TORRES, F., DARIO VIZZA, C., LAWRENCE, D., YANG, W., FELSER, J. M., QUINN, D. A. & GHOFRANI, H. A. 2015. Long-term safety and efficacy of imatinib in pulmonary arterial hypertension. *J Heart Lung Transplant*, 34, 1366-75.
- FUKUDA, R., ZHANG, H., KIM, J. W., SHIMODA, L., DANG, C. V. & SEMENZA, G. L. 2007. HIF-1 regulates cytochrome oxidase subunits to optimize efficiency of respiration in hypoxic cells. *Cell*, 129, 111-22.
- FUKUYAMA, K., YOSHIDA, M., YAMASHITA, A., DEYAMA, T., BABA, M., SUZUKI, A., MOHRI, H., IKEZAWA, Z., NAKAJIMA, H., HIRAI, S. & OHNO, S. 2000. MAPK upstream kinase (MUK)-binding inhibitory protein, a negative regulator of MUK/dual leucine zipper-bearing kinase/leucine zipper protein kinase. *J Biol Chem*, 275, 21247-54.
- FULDA, S., GALLUZZI, L. & KROEMER, G. 2010. Targeting mitochondria for cancer therapy. *Nat Rev Drug Discov*, 9, 447-64.
- GALIE, N., HOEPER, M. M., HUMBERT, M., TORBICKI, A., VACHIERY, J. L., BARBERA, J. A., BEGHETTI, M., CORRIS, P., GAINE, S., GIBBS, J. S., GOMEZ-SANCHEZ, M. A., JONDEAU, G., KLEPETKO, W., OPITZ, C., PEACOCK, A., RUBIN, L., ZELLWEGER, M. & SIMONNEAU, G. 2009a. Guidelines for the diagnosis and treatment of pulmonary hypertension. *Eur Respir J*, 34, 1219-63.
- GALIE, N., HOEPER, M. M., HUMBERT, M., TORBICKI, A., VACHIERY, J. L., BARBERA, J. A., BEGHETTI, M., CORRIS, P., GAINE, S., GIBBS, J. S., GOMEZ-SANCHEZ, M. A., JONDEAU, G., KLEPETKO, W., OPITZ, C., PEACOCK, A., RUBIN, L., ZELLWEGER, M. & SIMONNEAU, G. 2009b. Guidelines for the diagnosis and treatment of pulmonary hypertension: the Task Force for the Diagnosis and Treatment of Pulmonary

- Hypertension of the European Society of Cardiology (ESC) and the European Respiratory Society (ERS), endorsed by the International Society of Heart and Lung Transplantation (ISHLT). *Eur Heart J*, 30, 2493-537.
- GALIE, N., MANES, A. & BRANZI, A. 2004. The endothelin system in pulmonary arterial hypertension. *Cardiovasc Res*, 61, 227-37.
- GAN, J., LI, P., WANG, Z., CHEN, J., LIANG, X., LIU, M., XIE, W., YIN, R. & HUANG, F. 2013. Rosuvastatin suppresses platelet-derived growth factor-BB-induced vascular smooth muscle cell proliferation and migration via the MAPK signaling pathway. *Exp Ther Med*, 6, 899-903.
- GANDRE-BABBE, S. & VAN DER BLIEK, A. M. 2008. The novel tail-anchored membrane protein Mff controls mitochondrial and peroxisomal fission in mammalian cells. *Mol Biol Cell*, 19, 2402-12.
- GENNARO, G., MENARD, C., GIASSON, E., MICHAUD, S. E., PALASIS, M., MELOCHE, S. & RIVARD, A. 2003. Role of p44/p42 MAP kinase in the age-dependent increase in vascular smooth muscle cell proliferation and neointimal formation. *Arterioscler Thromb Vasc Biol*, 23, 204-10.
- GERACI, M. W., GAO, B., SHEPHERD, D. C., MOORE, M. D., WESTCOTT, J. Y., FAGAN, K. A., ALGER, L. A., TUDER, R. M. & VOELKEL, N. F. 1999. Pulmonary prostacyclin synthase overexpression in transgenic mice protects against development of hypoxic pulmonary hypertension. *J Clin Invest*, 103, 1509-15.
- GIAID, A. 1998. Nitric oxide and endothelin-1 in pulmonary hypertension. *Chest*, 114, 208s-212s.
- GIAID, A. & SALEH, D. 1995. Reduced expression of endothelial nitric oxide synthase in the lungs of patients with pulmonary hypertension. *N Engl J Med*, 333, 214-21.
- GIRGIS, R. E., MOZAMMEL, S., CHAMPION, H. C., LI, D., PENG, X., SHIMODA, L., TUDER, R. M., JOHNS, R. A. & HASSOUN, P. M. 2007. Regression of chronic hypoxic pulmonary hypertension by simvastatin. *Am J Physiol Lung Cell Mol Physiol*, 292, L1105-10.
- GONCHAROVA, E. A., AMMIT, A. J., IRANI, C., CARROLL, R. G., ESZTERHAS, A. J., PANETTIERI, R. A. & KRYMSKAYA, V. P. 2002. PI3K is required for proliferation and migration of human pulmonary vascular smooth muscle cells. *Am J Physiol Lung Cell Mol Physiol*, 283, L354-63.
- GONCHAROVA, E. A., KHAVIN, I. S., GONCHAROV, D. A. & KRYMSKAYA, V. P. 2012. Differential effects of formoterol on thrombin- and PDGF-induced proliferation of human pulmonary arterial vascular smooth muscle cells. *Respir Res*, 13, 109.
- GORDAN, J. D., BERTOUT, J. A., HU, C. J., DIEHL, J. A. & SIMON, M. C. 2007. HIF-2 α promotes hypoxic cell proliferation by enhancing c-myc transcriptional activity. *Cancer Cell*, 11, 335-47.
- GRANT, J. S., WHITE, K., MACLEAN, M. R. & BAKER, A. H. 2013. MicroRNAs in pulmonary arterial remodeling. *Cell Mol Life Sci*, 70, 4479-94.
- GRASEMANN, H., DHALIWAL, R., IVANOVSKA, J., KANTORES, C., MCNAMARA, P. J., SCOTT, J. A., BELIK, J. & JANKOV, R. P. 2015. Arginase inhibition prevents bleomycin-induced pulmonary hypertension, vascular remodeling, and collagen deposition in neonatal rat lungs. *Am J Physiol Lung Cell Mol Physiol*, 308, L503-10.

- GREEN, D. R., GALLUZZI, L. & KROEMER, G. 2011. Mitochondria and the autophagy-inflammation-cell death axis in organismal aging. *Science*, 333, 1109-12.
- GRIMWOOD, B. G. & WAGNER, R. P. 1976. Direct action of ethidium bromide upon mitochondrial oxidative phosphorylation and morphology. *Arch Biochem Biophys*, 176, 43-52.
- GRYGLEWSKI, R. J. 1980. The lung as a generator of prostacyclin. *Ciba Found Symp*, 78, 147-64.
- GRYGLEWSKI, R. J., CHLOPICKI, S. & SWIES, J. 2005. In vivo endothelial interaction between ACE and COX inhibitors. *Prostaglandins Leukot Essent Fatty Acids*, 72, 129-31.
- GU, Y., YU, X., LI, X., WANG, X., GAO, X., WANG, M., WANG, S., LI, X. & ZHANG, Y. 2019. Inhibitory effect of mabuterol on proliferation of rat ASMCs induced by PDGF-BB via regulating [Ca(2+)]_i and mitochondrial fission/fusion. *Chem Biol Interact*, 307, 63-72.
- GUERTIN, D. A. & SABATINI, D. M. 2007. Defining the role of mTOR in cancer. *Cancer Cell*, 12, 9-22.
- GUPTA, S., BARRETT, T., WHITMARSH, A. J., CAVANAGH, J., SLUSS, H. K., DERIJARD, B. & DAVIS, R. J. 1996. Selective interaction of JNK protein kinase isoforms with transcription factors. *Embo j*, 15, 2760-70.
- GUPTA, S., CAMPBELL, D., DERIJARD, B. & DAVIS, R. J. 1995. Transcription factor ATF2 regulation by the JNK signal transduction pathway. *Science*, 267, 389-93.
- HAN, J. & SUN, P. 2007. The pathways to tumor suppression via route p38. *Trends Biochem Sci*, 32, 364-71.
- HARA, K., MARUKI, Y., LONG, X., YOSHINO, K., OSHIRO, N., HIDAYAT, S., TOKUNAGA, C., AVRUCH, J. & YONEZAWA, K. 2002. Raptor, a binding partner of target of rapamycin (TOR), mediates TOR action. *Cell*, 110, 177-89.
- HASSOUN, P. M., PASRICHA, P. J., TEUFEL, E., LEE, S. L. & FANBURG, B. L. 1989. Hypoxia stimulates the release by bovine pulmonary artery endothelial cells of an inhibitor of pulmonary artery smooth muscle cell growth. *Am J Respir Cell Mol Biol*, 1, 377-84.
- HOCHEGGER, H., DEJSUPHONG, D., SONODA, E., SABERI, A., RAJENDRA, E., KIRK, J., HUNT, T. & TAKEDA, S. 2007. An essential role for Cdk1 in S phase control is revealed via chemical genetics in vertebrate cells. *J Cell Biol*, 178, 257-68.
- HOEPER, M. M., BARST, R. J., BOURGE, R. C., FELDMAN, J., FROST, A. E., GALIE, N., GOMEZ-SANCHEZ, M. A., GRIMMINGER, F., GRUNIG, E., HASSOUN, P. M., MORRELL, N. W., PEACOCK, A. J., SATOH, T., SIMONNEAU, G., TAPSON, V. F., TORRES, F., LAWRENCE, D., QUINN, D. A. & GHOFRANI, H. A. 2013. Imatinib mesylate as add-on therapy for pulmonary arterial hypertension: results of the randomized IMPRES study. *Circulation*, 127, 1128-38.
- HOMMA, N., NAGAOKA, T., MORIO, Y., OTA, H., GEBB, S. A., KAROOR, V., MCMURTRY, I. F. & OKA, M. 2007. Endothelin-1 and serotonin are involved in activation of RhoA/Rho kinase signaling in the chronically hypoxic hypertensive rat pulmonary circulation. *J Cardiovasc Pharmacol*, 50, 697-702.

- HONGFANG, J., CONG, B., ZHAO, B., ZHANG, C., LIU, X., ZHOU, W., SHI, Y., TANG, C. & JUNBAO, D. 2006. Effects of hydrogen sulfide on hypoxic pulmonary vascular structural remodeling. *Life Sci*, 78, 1299-309.
- HORITA, H., FURGESON, S. B., OSTRICKER, A., OLSZEWSKI, K. A., SULLIVAN, T., VILLEGAS, L. R., LEVINE, M., PARR, J. E., COOL, C. D., NEMENOFF, R. A. & WEISER-EVANS, M. C. 2013. Selective inactivation of PTEN in smooth muscle cells synergizes with hypoxia to induce severe pulmonary hypertension. *J Am Heart Assoc*, 2, e000188.
- HOSHIKAWA, Y., VOELKEL, N. F., GESELL, T. L., MOORE, M. D., MORRIS, K. G., ALGER, L. A., NARUMIYA, S. & GERACI, M. W. 2001. Prostacyclin receptor-dependent modulation of pulmonary vascular remodeling. *Am J Respir Crit Care Med*, 164, 314-8.
- HOU, Y., OKAMOTO, C., OKADA, K., KAWAO, N., KAWATA, S., UESHIMA, S. & MATSUO, O. 2007. c-Myc is essential for urokinase plasminogen activator expression on hypoxia-induced vascular smooth muscle cells. *Cardiovasc Res*, 75, 186-94.
- HOWARD, L. S., CROSBY, A., VAUGHAN, P., SOBOLEWSKI, A., SOUTHWOOD, M., FOSTER, M. L., CHILVERS, E. R. & MORRELL, N. W. 2012. Distinct responses to hypoxia in subpopulations of distal pulmonary artery cells contribute to pulmonary vascular remodeling in emphysema. *Pulm Circ*, 2, 241-9.
- HOWELL, K., PRESTON, R. J. & MCLOUGHLIN, P. 2003. Chronic hypoxia causes angiogenesis in addition to remodelling in the adult rat pulmonary circulation. *J Physiol*, 547, 133-45.
- HSU, S. P., HO, P. Y., LIANG, Y. C., HO, Y. S. & LEE, W. S. 2009. Involvement of the JNK activation in terbinafine-induced p21 up-regulation and DNA synthesis inhibition in human vascular endothelial cells. *J Cell Biochem*, 108, 860-6.
- HU, J., DISCHER, D. J., BISHOPRIC, N. H. & WEBSTER, K. A. 1998. Hypoxia regulates expression of the endothelin-1 gene through a proximal hypoxia-inducible factor-1 binding site on the antisense strand. *Biochem Biophys Res Commun*, 245, 894-9.
- HUMAR, R., KIEFER, F. N., BERNS, H., RESINK, T. J. & BATTEGAY, E. J. 2002. Hypoxia enhances vascular cell proliferation and angiogenesis in vitro via rapamycin (mTOR)-dependent signaling. *Faseb j*, 16, 771-80.
- HUMBERT, M., MONTANI, D., EVGENOV, O. V. & SIMONNEAU, G. 2013. Definition and classification of pulmonary hypertension. *Handb Exp Pharmacol*, 218, 3-29.
- HUMBERT, M., MORRELL, N. W., ARCHER, S. L., STENMARK, K. R., MACLEAN, M. R., LANG, I. M., CHRISTMAN, B. W., WEIR, E. K., EICKELBERG, O., VOELKEL, N. F. & RABINOVITCH, M. 2004a. Cellular and molecular pathobiology of pulmonary arterial hypertension. *J Am Coll Cardiol*, 43, 13s-24s.
- HUMBERT, M., SITBON, O., CHAOUAT, A., BERTOCCHI, M., HABIB, G., GRESSIN, V., YAICI, A., WEITZENBLUM, E., CORDIER, J. F., CHABOT, F., DROMER, C., PISON, C., REYNAUD-GAUBERT, M., HALOUN, A., LAURENT, M., HACHULLA, E. & SIMONNEAU, G. 2006. Pulmonary arterial hypertension in France: results from a national registry. *Am J Respir Crit Care Med*, 173, 1023-30.

- HUMBERT, M., SITBON, O. & SIMONNEAU, G. 2004b. Treatment of pulmonary arterial hypertension. *N Engl J Med*, 351, 1425-36.
- IHLE, J. N., WITTHUHN, B. A., QUELLE, F. W., YAMAMOTO, K., THIERFELDER, W. E., KREIDER, B. & SILVENNOINEN, O. 1994. Signaling by the cytokine receptor superfamily: JAKs and STATs. *Trends Biochem Sci*, 19, 222-7.
- IKEDA, Y., SHIRAKABE, A., BRADY, C., ZABLOCKI, D., OHISHI, M. & SADOSHIMA, J. 2015. Molecular mechanisms mediating mitochondrial dynamics and mitophagy and their functional roles in the cardiovascular system. *J Mol Cell Cardiol*, 78, 116-22.
- IP, Y. T. & DAVIS, R. J. 1998. Signal transduction by the c-Jun N-terminal kinase (JNK)--from inflammation to development. *Curr Opin Cell Biol*, 10, 205-19.
- ISHIHARA, N., NOMURA, M., JOFUKU, A., KATO, H., SUZUKI, S. O., MASUDA, K., OTERA, H., NAKANISHI, Y., NONAKA, I., GOTO, Y., TAGUCHI, N., MORINAGA, H., MAEDA, M., TAKAYANAGI, R., YOKOTA, S. & MIHARA, K. 2009. Mitochondrial fission factor Drp1 is essential for embryonic development and synapse formation in mice. *Nat Cell Biol*, 11, 958-66.
- JIN, N., HATTON, N., SWARTZ, D. R., XIA, X., HARRINGTON, M. A., LARSEN, S. H. & RHOADES, R. A. 2000. Hypoxia activates jun-N-terminal kinase, extracellular signal-regulated protein kinase, and p38 kinase in pulmonary arteries. *Am J Respir Cell Mol Biol*, 23, 593-601.
- JIN, R. C. & LOSCALZO, J. 2010. Vascular Nitric Oxide: Formation and Function. *J Blood Med*, 2010, 147-162.
- JOHNSON, G. L. & LAPADAT, R. 2002. Mitogen-activated protein kinase pathways mediated by ERK, JNK, and p38 protein kinases. *Science*, 298, 1911-2.
- JONES, R. G., PLAS, D. R., KUBEK, S., BUZZAI, M., MU, J., XU, Y., BIRNBAUM, M. J. & THOMPSON, C. B. 2005. AMP-activated protein kinase induces a p53-dependent metabolic checkpoint. *Mol Cell*, 18, 283-93.
- KALLUNKI, T., SU, B., TSIGELNY, I., SLUSS, H. K., DERIJARD, B., MOORE, G., DAVIS, R. & KARIN, M. 1994. JNK2 contains a specificity-determining region responsible for efficient c-Jun binding and phosphorylation. *Genes Dev*, 8, 2996-3007.
- KANG, D., KIM, S. H. & HAMASAKI, N. 2007. Mitochondrial transcription factor A (TFAM): roles in maintenance of mtDNA and cellular functions. *Mitochondrion*, 7, 39-44.
- KARBOWSKI, M., NORRIS, K. L., CLELAND, M. M., JEONG, S. Y. & YOULE, R. J. 2006. Role of Bax and Bak in mitochondrial morphogenesis. *Nature*, 443, 658-62.
- KASTAN, M. B., ONYEKWERE, O., SIDRANSKY, D., VOGELSTEIN, B. & CRAIG, R. W. 1991. Participation of p53 protein in the cellular response to DNA damage. *Cancer Res*, 51, 6304-11.
- KATO, M. & STAUB, N. C. 1966. Response of small pulmonary arteries to unilobar hypoxia and hypercapnia. *Circ Res*, 19, 426-40.
- KAWANABE, Y., HASHIMOTO, N. & MASAKI, T. 2002. Extracellular Ca²⁺ influx and endothelin-1-induced intracellular mitogenic cascades in rabbit internal carotid artery vascular smooth muscle cells. *J Cardiovasc Pharmacol*, 40, 307-14.

- KELLY, C., SMALLBONE, K. & BRADY, M. 2008. Tumour glycolysis: the many faces of HIF. *J Theor Biol*, 254, 508-13.
- KIM, F. Y., BARNES, E. A., YING, L., CHEN, C., LEE, L., ALVIRA, C. M. & CORNFIELD, D. N. 2015. Pulmonary artery smooth muscle cell endothelin-1 expression modulates the pulmonary vascular response to chronic hypoxia. *Am J Physiol Lung Cell Mol Physiol*, 308, L368-77.
- KIM, J. W. & DANG, C. V. 2005. Multifaceted roles of glycolytic enzymes. *Trends Biochem Sci*, 30, 142-50.
- KIM, J. W., TCHERNYSHYOV, I., SEMENZA, G. L. & DANG, C. V. 2006. HIF-1-mediated expression of pyruvate dehydrogenase kinase: a metabolic switch required for cellular adaptation to hypoxia. *Cell Metab*, 3, 177-85.
- KIMURA, S., EGASHIRA, K., CHEN, L., NAKANO, K., IWATA, E., MIYAGAWA, M., TSUJIMOTO, H., HARA, K., MORISHITA, R., SUEISHI, K., TOMINAGA, R. & SUNAGAWA, K. 2009. Nanoparticle-mediated delivery of nuclear factor kappaB decoy into lungs ameliorates monocrotaline-induced pulmonary arterial hypertension. *Hypertension*, 53, 877-83.
- KOLB, T. M., DAMICO, R. L. & HASSOUN, P. M. 2011. Linking new and old concepts: inflammation meets the Warburg phenomenon in pulmonary arterial hypertension. *J Mol Med (Berl)*, 89, 729-32.
- KOPPENOL, W. H., BOUNDS, P. L. & DANG, C. V. 2011. Otto Warburg's contributions to current concepts of cancer metabolism. *Nat Rev Cancer*, 11, 325-37.
- KOUREMBANAS, S., MARSDEN, P. A., MCQUILLAN, L. P. & FALLER, D. V. 1991. Hypoxia induces endothelin gene expression and secretion in cultured human endothelium. *J Clin Invest*, 88, 1054-7.
- KUSHNAREVA, Y., ANDREYEV, A. Y., KUWANA, T. & NEWMAYER, D. D. 2012. Bax activation initiates the assembly of a multimeric catalyst that facilitates Bax pore formation in mitochondrial outer membranes. *PLoS Biol*, 10, e1001394.
- KWASIBORSKI, P. J., KOWALCZYK, P., MROWKA, P., KWASIBORSKI, M., CWETSCH, A. & PRZYBYLSKI, J. 2012. [Selected, biochemical markers of hypoxia]. *Przegl Lek*, 69, 115-9.
- KYAW, M., YOSHIZUMI, M., TSUCHIYA, K., KIRIMA, K., SUZAKI, Y., ABE, S., HASEGAWA, T. & TAMAKI, T. 2002. Antioxidants inhibit endothelin-1 (1-31)-induced proliferation of vascular smooth muscle cells via the inhibition of mitogen-activated protein (MAP) kinase and activator protein-1 (AP-1). *Biochem Pharmacol*, 64, 1521-31.
- LAGNEUX, C., LEBRIN, F., DEMENGE, P., GODIN-RIBUOT, D. & RIBUOT, C. 2001. MAP-kinase dependent activation of kinin B1 receptor gene transcription after heat stress in rat vascular smooth muscle cells. *Int Immunopharmacol*, 1, 533-8.
- LANNER, M. C., RAPER, M., PRATT, W. M. & RHOADES, R. A. 2005. Heterotrimeric G proteins and the platelet-derived growth factor receptor-beta contribute to hypoxic proliferation of smooth muscle cells. *Am J Respir Cell Mol Biol*, 33, 412-9.
- LAPLANTE, M. & SABATINI, D. M. 2012. mTOR signaling in growth control and disease. *Cell*, 149, 274-93.

- LAVRENTIEVA, A., MAJORE, I., KASPER, C. & HASS, R. 2010. Effects of hypoxic culture conditions on umbilical cord-derived human mesenchymal stem cells. *Cell Commun Signal*, 8, 18.
- LEE, D. F., KUO, H. P., CHEN, C. T., WEI, Y., CHOU, C. K., HUNG, J. Y., YEN, C. J. & HUNG, M. C. 2008. IKKbeta suppression of TSC1 function links the mTOR pathway with insulin resistance. *Int J Mol Med*, 22, 633-8.
- LEE, H. J., RYU, J. M., JUNG, Y. H., OH, S. Y., LEE, S. J. & HAN, H. J. 2015. Novel Pathway for Hypoxia-Induced Proliferation and Migration in Human Mesenchymal Stem Cells: Involvement of HIF-1alpha, FASN, and mTORC1. *Stem Cells*, 33, 2182-95.
- LEE, Y., DOMINY, J. E., CHOI, Y. J., JURCZAK, M., TOLLIDAY, N., CAMPOREZ, J. P., CHIM, H., LIM, J. H., RUAN, H. B., YANG, X., VAZQUEZ, F., SICINSKI, P., SHULMAN, G. I. & PUIGSERVER, P. 2014. Cyclin D1-Cdk4 controls glucose metabolism independently of cell cycle progression. *Nature*, 510, 547-51.
- LI, L., BLUMENTHAL, D. K., MASAKI, T., TERRY, C. M. & CHEUNG, A. K. 2006. Differential effects of imatinib on PDGF-induced proliferation and PDGF receptor signaling in human arterial and venous smooth muscle cells. *J Cell Biochem*, 99, 1553-63.
- LI, P. F., DIETZ, R. & VON HARSDORF, R. 1997. Differential effect of hydrogen peroxide and superoxide anion on apoptosis and proliferation of vascular smooth muscle cells. *Circulation*, 96, 3602-9.
- LI, Y., LI, X., LIU, J., GUO, W., ZHANG, H. & WANG, J. 2017. Enhanced Rb/E2F and TSC/mTOR Pathways Induce Synergistic Inhibition in PDGF-Induced Proliferation in Vascular Smooth Muscle Cells. *PLoS One*, 12, e0170036.
- LIM, C. P. & CAO, X. 1999. Serine phosphorylation and negative regulation of Stat3 by JNK. *J Biol Chem*, 274, 31055-61.
- LIM, S., LEE, S. Y., SEO, H. H., HAM, O., LEE, C., PARK, J. H., LEE, J., SEUNG, M., YUN, I., HAN, S. M., LEE, S., CHOI, E. & HWANG, K. C. 2015. Regulation of mitochondrial morphology by positive feedback interaction between PKCdelta and Drp1 in vascular smooth muscle cell. *J Cell Biochem*, 116, 648-60.
- LIN, S. C., LIAO, W. L., LEE, J. C. & TSAI, S. J. 2014. Hypoxia-regulated gene network in drug resistance and cancer progression. *Exp Biol Med (Maywood)*, 239, 779-792.
- LIN, X., HE, Y., HOU, X., ZHANG, Z., WANG, R. & WU, Q. 2016. Endothelial Cells Can Regulate Smooth Muscle Cells in Contractile Phenotype through the miR-206/ARF6&NCX1/Exosome Axis. *PLoS One*, 11, e0152959.
- LING, Y., JOHNSON, M. K., KIELY, D. G., CONDLIFFE, R., ELLIOT, C. A., GIBBS, J. S., HOWARD, L. S., PEPKE-ZABA, J., SHEARES, K. K., CORRIS, P. A., FISHER, A. J., LORDAN, J. L., GAINE, S., COGHLAN, J. G., WORT, S. J., GATZOULIS, M. A. & PEACOCK, A. J. 2012. Changing demographics, epidemiology, and survival of incident pulmonary arterial hypertension: results from the pulmonary hypertension registry of the United Kingdom and Ireland. *Am J Respir Crit Care Med*, 186, 790-6.
- LIU, Q., SHAM, J. S., SHIMODA, L. A. & SYLVESTER, J. T. 2001. Hypoxic constriction of porcine distal pulmonary arteries: endothelium and endothelin dependence. *Am J Physiol Lung Cell Mol Physiol*, 280, L856-65.

- LIU, Y., SUZUKI, Y. J., DAY, R. M. & FANBURG, B. L. 2004. Rho kinase-induced nuclear translocation of ERK1/ERK2 in smooth muscle cell mitogenesis caused by serotonin. *Circ Res*, 95, 579-86.
- LUCAS, K. A., PITARI, G. M., KAZEROUNIAN, S., RUIZ-STEWART, I., PARK, J., SCHULZ, S., CHEPENIK, K. P. & WALDMAN, S. A. 2000. Guanylyl cyclases and signaling by cyclic GMP. *Pharmacol Rev*, 52, 375-414.
- LUO, Y., XU, D. Q., DONG, H. Y., ZHANG, B., LIU, Y., NIU, W., DONG, M. Q. & LI, Z. C. 2013. Tanshinone IIA inhibits hypoxia-induced pulmonary artery smooth muscle cell proliferation via Akt/Skp2/p27-associated pathway. *PLoS One*, 8, e56774.
- MA, J., ZHANG, Q., CHEN, S., FANG, B., YANG, Q., CHEN, C., MIELE, L., SARKAR, F. H., XIA, J. & WANG, Z. 2013. Mitochondrial dysfunction promotes breast cancer cell migration and invasion through HIF1alpha accumulation via increased production of reactive oxygen species. *PLoS One*, 8, e69485.
- MACLEAN, M. R., MCCULLOCH, K. M. & BAIRD, M. 1994. Endothelin ETA- and ETB-receptor-mediated vasoconstriction in rat pulmonary arteries and arterioles. *J Cardiovasc Pharmacol*, 23, 838-45.
- MADDOCKS, O. D. & VOUSDEN, K. H. 2011. Metabolic regulation by p53. *J Mol Med (Berl)*, 89, 237-45.
- MAGUIRE, J. J., KUC, R. E. & DAVENPORT, A. P. 2001. Vasoconstrictor activity of novel endothelin peptide, ET-1(1 - 31), in human mammary and coronary arteries in vitro. *Br J Pharmacol*, 134, 1360-6.
- MAHON, P. C., HIROTA, K. & SEMENZA, G. L. 2001. FIH-1: a novel protein that interacts with HIF-1alpha and VHL to mediate repression of HIF-1 transcriptional activity. *Genes Dev*, 15, 2675-86.
- MAI, S., KLINKENBERG, M., AUBURGER, G., BEREITER-HAHN, J. & JENDRACH, M. 2010. Decreased expression of Drp1 and Fis1 mediates mitochondrial elongation in senescent cells and enhances resistance to oxidative stress through PINK1. *J Cell Sci*, 123, 917-26.
- MAIR, K. M., MACLEAN, M. R., MORECROFT, I., DEMPSIE, Y. & PALMER, T. M. 2008. Novel interactions between the 5-HT transporter, 5-HT1B receptors and Rho kinase in vivo and in pulmonary fibroblasts. *Br J Pharmacol*, 155, 606-16.
- MANDAL, S., FREIJE, W. A., GUPTAN, P. & BANERJEE, U. 2010. Metabolic control of G1-S transition: cyclin E degradation by p53-induced activation of the ubiquitin-proteasome system. *J Cell Biol*, 188, 473-9.
- MANDEGAR, M., FUNG, Y. C., HUANG, W., REMILLARD, C. V., RUBIN, L. J. & YUAN, J. X. 2004. Cellular and molecular mechanisms of pulmonary vascular remodeling: role in the development of pulmonary hypertension. *Microvasc Res*, 68, 75-103.
- MARON, B. A. & LOSCALZO, J. 2013. Pulmonary hypertension: pathophysiology and signaling pathways. *Handb Exp Pharmacol*, 218, 31-58.
- MARSBOOM, G., TOTH, P. T., RYAN, J. J., HONG, Z., WU, X., FANG, Y. H., THENAPPAN, T., PIAO, L., ZHANG, H. J., POGORILER, J., CHEN, Y., MORROW, E., WEIR, E. K., REHMAN, J. & ARCHER, S. L. 2012. Dynamin-related protein 1-mediated mitochondrial mitotic fission permits

- hyperproliferation of vascular smooth muscle cells and offers a novel therapeutic target in pulmonary hypertension. *Circ Res*, 110, 1484-97.
- MARSHALL, C., MAMARY, A. J., VERHOEVEN, A. J. & MARSHALL, B. E. 1996. Pulmonary artery NADPH-oxidase is activated in hypoxic pulmonary vasoconstriction. *Am J Respir Cell Mol Biol*, 15, 633-44.
- MARSHALL, C. & MARSHALL, B. E. 1992. Hypoxic pulmonary vasoconstriction is not endothelium dependent. *Proc Soc Exp Biol Med*, 201, 267-70.
- MARTINEZ-LEMUS, L. A., HESTER, R. K., BECKER, E. J., JEFFREY, J. S. & ODOM, T. W. 1999. Pulmonary artery endothelium-dependent vasodilation is impaired in a chicken model of pulmonary hypertension. *Am J Physiol*, 277, R190-7.
- MCLAUGHLIN, V. V. & MCGOON, M. D. 2006. Pulmonary arterial hypertension. *Circulation*, 114, 1417-31.
- MICHELAKIS, E. D. 2003. The role of the NO axis and its therapeutic implications in pulmonary arterial hypertension. *Heart Fail Rev*, 8, 5-21.
- MICHELAKIS, E. D., HAMPL, V., NSAIR, A., WU, X., HARRY, G., HAROMY, A., GURTU, R. & ARCHER, S. L. 2002. Diversity in mitochondrial function explains differences in vascular oxygen sensing. *Circ Res*, 90, 1307-15.
- MICHIELS, C., DE LEENER, F., ARNOULD, T., DIEU, M. & REMACLE, J. 1994. Hypoxia stimulates human endothelial cells to release smooth muscle cell mitogens: role of prostaglandins and bFGF. *Exp Cell Res*, 213, 43-54.
- MILANINI, J., VINALS, F., POUYSSEGUR, J. & PAGES, G. 1998. p42/p44 MAP kinase module plays a key role in the transcriptional regulation of the vascular endothelial growth factor gene in fibroblasts. *J Biol Chem*, 273, 18165-72.
- MILEWICZ, D. M., KWARTLER, C. S., PAPKE, C. L., REGALADO, E. S., CAO, J. & REID, A. J. 2010. Genetic variants promoting smooth muscle cell proliferation can result in diffuse and diverse vascular diseases: evidence for a hyperplastic vasculomyopathy. *Genet Med*, 12, 196-203.
- MISHRA, P. & CHAN, D. C. 2014. Mitochondrial dynamics and inheritance during cell division, development and disease. *Nat Rev Mol Cell Biol*, 15, 634-46.
- MITRA, K., WUNDER, C., ROYSAM, B., LIN, G. & LIPPINCOTT-SCHWARTZ, J. 2009. A hyperfused mitochondrial state achieved at G1-S regulates cyclin E buildup and entry into S phase. *Proc Natl Acad Sci U S A*, 106, 11960-5.
- MIZUNO, S., ISHIZAKI, T., TOGA, H., SAKAI, A., ISAKOVA, J., TAALAIBEKOVA, E., BAISERKEEV, Z., KOJONAZAROV, B. & ALDASHEV, A. 2015. Endogenous Asymmetric Dimethylarginine Pathway in High Altitude Adapted Yaks. *Biomed Res Int*, 2015, 196904.
- MOLEDINA, S., DE BRUYN, A., SCHIEVANO, S., OWENS, C. M., YOUNG, C., HAWORTH, S. G., TAYLOR, A. M., SCHULZE-NEICK, I. & MUTHURANGU, V. 2011. Fractal branching quantifies vascular changes and predicts survival in pulmonary hypertension: a proof of principle study. *Heart*, 97, 1245-9.
- MONCADA, S., HIGGS, E. A. & COLOMBO, S. L. 2012. Fulfilling the metabolic requirements for cell proliferation. *Biochem J*, 446, 1-7.

- MONCADA, S. & VANE, J. R. 1981. Prostacyclin: its biosynthesis, actions and clinical potential. *Philos Trans R Soc Lond B Biol Sci*, 294, 305-29.
- MORGAN, D. O. 1995. Principles of CDK regulation. *Nature*, 374, 131-4.
- MORITA, M., GRAVEL, S. P., CHENARD, V., SIKSTROM, K., ZHENG, L., ALAIN, T., GANDIN, V., AVIZONIS, D., ARGUELLO, M., ZAKARIA, C., MCLAUGHLAN, S., NOUET, Y., PAUSE, A., POLLAK, M., GOTTLIEB, E., LARSSON, O., ST-PIERRE, J., TOPISIROVIC, I. & SONENBERG, N. 2013. mTORC1 controls mitochondrial activity and biogenesis through 4E-BP-dependent translational regulation. *Cell Metab*, 18, 698-711.
- MORRELL, N. W., ADNOT, S., ARCHER, S. L., DUPUIS, J., JONES, P. L., MACLEAN, M. R., MCMURTRY, I. F., STENMARK, K. R., THISTLETHWAITE, P. A., WEISSMANN, N., YUAN, J. X. & WEIR, E. K. 2009. Cellular and molecular basis of pulmonary arterial hypertension. *J Am Coll Cardiol*, 54, S20-31.
- MUBARAK, K. K. 2010. A review of prostaglandin analogs in the management of patients with pulmonary arterial hypertension. *Respir Med*, 104, 9-21.
- MUNOZ, J. P., IVANOVA, S., SANCHEZ-WANDELMER, J., MARTINEZ-CRISTOBAL, P., NOGUERA, E., SANCHO, A., DIAZ-RAMOS, A., HERNANDEZ-ALVAREZ, M. I., SEBASTIAN, D., MAUVEZIN, C., PALACIN, M. & ZORZANO, A. 2013. Mfn2 modulates the UPR and mitochondrial function via repression of PERK. *Embo j*, 32, 2348-61.
- MURPHY, E. & STEENBERGEN, C. 2011. What makes the mitochondria a killer? Can we condition them to be less destructive? *Biochim Biophys Acta*, 1813, 1302-8.
- MURRAY, T. R., CHEN, L., MARSHALL, B. E. & MACARAK, E. J. 1990. Hypoxic contraction of cultured pulmonary vascular smooth muscle cells. *Am J Respir Cell Mol Biol*, 3, 457-65.
- MUTHUSAMY, V. & PIVA, T. J. 2013. A comparative study of UV-induced cell signalling pathways in human keratinocyte-derived cell lines. *Arch Dermatol Res*, 305, 817-33.
- NAIR, S., SOBOTKA, K. S., JOSHI, P., GRESSENS, P., FLEISS, B., THORNTON, C., MALLARD, C. & HAGBERG, H. 2019. Lipopolysaccharide-induced alteration of mitochondrial morphology induces a metabolic shift in microglia modulating the inflammatory response in vitro and in vivo. *Glia*, 67, 1047-1061.
- NAKAMURA, K., AKAGI, S., OGAWA, A., KUSANO, K. F., MATSUBARA, H., MIURA, D., FUKU, S., NISHII, N., NAGASE, S., KOHNO, K., MORITA, H., OTO, T., YAMANAKA, R., OTSUKA, F., MIURA, A., YUTANI, C., OHE, T. & ITO, H. 2012. Pro-apoptotic effects of imatinib on PDGF-stimulated pulmonary artery smooth muscle cells from patients with idiopathic pulmonary arterial hypertension. *Int J Cardiol*, 159, 100-6.
- NORTHWOOD, I. C., GONZALEZ, F. A., WARTMANN, M., RADEN, D. L. & DAVIS, R. J. 1991. Isolation and characterization of two growth factor-stimulated protein kinases that phosphorylate the epidermal growth factor receptor at threonine 669. *J Biol Chem*, 266, 15266-76.
- ONG, S. B., SUBRAYAN, S., LIM, S. Y., YELLON, D. M., DAVIDSON, S. M. & HAUSENLOY, D. J. 2010. Inhibiting mitochondrial fission protects the heart against ischemia/reperfusion injury. *Circulation*, 121, 2012-22.

- OPARIL, S., CHEN, S. J., MENG, Q. C., ELTON, T. S., YANO, M. & CHEN, Y. F. 1995. Endothelin-A receptor antagonist prevents acute hypoxia-induced pulmonary hypertension in the rat. *Am J Physiol*, 268, L95-100.
- OWENS, G. K., KUMAR, M. S. & WAMHOFF, B. R. 2004. Molecular regulation of vascular smooth muscle cell differentiation in development and disease. *Physiol Rev*, 84, 767-801.
- OWUSU-ANSAH, E., YAVARI, A., MANDAL, S. & BANERJEE, U. 2008. Distinct mitochondrial retrograde signals control the G1-S cell cycle checkpoint. *Nat Genet*, 40, 356-61.
- PAFFETT, M. L. & WALKER, B. R. 2007. Vascular adaptations to hypoxia: molecular and cellular mechanisms regulating vascular tone. *Essays Biochem*, 43, 105-19.
- PALMER, R. M., ASHTON, D. S. & MONCADA, S. 1988. Vascular endothelial cells synthesize nitric oxide from L-arginine. *Nature*, 333, 664-6.
- PAPANDREOU, I., CAIRNS, R. A., FONTANA, L., LIM, A. L. & DENKO, N. C. 2006. HIF-1 mediates adaptation to hypoxia by actively downregulating mitochondrial oxygen consumption. *Cell Metab*, 3, 187-97.
- PARONE, P. A., DA CRUZ, S., TONDERA, D., MATTENBERGER, Y., JAMES, D. I., MAECHLER, P., BARJA, F. & MARTINOU, J. C. 2008. Preventing mitochondrial fission impairs mitochondrial function and leads to loss of mitochondrial DNA. *PLoS One*, 3, e3257.
- PARRA, V., BRAVO-SAGUA, R., NORAMBUENA-SOTO, I., HERNANDEZ-FUENTES, C. P., GOMEZ-CONTRERAS, A. G., VERDEJO, H. E., MELLADO, R., CHIONG, M., LAVANDERO, S. & CASTRO, P. F. 2017. Inhibition of mitochondrial fission prevents hypoxia-induced metabolic shift and cellular proliferation of pulmonary arterial smooth muscle cells. *Biochim Biophys Acta Mol Basis Dis*, 1863, 2891-2903.
- PAULIN, R. & MICHELAKIS, E. D. 2014. The metabolic theory of pulmonary arterial hypertension. *Circ Res*, 115, 148-64.
- PEACOCK, A. J., MURPHY, N. F., MCMURRAY, J. J., CABALLERO, L. & STEWART, S. 2007. An epidemiological study of pulmonary arterial hypertension. *Eur Respir J*, 30, 104-9.
- PEARSON, G., ROBINSON, F., BEERS GIBSON, T., XU, B. E., KARANDIKAR, M., BERMAN, K. & COBB, M. H. 2001. Mitogen-activated protein (MAP) kinase pathways: regulation and physiological functions. *Endocr Rev*, 22, 153-83.
- PEREZ, J., HILL, B. G., BENAVIDES, G. A., DRANKA, B. P. & DARLEY-USMAR, V. M. 2010. Role of cellular bioenergetics in smooth muscle cell proliferation induced by platelet-derived growth factor. *Biochem J*, 428, 255-67.
- PETI, W. & PAGE, R. 2013. Molecular basis of MAP kinase regulation. *Protein Sci*, 22, 1698-710.
- PIETRA, G. G., CAPRON, F., STEWART, S., LEONE, O., HUMBERT, M., ROBBINS, I. M., REID, L. M. & TUDER, R. M. 2004. Pathologic assessment of vasculopathies in pulmonary hypertension. *J Am Coll Cardiol*, 43, 25s-32s.
- PISARCIK, S., MAYLOR, J., LU, W., YUN, X., UNDEM, C., SYLVESTER, J. T., SEMENZA, G. L. & SHIMODA, L. A. 2013. Activation of hypoxia-inducible factor-1 in pulmonary arterial smooth muscle cells by endothelin-1. *Am J Physiol Lung Cell Mol Physiol*, 304, L549-61.

- PLATOSHYN, O., YU, Y., GOLOVINA, V. A., MCDANIEL, S. S., KRICK, S., LI, L., WANG, J. Y., RUBIN, L. J. & YUAN, J. X. 2001. Chronic hypoxia decreases K(V) channel expression and function in pulmonary artery myocytes. *Am J Physiol Lung Cell Mol Physiol*, 280, L801-12.
- PRESTON, I. R., HILL, N. S., WARBURTON, R. R. & FANBURG, B. L. 2006. Role of 12-lipoxygenase in hypoxia-induced rat pulmonary artery smooth muscle cell proliferation. *Am J Physiol Lung Cell Mol Physiol*, 290, L367-74.
- PULIDO, T., ADZERIKHO, I., CHANNICK, R. N., DELCROIX, M., GALIE, N., GHOFRANI, H. A., JANSA, P., JING, Z. C., LE BRUN, F. O., MEHTA, S., MITTELHOLZER, C. M., PERCHENET, L., SASTRY, B. K., SITBON, O., SOUZA, R., TORBICKI, A., ZENG, X., RUBIN, L. J. & SIMONNEAU, G. 2013. Macitentan and morbidity and mortality in pulmonary arterial hypertension. *N Engl J Med*, 369, 809-18.
- RABINOVITCH, M. 2008. Molecular pathogenesis of pulmonary arterial hypertension. *J Clin Invest*, 118, 2372-9.
- RATHORE, R., ZHENG, Y. M., LI, X. Q., WANG, Q. S., LIU, Q. H., GINNAN, R., SINGER, H. A., HO, Y. S. & WANG, Y. X. 2006. Mitochondrial ROS-PKCepsilon signaling axis is uniquely involved in hypoxic increase in [Ca²⁺]_i in pulmonary artery smooth muscle cells. *Biochem Biophys Res Commun*, 351, 784-90.
- RAY, L. B. & STURGILL, T. W. 1987. Rapid stimulation by insulin of a serine/threonine kinase in 3T3-L1 adipocytes that phosphorylates microtubule-associated protein 2 in vitro. *Proc Natl Acad Sci U S A*, 84, 1502-6.
- REHMAN, J., ZHANG, H. J., TOTH, P. T., ZHANG, Y., MARSBOOM, G., HONG, Z., SALGIA, R., HUSAIN, A. N., WIETHOLT, C. & ARCHER, S. L. 2012. Inhibition of mitochondrial fission prevents cell cycle progression in lung cancer. *Faseb j*, 26, 2175-86.
- REICHERT, A. S. & NEUPERT, W. 2002. Contact sites between the outer and inner membrane of mitochondria-role in protein transport. *Biochim Biophys Acta*, 1592, 41-9.
- REID, L. M. 1986. Structure and function in pulmonary hypertension. New perceptions. *Chest*, 89, 279-88.
- REN, W., WATTS, S. W. & FANBURG, B. L. 2011. Serotonin transporter interacts with the PDGFbeta receptor in PDGF-BB-induced signaling and mitogenesis in pulmonary artery smooth muscle cells. *Am J Physiol Lung Cell Mol Physiol*, 300, L486-97.
- RENSEN, S. S., DOEVENDANS, P. A. & VAN EYS, G. J. 2007. Regulation and characteristics of vascular smooth muscle cell phenotypic diversity. *Neth Heart J*, 15, 100-8.
- REUTER, C. W., MORGAN, M. A. & BERGMANN, L. 2000. Targeting the Ras signaling pathway: a rational, mechanism-based treatment for hematologic malignancies? *Blood*, 96, 1655-69.
- RICARD, N., TU, L., LE HIRESS, M., HUERTAS, A., PHAN, C., THUILLET, R., SATTLER, C., FADEL, E., SEFERIAN, A., MONTANI, D., DORFMULLER, P., HUMBERT, M. & GUIGNABERT, C. 2014. Increased pericyte coverage mediated by endothelial-derived fibroblast growth factor-2 and interleukin-6 is a source of smooth muscle-like cells in pulmonary hypertension. *Circulation*, 129, 1586-97.

- RICH, S., DANTZKER, D. R., AYRES, S. M., BERGOFKY, E. H., BRUNDAGE, B. H., DETRE, K. M., FISHMAN, A. P., GOLDRING, R. M., GROVES, B. M., KOERNER, S. K. & ET AL. 1987. Primary pulmonary hypertension. A national prospective study. *Ann Intern Med*, 107, 216-23.
- RICHTER, J. D. & SONENBERG, N. 2005. Regulation of cap-dependent translation by eIF4E inhibitory proteins. *Nature*, 433, 477-80.
- ROBELLET, X., THATTIKOTA, Y., WANG, F., WEE, T. L., PASCARIU, M., SHANKAR, S., BONNEIL, E., BROWN, C. M. & D'AMOURS, D. 2015. A high-sensitivity phospho-switch triggered by Cdk1 governs chromosome morphogenesis during cell division. *Genes Dev*, 29, 426-39.
- ROBINSON, M. J. & COBB, M. H. 1997. Mitogen-activated protein kinase pathways. *Curr Opin Cell Biol*, 9, 180-6.
- ROSDAH, A. A., J, K. H., DELBRIDGE, L. M., DUSTING, G. J. & LIM, S. Y. 2016. Mitochondrial fission - a drug target for cytoprotection or cytodestruction? *Pharmacol Res Perspect*, 4, e00235.
- ROUX, P. P. & BLENIS, J. 2004. ERK and p38 MAPK-activated protein kinases: a family of protein kinases with diverse biological functions. *Microbiol Mol Biol Rev*, 68, 320-44.
- RUBIN, B., COOLEY, M. A., LE BORGNE DE KAOUEL, C., TAYLOR, R. B. & GOLSTEIN, P. 1980. Production and main characteristics of a fetal calf serum-specific cell line that induces T and B cell differentiation. *Scand J Immunol*, 12, 401-9.
- RUBIN, L. J., BADESCH, D. B., BARST, R. J., GALIE, N., BLACK, C. M., KEOGH, A., PULIDO, T., FROST, A., ROUX, S., LECONTE, I., LANDZBERG, M. & SIMONNEAU, G. 2002. Bosentan therapy for pulmonary arterial hypertension. *N Engl J Med*, 346, 896-903.
- RUDIJANTO, A. 2007. The role of vascular smooth muscle cells on the pathogenesis of atherosclerosis. *Acta Med Indones*, 39, 86-93.
- RYAN, J., DASGUPTA, A., HUSTON, J., CHEN, K. H. & ARCHER, S. L. 2015. Mitochondrial dynamics in pulmonary arterial hypertension. *J Mol Med (Berl)*, 93, 229-42.
- SAGIRKAYA, H., MISIRLIOGLU, M., KAYA, A., FIRST, N. L., PARRISH, J. J. & MEMILI, E. 2007. Developmental potential of bovine oocytes cultured in different maturation and culture conditions. *Anim Reprod Sci*, 101, 225-40.
- SAKAO, S., TATSUMI, K. & VOELKEL, N. F. 2009. Endothelial cells and pulmonary arterial hypertension: apoptosis, proliferation, interaction and transdifferentiation. *Respir Res*, 10, 95.
- SALABEI, J. K. & HILL, B. G. 2013. Mitochondrial fission induced by platelet-derived growth factor regulates vascular smooth muscle cell bioenergetics and cell proliferation. *Redox Biol*, 1, 542-51.
- SALCEDA, S. & CARO, J. 1997. Hypoxia-inducible factor 1alpha (HIF-1alpha) protein is rapidly degraded by the ubiquitin-proteasome system under normoxic conditions. Its stabilization by hypoxia depends on redox-induced changes. *J Biol Chem*, 272, 22642-7.
- SARBASSOV, D. D., ALI, S. M., KIM, D. H., GUERTIN, D. A., LATEK, R. R., ERDJUMENT-BROMAGE, H., TEMPST, P. & SABATINI, D. M. 2004. Rictor, a novel binding partner of mTOR, defines a rapamycin-insensitive and raptor-independent pathway that regulates the cytoskeleton. *Curr Biol*, 14, 1296-302.

- SAVAI, R., AL-TAMARI, H. M., SEDDING, D., KOJONAZAROV, B., MUECKE, C., TESKE, R., CAPECCHI, M. R., WEISSMANN, N., GRIMMINGER, F., SEEGER, W., SCHERMULY, R. T. & PULLAMSETTI, S. S. 2014. Pro-proliferative and inflammatory signaling converge on FoxO1 transcription factor in pulmonary hypertension. *Nat Med*, 20, 1289-300.
- SAVAI, R., PULLAMSETTI, S. S., KOLBE, J., BIENIEK, E., VOSWINCKEL, R., FINK, L., SCHEED, A., RITTER, C., DAHAL, B. K., VATER, A., KLUSSMANN, S., GHOFRANI, H. A., WEISSMANN, N., KLEPETKO, W., BANAT, G. A., SEEGER, W., GRIMMINGER, F. & SCHERMULY, R. T. 2012. Immune and inflammatory cell involvement in the pathology of idiopathic pulmonary arterial hypertension. *Am J Respir Crit Care Med*, 186, 897-908.
- SCHERMULY, R. T., DONY, E., GHOFRANI, H. A., PULLAMSETTI, S., SAVA I, R., ROTH, M., SYDYKOV, A., LAI, Y. J., WEISSMANN, N., SEEGER, W. & GRIMMINGER, F. 2005. Reversal of experimental pulmonary hypertension by PDGF inhibition. *J Clin Invest*, 115, 2811-21.
- SCHERMULY, R. T., KREISSELMEIER, K. P., GHOFRANI, H. A., YILMAZ, H., BUTROUS, G., ERMERT, L., ERMERT, M., WEISSMANN, N., ROSE, F., GUENTHER, A., WALMRATH, D., SEEGER, W. & GRIMMINGER, F. 2004. Chronic sildenafil treatment inhibits monocrotaline-induced pulmonary hypertension in rats. *Am J Respir Crit Care Med*, 169, 39-45.
- SCHOFIELD, C. J. & RATCLIFFE, P. J. 2004. Oxygen sensing by HIF hydroxylases. *Nat Rev Mol Cell Biol*, 5, 343-54.
- SCHULTZ, K., FANBURG, B. L. & BEASLEY, D. 2006. Hypoxia and hypoxia-inducible factor-1 α promote growth factor-induced proliferation of human vascular smooth muscle cells. *Am J Physiol Heart Circ Physiol*, 290, H2528-34.
- SCOTT, P. H., PAUL, A., BELHAM, C. M., PEACOCK, A. J., WADSWORTH, R. M., GOULD, G. W., WELSH, D. & PLEVIN, R. 1998. Hypoxic stimulation of the stress-activated protein kinases in pulmonary artery fibroblasts. *Am J Respir Crit Care Med*, 158, 958-62.
- SEMENZA, G. L. 2007. Oxygen-dependent regulation of mitochondrial respiration by hypoxia-inducible factor 1. *Biochem J*, 405, 1-9.
- SEMENZA, G. L., JIANG, B. H., LEUNG, S. W., PASSANTINO, R., CONCORDET, J. P., MAIRE, P. & GIALLONGO, A. 1996. Hypoxia response elements in the aldolase A, enolase 1, and lactate dehydrogenase A gene promoters contain essential binding sites for hypoxia-inducible factor 1. *J Biol Chem*, 271, 32529-37.
- SEO, B., OEMAR, B. S., SIEBENMANN, R., VON SEGESSER, L. & LUSCHER, T. F. 1994. Both ETA and ETB receptors mediate contraction to endothelin-1 in human blood vessels. *Circulation*, 89, 1203-8.
- SHAM, J. S., CRENSHAW, B. R., JR., DENG, L. H., SHIMODA, L. A. & SYLVESTER, J. T. 2000. Effects of hypoxia in porcine pulmonary arterial myocytes: roles of K(V) channel and endothelin-1. *Am J Physiol Lung Cell Mol Physiol*, 279, L262-72.
- SHARP, W. W., FANG, Y. H., HAN, M., ZHANG, H. J., HONG, Z., BANATHY, A., MORROW, E., RYAN, J. J. & ARCHER, S. L. 2014. Dynamin-related protein 1 (Drp1)-mediated diastolic dysfunction in myocardial ischemia-

- reperfusion injury: therapeutic benefits of Drp1 inhibition to reduce mitochondrial fission. *Faseb j*, 28, 316-26.
- SHAUL, Y. D. & SEGER, R. 2007. The MEK/ERK cascade: from signaling specificity to diverse functions. *Biochim Biophys Acta*, 1773, 1213-26.
- SHEIKH, A. Q., LIGHTHOUSE, J. K. & GREIF, D. M. 2014. Recapitulation of developing artery muscularization in pulmonary hypertension. *Cell Rep*, 6, 809-17.
- SHEN, Y. J., ZHU, X. X., YANG, X., JIN, B., LU, J. J., DING, B., DING, Z. S. & CHEN, S. H. 2014. Cardamonin inhibits angiotensin II-induced vascular smooth muscle cell proliferation and migration by downregulating p38 MAPK, Akt, and ERK phosphorylation. *J Nat Med*, 68, 623-9.
- SHIMODA, L. A., SYLVESTER, J. T. & SHAM, J. S. 2000. Mobilization of intracellular Ca(2+) by endothelin-1 in rat intrapulmonary arterial smooth muscle cells. *Am J Physiol Lung Cell Mol Physiol*, 278, L157-64.
- SIMONNEAU, G., GATZOULIS, M. A., ADATIA, I., CELERMAJER, D., DENTON, C., GHOFRANI, A., GOMEZ SANCHEZ, M. A., KRISHNA KUMAR, R., LANDZBERG, M., MACHADO, R. F., OLSCHIEWSKI, H., ROBBINS, I. M. & SOUZA, R. 2013. Updated clinical classification of pulmonary hypertension. *J Am Coll Cardiol*, 62, D34-41.
- SIMONNEAU, G., ROBBINS, I. M., BEGHETTI, M., CHANNICK, R. N., DELCROIX, M., DENTON, C. P., ELLIOTT, C. G., GAINE, S. P., GLADWIN, M. T., JING, Z. C., KROWKA, M. J., LANGLEBEN, D., NAKANISHI, N. & SOUZA, R. 2009. Updated clinical classification of pulmonary hypertension. *J Am Coll Cardiol*, 54, S43-54.
- SITBON, O., BADESCH, D. B., CHANNICK, R. N., FROST, A., ROBBINS, I. M., SIMONNEAU, G., TAPSON, V. F. & RUBIN, L. J. 2003. Effects of the dual endothelin receptor antagonist bosentan in patients with pulmonary arterial hypertension: a 1-year follow-up study. *Chest*, 124, 247-54.
- SITBON, O., HUMBERT, M., JAIS, X., IOOS, V., HAMID, A. M., PROVENCHER, S., GARCIA, G., PARENT, F., HERVE, P. & SIMONNEAU, G. 2005. Long-term response to calcium channel blockers in idiopathic pulmonary arterial hypertension. *Circulation*, 111, 3105-11.
- SMITH, G. & GALLO, G. 2017. To mdivi-1 or not to mdivi-1: Is that the question? *Dev Neurobiol*, 77, 1260-1268.
- SMITH, R. A., HARTLEY, R. C., COCHEME, H. M. & MURPHY, M. P. 2012. Mitochondrial pharmacology. *Trends Pharmacol Sci*, 33, 341-52.
- SO, E. C., HSING, C. H., LIANG, C. H. & WU, S. N. 2012. The actions of mdivi-1, an inhibitor of mitochondrial fission, on rapidly activating delayed-rectifier K(+) current and membrane potential in HL-1 murine atrial cardiomyocytes. *Eur J Pharmacol*, 683, 1-9.
- SOMLYO, A. P. & SOMLYO, A. V. 1994. Signal transduction and regulation in smooth muscle. *Nature*, 372, 231-6.
- SOMMER, N., DIETRICH, A., SCHERMULY, R. T., GHOFRANI, H. A., GUDERMANN, T., SCHULZ, R., SEEGER, W., GRIMMINGER, F. & WEISSMANN, N. 2008. Regulation of hypoxic pulmonary vasoconstriction: basic mechanisms. *Eur Respir J*, 32, 1639-51.
- SPRAGUE, A. H. & KHALIL, R. A. 2009. Inflammatory cytokines in vascular dysfunction and vascular disease. *Biochem Pharmacol*, 78, 539-52.
- STACEY, D. W. 2003. Cyclin D1 serves as a cell cycle regulatory switch in actively proliferating cells. *Current Opinion in Cell Biology*, 15, 158-163.

- STACHER, E., GRAHAM, B. B., HUNT, J. M., GANDJEVA, A., GROSHONG, S. D., MCLAUGHLIN, V. V., JESSUP, M., GRIZZLE, W. E., ALDRED, M. A., COOL, C. D. & TUDER, R. M. 2012. Modern age pathology of pulmonary arterial hypertension. *Am J Respir Crit Care Med*, 186, 261-72.
- STAWOWY, P., BLASCHKE, F., KILIMNIK, A., GOETZE, S., KALLISCH, H., CHRETIEN, M., MARCINKIEWICZ, M., FLECK, E. & GRAF, K. 2002. Proprotein convertase PC5 regulation by PDGF-BB involves PI3-kinase/p70(s6)-kinase activation in vascular smooth muscle cells. *Hypertension*, 39, 399-404.
- STENMARK, K. R., DAVIE, N., FRID, M., GERASIMOVSKAYA, E. & DAS, M. 2006a. Role of the adventitia in pulmonary vascular remodeling. *Physiology (Bethesda)*, 21, 134-45.
- STENMARK, K. R., FAGAN, K. A. & FRID, M. G. 2006b. Hypoxia-induced pulmonary vascular remodeling: cellular and molecular mechanisms. *Circ Res*, 99, 675-91.
- STENMARK, K. R., FRID, M., NEMENOFF, R., DEMPSEY, E. C. & DAS, M. 1999. Hypoxia induces cell-specific changes in gene expression in vascular wall cells: implications for pulmonary hypertension. *Adv Exp Med Biol*, 474, 231-58.
- STEUDEL, W., ICHINOSE, F., HUANG, P. L., HURFORD, W. E., JONES, R. C., BEVAN, J. A., FISHMAN, M. C. & ZAPOL, W. M. 1997. Pulmonary vasoconstriction and hypertension in mice with targeted disruption of the endothelial nitric oxide synthase (NOS 3) gene. *Circ Res*, 81, 34-41.
- STEWART, D. J., LEVY, R. D., CERNACEK, P. & LANGLEBEN, D. 1991. Increased plasma endothelin-1 in pulmonary hypertension: marker or mediator of disease? *Ann Intern Med*, 114, 464-9.
- STIEBELLEHNER, L., FRID, M. G., REEVES, J. T., LOW, R. B., GNANASEKHARAN, M. & STENMARK, K. R. 2003. Bovine distal pulmonary arterial media is composed of a uniform population of well-differentiated smooth muscle cells with low proliferative capabilities. *Am J Physiol Lung Cell Mol Physiol*, 285, L819-28.
- STOTZ, W. H., LI, D. & JOHNS, R. A. 2004. Exogenous nitric oxide upregulates p21(waf1/cip1) in pulmonary microvascular smooth muscle cells. *J Vasc Res*, 41, 211-9.
- SUEN, D. F., NORRIS, K. L. & YOULE, R. J. 2008. Mitochondrial dynamics and apoptosis. *Genes Dev*, 22, 1577-90.
- SUN, Z., NIE, X., SUN, S., DONG, S., YUAN, C., LI, Y., XIAO, B., JIE, D. & LIU, Y. 2017. Long Non-Coding RNA MEG3 Downregulation Triggers Human Pulmonary Artery Smooth Muscle Cell Proliferation and Migration via the p53 Signaling Pathway. *Cell Physiol Biochem*, 42, 2569-2581.
- SUTENDRA, G., BONNET, S., ROCHEFORT, G., HAROMY, A., FOLMES, K. D., LOPASCHUK, G. D., DYCK, J. R. & MICHELAKIS, E. D. 2010. Fatty acid oxidation and malonyl-CoA decarboxylase in the vascular remodeling of pulmonary hypertension. *Sci Transl Med*, 2, 44ra58.
- SUTENDRA, G. & MICHELAKIS, E. D. 2014. The metabolic basis of pulmonary arterial hypertension. *Cell Metab*, 19, 558-73.
- SZABADKAI, G., SIMONI, A. M., CHAMI, M., WIECKOWSKI, M. R., YOULE, R. J. & RIZZUTO, R. 2004. Drp-1-dependent division of the mitochondrial network blocks intraorganellar Ca²⁺ waves and protects against Ca²⁺-mediated apoptosis. *Mol Cell*, 16, 59-68.

- TAGUCHI, N., ISHIHARA, N., JOFUKU, A., OKA, T. & MIHARA, K. 2007. Mitotic phosphorylation of dynamin-related GTPase Drp1 participates in mitochondrial fission. *J Biol Chem*, 282, 11521-9.
- TAIT, S. W. & GREEN, D. R. 2010. Mitochondria and cell death: outer membrane permeabilization and beyond. *Nat Rev Mol Cell Biol*, 11, 621-32.
- TANAKA, A. & YOULE, R. J. 2008. A chemical inhibitor of DRP1 uncouples mitochondrial fission and apoptosis. *Mol Cell*, 29, 409-10.
- TANG, H., TAO, A., SONG, J., LIU, Q., WANG, H. & RUI, T. 2017. Doxorubicin-induced cardiomyocyte apoptosis: Role of mitofusin 2. *Int J Biochem Cell Biol*, 88, 55-59.
- TCHAKARSKA, G., ROUSSEL, M., TROUSSARD, X. & SOLA, B. 2011. Cyclin D1 inhibits mitochondrial activity in B cells. *Cancer Res*, 71, 1690-9.
- TEE, A. R., MANNING, B. D., ROUX, P. P., CANTLEY, L. C. & BLENIS, J. 2003. Tuberous sclerosis complex gene products, Tuberin and Hamartin, control mTOR signaling by acting as a GTPase-activating protein complex toward Rheb. *Curr Biol*, 13, 1259-68.
- TEN FREYHAUS, H., DAGNELL, M., LEUCHS, M., VANTLER, M., BERGHAUSEN, E. M., CAGLAYAN, E., WEISSMANN, N., DAHAL, B. K., SCHERMULY, R. T., OSTMAN, A., KAPPERT, K. & ROSENKRANZ, S. 2011. Hypoxia enhances platelet-derived growth factor signaling in the pulmonary vasculature by down-regulation of protein tyrosine phosphatases. *Am J Respir Crit Care Med*, 183, 1092-102.
- THOMPSON, K. & RABINOVITCH, M. 1996. Exogenous leukocyte and endogenous elastases can mediate mitogenic activity in pulmonary artery smooth muscle cells by release of extracellular-matrix bound basic fibroblast growth factor. *J Cell Physiol*, 166, 495-505.
- TIAN, L., POTUS, F., WU, D., DASGUPTA, A., CHEN, K. H., MEWBURN, J., LIMA, P. & ARCHER, S. L. 2018. Increased Drp1-Mediated Mitochondrial Fission Promotes Proliferation and Collagen Production by Right Ventricular Fibroblasts in Experimental Pulmonary Arterial Hypertension. *Front Physiol*, 9, 828.
- TOCHHAWNG, L., DENG, S., PERVAIZ, S. & YAP, C. T. 2013. Redox regulation of cancer cell migration and invasion. *Mitochondrion*, 13, 246-53.
- TODD, J. R., SCURR, L. L., BECKER, T. M., KEFFORD, R. F. & RIZOS, H. 2014. The MAPK pathway functions as a redundant survival signal that reinforces the PI3K cascade in c-Kit mutant melanoma. *Oncogene*, 33, 236-45.
- TODOROVICH-HUNTER, L., JOHNSON, D. J., RANGER, P., KEELEY, F. W. & RABINOVITCH, M. 1988. Altered elastin and collagen synthesis associated with progressive pulmonary hypertension induced by monocrotaline. A biochemical and ultrastructural study. *Lab Invest*, 58, 184-95.
- TORRES, G., MORALES, P. E., GARCIA-MIGUEL, M., NORAMBUENA-SOTO, I., CARTES-SAAVEDRA, B., VIDAL-PENA, G., MONCADA-RUFF, D., SANHUEZA-OLIVARES, F., SAN MARTIN, A. & CHIONG, M. 2016. Glucagon-like peptide-1 inhibits vascular smooth muscle cell dedifferentiation through mitochondrial dynamics regulation. *Biochem Pharmacol*, 104, 52-61.

- TUDER, R. M., COOL, C. D., GERACI, M. W., WANG, J., ABMAN, S. H., WRIGHT, L., BADESCH, D. & VOELKEL, N. F. 1999. Prostacyclin synthase expression is decreased in lungs from patients with severe pulmonary hypertension. *Am J Respir Crit Care Med*, 159, 1925-32.
- TUDER, R. M., DAVIS, L. A. & GRAHAM, B. B. 2012. Targeting energetic metabolism: a new frontier in the pathogenesis and treatment of pulmonary hypertension. *Am J Respir Crit Care Med*, 185, 260-6.
- USHIO-FUKAI, M., GRIENDLING, K. K., BECKER, P. L., HILENSKI, L., HALLERAN, S. & ALEXANDER, R. W. 2001. Epidermal growth factor receptor transactivation by angiotensin II requires reactive oxygen species in vascular smooth muscle cells. *Arterioscler Thromb Vasc Biol*, 21, 489-95.
- VAN LANGENDONCKT, A., DONNAY, I., SCHUURBIERS, N., AUQUIER, P., CAROLAN, C., MASSIP, A. & DESSY, F. 1997. Effects of supplementation with fetal calf serum on development of bovine embryos in synthetic oviduct fluid medium. *J Reprod Fertil*, 109, 87-93.
- VENDER, R. L. 1992. Role of endothelial cells in the proliferative response of cultured pulmonary vascular smooth muscle cells to reduced oxygen tension. *In Vitro Cell Dev Biol*, 28a, 403-9.
- VOELKEL, N. F. & TUDER, R. M. 1995. Cellular and molecular mechanisms in the pathogenesis of severe pulmonary hypertension. *Eur Respir J*, 8, 2129-38.
- VOELKEL, N. F. & TUDER, R. M. 1997. Cellular and molecular biology of vascular smooth muscle cells in pulmonary hypertension. *Pulm Pharmacol Ther*, 10, 231-41.
- VOUSDEN, K. H. & RYAN, K. M. 2009. p53 and metabolism. *Nat Rev Cancer*, 9, 691-700.
- WAKASUGI, T., SHIMIZU, I., YOSHIDA, Y., HAYASHI, Y., IKEGAMI, R., SUDA, M., KATSUUMI, G., NAKAO, M., HOYANO, M., KASHIMURA, T., NAKAMURA, K., ITO, H., NOJIRI, T., SOGA, T. & MINAMINO, T. 2019. Role of smooth muscle cell p53 in pulmonary arterial hypertension. *PLoS One*, 14, e0212889.
- WALDMAN, T., KINZLER, K. W. & VOGELSTEIN, B. 1995. p21 is necessary for the p53-mediated G1 arrest in human cancer cells. *Cancer Res*, 55, 5187-90.
- WALKER, A. M., LANGLEBEN, D., KORELITZ, J. J., RICH, S., RUBIN, L. J., STROM, B. L., GONIN, R., KEAST, S., BADESCH, D., BARST, R. J., BOURGE, R. C., CHANNICK, R., FROST, A., GAINE, S., MCGOON, M., MCLAUGHLIN, V., MURALI, S., OUDIZ, R. J., ROBBINS, I. M., TAPSON, V., ABENHAIM, L. & CONSTANTINE, G. 2006. Temporal trends and drug exposures in pulmonary hypertension: an American experience. *Am Heart J*, 152, 521-6.
- WALKER, J., UNDEM, C., YUN, X., LADE, J., JIANG, H. & SHIMODA, L. A. 2016. Role of Rho kinase and Na⁺/H⁺ exchange in hypoxia-induced pulmonary arterial smooth muscle cell proliferation and migration. *Physiol Rep*, 4.
- WALLACE, D. C. 2005. A mitochondrial paradigm of metabolic and degenerative diseases, aging, and cancer: a dawn for evolutionary medicine. *Annu Rev Genet*, 39, 359-407.
- WALLACE, D. C., FAN, W. & PROCACCIO, V. 2010. Mitochondrial energetics and therapeutics. *Annu Rev Pathol*, 5, 297-348.

- WAN, Y. Y., ZHANG, J. F., YANG, Z. J., JIANG, L. P., WEI, Y. F., LAI, Q. N., WANG, J. B., XIN, H. B. & HAN, X. J. 2014. Involvement of Drp1 in hypoxia-induced migration of human glioblastoma U251 cells. *Oncol Rep*, 32, 619-26.
- WANG, C., LI, Z., LU, Y., DU, R., KATIYAR, S., YANG, J., FU, M., LEADER, J. E., QUONG, A., NOVIKOFF, P. M. & PESTELL, R. G. 2006. Cyclin D1 repression of nuclear respiratory factor 1 integrates nuclear DNA synthesis and mitochondrial function. *Proc Natl Acad Sci U S A*, 103, 11567-72.
- WANG, G. L., JIANG, B. H., RUE, E. A. & SEMENZA, G. L. 1995. Hypoxia-inducible factor 1 is a basic-helix-loop-helix-PAS heterodimer regulated by cellular O₂ tension. *Proc Natl Acad Sci U S A*, 92, 5510-4.
- WANG, J., LI, J., SANTANA-SANTOS, L., SHUDA, M., SOBOL, R. W., VAN HOUTEN, B. & QIAN, W. 2015a. A novel strategy for targeted killing of tumor cells: Induction of multipolar acentrosomal mitotic spindles with a quinazolinone derivative mdivi-1. *Mol Oncol*, 9, 488-502.
- WANG, J., SHIMODA, L. A., WEIGAND, L., WANG, W., SUN, D. & SYLVESTER, J. T. 2005. Acute hypoxia increases intracellular [Ca²⁺] in pulmonary arterial smooth muscle by enhancing capacitative Ca²⁺ entry. *Am J Physiol Lung Cell Mol Physiol*, 288, L1059-69.
- WANG, J., WEIGAND, L., FOXSON, J., SHIMODA, L. A. & SYLVESTER, J. T. 2007. Ca²⁺ signaling in hypoxic pulmonary vasoconstriction: effects of myosin light chain and Rho kinase antagonists. *Am J Physiol Lung Cell Mol Physiol*, 293, L674-85.
- WANG, J. N., SHI, N. & CHEN, S. Y. 2012. Manganese superoxide dismutase inhibits neointima formation through attenuation of migration and proliferation of vascular smooth muscle cells. *Free Radic Biol Med*, 52, 173-81.
- WANG, L., XIONG, H., WU, F., ZHANG, Y., WANG, J., ZHAO, L., GUO, X., CHANG, L. J., ZHANG, Y., YOU, M. J., KOOCHKEPOUR, S., SALEEM, M., HUANG, H., LU, J. & DENG, Y. 2014a. Hexokinase 2-mediated Warburg effect is required for PTEN- and p53-deficiency-driven prostate cancer growth. *Cell Rep*, 8, 1461-74.
- WANG, L., YU, T., LEE, H., O'BRIEN, D. K., SESAKI, H. & YOON, Y. 2015b. Decreasing mitochondrial fission diminishes vascular smooth muscle cell migration and ameliorates intimal hyperplasia. *Cardiovasc Res*, 106, 272-83.
- WANG, P., XU, J., HOU, Z., WANG, F., SONG, Y., WANG, J., ZHU, H. & JIN, H. 2016. miRNA-34a promotes proliferation of human pulmonary artery smooth muscle cells by targeting PDGFRA. *Cell Prolif*, 49, 484-93.
- WANG, W., LIU, J., MA, A., MIAO, R., JIN, Y., ZHANG, H., XU, K., WANG, C. & WANG, J. 2014b. mTORC1 is involved in hypoxia-induced pulmonary hypertension through the activation of Notch3. *J Cell Physiol*, 229, 2117-25.
- WANG, X. P., ZHANG, W., LIU, X. Q., WANG, W. K., YAN, F., DONG, W. Q., ZHANG, Y. & ZHANG, M. X. 2014c. Arginase I enhances atherosclerotic plaque stabilization by inhibiting inflammation and promoting smooth muscle cell proliferation. *Eur Heart J*, 35, 911-9.
- WANG, Z., FAN, M., CANDAS, D., ZHANG, T. Q., QIN, L., ELDRIDGE, A., WACHSMANN-HOGIU, S., AHMED, K. M., CHROMY, B. A., NANTAJIT, D., DURU, N., HE, F., CHEN, M., FINKEL, T., WEINSTEIN, L. S. & LI, J. J. 2014d. Cyclin B1/Cdk1 coordinates

- mitochondrial respiration for cell-cycle G2/M progression. *Dev Cell*, 29, 217-32.
- WARBURG, O. 1956. On the origin of cancer cells. *Science*, 123, 309-14.
- WAYPA, G. B., GUZY, R., MUNGAI, P. T., MACK, M. M., MARKS, J. D., ROE, M. W. & SCHUMACKER, P. T. 2006. Increases in mitochondrial reactive oxygen species trigger hypoxia-induced calcium responses in pulmonary artery smooth muscle cells. *Circ Res*, 99, 970-8.
- WEBER, D. S., TANIYAMA, Y., ROCIC, P., SESHIAH, P. N., DECHERT, M. A., GERTHOFFER, W. T. & GRIENGLING, K. K. 2004. Phosphoinositide-dependent kinase 1 and p21-activated protein kinase mediate reactive oxygen species-dependent regulation of platelet-derived growth factor-induced smooth muscle cell migration. *Circ Res*, 94, 1219-26.
- WEI, L., DENG, W., CHENG, Z., GUO, H., WANG, S., ZHANG, X., HE, Y. & TANG, Q. 2016. Effects of hesperetin on platelet-derived growth factor-BB-induced pulmonary artery smooth muscle cell proliferation. *Mol Med Rep*, 13, 955-60.
- WEIR, E. K. & ARCHER, S. L. 1995. The mechanism of acute hypoxic pulmonary vasoconstriction: the tale of two channels. *Faseb j*, 9, 183-9.
- WEIR, E. K., LOPEZ-BARNEO, J., BUCKLER, K. J. & ARCHER, S. L. 2005. Acute oxygen-sensing mechanisms. *N Engl J Med*, 353, 2042-55.
- WEIR, E. K. & OLSCHESKI, A. 2006. Role of ion channels in acute and chronic responses of the pulmonary vasculature to hypoxia. *Cardiovasc Res*, 71, 630-41.
- WELSH, D. J., PEACOCK, A. J., MACLEAN, M. & HARNETT, M. 2001. Chronic hypoxia induces constitutive p38 mitogen-activated protein kinase activity that correlates with enhanced cellular proliferation in fibroblasts from rat pulmonary but not systemic arteries. *Am J Respir Crit Care Med*, 164, 282-9.
- WESTERMANN, B. 2010. Mitochondrial fusion and fission in cell life and death. *Nat Rev Mol Cell Biol*, 11, 872-84.
- WILSON, J. L., YU, J., TAYLOR, L. & POLGAR, P. 2015. Hyperplastic Growth of Pulmonary Artery Smooth Muscle Cells from Subjects with Pulmonary Arterial Hypertension Is Activated through JNK and p38 MAPK. *PLoS One*, 10, e0123662.
- WOODGETT, J. R., AVRUCH, J. & KYRIAKIS, J. M. 1995. Regulation of nuclear transcription factors by stress signals. *Clin Exp Pharmacol Physiol*, 22, 281-3.
- XIN, X., JOHNSON, A. D., SCOTT-BURDEN, T., ENGLER, D. & CASSCELLS, W. 1994. The predominant form of fibroblast growth factor receptor expressed by proliferating human arterial smooth muscle cells in culture is type I. *Biochem Biophys Res Commun*, 204, 557-64.
- XU, W., KANEKO, F. T., ZHENG, S., COMHAIR, S. A., JANOCHA, A. J., GOGGANS, T., THUNNISSEN, F. B., FARVER, C., HAZEN, S. L., JENNINGS, C., DWEIK, R. A., ARROLIGA, A. C. & ERZURUM, S. C. 2004. Increased arginase II and decreased NO synthesis in endothelial cells of patients with pulmonary arterial hypertension. *Faseb j*, 18, 1746-8.
- YAMAUCHI, J., NAGAO, M., KAZIRO, Y. & ITOH, H. 1997. Activation of p38 mitogen-activated protein kinase by signaling through G protein-coupled receptors. Involvement of Gbetagamma and Galphaq/11 subunits. *J Biol Chem*, 272, 27771-7.

- YAMBOLIEV, I. A., CHEN, J. & GERTHOFFER, W. T. 2001. PI 3-kinases and Src kinases regulate spreading and migration of cultured VSMCs. *Am J Physiol Cell Physiol*, 281, C709-18.
- YAMBOLIEV, I. A. & GERTHOFFER, W. T. 2001. Modulatory role of ERK MAPK-caldesmon pathway in PDGF-stimulated migration of cultured pulmonary artery SMCs. *Am J Physiol Cell Physiol*, 280, C1680-8.
- YANAGISAWA, M., KURIHARA, H., KIMURA, S., TOMOBE, Y., KOBAYASHI, M., MITSUI, Y., YAZAKI, Y., GOTO, K. & MASAKI, T. 1988. A novel potent vasoconstrictor peptide produced by vascular endothelial cells. *Nature*, 332, 411-5.
- YANG, G., LI, J. Q., BO, J. P., WANG, B., TIAN, X. R., LIU, T. Z. & LIU, Z. L. 2015. Baicalin inhibits PDGF-induced proliferation and migration of airway smooth muscle cells. *Int J Clin Exp Med*, 8, 20532-9.
- YANG, X. P., PEI, Z. H. & REN, J. 2009. Making up or breaking up: the tortuous role of platelet-derived growth factor in vascular ageing. *Clin Exp Pharmacol Physiol*, 36, 739-47.
- YE, X. W., YU, H., JIN, Y. K., JING, X. T., XU, M., WAN, Z. F. & ZHANG, X. Y. 2015. miR-138 inhibits proliferation by targeting 3-phosphoinositide-dependent protein kinase-1 in non-small cell lung cancer cells. *Clin Respir J*, 9, 27-33.
- YI, E. S., KIM, H., AHN, H., STROTHER, J., MORRIS, T., MASLIAH, E., HANSEN, L. A., PARK, K. & FRIEDMAN, P. J. 2000. Distribution of obstructive intimal lesions and their cellular phenotypes in chronic pulmonary hypertension. A morphometric and immunohistochemical study. *Am J Respir Crit Care Med*, 162, 1577-86.
- YING-FANG, S., JING-FANG, H., HUAN-ZHANG, L. & HAO-WEN, Q. 2007. Effect of platelet-activating factor on cell proliferation & NF-kappaB activation in airway smooth muscle cells in rats. *Indian J Med Res*, 126, 139-45.
- YOSHIDA, T., AZUMA, H., AIHARA, K., FUJIMURA, M., AKAIKE, M., MITSUI, T. & MATSUMOTO, T. 2005. Vascular smooth muscle cell proliferation is dependent upon upregulation of mitochondrial transcription factor A (mtTFA) expression in injured rat carotid artery. *Atherosclerosis*, 178, 39-47.
- YU, A. Y., SHIMODA, L. A., IYER, N. V., HUSO, D. L., SUN, X., MCWILLIAMS, R., BEATY, T., SHAM, J. S., WIENER, C. M., SYLVESTER, J. T. & SEMENZA, G. L. 1999. Impaired physiological responses to chronic hypoxia in mice partially deficient for hypoxia-inducible factor 1alpha. *J Clin Invest*, 103, 691-6.
- YU, J. S. & CUI, W. 2016. Proliferation, survival and metabolism: the role of PI3K/AKT/mTOR signalling in pluripotency and cell fate determination. *Development*, 143, 3050-60.
- YU, T., JHUN, B. S. & YOON, Y. 2011. High-glucose stimulation increases reactive oxygen species production through the calcium and mitogen-activated protein kinase-mediated activation of mitochondrial fission. *Antioxid Redox Signal*, 14, 425-37.
- YU, Y., SWEENEY, M., ZHANG, S., PLATOSHYN, O., LANDSBERG, J., ROTHMAN, A. & YUAN, J. X. 2003. PDGF stimulates pulmonary vascular smooth muscle cell proliferation by upregulating TRPC6 expression. *Am J Physiol Cell Physiol*, 284, C316-30.

- YUAN, J. X., ALDINGER, A. M., JUHASZOVA, M., WANG, J., CONTE, J. V., JR., GAINES, S. P., ORENS, J. B. & RUBIN, L. J. 1998. Dysfunctional voltage-gated K⁺ channels in pulmonary artery smooth muscle cells of patients with primary pulmonary hypertension. *Circulation*, 98, 1400-6.
- ZAMZAMI, N. & KROEMER, G. 2001. The mitochondrion in apoptosis: how Pandora's box opens. *Nat Rev Mol Cell Biol*, 2, 67-71.
- ZHAN, Y., KIM, S., IZUMI, Y., IZUMIYA, Y., NAKAO, T., MIYAZAKI, H. & IWAO, H. 2003. Role of JNK, p38, and ERK in platelet-derived growth factor-induced vascular proliferation, migration, and gene expression. *Arterioscler Thromb Vasc Biol*, 23, 795-801.
- ZHANG, H., GONG, Y., WANG, Z., JIANG, L., CHEN, R., FAN, X., ZHU, H., HAN, L., LI, X., XIAO, J. & KONG, X. 2014. Apelin inhibits the proliferation and migration of rat PASMCs via the activation of PI3K/Akt/mTOR signal and the inhibition of autophagy under hypoxia. *J Cell Mol Med*, 18, 542-53.
- ZHANG, J., JIN, N., LIU, Y. & RHOADES, R. A. 1998. Hydrogen peroxide stimulates extracellular signal-regulated protein kinases in pulmonary arterial smooth muscle cells. *Am J Respir Cell Mol Biol*, 19, 324-32.
- ZHANG, S. X., GOZAL, D., SACHLEBEN, L. R., JR., RANE, M., KLEIN, J. B. & GOZAL, E. 2003. Hypoxia induces an autocrine-paracrine survival pathway via platelet-derived growth factor (PDGF)-B/PDGF-beta receptor/phosphatidylinositol 3-kinase/Akt signaling in RN46A neuronal cells. *Faseb j*, 17, 1709-11.
- ZHANG, W. & LIU, H. T. 2002. MAPK signal pathways in the regulation of cell proliferation in mammalian cells. *Cell Res*, 12, 9-18.
- ZHAO, J., ZHANG, J., YU, M., XIE, Y., HUANG, Y., WOLFF, D. W., ABEL, P. W. & TU, Y. 2013. Mitochondrial dynamics regulates migration and invasion of breast cancer cells. *Oncogene*, 32, 4814-24.
- ZHAO, L., MASON, N. A., MORRELL, N. W., KOJONAZAROV, B., SADYKOV, A., MARIPOV, A., MIRRAKHIMOV, M. M., ALDASHEV, A. & WILKINS, M. R. 2001. Sildenafil inhibits hypoxia-induced pulmonary hypertension. *Circulation*, 104, 424-8.
- ZHOU, W. M., WU, G. L., HUANG, J., LI, J. G., HAO, C., HE, Q. M., CHEN, X. D., WANG, G. X. & TU, X. H. 2019. Low expression of PDK1 inhibits renal cell carcinoma cell proliferation, migration, invasion and epithelial mesenchymal transition through inhibition of the PI3K-PDK1-Akt pathway. *Cell Signal*, 56, 1-14.
- ZHUANG, X., MAIMAITIJANG, A., LI, Y., SHI, H. & JIANG, X. 2017. Salidroside inhibits high-glucose induced proliferation of vascular smooth muscle cells via inhibiting mitochondrial fission and oxidative stress. *Exp Ther Med*, 14, 515-524.